

DOCTORAL THESIS

Hygrothermal Criteria for Design of Cross-Laminated Timber External Walls with Ventilated Facades

Villu Kukk

TALLINN UNIVERSITY OF TECHNOLOGY
DOCTORAL THESIS
33/2022

Hygrothermal Criteria for Design of Cross-Laminated Timber External Walls with Ventilated Facades

VILLU KUKK



TALLINN UNIVERSITY OF TECHNOLOGY

School of Engineering

Department of Civil Engineering and Architecture

This dissertation was accepted for the defence of the degree 20/05/2022

Supervisor: Prof. Targo Kalamees
School of Engineering
Department of Civil Engineering and Architecture
Nearly Zero Energy Buildings Research Group
Tallinn University of Technology
Tallinn, Estonia

Co-supervisor: Prof. Jaan Kers
School of Engineering
Department of Materials and Environmental Technology
Head of Laboratory of Wood Technology
Tallinn University of Technology
Tallinn, Estonia

Opponents: Berit Time, Chief Scientist
Department of Architecture, Materials and Structures
SINTEF Norwegian Independent Research Organisation
Trondheim, Norway

Prof. Thomas Bednar
Faculty of Civil Engineering
Institute of Material Technology, Building Physics, and Building Ecology
Head of Research Group for Building Physics and Sound Protection
TU Wien
Wien, Austria

Defence of the thesis: 21/06/2022, Tallinn

Declaration:

Hereby I declare that this doctoral thesis, my original investigation and achievement, submitted for the doctoral degree at Tallinn University of Technology, has not been submitted for doctoral or equivalent academic degree.

Villu Kukk

signature



European Union
European Regional
Development Fund



Investing
in your future

Copyright: Villu Kukk, 2022

ISSN 2585-6898 (publication)

ISBN 978-9949-83-837-0 (publication)

ISSN 2585-6901 (PDF)

ISBN 978-9949-83-838-7 (PDF)

Printed by Koopia Niini & Rauam

TALLINNA TEHNIKAÜLIKOOL
DOKTORITÖÖ
33/2022

Soojus- ja niiskustehnilised kriteeriumid tuulduva fassaadiga ristkihtliimpuidust välisseinte projekteerimiseks

VILLU KUKK



To Luule and Urmas

Abstract

Hygrothermal Criteria for Design of Cross-Laminated Timber External Walls with Ventilated Facades

Wooden buildings are the most sensitive objects in terms of moisture safety; large-scale buildings made of mass timber elements require even more attention. Regarding hygrothermal performance, one of the main concerns about wooden buildings is the durability of wood related to moisture damages. However, no studies have clearly determined the hygrothermal criteria for designing CLT external walls. Criteria considering the high initial MC of the CLT panels, the water vapour resistance of an additional air and vapour barrier, the effect of interior insulation and the dry-out capacity of the wall assembly should be established. As compared to concrete buildings, construction of modern large-scale mass-timber buildings can be less time consuming and easier. Without proper weather protection, there is a high probability of wood getting soaked by exposure to weather, which can cause moisture problems during the service life. Therefore, the main objective of this thesis is to determine hygrothermal criteria for CLT external wall that are applicable to secure the air-tightness and moisture safety of the building envelope.

Data for analysing air permeability properties and hygrothermal performance of the CLT envelope was gathered from laboratory experiments, climate chamber test and exposing external test walls to real outdoor climate conditions. Results from the experiments were first used to create and validate the simulation models and later to analyse data for establishing the hygrothermal criteria. Mould growth risk on the CLT and wind barrier surface was used to evaluate the hygrothermal performance.

The seasonal change in the indoor environment in cold and humid climate and initial MC of wood significantly affect the crack formation in the CLT panel. The size of the penetrating crack affects the size of the air leakage with increasing air pressure difference. A single middle layer is not sufficient to prevent air leakage through the cracks and therefore 3-layer CLT panel may require an additional air barrier. Having at least 5 layers are sufficient for ensuring the airtightness of CLT panels as the probability of crack formation through panel thickness is minimal. The effect of a change in indoor RH on the size of air leakages is small compared to the impact of built-in moisture. Therefore the 5-layer CLT panel can be used as an air-tight layer in external wall construction as long as its initial low MC (about 13 %) is maintained. The key factors in safe hygrothermal design of the CLT external envelope with ventilated facade are sufficient dry-out capacity and maintenance of low initial MC of CLT during construction phase. It was found that the vapour resistance of the wind barrier should not exceed $S_d \leq 0.03$ m with thermal resistance of $R \leq 0.075$ (m²·K)/W. The CLT initial MC of the external surface (depth 30 mm) should not exceed 20 % and core remains factory-dry (13 %) or the vapour resistance (S_d) of an additional air and vapour barrier should not exceed $S_d \leq 0.25$ m if the CLT envelope is not fully weather protected and is externally insulated with vapour open materials. In the case of vapour tight external or internal insulation, initial moisture content of the CLT surface should not exceed 16 % to prevent mould growth risk. Construction of CLT building during spring (April-May) causes the lowest risk for mould growth.

Keywords: *Cross-laminated timber, CLT, cracks formation, water vapour transmission, air permeability, production technology, initial moisture content, moisture safety, hygrothermal performance, hygrothermal criteria, external wall, ventilated façade.*

Kokkuvõte

Soojus- ja niiskustehnilised kriteeriumid tuulduva fassaadiga ristkihtliimpuidust välisseinte projekteerimiseks

Niiskus- ja soojustehnilise toimivuse seisukohalt on puithoonete ehitusel oluline vältida niiskuskahjustuste teket välispiiretes. Ristkihtliimpuit hoonete ehitamisel napib teavet, mis selgelt määraksid niiskus- ja soojustehnilised tingimused ja kriteeriumid, mille järgi hooned niiskusturvaliselt projekteerid ja ehitada. Määrata on vaja kriteeriumid, mis arvestaksid ristkihtliimpuidu algniiskussisalduse välja kuivamisega, õhu- ja aurutõkke veeaurutakistuse suurusega, seespoolse soojustuse kasutamise ja välispiirete väljakuivamise võimekusega. Modernsete suuremõõtmeliste massiivpuidust hoonete ehitamine on oluliselt vähem aega nõudev ja lihtsam paigaldada võrreldes tänapäeva betoonhoonetega. Ilma korrektse ilmastiku kaitseta on suur tõenäosus, et sademetele avatud massiivpuidust elemendid märguvad ja see võib kaasa tuua niiskuskahjustused. Sellest tulenevalt on selle töö eesmärgiks seada niiskustehnilised kriteeriumid ristkihtliimpuidust välisseinte projekteerimiseks, mille rakendamisel on võimalik tagada hoone õhupidavus ja niiskusturvalisus arvestades seejuures ristkihtliimpuidu ehituse, tootmistehnoloogia ja ehitusaegse niiskusega.

Andmed ristkihtliimpuidust välispiirete õhupidavuse omaduste ja niiskustehnilise toimivuse analüüsiks koguti laboratoorsetest katsetest ja kliimakambri ja väli mõõtmistelt. Mõõtetulemuste põhjal koostati ja valideeriti simulatsiooni mudelid, mis hiljem andmeanalüüsil kasutati niiskustehniliste kriteeriumite seadmisel. Hallituse kasvu ohtu ristkihtliimpuidu ja tuuletõkke pinnal arvestati niiskustehnilise toimivuse hindamiskriteeriumiks.

Hooajalise siseruumi suhtelise õhuniiskuse muutus mõjutab oluliselt ristkihtliimpuidus tekkivate pragude kasvu ja suurust. See omakorda mõjutab märgatavalt õhulekete kasvu paneelides õhurõhu erinevuse suurenemisel. Üksik vahekiht ristkihtliimpuitpaneelis ei ole piisav vältimaks õhulukete tekkimist läbi paneeli pragude ja seetõttu vajab 3-kihiline ristkihtliimpuitpaneel eraldi õhutõkke kihti. Ristkihtliimpuitpaneel vähemalt 5 kihiga on piisav arvestamiseks seda kui õhupidavat kihti. Võrreldes ehitusaegse niiskusega, on hooajalise siseruumi suhtelise õhuniiskuse muutuse mõju väike ja seetõttu saab 5 kihilist paneeli pidada õhupidavaks vaid juhul, kui selle madal algniiskus on ehituse aeg tagatud. Peamised tegurid ristkihtliimpuidust välispiirde niiskustehnilise toimivuse tagamiseks on aga piisav väljakuivamise võimekus ja samal ajal madala algniiskuse tagamine ehitusel. Andmeanalüüsi tulemusel leiti, et ilmasitku kaitse puudumisel ei tohiks välispiirde tuuletõkke veeaurutakistus (S_d) ületada 0.03 m; ristkihtliimpuidu algniiskussisaldus ei tohiks ületada 20 % või õhu- ja arutõkke veeaurutakistus (S_d) ei tohiks ületada 0.03 m kui välispiire on veeauru läbilaskva materjaliga soojustatud. Kui välispiire on soojustatud veeaurutiheda soojustusega, ei tohiks paneeli algniiskussisaldus ületada 16 %, et vältida hallituse kasvu ohtu. Ristkihtliimpuitpaneelide paigaldus kevadel toob kaasa väikseima hallituse riksi ohtu.

Märksõnad: Ristkihtliimpuit, CLT, pragude teke, veeauru läbivus, õhupidavus, tootmistehnoloogia, algniiskussisaldus, niiskusturvalisus, soojus- ja niiskustehniline toimivus, niiskustehnilised kriteeriumid, välissein, tuulutatav fassaad.

Acknowledgements

The author wishes to express his sincere gratitude to all collaborators for their support in the process of the preparation of this PhD work.

First, my deepest gratitude is due to my supervisors, Professor Targo Kalamees and Professor Jaan Kers, for their support, motivation and guidance throughout my doctoral studies and for introducing the possibilities of research in my topic. I appreciate the opportunity to attend conferences, working meetings and doctoral courses in various countries. I am grateful for their time and continuous support during all these years and for being a personal example of thoroughness, creativity and punctuality in the work to be followed.

My sincere thanks go to my supervisors at Concordia University in Montreal, Canada, Professor Hua Ge and Dr Lin Wang for their valuable collaboration and scientific support.

I am thankful to researchers Paul Klõšeiko, Simo Ilomets, Endrik Arumägi, Kristo Kalbe, and Heikko Kallakas from this university for their professional help and discussion.

I extend my gratitude to all the members of the Nearly Zero Energy Buildings Research Group and Wood Technology Laboratory for their motivation and support.

I wish to thank the graduate students and co-authors of my publications for their assistance and collaboration – Giovanni Luciani, Ricardo Horta, Martin Püssa, Adeniyi Bella, Annegrete Külaots, Laura Kaljula, and Raina Lipand.

I acknowledge Estonian glulam producer Peetri Puit OÜ for their constructive discussions from a practical point of view and for supplying CLT specimens.

I would like to thank the organizations that have rewarded my studies with scholarships – Riigi Kinnisvara AS, Sihtasutus Professor Karl Õigeri Stipendiumifond, City Government of Tallinn, and Estonian Education and Youth Board (former Archimedes Foundation).

My dearest thanks are due to my family members for their unlimited support during my scientific studies – my parents Luule and Urmas for their wisdom and shared experience, my cousin Mirle and her family for their loving care, my brother Uku and his family for their encouragement, and my sister Marta for her supporting kind words. Also, my closest friends and relatives are gratefully acknowledged for their support.

Financial support

The thesis would not have been completed without the financial support provided to me. My sincere gratitude to all these institutions.

The research work on which this thesis is based was carried out at the Nearly Zero Energy Buildings Research Group, Department of Civil Engineering and Architecture, School of Engineering at Tallinn University of Technology.

This research was supported financially by the Estonian Research Council with Personal research funding PRG483 “Moisture safety of interior insulation, constructional moisture, and thermally efficient building envelope”, Estonian Centre of Excellence in Zero Energy and Resource Efficient Smart Buildings and Districts, ZEBE, grant TK146 funded by the European Regional Development Fund and by the European Commission through the H2020 project Finest Twins (grant No. 856602).

Short-term visits and research for the thesis was supported by the Estonian Education and Youth Board (former Archimedes Foundation) and by development of cooperation and innovation of universities, the sub-measure “Doctoral Schools”.

Contents

List of publications	13
Author's contribution to the publications	14
Abbreviations	15
Symbols	16
Greek letters	17
Subscripts	18
1 Introduction	19
1.1 Objectives and content of the study	20
1.2 Novelty and practical application	21
1.3 Limitations of the work	22
2 Design and performance of mass-timber envelopes	24
2.1 Mass-timber panel as structural element	24
2.2 Hygrothermal properties of mass-timber panel	24
2.3 Air leakages in mass-timber envelopes	26
2.4 Hygrothermal performance of mass-timber envelopes	28
2.5 Hygrothermal criteria for design of wooden buildings	29
3 Materials and methods	31
3.1 Measurements	31
3.1.1 Measurement devices	31
3.1.1.1 Determination of moisture content in wood	31
3.1.1.2 Determination of cracks formation	31
3.1.1.3 Determination of air permeability	31
3.1.1.4 Determination of temperature and RH in external test walls	31
3.1.2 Material properties	32
3.1.2.1 Cracks formation	32
3.1.2.2 Vapour permeability	35
3.1.2.3 Air permeability	36
3.1.3 Hygrothermal performance of CLT external walls in the climate chamber test	38
3.1.4 Hygrothermal performance and air leakages of CLT external walls exposed to real outdoor conditions	40
3.1.4.1 The test setup	40
3.1.4.2 Air leakages in external test walls	43
3.1.4.3 Hygrothermal performance	45
3.2 Modelling	46
3.2.1 Simulation software	46
3.2.2 Simulation models	47
3.2.2.1 Simulation models of test walls from climate chamber test	47
3.2.2.2 Simulation models of test walls from test facility measurements	48
3.2.3 Material properties	48
3.2.4 Structure of stochastic analysis	49
3.2.4.1 Discrete random variables	50
3.2.4.2 Uniformly distributed continuous random variables	50
3.2.4.3 Boundary conditions for data analysis	51
3.3 Data analysis	54
3.3.1 Validation of simulation models	54
3.3.2 Evaluation criteria	54

3.3.3 Probability of hygrothermal performance	55
3.3.4 Partial correlation coefficient	55
4 Results and discussion.....	56
4.1 Air leakages	56
4.1.1 CLT as a material	56
4.1.1.1 Cracks size and locations in the CLT panel	56
4.1.1.2 Impact of cracks on the water vapour resistance and air permeability properties of the CLT panel.....	57
4.1.1.3 Impact of indoor seasonal RH change on the crack formation and air permeability properties of the CLT panel	59
4.1.2 Air leakages of CLT external wall.....	63
4.2 Hygrothermal performance of CLT external walls	67
4.2.1 Measurements	67
4.2.1.1 Climate chamber test: Impact of interior layer properties	67
4.2.1.2 CLT external test walls exposed to real outdoor conditions	68
4.2.2 Modelling	75
4.2.2.1 Simulation models of test walls from climate chamber test.....	75
4.2.2.2 Simulation models of test walls from test facility measurements.....	76
4.2.3 Data analysis	83
4.2.3.1 Impact of interior layer properties on moisture dry-out of CLT external walls	83
4.2.3.2 Stochastic analysis.....	85
4.3 Hygrothermal design criteria	93
4.3.1 Parameter study.....	93
4.3.1.1 The interior surface of CLT	93
4.3.1.2 The exterior surface of CLT	94
4.3.1.3 The interior surface of the wind barrier.....	95
4.3.2 Variations in hygrothermal criteria	97
4.3.3 Use of hygrothermal criteria in practice	98
5 Conclusions	100
5.1 Air leakages in the CLT panel and external wall	100
5.2 Hygrothermal performance of CLT external walls	101
5.3 Hygrothermal design criteria	102
6 Future studies	104
References	105
Publications.....	113
PUBLICATION I.....	115
PUBLICATION II.....	123
PUBLICATION III.....	141
PUBLICATION IV	151
PUBLICATION V	163
PUBLICATION VI	183
Curriculum vitae.....	210
Elulookirjeldus.....	211
Publications / Teaduspublikatsioonid	212

List of publications

The list of author's publications, on the basis of which the thesis has been prepared:

- I Kukk, V.; Luciani, G.; Püssa, M.; Horta, R.; Kallakas, H.; Kers, J.; Kalamees, T., 2017. Impact of cracks to the hygrothermal properties of CLT water vapour resistance and air permeability. *Energy Procedia*, 132: The 11th Nordic Symposium on Building Physics, Trondheim, Norway, 11-14 June 2017. Ed. S. Geving, B. Time. Elsevier, 741–746.
- II Kukk, V.; Kalamees, T.; Kers, J., 2019. The effects of production technologies on the air permeability and crack development of cross-laminated timber. *Journal of Building Physics*, 43 (3), 171–186.
- III Kukk, V.; Bella, A.; Kers, J.; Kalamees, T., 2021. Airtightness of cross-laminated timber envelopes: Influence of moisture content, indoor humidity, orientation, and assembly. *Journal of Building Engineering*, 44.
- IV Kukk, V.; Külaots, A.; Kers, J.; Kalamees, T., 2019. Influence of interior layer properties to moisture dry-out of CLT walls. *Canadian Journal of Civil Engineering*, 46 (11), 1001–1009.
- V Kukk, V.; Kaljula, L.; Kers, J.; Kalamees, T., 2022. Designing highly insulated cross-laminated timber external walls in terms of hygrothermal performance: Field measurements and simulations. *Building and Environment*, 212.
- VI Kukk, V.; Kers, J.; Kalamees, T.; Wang, L.; Ge, H., 2022. Impact of built-in moisture on the design of hygrothermally safe cross-laminated timber external walls: A stochastic approach. *Building and Environment* (Submitted 21.03.2022, Under review).

Author's contribution to the publications

Contribution to the publications in this thesis are:

- I The climate chamber test, water vapour permeability and air leakage measurements were conducted by the author with the help of MSc students, guided by the supervisors Prof. Targo Kalamees and Prof. Jaan Kers. The method was developed by the author in cooperation with the supervisors. Data analysis was done by the author and the results were discussed with the co-authors. The article was written by the author in cooperation with the supervisors.
- II The research questions and measurement method were developed by the author in cooperation with the supervisors. The conditioning of the CLT panels, the dimensions of cracks and air leakage measurements were carried out by the MSc students with the help of the author, guided by the supervisors Prof. Targo Kalamees and Prof. Jaan Kers. Data analysis was done by the author and the results were discussed with the co-authors. The article was written by the author in cooperation with the supervisors.
- III The research questions and methodology were developed by the author in cooperation with the MSc student and with the supervisors Prof. Targo Kalamees and Prof. Jaan Kers. The air leakage measurements of CLT external test walls were taken by a MSc student with the help of the author, guided by the supervisors. Data analysis was done by the author and the results were discussed with the co-authors. The article was written by the author in cooperation with the supervisors.
- IV The research questions and methodology were developed by the author in cooperation with the supervisors Prof. Targo Kalamees and Prof. Jaan Kers. The hygrothermal parameters of CLT external test walls in the climate chamber test were measured by a MSc student with the help of the author, guided by the supervisors. The validation of simulation models, data analysis and discussion were done by the author and the MSc student in cooperation with the supervisors. The article was written by the author in cooperation with the supervisors.
- V The design of CLT external test walls, material selection and the measurements method were developed by the author in cooperation with the supervisors Prof. Targo Kalamees and Prof. Jaan Kers. The hygrothermal parameters of CLT external test walls exposed to the real outdoor climate conditions were measured by a MSc student with the help of the author, guided by the supervisors Prof. Targo Kalamees and Prof. Jaan Kers. The validation of simulation models, data analysis and discussion were done by the author and the MSc student in cooperation with the supervisors. The article was written by the author in cooperation with the supervisors.
- VI The stochastic analysis and hygrothermal criteria were set by the author, guided by the supervisors Prof. Targo Kalamees and Prof. Jaan Kers. The method was developed by the co-authors Prof. Hua Ge and Lin Wang and customized by the author in cooperation with the supervisors. Data analysis and discussion was done by the author in cooperation with the supervisors. The article was written by the author in cooperation with the supervisors.

Abbreviations

13/20MW	CLT test wall type: $MC_{CLT} \approx 13/20$ %, internally insulated with mineral wool
13/20PIR	CLT test wall type: $MC_{CLT} \approx 13/20$ %, internally insulated with PIR
13BE3L	CLT specimen: $MC \approx 13$ %, bonded edges, 3-layer
13BE5L	CLT specimen: $MC \approx 13$ %, bonded edges, 5-layer
13WBE3L	CLT specimen: $MC \approx 13$ %, without bonded edges, 3-layer
13WBE5L	CLT specimen: $MC \approx 13$ %, without bonded edges, 5-layer
1D	One (1) Dimensional
2D	Two (2) Dimensional
6BE3L	CLT specimen: $MC \approx 6$ %, bonded edges, 3-layer
6BE5L	CLT specimen: $MC \approx 6$ %, bonded edges, 5-layer
6WBE3L	CLT specimen: $MC \approx 6$ %, without bonded edges, 3-layer
6WBE5L	CLT specimen: $MC \approx 6$ %, without bonded edges, 5-layer
ACH	Air Change Rate per Hour (1/h)
ASHRAE	American Society of Heating, Refrigerating and Air-Conditioning Engineers
CHAMPS	Coupled Heat, Air, Moisture, Pollutant Simulation
CLT	Cross-Laminated Timber
CS1-4	Small-scale CLT specimens (0.1 × 0.1 m)
EMC	Equilibrium Moisture Content
EPDM	Ethylene Propylene Diene Monomer (rubber)
EPS	Expanded Polystyrene insulation
ETICS	External Thermal Insulation Composite System
EW11-52	CLT test wall type (test facility measurements)
FSP	Fibre Saturation Point
HAM	Heat, Air, Moisture
MC	Moisture Content (% , kg/kg, m^3/m^3)
MW	Mineral Wool
NRMSE	Normalized Root-Mean-Square-Error
nZEB	Nearly Zero Energy Building
PCC	Partial Correlation Coefficient
PIR	Polyisocyanurate insulation
RH	Relative Humidity (%)
RMSE	Root-Mean-Square-Error
S1-4	Large scale CLT specimen (0.5 × 0.5 m)
XPS	Extruded Polystyrene insulation

Symbols

Δv	moisture excess, g/m ³
A_w	water absorption coefficient, kg/(m ² ·s ^{0.5})
C	air flow coefficient, m ³ /h·Pa ⁿ
D	conduction coefficient, kg/(m·s)
h	specific enthalpy, J/kg
H	enthalpy, J/m ³
j	flux, kg/m ² s
M	mould growth index, -
n	air flow exponent, -
P	air pressure, Pa
P_v	partial pressure of water vapour, Pa
Q	thermal energy, J
q_{50}	air leakage rate at 50 Pa, m ³ /(h·m ²)
R	thermal resistance, (m ² ·K)/W
S_d	equivalent air layer thickness, m
t	temperature, °C
T	Temperature, temperature difference, K
U	thermal transmittance, W/(m ² ·K)
u	specific internal energy, J/kg
\dot{V}	air flow rate, m ³ /h
Z	water vapour resistance, m ² ·s·Pa/kg

Greek letters

Δ	delta, difference
Δv	moisture excess, g/m ³
∇	nabla, magnitude
μ	water vapour diffusion resistance factor, -
δ	vapour permeability, kg/(m·s·Pa)
λ	lambda, thermal conductivity, W/(m·K)
ρ	density, kg/m ³
φ	relative humidity, -

Subscripts

a	air
AVB	additional air and vapour barrier
CLT_ES	the exterior surface of CLT
CLT_IS	the interior surface of CLT
conv	convection
diff	diffusion
e	exterior
g	gas
i	interior
IL	interior layer
l	liquid
REV	reference volume
s	surface
si	interior surface
se	exterior surface
sat	saturation
v	vapour
VOC	Volatile Organic Compound
w	water
WB	wind barrier

1 Introduction

Using wood in building design and construction can reduce the environmental impact on air up to 59 % compared to using traditional materials such as brick (Santi et al. 2016). Alongside traditional materials, cross-laminated timber (CLT) is increasingly used in the building design because of its rigidity, strength and low density, as well as high water vapour diffusion control, low thermal conductivity and environmental aspects, as compared to steel and concrete. According to the EN 16351 (2015), a CLT panel is a multi-layer wooden composite structure made of lumber, usually softwood such as spruce and pine, produced of at least three orthogonally bonded layers.

Wood is known as a hygroscopic material that can lose and absorb moisture from air depending on the ambient environment. Moisture loss and absorption from ambient air regulate the equilibrium moisture content (EMC) of the wood. The change of EMC in wood has a major role in crack formation as the wood shrinks and swells below the fibre saturation point (FSP), depending on the relative humidity (RH) and temperature of the ambient environment (Rubin Shmulsky and Jones 2011). Several studies have shown that the crack formation on the CLT panel surface influences its air permeability properties. In her research, Time (2020) indicated that external walls with 3-layer CLT panels need an additional air barrier layer. Skogstad et al. (2011) from SINTEF (Norwegian independent research organisation) studied the air permeability properties of the CLT panel and its connections (wall, wall to ceiling, wall to wall). They found that moisture content decrease (caused by a decrease in ambient indoor air RH) from 0.14 to 0.10 kg/kg caused air leakage in CLT connections to increase up to 10 times (mostly in the wall to wall connections).

There is a need for more in-depth knowledge of which production technology (e.g., number of layers, glued edges, initial moisture content) ensures airtightness of a CLT panel when exposed to the seasonal indoor climate change and how large the air leakages of CLT panels are compared to the requirements for the building air permeability. When designing a CLT building, it is important to know which CLT panel can be considered as an airtight layer or which airtightness solution can be used for different panels. There are three main suggested technologies to improve the airtightness of CLT envelopes: first, to use sealing products between CLT elements; second, to give an additional cover to the CLT joints; third, to cover the whole envelope with an airtight membrane (Herms 2020). The first two technologies are more cost-effective than the third and are the most commonly used. The third is the most reliable technology; it is mostly used if the panel itself cannot be considered as an airtight layer.

The effect of built-in moisture on the air permeability properties of CLT panels has not been thoroughly studied. Wood shrinkage from built-in moisture content (e.g., exposure to rainwater during the construction phase) is higher than shrinkage that occurs as the wood dries out from its factory moisture content level ($\approx 13\%$) during service life. Several studies have shown that CLT panels are most likely to get soaked during the construction phase without proper weather protection (Kalbe, Kukk, and Kalamees 2020; Liisma et al. 2019; Mjörnell and Olsson 2019a; Niklewski, Fredriksson, and Isaksson 2016; Olsson 2020a; Schmidt et al. 2019) whereas the moisture content of precipitation exposed to CLT elements exceeds 25 % and in some cases even more than 30 % (Kalbe et al. 2020; Liisma et al. 2019).

Airtightness is an important property of a building envelope. Air leakages occur in the building envelope as infiltration and exfiltration, both may cause a significant increase in

total energy consumption. In addition to energy loss, air exfiltration can lead to moisture damage inside the external envelope through moisture convection.

Sufficient airtightness together with the moisture safe construction of CLT buildings are the key factors in terms of safe hygrothermal performance. Mass timber panels as CLT are sensitive to moisture in their hygrothermal performance. Exposure to excess moisture can lead to the growth of mould and rot. Mould is harmful to human health (Caillaud et al. 2018; 2009), and rot damages the mechanical properties of wood (Curling, Clausen, and Winandy 2002). However, it has been argued that no clear indication of the critical moisture conditions for CLT envelopes related to moisture content exists (Olsson 2021).

Several studies have addressed the hygrothermal performance of CLT external envelopes using different wall configurations, evaluation criteria, and methodologies (field measurements vs. simulations). McClung et al. (2014) and Wang and Ge (2016) used both field measurements and stochastic analysis to analyse low and high water vapour permeable wall assemblies with built-in moisture dry-out. Their evaluation is based on a certain level of MC alone, to find out whether the results exceeded 20 % (growth of mould) or < 26 % (growth of decay) without determining actual mould or decay risk. Cho et al. (2019), Yoo et al. (2021), Al-Sayegh (2012), Byttebier (2018), and Kordziel et al. (2020) evaluated the hygrothermal performance of the CLT external envelope only in a stationary situation, without considering any soaking scenarios of CLT. In the studies addressing high CLT moisture content, either the risk of mould growth on the CLT surface is not evaluated or only a single wall assembly is used. Thus, the information on the hygrothermal performance of the CLT external envelope built without proper weather protection where the CLT achieves a high moisture content is scarce. In particular, there is little information on the variations in the performance of different wall assemblies with high initial CLT moisture content. Based on the research topics highlighted, my choice for the PhD thesis was “Hygrothermal Criteria for Design of Cross-Laminated Timber External Walls”.

1.1 Objectives and content of the study

The main objective of this thesis is to determine hygrothermal performance criteria for CLT external wall that are applicable to secure the air-tightness and moisture safety of the building envelope considering the design, production technology and built-in moisture of the CLT panel. To achieve the objectives, the following research questions were set:

- What is the impact of the production technologies on the crack formation and air permeability properties of the CLT panel?
- How does the construction phase and service life conditions affect the air permeability of the CLT external wall?
- How does the initial moisture content of CLT affect the hygrothermal performance of external walls having different drying potential towards indoor?
- What is the impact of different CLT external wall assembly properties on the hygrothermal performance of CLT external walls?
- What are the hygrothermal criteria for the design of CLT external walls?

Responses to the research questions are given in six scientific publications, five of which are journal articles and one is a pre-reviewed conference paper. The first three

publications address research on the air permeability properties of CLT panels and the rest of the three the hygrothermal performance of CLT envelopes.

Crack formation and propagation on the CLT panel surface and its impact on the air permeability properties of the panel are described in PUBLICATION I. The crack formation was examined by means of a climate chamber test in which the CLT panels were surrounded by controlled climatic conditions that favoured shrinkage and swelling of the CLT. The impact of the position and dimensions of cracks on air permeability was studied by two miniature CLT specimens with drilled holes of 2 and 6 mm for crack imitation.

The impact of production technologies such as edge bonding, initial moisture content of lamination (≈ 6 and ≈ 13 %), and the number of lamination layers (3 and 5) on the air-permeability properties of CLT panels were evaluated in PUBLICATION II. Air leakages and crack growth on the surface were measured after the panels were conditioned under the conditions of the seasonal change in indoor humidity regime in cold and humid climates, from RH 75 % to 15 %, imitating the period from summer to winter.

The effect of high initial MC of CLT on the air permeability properties of an external wall compared to indoor RH change, insulation type and façade orientation was investigated in PUBLICATION III. To evaluate the effect, the measured air leakages in the external walls with the factory-dry and soaked (before installation) CLT panels were compared.

The hygrothermal performance of the internally and externally insulated CLT external walls was studied in PUBLICATION IV. A comparison of the mould growth risk on the CLT surface was made between the walls having water vapour-tight and vapour permeable interior insulation layer. Built-in moisture (initial MC) was a factor used for the comparison of the two different interior insulation types to determine the critical MC for both solutions.

Field measurements of temperature and RH between material layers were carried out in different types of highly insulated CLT external walls. The impact of different assemblies (vapour permeable and low permeable insulation and interior layers), façade orientation, and initial MC on the hygrothermal performance of CLT external walls were evaluated and the results were published in PUBLICATION V. Based on the field measurements, the simulation models were created and validated.

Finally, the stochastic analysis was done based on the validated simulation models to provide a more comprehensive overview of the hydrothermal performance of CLT external walls. The limit values as hygrothermal criteria based on the stochastic analysis for the design of CLT external walls in terms of moisture conditions to ensure safe hygrothermal performance were set in PUBLICATION VI. The results can be used for moisture safety planning in large-scale CLT construction.

1.2 Novelty and practical application

The newly acquired knowledge about the air permeability properties and hygrothermal performance of highly insulated CLT external walls discussed in this thesis is as follows:

- The indoor low RH (25 %) during the winter in cold and humid climate content (e.g., Northern Europe) causes a significant crack formation on the CLT surface.
- Seasonal (summer to winter) changes in the indoor climate cause such large cracks on the 3-layer CLT panel surface that the panel alone is not sufficient to function as an airtight layer.
- Built-in moisture in the CLT panels has larger impact weakening the airtightness of the external wall compared to the effect of a seasonal change in indoor RH.

- The risk of mould growth can occur even at 16 % of the initial MC of CLT when the interior insulation is used in the CLT external wall.
- The use of low vapour permeable external insulation can be beneficial against vapour permeable insulation if the factory-dry CLT MC ($\approx 13\%$) is maintained during the construction phase and insulation is installed airtightly.
- Cellulose insulation can be a safer choice when selecting water vapour permeable insulation for the external wall in case the construction is planned without weather protection.
- Hygrothermal criteria for designing moisture safe CLT external walls: the vapour resistance (S_d) of the wind barrier should not exceed 0.03 m; the CLT initial moisture content of the external surface should not exceed 20 % or the vapour resistance (S_d) of additional air and vapour barrier should not exceed 0.25 m if the CLT envelope is not fully weather protected and is externally insulated with vapour open materials; in the case of vapour tight external or internal insulation, the initial moisture content of the CLT surface should not exceed 16 % to prevent mould growth risk.

Practical application of new knowledge:

- Use of production technologies such as edge bonding together with initially drier laminations can avoid large crack growth on the surface of a CLT panel and sufficient airtightness can be achieved by including at least 5 layers of laminations.
- The 5-layer CLT panel can be used as an air-tight layer in external walls as long as its initial low moisture content ($\approx 13\%$) is maintained during the construction phase. The 3-layer CLT panel requires an additional airtight layer.
- In the cold and humid climate conditions, it is recommended to install the CLT panels and cover with the remaining wall layers in spring as the risk of mould growth in spring is the lowest. The greatest risk of mould growth occurs when CLT is covered in late summer (August-September).
- The use of hygrothermal criteria during the design process allows the engineer to develop the moisture safety plan and facilitates the selection of materials to ensure sufficient dry-out capacity of the CLT external walls. The constructor can use the criteria as requirements to manage the construction phase of CLT building in terms of moisture safety.

1.3 Limitations of the work

The air permeability measurements were made only on small scale CLT panels and external walls. However, several studies have indicated that the most problematic locations in terms of built-in moisture are the joint areas (Fedorik and Haapala 2017; Kalbe et al. 2020). Therefore, future research should focus on the air permeability properties of particular CLT external wall joints.

The results of hygrothermal calculations were obtained through simplified 1D calculations. This eliminates small features such as air leakages and rain intrusion. Field measurements of CLT external walls (PUBLICATION V) discovered a small air exchange between the PIR insulation and the CLT panel that significantly decreased the moisture accumulation. Wang and Ge (2016) highlighted the significance of the rain leakage impact on the hygrothermal performance of the CLT external wall during the service life.

Therefore, future studies should use multidimensional calculations to evaluate the impact of additional features such as air and rain leakage on the hygrothermal criteria.

The stochastic analysis (PUBLICATION VI) of this study was limited to CLT external walls with a ventilated façade. External thermal insulation composite system (ETICS) in a timber structure external envelope has not been recommended as a solution because of high risk of moisture damage (Samuels, Mjörnell, and Jansson 2008). On the other hand, it has been considered as a more cost-effective alternative to a ventilated façade as well as a hygrothermally safe solution when using vapour open insulation materials (Günther, Ringhofer, Schickhofer 2016; Kukk, Kers, and Kalamees 2019). Therefore, a future study should further explore ETICS solutions for mass timber structures using stochastic analysis.

2 Design and performance of mass-timber envelopes

2.1 Mass-timber panel as structural element

A CLT panel is a multi-layer wooden composite structure made of strength graded lumber, usually softwood such as spruce (*Picea abies*) and pine (*Pinus sylvestris*), produced of at least three orthogonally bonded layers of laminations, EN 16351 (2015), see Figure 2.1, a. Originally developed in Lausanne and Zurich, Switzerland in the 1990s, modern CLT was developed in 1996 as a joint research effort between industry and academia. Until the early 2000s, advancement was very slow; however, later construction with CLT increased dramatically, mainly by green building movement, also because of better efficiencies and improved marketing (Brandner et al. 2016; Gagnon and Pirvu 2011). The use of CLT has paved the way for the construction of high-rise and large-scale wooden buildings because of its versatility (isotropy) in mechanical properties compared to a traditional timber(-frame) structure (anisotropy) (Van De Kuilen et al. 2011). One of the first wooden high-rise (nine-story) buildings to be built entirely of CLT panels is the Murray Grove building in London, completed in 2009 (Lomholt 2009). Currently, the tallest wooden building is Mjøstårnet, an 18-storey tower in Brumunddal, Norway, built as a combination of mass-timber (including CLT) and timber-frame constructions (Pintos 2019). The construction of CLT buildings in Estonia has also increased over the last decade. The first passive house in Estonia was made of CLT in 2013 (Reinberg et al. 2013). In recent years, several large-scale CLT panels have been built in Estonia as well (Kalbe et al. 2020; Liisma et al. 2019). Figure 2.1, b shows main load-bearing structures of a large-scale building made of CLT panels. In terms of moisture safety, wooden buildings have been the most sensitive objects; large-scale buildings made of mass timber elements require even more attention.

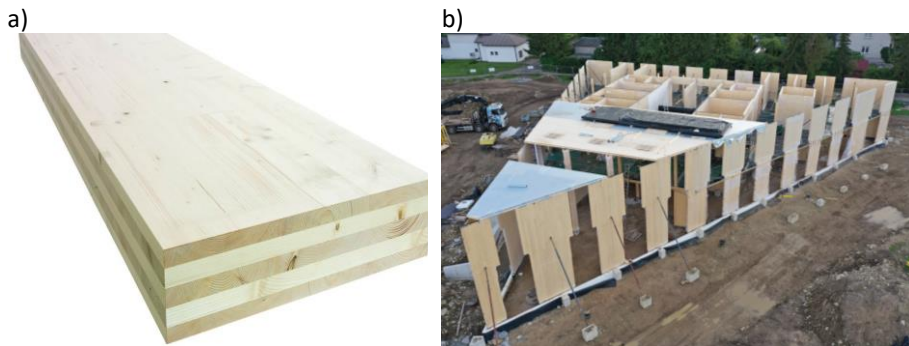


Figure 2.1. An image of a 5-layer CLT panel (a) and a building construction made of CLT panels (b).

2.2 Hygrothermal properties of mass-timber panel

Hygrothermal properties are the basis for designing moisture safe mass timber envelopes. The properties of mass-timber elements, such as CLT, are similar to solid wood. However, certain differences (bonding layer, alternation of longitudinal and transverse directions due to the arrangement of layers of laminations) occur in the properties of mass-timber elements.

The thermal conductivity of wood depends on the direction of the wood grain, being twice lower across the grain than along the grain (Asdrubali et al. 2017). The thermal

conductivity of wood also depends linearly on the moisture content and density, see Figure 2.2 a and can be expressed by Equation (1) (TenWolde, McNatt, and Krahn 1988).

$$\lambda = \rho(a_0 + a_1 \cdot MC) + k_0, \quad (\text{W}/(\text{m} \cdot \text{K})) \quad (1)$$

where λ is the thermal conductivity of wood ($\text{W}/(\text{m}\cdot\text{K})$), ρ is the dry density (kg/m^3), MC is the moisture content in percentage (%), and a_0 , a_1 and k_0 are constants. Measured thermal conductivity of CLT in the laboratory with MC of 11 % were found to range from 0.103-0.106 $\text{W}/(\text{m}\cdot\text{K})$ at 20 °C (AlSayegh 2012; Byttebier 2018). On-site measurements have shown thermal conductivity of $0.111 \pm 0.005 \text{ W}/(\text{m}\cdot\text{K})$ of CLT with MC of 10 % (Flexeder et al. 2021).

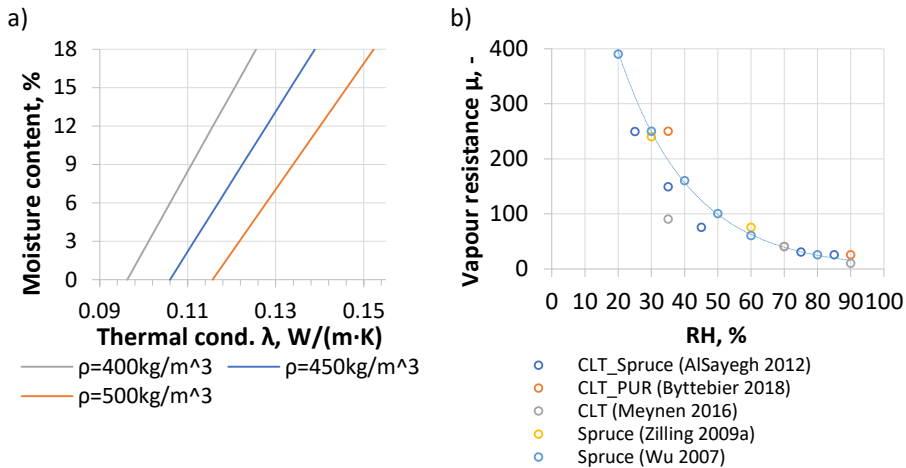


Figure 2.2. Functions of thermal conductivity (a) and vapour diffusion resistance (b) of mass timber across the wood grain.

Most of the laboratory measurements of the water vapour resistance of CLT have been described as an isothermal process where the resistance is inversely proportional to the RH (AlSayegh 2012; Byttebier 2018; Meynen 2016; Wu 2007; Zilling 2009), see Figure 2.2 b. The isothermal water vapour resistance of wood includes a combination of vapour diffusion and liquid conductivity. Vapour diffusion dominates the total moisture transport in the wood up to 60 % RH, from where the conductivity of the liquid is expected to dominate due to capillary condensation (Hagentoft 2001; Vinha et al. 2005).

Wood as hygroscopic material is able to interact moisture from ambient air. This phenomenon is called sorption, which in turn is divided into absorption (absorbing moisture from ambient air) and desorption (losing moisture to ambient air), both strongly depend on RH and temperature of ambient air (Rubin. Shmulsky and Jones 2011). The equilibrium moisture content (EMC) of wood is regulated by sorption through exposure to RH and temperature, see Figure 2.3, b (Absetz 1993; AlSayegh 2012; Time 1998; Tveit 1966). When MC of wood is lower than expected EMC, then wood absorbs moisture from ambient air and vice versa to achieve equilibrium. Although, moisture sorption to an equilibrium is rather rare in wooden construction of building as it is exposed to the rapid environmental climate changes (Time 1998).

Water absorption coefficient, A_w ($\text{kg}/(\text{m}^2\cdot\text{s}^{0.5})$), characterize the liquid water absorption capacity through a material surface (Wang et al. 2021). Water absorption of wood is determined by the direction of the grain. Wood absorbs liquid water around 10 times faster along the grain than across the grain (Rubin. Shmulsky and Jones 2011).

The water absorption coefficient across the grain of the CLT panel is found in the range of 0.0016-0.0028 kg/(m²·s^{0.5}) (AlSayegh 2012; Byttebier 2018; Kordziel et al. 2020; Lipand, Kukk, and Kalamees 2021) and along the grain between 0.0107-0.0163 kg/(m²·s^{0.5}) (AlSayegh 2012; Byttebier 2018). These results are showing that the CLT is significantly more sensitive to wetting from the cut-edges compared to the plane surface.

2.3 Air leakages in mass-timber envelopes

The change of EMC in wood has a major role in crack formation as the wood shrinks and swells below the fibre saturation point (FSP) (Rubin Shmulsky and Jones 2011). The largest shrinkage and swelling in wood occurs tangentially, see Figure 2.3 a. Shrinkage of wood can cause dimensional deformations in timber. In cross-section, shrinkage can change shape of timber board cut-edge depending on the location from which the cutouts of the log were made, see Figure 2.3, c. The same applies to the longitudinal direction of timber board, which may crook, twist, cup, bow and crack due to enviromental changes, Figure 2.3, d. Previous studies have mainly focused on the effect of dimensional deformations in mass timber panels on mechanical properties (Huang et al. 2022; Nairn 2017, 2019; Tuhkanen, Mölder, and Schickhofer 2018) and little information is available on the effect on hygrothermal properties.

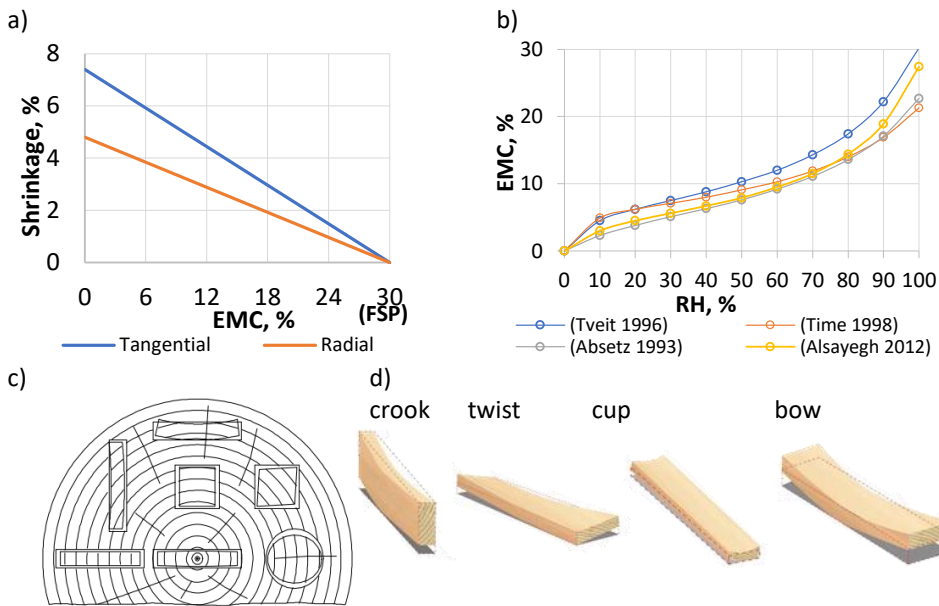


Figure 2.3. Tangential shrinkage (a) and sorption curve of spruce (b) (Rubin. Shmulsky and Jones 2011); dimensional deformations of timber in the cross-section (c) and in longitudinal direction (d) due to shrinkage of wood.

Most common dimensional deformations on the surface of the CLT panel are gaps and cracks between (Figure 2.4, a) and in the middle (Figure 2.4, b) of the laminations (Brandner 2013). The seasonal indoor RH in cold and humid climate can vary from 75 % (in summer) to less than 30 % (in heating period, winter) (Ilomets, Kalamees, and Vinha 2017), which may lead to the EMC change of wood up to 7 %, see Figure 2.3, b. As the edges of laminations in the CLT panel shrink tangentially, the seasonal shrinkage can grow up to 1.7 % when exposed to the indoor environment. In case of built-in moisture,

the shrinkage of laminations in CLT can be even larger. The gaps and cracks have been observed in laminations of CLT in a building envelope. However, it has been stated that the CLT panel is airtight after production (AlSayegh 2012; Byttebier 2018; GUT 2013). Skogstad et al. (2011) from SINTEF (Norwegian independent research organisation) studied the air permeability properties of the CLT panel and its joints (wall, wall to ceiling, wall to wall) and found that the moisture content decrease (caused by a decrease in ambient indoor air RH) from 0.14 to 0.1 kg/kg caused air leakage in CLT joints to increase up to 10 times (mostly in wall to wall connections). They concluded that CLT constructions need to be designed with sealed joints to maintain their airtightness. Janols et al. (2013) measured air leakages in a small 3-layer CLT test building over a six-month period from July (right after the building was installed) to December. The results showed that the CLT building was sufficiently airtight, having maximum air leakage $0.37 \text{ l/m}^2\cdot\text{s}$ at the pressure difference of ΔP 50 Pa (target $< 0.5 \text{ l/m}^2\cdot\text{s}$). However, the results showed considerable effect of seasonal change as the air leakage increased from $0.3 \text{ l/m}^2\cdot\text{s}$ (July) to $0.37 \text{ l/m}^2\cdot\text{s}$ (December).

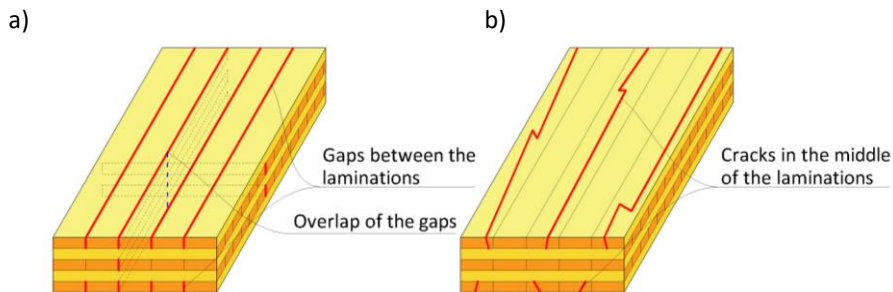


Figure 2.4. Gaps between the laminations, which may develop, overlapping of the gaps (a), and cracks in the middle of the laminations (b) in the top layers of CLT due to swelling and shrinkage of the wood.

Hermes (2020) proposed three main technologies to improve airtightness of CLT envelopes: firstly, using sealing products between CLT elements; secondly, giving an additional cover to the CLT joints with adhesive tape or with bitumen or airtight membrane strips; thirdly, covering the whole envelope with an airtight membrane. The first two technologies are more cost-effective compared to the third and are the most commonly used. The third is the most reliable technology and mostly used if the panel itself is not airtight. For all technologies, it is assumed that the lamination shrinkage of the CLT panel is minimal and is related only to changes in the indoor RH, not to built-in moisture. Hallik and Kalamees (2019) mapped the airtightness of Estonian wooden buildings with a construction year <1945 to 2009+. They concluded that the effect of minimum requirements for energy performance has been significant as the median air leakage (q_{50}) at ΔP 50 Pa decreased from $13.9 \text{ m}^3/\text{h}\cdot\text{m}^2$ (old buildings <1994) to $1.1 \text{ m}^3/\text{h}\cdot\text{m}^2$ (new wooden buildings constructed after 2009). Their study also included a comparison of pre-fabricated and built on-site new timber-frame and traditional mass timber buildings made of logs. They found that pre-fabrication significantly improves airtightness of wooden building, having median air leakage $0.9 \text{ m}^3/\text{h}\cdot\text{m}^2$ (timber-frame buildings) and $1.6 \text{ m}^3/\text{h}\cdot\text{m}^2$ (log buildings) compared to on-site built buildings 3.4 and $3.6 \text{ m}^3/\text{h}\cdot\text{m}^2$ (timber-frame and log buildings respectively). However, the median air leakage of pre-fabricated timber-frame buildings was found considerably smaller than in pre-fabricated mass timber log buildings (0.9 vs $1.6 \text{ m}^3/\text{h}\cdot\text{m}^2$). Eskola et al. (2016) measured

air leakages from Estonian historic residential buildings built between 1650 and 1938, among which most were traditional massive timber buildings made of logs. The study showed that the historic mass timber (log) buildings have large air leakages, average $15.8 \text{ m}^3/\text{h}\cdot\text{m}^2$ (in the range of 4 and $36 \text{ m}^3/\text{h}\cdot\text{m}^2$).

Modern mass timber building made from CLT can level or even improve the airtightness compared with the modern timber-frame buildings. However, more information is needed regarding technologies to be used under different moisture conditions to achieve sufficient airtightness. The moisture conditions can help determine whether only the sealing of the joints is sufficient to achieve airtightness or the entire envelope must be covered with an additional airtight layer.

2.4 Hygrothermal performance of mass-timber envelopes

Timber is one of the main building materials aside to concrete, steel and brick, both today and historically. Due to higher sensitivity to moisture and moisture damages, the hygrothermal performance of timber envelopes has been the centre of focus of many studies (Alev and Kalamees 2016; Arumägi, Pihlak, and Kalamees 2015; Geving, Karagiozis, and Salonvaara 2016; Langmans, Klein, and Roels 2013; Pihelo and Kalamees 2016; Tijskens, Roels, and Janssen 2021; Vinha 2007; Wang and Ge 2018). Most studies on hygrothermal properties have been made on timber-frame building envelopes and historical mass timber envelopes such as log houses. For mass-timber such as CLT envelope, as the newest material compared to the aforementioned, studies are scarce. However, the studies on the hygrothermal performance of CLT envelopes have all used different wall configurations, evaluation criteria, and methodologies (field measurements vs. simulations).

In their in-depth study of the hygrothermal performance of CLT external walls, McClung et al. (2014) and Wang and Ge (2016) used both field measurements and stochastic analysis. They used low and high water vapour permeable wall assemblies for the variables to study the effect of built-in moisture dry-out. They concluded that use of an additional water resistive barrier with low vapour permeability between external insulation and CLT panel can cause higher moisture problems (keeping the MC of CLT surface close to 20 %) when rain leakage should intrude behind the barrier and accumulate on the exterior surface of CLT. Vapour tight barrier in this case would prevent the CLT from drying out. In case of high vapour permeable water resistive barrier, the rain leakage has less significant impact and caused no risk of moisture problems. They also concluded that the hygrothermal properties of CLT have dominant influence on CLT MC when vapour tight barrier is used. When vapour permeable barrier is used, the hygrothermal performance of CLT envelope is dominated by ambient conditions such as air exchange rate in the ventilation gap of façade glazing. Their evaluation was based on the moisture content alone (< 20 % and < 26 %), with mould and decay as the evaluation criteria. Mould, for example, grows on the surface of a material; one of the most common ways to estimate the growth is to use the mould growth index, which is calculated from the relative humidity and temperature near the surface (Viitanen et al. 2011). Therefore, it is not sufficient to determine the MC alone in the risk evaluation of primary moisture damages – mould growth. Cho et al. (2019) studied the hygrothermal performance of CLT external walls with low vapour permeance internal and external insulation systems. Hygrothermal performance was evaluated by the mould growth index using the Korean cold and humid climate. They concluded that using the external insulation system in the CLT external wall gives better long-term dry-out capacity than

using internal insulation. However, they found that all of the wall layers had low mould growth risk with low moisture content CLT panels. Hygrothermal performance of CLT external walls insulated with different insulation materials was studied by Yoo et al. (2021). The results of the research were obtained by simulation with a calculation model in a stationary situation, the properties of the material were found through laboratory tests, and the Korean cold and humid climate data were used for external boundary conditions. They concluded that the application of vapour impermeable XPS and EPS insulation is not sensitive to moisture accumulation between the CLT and insulation in the stationary situation and RH remained stably low, below 60 %, during the simulation period. Using mineral wool, the RH between the insulation and the CLT was higher and fluctuated more significantly than with the use of vapour impermeable insulations XPS and EPS, but still remained below 60 %. It was concluded that water vapour condensation is more likely to occur when mineral wool is used compared with the use of water vapour impermeable insulations. However, both Cho et al. and Yoo et al., they addressed only a stationary situation, without considering any wetting scenarios of CLT; their approach used simulation without validation based on the field or laboratory measurements. Chang et al. (2021) studied the effect of future climate to the hygrothermal performance of CLT modular construction. The modular CLT construction varied from four different types of external insulation: mineral wool, expanded polystyrene, extruded polystyrene and wood-fibre insulation. They concluded first that no long-term moisture problem occurred in the external envelope. However, future climate change predicted the increase of MC of external insulation. The mould growth risk was evaluated by using the critical RH (Viitanen and Ojanen 2007) as a limit value and no exposure time was included. Externally insulated envelopes with XPS were only examples where RH did not exceed the critical limit in the studied locations. This confirms the beneficial of water vapor tight insulation used in the CLT external wall in the stationary situation. However, without consideration of built-in moisture and possible air leakages. Al-Sayegh (2012), Byttebier (2018) and Kordziel et al. (2020) determined the hygrothermal properties of the CLT panel first by laboratory experiments and then used the data to create a simulation model and evaluate the hygrothermal performance in a stationary state.

In summary, previous studies have evaluated the hygrothermal performance of CLT envelopes in the steady state, i.e., only at low initial CLT moisture content. In the studies addressing high CLT moisture content, either the risk of mould growth on the CLT surface is not evaluated or only a single wall assembly is used. Thus, the information on the hygrothermal performance of the CLT external envelope built without proper weather protection where the CLT achieves a high moisture content is scarce. In particular, there is little information on the variations in the performance of different wall assemblies at high initial CLT moisture content.

2.5 Hygrothermal criteria for design of wooden buildings

One of the main concerns about wooden buildings in terms of hygrothermal performance is the durability of wood related to moisture damages. Moisture damage, such as fungi and rot, reduces the durability of wood (Brischke, Welzbacher, and Rapp 2006; Curling et al. 2002), and mould fungi is harmful to human health (WHO 2009; Caillaud et al. 2018). If rot requires a high MC of wood and a humid environment for growth, then the fungi such as mould on the surface of the wood are already formed in a significantly drier environment. The risk of mould growth depends on the combination of RH, temperature, exposure time, material sensitivity, and durability (Viitanen and

Ojanen 2007). Possible risk of mould growth of wood surface can occur from RH of 80 % in the temperature range from 0 °C to 50 °C; detailed relation is shown in Figure 2.5. CLT is produced mainly from spruce and pine, and according to the EN 350 (2016) both species are considered between “Slightly durable” and “Not durable” in the durability classification, which means that both are sensitive to attack by decay fungi. According to the EN 335 (2013), the development of fungi starts from wood MC of $\geq 20\%$. Wood-rotting fungi starts to grow from $\geq 25\%$ of MC (Schmidt 2010).

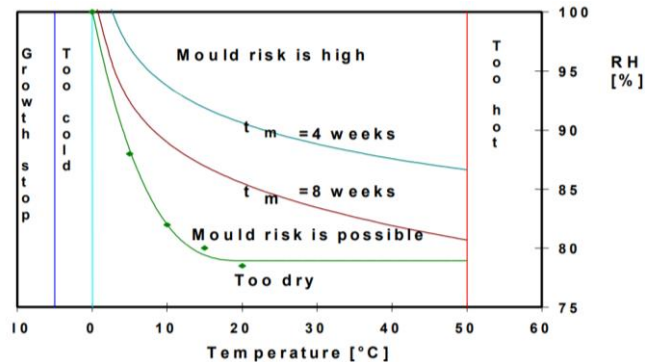


Figure 2.5. Favourable environmental conditions for mould growth on the wood surface (Viitanen and Ojanen 2007).

Risk of mould growth and moisture condensation are two main evaluation criteria for wooden buildings (Vinha 2007). Juha Vinha (2007) has evaluated the hygrothermal performance of timber frame external walls and found criteria for vapour resistance of the interior vapour barriers. He concluded that at least $\frac{3}{4}$ of the thermal insulation should be outside the vapour barrier, and the plastic vapour barrier (vapour impermeable) should be used as the interior layer when vapour resistance of wind barrier is more than >500 s/m in cold and humid climate. The minimum ratio of vapour resistance of vapour and wind barrier should be up to 80:1, and in case of highly vapour permeable wind barrier, the minimum ratio is up to 40:1. Alev and Kalamees (2016) set hygrothermal criteria for interiorly insulated traditional mass-timber envelopes made of logs in cold and humid climate. They concluded that the maximum thermal resistance of interior insulation should not be more than the resistance of the external wall before interior insulation. The vapour resistance (S_d) of the vapour barrier should not be less than 2 m and initial MC of logs; before the installation of interior insulation, it should not exceed 12 % to avoid mould growth risk on logs surface.

Given the complexity of large-scale buildings made of CLT, CLT structures get soaked during construction if full weather protection is not implemented (Kalbe et al. 2020; Liisma et al. 2019; Mjörnell and Olsson 2019b; Niklewski et al. 2016; Olsson 2020b; Wang, Wang, and Ge 2020). Most critical locations are structural joints where water is absorbed at the longitudinal fibre direction from the cut-edge of the panel, and the moisture content (MC) can increase up to 30 % (Kalbe et al. 2020). However, it has been argued that no clear indication of the critical moisture conditions for CLT envelopes related to the moisture content exist (Olsson 2021). There is a gap in research that would clearly determine the hygrothermal criteria for designing CLT external walls. Criteria considering the dry-out of the initial MC of the CLT panels, the water vapor resistance of an additional air and vapour barrier, the effect of interior insulation and the dry-out capacity of the wall assembly should be established.

3 Materials and methods

The present thesis includes measurements with small- and large-scale (0.1 × 0.1 m and 0.4 × 1.4 m) CLT specimens to determine material properties such as water vapour resistance and air permeability; measurements with small scale (0.9 × 0.9 m) CLT external test walls do determine hygrothermal behaviour; modelling and validation of simulation models based on the measurement results; and data analysis to determine hygrothermal performance and criteria of design of CLT external walls. The following chapter describes in detail the materials and methods used in this thesis.

3.1 Measurements

3.1.1 Measurement devices

3.1.1.1 Determination of moisture content in wood

The MC of wood was measured according to the EN 13183-2 (2002) by the electrical resistance method. Measurements were done by an electronic wood moisture meter GANN Hydromette H35 together with the ram-in electrode and electrode pins with Teflon insulation 45-60 mm long. Teflon insulated pins provided MC measurements at different depths in wood. The measuring range of GANN Hydromette H35 was 4 to 30 % of dry mass. The accuracy of the device was controlled with the Test Adapter, which has a fixed electrical resistance.

3.1.1.2 Determination of cracks formation

Cracks width and length were measured by using a ruler and a crack width gauge on the external surface of each panel that was exposed to the set environment in the climate chamber, the methodology developed by Brischke and Humar (2014).

3.1.1.3 Determination of air permeability

The air leakages were measured and equipment was selected according to the EN 12114 (2000) standard. The equipment used for the air leakage measurements consisted of the following: air flow meter with integrated flow adjustment valve SMC_PFM 710 (flow rate range 0.2-10 l/min; minimum unit setting 0.01 l/min; repeatability ±1 %); manometer for measuring air pressure difference Huba Control 699 (Pressure range 0-1600 Pa; tolerance 0.7 %).

3.1.1.4 Determination of temperature and RH in external test walls

The temperature and RH (t &RH) were measured between the material layers in the CLT external test walls with the following sensors:

- **t &RH** – Omnisense A-1 Temperature and Humidity sensors with an accuracy of ±0.3 °C from 0 ° to 60 °C (temp. sensor) and ±2.0 % from 0 % to 100 % (RH sensor). (Climate chamber test and measurements in test facility);
- **Surface temperature, t_s** – Hobo UX120-006M logger together with TMC6-HD/E sensors with an accuracy of ±0.25°C from 0 ° to 50 °C (Climate chamber test); Uniflex t_s sensor, accuracy ±0.5 °C from -10 to 85 °C (measurements in test facility).

3.1.2 Material properties

3.1.2.1 Cracks formation

The impact of low indoor RH during winter in cold and humid climate on the crack formation on the CLT panel surfaces was determined by using four specimens (S1-S4) of 95 mm thick five-layer CLT panels (layer thickness 19 mm), made of spruce (*Picea abies*) with side dimensions of 470 x 500 mm. First two panels (S1 and S2) were pre-stored before testing for about two weeks at 15 °C and a relative humidity (RH) of 40 %, simulating the environment of an indoor storage room, see Table 3.1. Measured MC on the surface of these panels was 11 %, the methodology described in section 3.1.1.1. The rest of the two panels (S3 and S4) were pre-stored for a week before testing at 10 °C and a RH of 95 % (Table 3.1), simulating an outdoor storage environment during the autumn season. Measured MC on the surface of these panels was 17 % and 18 % respectively. Panel edges were given two coats of polyurethane acrylic paint to avoid moisture dry-out from the cut edge (towards longitudinal fibre direction). The CLT panels were placed into a climate chamber (ILKA PTK-3018) doorway for 92 days, see Figure 3.1. The CLT panels in the test wall were separated with mineral wool and vapour barrier tape (Gerband 586, 50 mm wide) to prevent any major air leakages. The RH of 25 % was selected for the indoor environment in the climate chamber at 20 °C, which can occur indoors in the cold and humid climate during the winter heating period. Cracks width and length were measured on the external surface of each panel that was exposed to the simulated environment in the climate chamber, the methodology described in section 3.1.1.2. No other sides of the panels were considered.

Table 3.1. CLT specimens pre-conditioned in climate chamber.

CLT specimen	Pre-conditioning	Initial surface MC
S1 S2	at 40 % RH and 15°C	≈17 %
S3 S4	at 95 % RH and 10°C	≈12 %



Figure 3.1. CLT specimens placed inside the climate chamber ILKA PTK-3018 doorway.

The impact of seasonal change in indoor RH during the period from summer to winter on the crack formation on the CLT panel surfaces was determined using large-scale CLT specimens produced with three different technologies; parameters are given in Table 3.2. The selection of the parameters of the production technologies (number of layers, edge bonding and initial MC of laminations) was determined by their direct impact on the panel air permeability. Three specimens were made for each technology combination. Accordingly, 24 specimens of rectangular-shaped cross-laminated timber panels constructed from spruce wood (*Picea abies*), with dimensions of 1.4 x 0.4 m (0.56 m²) and thickness of 30 mm, were designed and produced for the air permeability and crack evaluation test (Figure 3.2, a). A small part of the flat sides of the panels was covered with adhesive tape and mastic and therefore the measurement area of each specimen for the air permeability test was considered as 0.52 m² (1.375 x 0.375 m). Layer thickness of the 3-layer panels was 10 mm and 6 mm of the 5-layer panels. The initial MC of 13 % represented the common moisture level of laminations in the production of the CLT panels. The initial MC of 6 % represented the minimum moisture level of laminations that is required for bonding with moisture curing one-component polyurethane adhesive, which was used in the production of the CLT specimens.

Table 3.2. Parameters and ID of CLT specimens produced with different technologies.

Edge bonding	Number of layers and initial MC of laminations			
	3-layer panel, thickness of one layer 10 mm		5-layer panel, thickness of one layer 6 mm	
Edge bonded panels	13BE3L Init. MC ≈13 %	6BE3L Init. MC ≈6 %	13BE5L Init. MC ≈13 %	6BE5L Init. MC ≈6 %
Panels without edge bonding	13WBE3L Init. MC ≈13 %	6WBE3L Init. MC ≈6 %	13WBE5L Init. MC ≈13 %	6WBE5L Init. MC ≈6 %

Specimens were marked as follows: 6/13 W/BE 3/5L, where 6/13 defines panel's initial MC of laminations (MC of 6 % and MC of 13 %); WBE- without bonded edge panels and BE- with bonded edge panels; 3/5L- panels with 3 or 5 layers. When panels are marked without "6/13", then the specimens are separately divided by the initial MC of laminations.

The laboratory test process consisted of four steps of specimen conditioning in environments with different RH supplied by a climate chamber (Figure 3.2, a). Before and after each conditioning step, the three following parameters were measured and recorded during a laboratory test: MC of panels, crack area on panel's top surfaces and air permeability. Conditioning steps started from RH of 75 % and continued with RH of 43, 30 and 15 %, representing the typical decrease of RH in an indoor environment during the period from summer to winter in the Nordic climate (Ilomets et al. 2017). The minimum duration of each conditioning step was 30 days, which was calculated to be sufficient for the specimens to attain equilibrium moisture content (EMC). The minimum duration time for conditioning was calculated with hygrothermal software WUFI 6; the simulation results are shown in Figure 3.3. The temperature was at a constant 20 °C during the simulation, initial state for conditioning at 75 % RH was a selected EMC of 18 % (represents the EMC at RH of 90 % at 20 °C). Each conditioning at RH of 75, 43, 30, and 15 % was done several times at various time periods until 30 days was found to be sufficient minimum time to attain EMC for a 30-mm thick CLT panel made from spruce.

As shown in Figure 3.4, at 20 °C, the average EMC after conditioning in RH of 75 % was 13.2 % over all specimens, which was close to the expected EMC of about 14 %. After conditioning in RH of 43 %, the average EMC was 9.3 % (expected EMC of about 8.5 %), decrease in EMC was $\Delta\text{EMC} = -3.9\%$ in RH change from 75 % to 43 %. After conditioning at RH of 30 %, the average EMC was 7.4 % (expected EMC of about 6.5 %) and decrease in EMC was $\Delta\text{EMC} = -1.9\%$ in RH change from 43 to 30 %. After the final conditioning step (RH 15 %), the average EMC was 5.4 % (expected EMC of about 4.7 %) and the decrease in EMC was $\Delta\text{EMC} = -2\%$ in RH change from 30 to 15 %. Total EMC loss after the final conditioning step (RH change from 75 % to 15 %) was $\Delta\text{EMC} = -7.8\%$ over all specimens. The expected result of EMC after each conditioning step in different RH was close in all specimens compared with the reference values (Rubin, Shmulsky and Jones 2011).

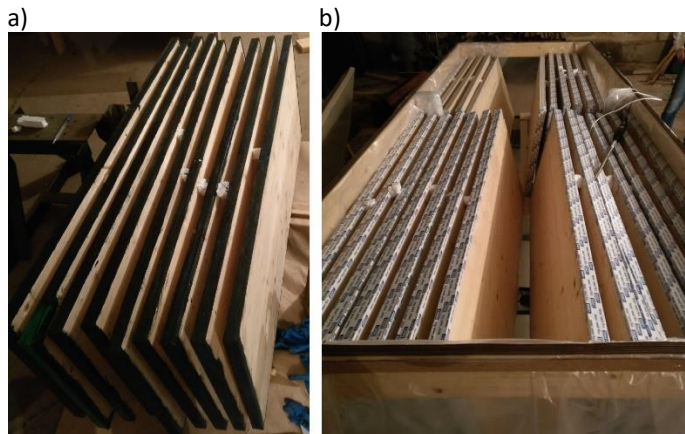


Figure 3.2. CLT specimens (Table 3.2) with coated edges (a) and conditioning in the climate chamber (b).

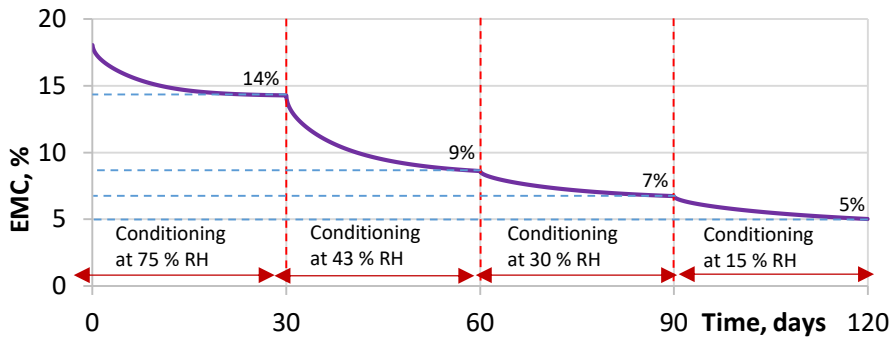


Figure 3.3. WUFI hygrothermal simulation of EMC (%) at 20 °C of a 30-mm thick CLT panel made from spruce at different RH conditions in a 30-day interval.

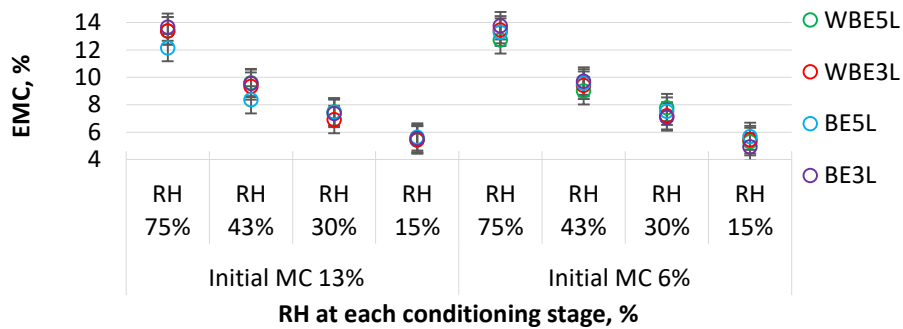


Figure 3.4 EMC of CLT specimens (Table 3.2) after each conditioning step.

Average MC of each specimen was calculated from the three measurements taken from different locations in one panel, the methodology described in section 3.1.1.1. Cracks were measured from both flat sides of the panel and total crack area was summed for each specimen, the methodology described in section 3.1.1.2. Cracks were defined as gaps between the laminations (Figure 2.4, a) and cracks in the middle of the lamination (Figure 2.4, b). Gaps between the laminations develop due to shrinkage of the edges of the wooden boards. Cracks appearing in the middle of the lamination (board) are expected to occur in edge bonded panels. The rigid bond connection between the edges of the boards causes internal stresses over the cross-section of the board during shrinkage and, as a consequence, cracks can form in the middle of board top surface (Brandner, 2013). Regarding airtightness of the CLT panel, the worst resulting scenario in crack development is when gaps or cracks will overlap through all layers, thereby creating a hole through the entire thickness of the panel (Figure 2.4, a). It is most likely that the overlapping will happen with gaps between the layers in three- (3-) layer panels. For three- (3-) layer panels, if gaps in the outer layers occur in alignment (a gap appears in the same line in the top and bottom layers), then the appearance of a single gap in the middle layer is enough to result in an overlapping of gaps through the entire panel.

3.1.2.2 Vapour permeability

The impact of the crack size on water vapour transmission in CLT was studied by measuring vapour permeability according to ISO 12572 (2016) standard. Vapour permeability of small-scale CLT specimens was measured by the dry cup test method. Four types of square shape specimens (CS1-CS4), 5 specimens for each type, a total of 20 specimens were used for carrying out the test, see Table 3.3. Specimens were made from planed timber laminations of spruce (*Picea abies*) with a length of 110 mm. The first two types were made for reference measurements: first type was a 6-mm thick one-layer timber lamination (solid timber board), the second was a 12-mm thick 2-layer glued laminated panel. Type 3 and 4 specimens were 2-layer glued laminated panels having a drilled hole in the middle of the specimen, with a diameter of 2 and 6 mm respectively. Drilled holes were made to imitate the cracks in the CLT panel, the 2-mm hole imitated the crack with the width of 2 mm, and 6 mm was selected as maximum allowed gap between laminations according to the EN 16351 (2015). The specimens were placed and sealed in the test cup filled with desiccant of CaCl₂ (particle size < 3 mm), which created near 0 % RH inside the cup, see Figure 3.5 a. During the measurements, the test cup was placed in the climate chamber with the surrounding conditions

of 23 °C ±0.5 °C and RH 50 %, see Figure 3.5 b. Final results were taken when the five last weightings showed a constant value in mass change.

Table 3.3. Small-scale (100 × 100 mm) CLT test specimen types.

Specimen type ID	Number and thickness of laminations	Hole drilled through specimen
CS1	1×6 mm	-
CS2	2×6 mm	-
CS3	2×6 mm	∅ = 2 mm
CS4	2×6 mm	∅ = 6 mm

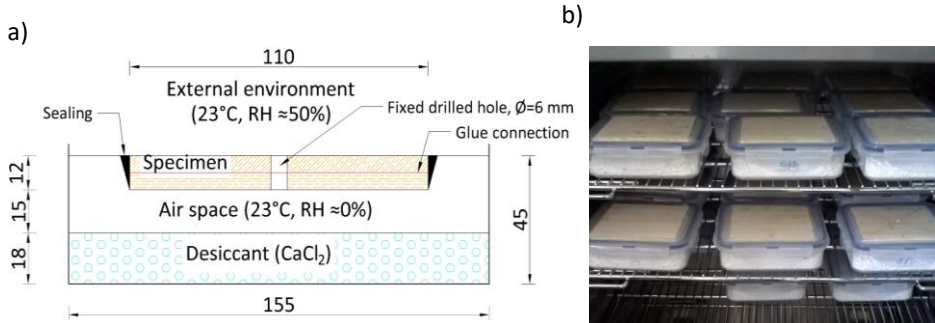


Figure 3.5. Test cup scheme to measure the water vapour transmission of planed and glued solid wood panel with a 6-mm diameter hole in the middle (a); and test cups placed into the climate chamber (b).

3.1.2.3 Air permeability

The air permeability was measured from both small- (from vapour permeability test) and large-scale (crack formation during seasonal change of indoor RH) CLT specimens. Air permeability measurements of the CLT specimens were carried out under laboratory conditions in accordance with the EN 12114 (2000) standard.

Small-scale specimens (CS1-CS4) were used to study the impact of cracks size on the air permeability of CLT and large-scale specimens (13BE3L-6WBE5L) and the effect of seasonal indoor RH change. The small-scale CLT specimens were placed into 0.4 x 0.4 m hermetic test rig made from stainless steel and were sealed with ethylene propylene diene monomer (EPDM) rubber (Figure 3.6, a, b). The large-scale CLT panels were placed into 0.46 x 1.46 m hermetic test rig made from powder coated steel and were sealed with EPDM rubber as well (Figure 3.6, c, d). A detailed description of the measurement equipment is given in section 3.1.1.3. To avoid any air leakages between the connection of the test rig and specimens, all large-scale CLT specimen edges were coated with airtight liquid mastic and sealed with vapour and airtight adhesive tape (Figure 3.2).

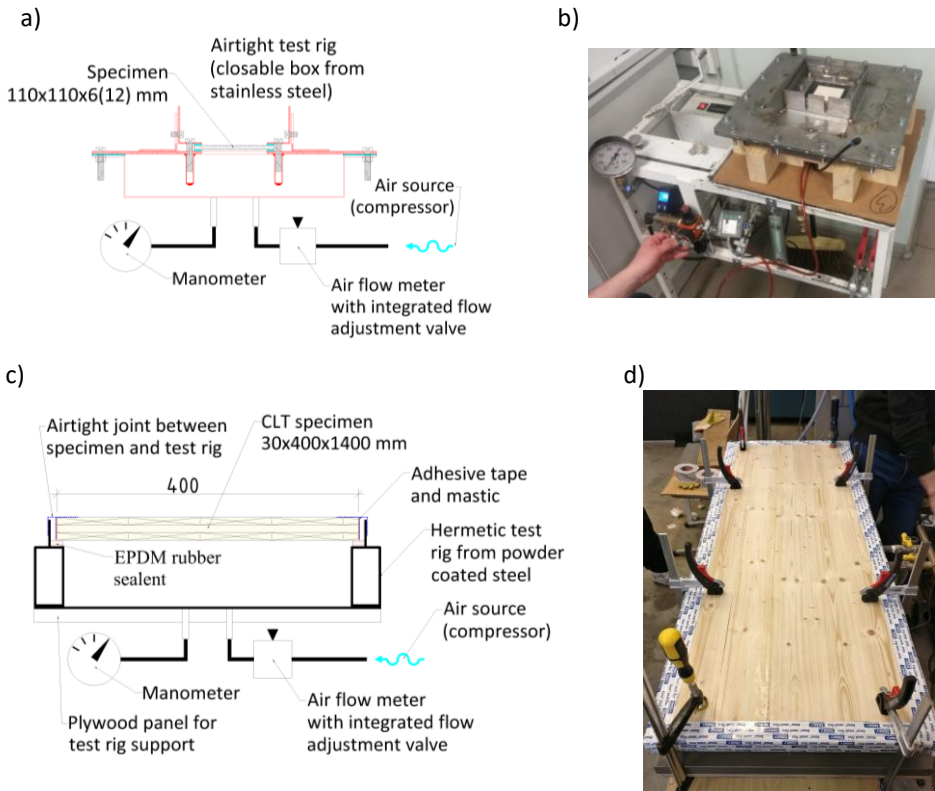


Figure 3.6. Complex scheme of equipment for the air permeability test (a, c); and small- (b) and large- (d) scale CLT specimen attached and sealed to a hermetic test rig.

Air leakage was measured only with positive pressure and the maximum (ΔP_{\max}), and minimum (ΔP_{\min}) pressure differences were selected to be 500 Pa and 50 Pa. The measurements were carried out in two stages. In the first stage, the leakage was measured by applying three overpressure impulses at a pressure difference of 550 Pa (each impulse was created with the pressure difference 10 % greater than ΔP_{\max}). In the second stage, the measurements were carried out at seven measuring points distributed in a geometric series of logarithmically growing pressure differences between, including ΔP_{\min} and ΔP_{\max} . Pressure difference in each measuring point was calculated by Equation (2) in accordance with the EN 12114 (2000) standard: $\Delta P_1 = 50$ Pa, $\Delta P_2 = 73$ Pa, $\Delta P_3 = 108$ Pa, $\Delta P_4 = 158$ Pa, $\Delta P_5 = 232$ Pa, $\Delta P_6 = 341$ Pa and $\Delta P_7 = 500$ Pa. Each applied pressure difference, in both the first and the second stage, was held at least three seconds.

$$\Delta P_i = 10^{i \frac{\log \Delta P_{\max} - \log \Delta P_{\min}}{N} + \log \Delta P_{\min}}, (\text{Pa}) \quad (2)$$

where ΔP_i (Pa) is the pressure difference in each measuring point and N – total number of measuring points.

Measurements at different measuring points show the relation between the airflow (air leakage) and the pressure difference, which is characterised by the power function Equation (3) in accordance with the EN 12114 (2000) standard:

$$\dot{V} = C \cdot \Delta P^n, (\text{m}^3/\text{h}) \quad (3)$$

where \dot{V} (m^3/h) is the air flow rate, ΔP (Pa) is the pressure difference, C ($\text{m}^3/\text{h}\cdot\text{Pa}^n$) is the flow coefficient and n [-] is the flow exponent.

3.1.3 Hygrothermal performance of CLT external walls in the climate chamber test

The hygrothermal performance of CLT external walls was first evaluated by the climate chamber test with controlled climatic boundary conditions. Four CLT external test walls (Figure 3.7) with side dimensions of 0.79 m × 0.86 m were constructed using five-layer (5 × 20 mm) CLT panels with a thickness of 100 mm (Figure 3.7, a, c). Two levels for the target initial MC in CLT panels were selected: 13 % and 20 %. The measured initial MC varied from the target: two of the walls had CLT panels with the initial MC of 12 % and the rest of the two respectively had initial MC of 19 % and 21 %, the method is described in section 3.1.1.1. The higher initial MC was gained by soaking the CLT panels in a pool filled with water and the MC was measured by weighing the panels at fixed intervals. Weighing was continued until the calculated weight corresponding to the desired MC was achieved. During the four weeks of soaking only the top layers of CLT panels achieved desired high initial MC and the middle layers retained the initial MC. Later, in the simulations, the high initial MC only in the top layers was considered as well. The higher initial MC in a CLT panel represents the situation where the CLT has been exposed to excess water (rainwater, water leakages, melting snow) during the construction without proper weather protection.

CLT external test walls were designed with two different insulation solutions, using both interior and exterior insulation. External insulation in all test walls was 200 mm thick mineral wool covered with a 30-mm thick mineral wool wind barrier. Two different types of interior insulation were used: two of the test walls were internally insulated with 30 mm thick polyisocyanurate (PIR) insulation covered from both sides with aluminum foil ($S_d > 800$ m), which was considered as a vapour impermeable layer and the dry-out of CLT would be in one direction only (towards to outdoor). The rest of the two test wall was internally insulated with mineral wool insulation, which had a layer with variable vapour diffusion resistance depending on the relative humidity ($S_d \approx 13$ m @ RH 20 % and $S_d \approx 0.5$ m @ RH 80 %). The dry-out of CLT in the second solution is towards both indoor and outdoor. The interior insulation was covered with a gypsum board in all test walls. The edges of all test walls and CLT panels were covered with 18-mm thick film faced plywood boards ($Z_{RH90\%} = 1.14 \cdot 10^{10}$ $\text{m}^2\text{sPa}/\text{kg}$) and sealed with polyurethane foam and airtight adhesive tape to minimize two-dimensional moisture movement through the wall. The purpose of using a tape and polyurethane foam for sealing was to create an airtight connection between the CLT and the film faced plywood to prevent any convective moisture movement. Also, the narrow edges of the CLT panels were covered with a moisture and air barrier liquid mastic ($Z_p = 3.92 \cdot 10^{11}$ $\text{m}^2\text{sPa}/\text{kg}$) for the same reason as the adhesive tape was used. Test walls were marked as: 13/20 depending on the initial MC and PIR/MW depending on the interior insulation material (PIR board or mineral wool (MW)). The calculated thermal transmittance of all test walls was the same, $U=0.12$ $\text{W}/(\text{m}^2\cdot\text{K})$.

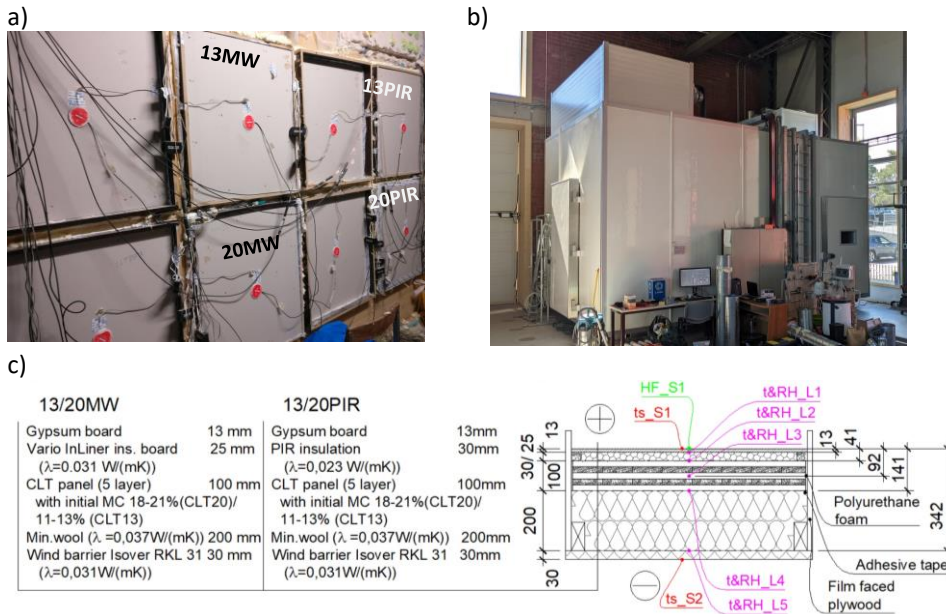


Figure 3.7. Interior view of the test walls (a) and cross-section of a climatic chambers (b); material layer lists of the test walls and placement of measuring sensors in the wall section (c).

The temperature (t) and RH were measured between the material layers in the test walls; locations are shown in Figure 3.7, c. A detailed description of the measuring sensors is given in section 3.1.1.4. Sensors were marked as follows: $t\&RH/ts_L/S1$, where $t\&RH/ts$ defines the measured quantity ($t\&RH$ – temperature and RH, ts – surface temperature) and $L/S1$ shows the location of the sensor ($L1, 2, 3...$ – Location 1, 2, 3...; $S1$ – internal surface, $S2$ – external surface).

Test walls were built in a large-scale climate chamber where it was possible to create controlled indoor and outdoor climatic conditions on both sides of the test walls, see Figure 3.7, b. The total test duration in the climate chamber was 86 days and during the experiment, Northern European climate conditions from autumn to spring were applied (Kalamees and Vinha 2003), as seen in Figure 3.8. The duration of autumn conditions ($RH_i \approx 50\%$, $RH_e \approx 80\%$, $t_i \approx +21\text{ }^\circ\text{C}$ and $t_e \approx +10\text{ }^\circ\text{C}$, $\Delta v \approx 1.6\text{ g/m}^3$) was 40 days, which was the longest period. The 40 days were selected with the consideration that within that time the top layers (20 mm thick) of CLT will dry out and achieve EMC, according to Figure 3.3. The winter conditions ($RH_i \approx 35\%$, $RH_e \approx 80\%$, $t_i \approx +21\text{ }^\circ\text{C}$ and $t_e \approx -10\text{ }^\circ\text{C}$, $\Delta v \approx 4.5\text{ g/m}^3$) together with a transition period (5 days) was 26 days, and spring conditions ($RH_i \approx 50\%$, $RH_e \approx 45\%$ to 70% in one cycle per day, $t_i \approx +21\text{ }^\circ\text{C}$ and $t_e \approx 0\text{ }^\circ\text{C}$ to $+15\text{ }^\circ\text{C}$ in one cycle per day, $\Delta v \approx 7$ to 0.18 g/m^3 in one cycle per day) was 20 days (including a transition period of 3 days). The test duration was shortened to 86 days compared to the usual 9 months with three seasons due to practical reasons and time limitations. The fluctuations in cycle per day of outdoor temperature and RH in spring conditions were applied for simulating the effect of solar radiation. It was considered equivalent to temperature change in the outdoor environment in springtime due to solar radiation during a one-day cycle in general. The outdoor temperature increase during daytime and the decrease in the night was according to the exposure of the sun in general. The average change of the outdoor temperature was calculated using the climate data from March to May of the Estonian

moisture reference year (Kalamees and Vinha 2004). Outdoor climatic boundary conditions were considered to be the environment in the ventilation gap between the wind barrier and the external façade, and therefore any additional weather phenomena (e.g., rain load) were not applied. For that reason, an external façade was not added to the test walls. Large peaks between days 49 and 56 appeared because of technical reasons with the climate chamber. The climate chamber was switched off due to a malfunction for six (6) days, and therefore the temperature increased and the RH decreased inside the chamber.

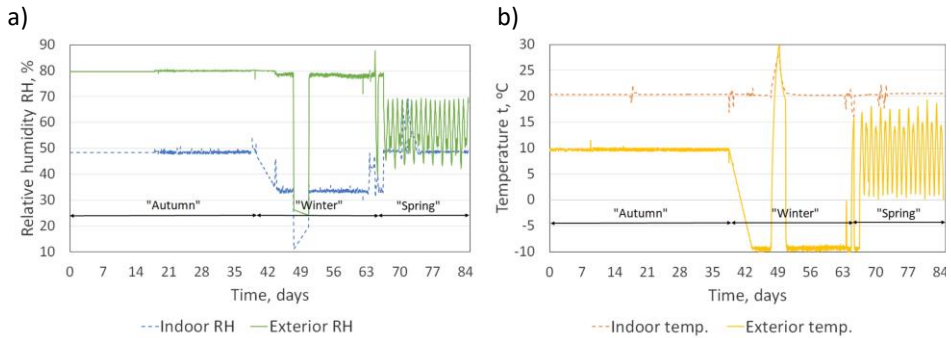


Figure 3.8. Indoor and outdoor climatic boundary conditions in climate chamber: relative humidity (a) and temperature (b).

3.1.4 Hygrothermal performance and air leakages of CLT external walls exposed to real outdoor conditions

3.1.4.1 The test setup

In addition to the climate chamber test, the air permeability properties and hygrothermal performance of the CLT external walls were also evaluated in real climate conditions. For this purpose, field measurements were performed where the CLT external test walls were placed in a test facility to function as a real external wall and be exposure to real outdoor conditions. Five CLT external wall types (EW 1-5) with side dimensions 850 x 850 mm were designed to study the hygrothermal performance, see Figure 3.9. For each wall type, four test walls were prefabricated in the laboratory (a total of 20 test walls) and installed as part of the external wall into the nZEB technological test facility on TalTech campus, Tallinn, Estonia, see Figure 3.10. Half of the test walls from each type were facing north, and the other half were facing south (marked EW nn N/S). The test walls were also divided by the initial moisture content (MC) of the CLT. Half of the test walls were with the CLT surface MC of 26 % and marked as EW n1; and the other half were manufactured with factory-dry CLT, MC up to 13 % and marked as EW n2. Higher CLT surface MC was achieved by soaking the panels in a water-filled pool for 24 days. To prevent both large water absorption along the wood grain (longitudinal direction) during soaking and rapid dry-out of the cut-edges of the CLT panel during the test, the narrow CLT edges (cut-edges) were painted with a waterproof polymer-based mastic. The high MC of the soaked CLT was measured by two methods. During soaking, the MC was determined by weighing. The aim was to achieve an MC of 25 % by weight. The panels were then kept outdoors for one week for conditioning; later, before the panels were used to prefabricate the test walls, the surface moisture content was measured by the electrical resistance method using electrodes (pins). The surface MC

varied between 24 and 27 % in different panels and the MC also varied in the surface area. Therefore, in another study, the moisture distribution in the CLT panel was determined when the panel surface was placed in contact with water (Lipand et al. 2021). According to the panel surface, the surface high MC depth of 30 mm was later selected when creating the simulation model.

All external wall types were designed with a 5-layer 100 mm thick (layer thickness 20 mm) CLT panel (produced from Norway spruce, *Picea abies*), ventilated (ventilation gap 28 mm) wooden cladding (22 mm) façade, and a mineral wool wind barrier (30 mm). Three (EW 1-3) of the five test wall types were insulated with different insulation materials and the CLT was exposed to the indoor environment, see Figure 3.9 a, b, c. In the other two wall types (EW 4-5), the CLT was covered with different interior layers and insulated with water vapour permeable mineral wool, see Figure 3.9 d, e. Test wall type 1 (EW 1) was insulated with 300 mm thick glass wool insulation ($\lambda = 0.037 \text{ W}/(\text{m}\cdot\text{K})$), type 2 (EW 2) with 330 mm thick cellulose insulation ($\lambda = 0.041 \text{ W}/(\text{m}\cdot\text{K})$), and type 3 with 200 mm thick polyisocyanurate (PIR) ($\lambda = 0.022 \text{ W}/(\text{m}\cdot\text{K})$). Mineral wool (glass wool in this study) was selected for insulation because it is the most common type of insulation used in the production of prefabricated wooden buildings. Cellulose insulation was selected because it provides the benefit of moisture buffering effect that can smoothen down the humidity peak levels and dynamics of the indoor air and prevents mould growth better than non-hygroscopic insulations (such as mineral wool) (Ojanen and Laaksonen 2016; Pihelo, Kikkas, and Kalamees 2016). PIR insulation has been used most frequently in the prefabrication industry due to its very low thermal conductivity, which allows significant reduction of the wall thickness while still achieving very low thermal transmittance. Thermal transmittance was designed to be the same for all wall types ($U = 0.1 \text{ W}/(\text{m}^2\cdot\text{K})$); therefore, thickness of the insulation varied. Thermal transmittance of each wall type was calculated at 13 % CLT MC, and in the oven-dry state (0 % of MC) of the remaining materials according to the standard EN ISO 6946:2017 by Equation (4).

$$U = \frac{1}{R_{si} + R_1 + R_2 + \dots + R_n + R_{se}}, \quad \text{W}/(\text{m}^2 \cdot \text{K}) \quad (4)$$

where U ($\text{W}/(\text{m}^2\cdot\text{K})$) is thermal transmittance of the external wall and R_T is total thermal resistance of the external wall, which was found by summing the resistance of the interior (R_{si}) and exterior (R_{se}) surface and the resistance of each wall material layer ($R_1, R_2, \dots R_n$). The resistances of the material layers were calculated according to the thermal conductivity given by the manufacturers.

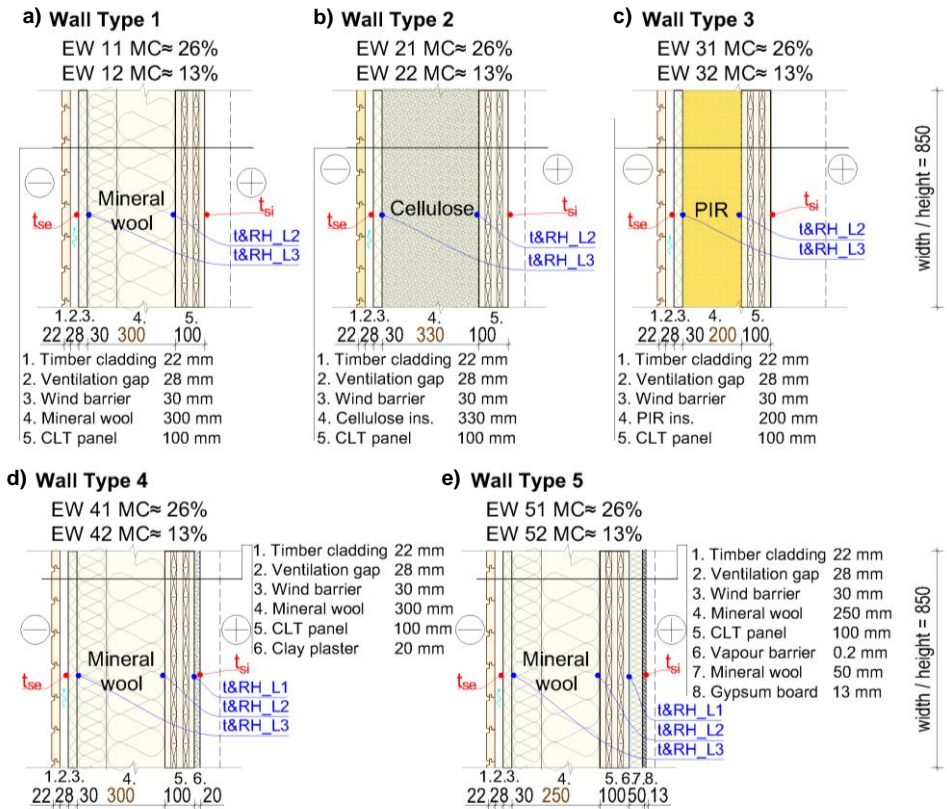


Figure 3.9. Cross-sections of CLT external test wall types.

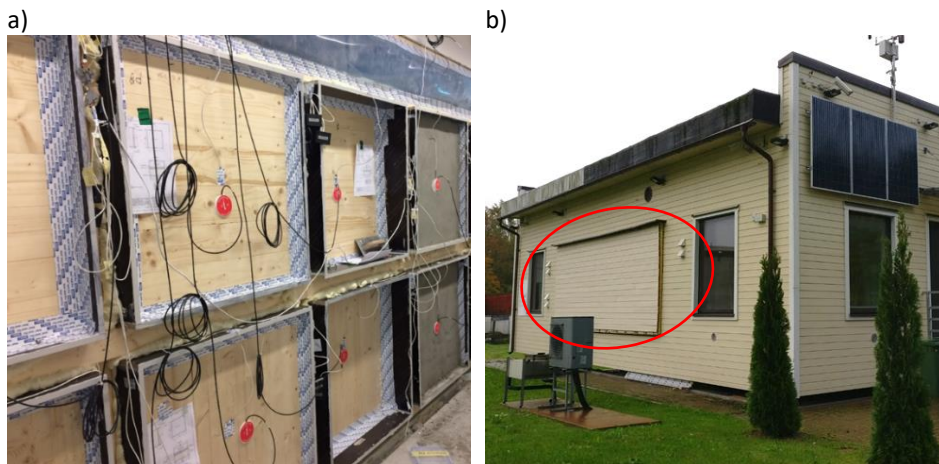


Figure 3.10. Test walls installed as part of the external wall of the TalTech nZEB test facility, interior view (a) and exterior view (b, marked with a red circle).

3.1.4.2 Air leakages in external test walls

During the field measurements, the air permeability of CLT external test walls was measured first. Air permeability was measured only in the external test walls where the CLT internal surface was exposed to the indoor environment (EW1-3) to exclude the effect of interior layer and to evaluate the effect of indoor RH change, see Figure 3.11 and Figure 3.9. The measurements were carried out in accordance with EN 12114 (2000) under real climate conditions. An airtight chamber was installed into the external wall. The airtight chamber was made of 18-mm thick film plywood and it was exposed to both the indoor and outdoor climate. Measurement equipment consisted of a hermetic test rig made with flat stainless steel and plywood board, which was used to cover the test wall and sealed with EPDM rubber, see Figure 3.12, a, b. A detailed description of the measurement equipment is given in section 3.1.1.3.

To ensure the airtightness of the connection between the CLT panel and the plywood airtight chamber, one of the sealing methods mentioned in the introduction was used, according to which the connection was sealed with an adhesive tape. Figure 3.10, a, shows that the tape was applied to the corners of the connection on both sides of the CLT, as well as to the corners of the plywood chamber to prevent any possible air leakage locations between the plywood and the CLT. In addition, the joint between the CLT and the plywood was filled with polyurethane foam in the thickness of the panel to ensure the rigidity of the CLT in the plywood chamber.

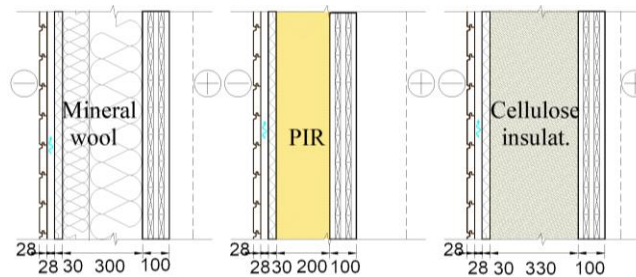


Figure 3.11. Cross-sections of CLT external test wall types from which air leakages were measured.

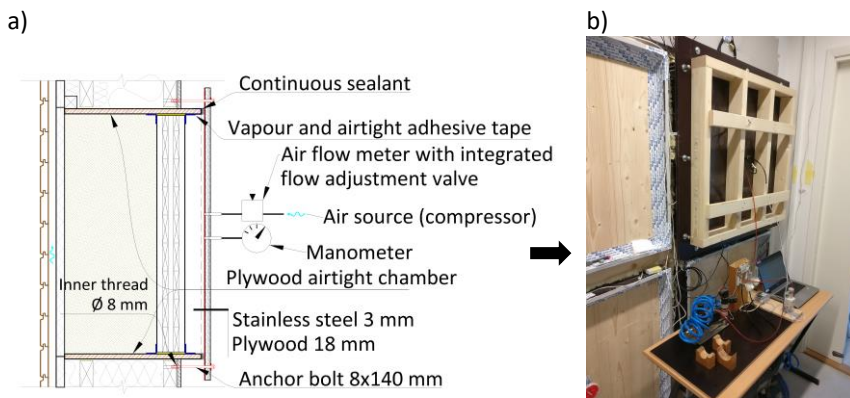


Figure 3.12. Equipment kit scheme for the air permeability test of CLT test walls (a) and performing an air permeability test (b).

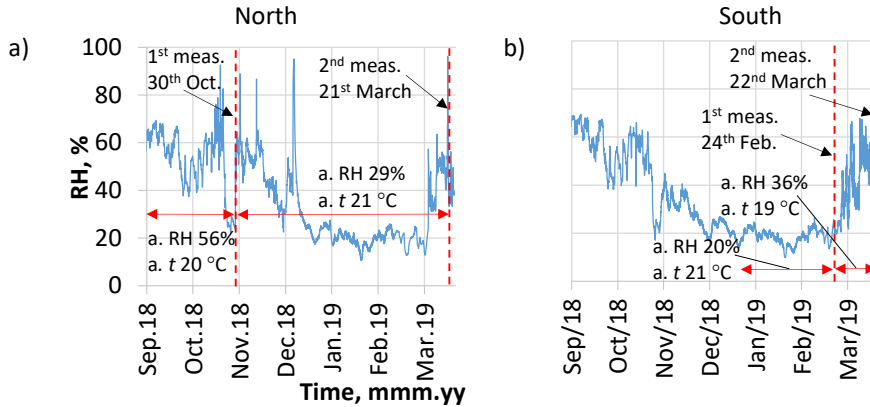


Figure 3.13. Measurement times together with the environment properties of the northern (a) and southern (b) side CLT test walls.

Air leakage was measured twice with different indoor humidity levels. The first measurements for the northern side walls were made on 30th October, with the average indoor RH of the last three months being 56 % at 20 °C (Figure 3.13, a). The first measurements for the southern side walls were made on 24th February, with the average indoor RH of the last two months being 20 % at 21 °C (Figure 3.13, b). The second measurements for both northern and southern walls were made on 22nd March. The average indoor RH of the last three months was 29 % at 21 °C for the northern walls (Figure 3.13, a), and the difference between the first and the second measurement time was $\Delta RH_{N(M2-M1)} = -27\%$. For the southern walls, the average indoor RH of the last month before the second measurement was 36 % at 19 °C (Figure 3.13, b), and the difference between the first and the second measurement time was $\Delta RH_{S(M2-M1)} = 16\%$.

Air leakage measurements were made with only positive pressure. The maximum pressure difference (ΔP_{max}) was selected to be 500 Pa for the first measurement and 100 Pa for the second measurement. The minimum pressure difference (ΔP_{min}) was selected as 50 Pa and 25 Pa, respectively. The measurements included two stages; in the first stage, three overpressure impulses were applied at a pressure difference of 550 and 110 Pa (each impulse was created with a pressure difference of 10 % greater than ΔP_{max}). The measurements in the second stage were carried out at seven pressure steps. The steps were divided into a geometric series of logarithmically growing pressure differences between and including ΔP_{min} and ΔP_{max} . Pressure differences in the pressure steps were found by Equation (2); it is the same as described in section 3.1.2.3. The first series of measurements included 7 pressure steps with pressure differences of $\Delta P_1 = 50$ Pa, $\Delta P_2 = 73$ Pa, $\Delta P_3 = 108$ Pa, $\Delta P_4 = 158$ Pa, $\Delta P_5 = 232$ Pa, $\Delta P_6 = 341$ Pa, and $\Delta P_7 = 500$ Pa; the second series included $\Delta P_1 = 25$ Pa, $\Delta P_2 = 31$ Pa, $\Delta P_3 = 40$ Pa, $\Delta P_4 = 50$ Pa, $\Delta P_5 = 63$ Pa, $\Delta P_6 = 79$ Pa, and $\Delta P_7 = 100$ Pa. Each applied pressure difference at each pressure step was held for at least three seconds.

Analysis of the CLT external test walls was done based only on the results at a pressure difference of 50 Pa. The pressure difference of 50 Pa was chosen according to the air leakage rate (q_{ES0}) given in EN ISO 9972 (2015). In this way, it is possible to compare the results of this research with the air tightness requirements set for buildings in Europe.

Given the small size of the test walls, the limit value of $1.0 \text{ m}^3/(\text{m}^2\text{h})$, with 10 % reserve ($0.9 + 0.1 \text{ m}^3/(\text{m}^2\text{h})$), was set for the measurement results, above which the wall was

considered not sufficiently airtight within the recommended norms of new nearly zero energy buildings and detached houses (Hallik and Kalamees 2019) when the results values should be applied to the whole building.

Due to the complexity of the measurement setup and large amount of time involved to perform the measurement, only one measurement was performed at each measuring point and the measurement uncertainty was calculated according to the accuracy of the equipment. Possible air leakages that could have significantly increased the uncertainty were checked at the sealed connection between the hermetic test rig and the test wall with a smoke tester at a pressure difference of 1000 Pa. The uncertainty of the smallest measured result of $0.06 \text{ m}^3/(\text{m}^2\cdot\text{h})$ at the air flow measurement device repeatability of $\pm 1\%$ is $0.0001 \text{ m}^3/(\text{m}^2\cdot\text{h})$ and the largest measured result of $0.9 \text{ m}^3/(\text{m}^2\cdot\text{h})$ has an uncertainty of $0.001 \text{ m}^3/(\text{m}^2\cdot\text{h})$; therefore, the uncertainties due to their insignificant values were not added to the results.

3.1.4.3 Hygrothermal performance

At the same time, the air permeability test was carried out, the temperature (t) and relative humidity (RH) were measured between the material layers in test walls during the field measurements. Temperature and RH sensors ($t\&RH$) were placed as follows: between the CLT and the external insulation (L2, see Figure 3.9), between the external insulation and the wind barrier (L3, see Figure 3.9), and between the interior layer and the CLT (L1, see Figure 3.9). Measurements between the interior layer and the CLT were made only in wall types 4 and 5, see Figure 3.9, d, e. The indoor surface temperature (t_{si}) of each wall was measured by sensors located in the interior layer surface; outdoor surface temperature sensors (t_{se}) were located on the wind barrier surface. Measurement results were logged and saved at an hourly interval. A detailed description of the measuring sensors is given in section 3.1.1.4.

The indoor climate was controlled by automated heating and humidifiers. The target indoor temperature of both the northern and the southern walls was $21 \text{ }^\circ\text{C}$ (Figure 3.14, b); the target moisture excess $\Delta v_{te\leq 0^\circ\text{C}} = 3 \text{ g/m}^3$ in the cold period (less than $0 \text{ }^\circ\text{C}$) and $\Delta v_{te\geq 20^\circ\text{C}} = 0.5 \text{ g/m}^3$ in the warm period (from $20 \text{ }^\circ\text{C}$). Moisture excess $\Delta v 3 \text{ g/m}^3$ in the cold period applies to residential buildings with an occupancy of $32 \text{ m}^2/\text{person}$ (Ilomets et al. 2017). Indoor RH is shown in Figure 3.14, a. Hourly measured values of outdoor RH (Figure 3.15, a), temperature (Figure 3.15, b), diffuse (Figure 3.15, c) and direct (Figure 3.15, d) shortwave radiation on the horizontal area, wind direction (Figure 3.15, e) and velocity (Figure 3.15, f), and rainfall intensity (Figure 3.15, g) on the horizontal area were obtained from the nearest weather station located 3 km from the test facility.

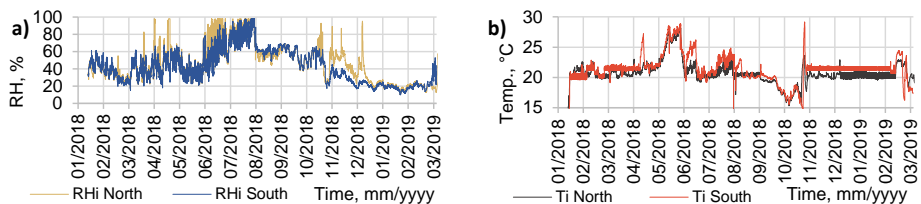


Figure 3.14. Indoor RH (a) and temperature (b) in both northern and southern test rooms.

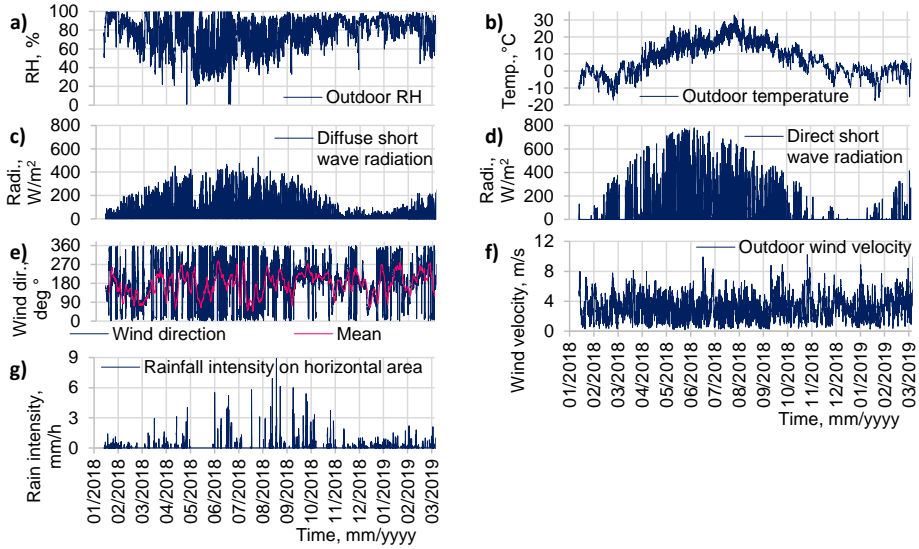


Figure 3.15. Outdoor RH (a), temperature (b), diffuse (c) and direct (d) short wave radiation on the horizontal area, wind direction (e) and velocity (f) and rainfall intensity (g) on the horizontal area.

Field measurements of the test walls started on 16 January 2018 and finished on 6 March 2019. The methodology was developed on the example of research by McClung R. et al. (2014) and adapted according to the objectives of this work.

3.2 Modelling

3.2.1 Simulation software

The simulation models for the test walls from both climate chamber test and field measurements were made by using Delphin 5.9.3 software, which is a simulation program used for coupled heat, air, moisture, pollutant simulation (CHAMPS) modelling of porous building materials. CHAMPS modelling covers the description of field (between volume elements including material interfaces) fluxes and storage, which is done by a set of balance equations (Nicolai and Grunewald 2003):

- Moisture mass balance (with an assumption that ice do not form), Equation (5)

$$\frac{\partial}{\partial t} \rho_{REV}^{m_{w+v}} = - \frac{\partial}{\partial x} [j_{conv}^{m_w} + j_{conv}^{m_v} + j_{diff}^{m_v}] + \sigma_{REV}^{m_{w+v}} \quad (5)$$

where $\rho_{REV}^{m_{w+v}}$ is moisture density in reference volume (liquid water + vapour) (kg/m^3); $j_{conv}^{m_w}$ is convective liquid (capillary) water flux ($\text{kg}/\text{m}^2\text{s}$); $j_{conv}^{m_v}$ is convective water vapor flux (in case of air flux) ($\text{kg}/\text{m}^2\text{s}$); $j_{diff}^{m_v}$ is diffusive water vapor flux ($\text{kg}/\text{m}^2\text{s}$); $\sigma_{REV}^{m_{w+v}}$ is moisture sources/sinks in reference volume ($\text{kg}/\text{m}^3\text{s}$).

- The air mass balance, Equation (6)

$$\frac{\partial}{\partial t} \rho_{REV}^{m_a} = - \frac{\partial}{\partial x} [j_{conv}^{m_a}] + \sigma_{REV}^{m_a} \quad (6)$$

where $\rho_{REV}^{m_a}$ is air mass density in reference volume (kg/m^3); $j_{conv}^{m_a}$ is convective air mass flux ($\text{kg}/\text{m}^2\text{s}$); $\sigma_{REV}^{m_a}$ is air sources/sinks in reference volume ($\text{kg}/\text{m}^3\text{s}$).

- The energy balance, Equation (7)

$$\frac{\partial}{\partial t} \rho_{REV}^U = - \frac{\partial}{\partial x} \left[j_{diff}^Q + u_l \cdot j_{conv}^{m_l} + u_g \cdot j_{conv}^{m_g} + h_v \cdot j_{diff}^{m_v} + h_{VOC,g} \cdot j_{diff}^{m_{VOC,g}} \right] + \sigma_{REV}^U \quad (7)$$

where ρ_{REV}^U is internal energy density in reference volume (J/m^3); j_{diff}^Q is heat conduction (W/m^2); $j_{conv}^{m_l}$ convective flux of the liquid phase (mainly water) (kg/m^2s); $j_{conv}^{m_g}$ is convective flux of the gas phase (kg/m^2s); $j_{diff}^{m_v}$ is diffusive water vapor flux (kg/m^2s); $j_{diff}^{m_{VOC,g}}$ is diffusive gas phase VOC flux (kg/m^2s); u_l is specific internal energy of liquid phase (J/kg); u_g is specific internal energy of gas phase (J/kg); h_v is specific enthalpy of water vapor (J/kg); $h_{VOC,g}$ is specific enthalpy of gaseous VOC (J/kg); σ_{REV}^U is energy sources and sinks in reference volume (W/m^3).

EMC of CLT specimens were calculated in section 3.1.2.1 (Figure 3.3) with Heat, Air and Moisture (HAM) simulation software WUFI 6. The simulation software is using the following balance equations (Holm and Künzle 2003):

- Moisture transfer, Equation (8)

$$\frac{\partial w}{\partial \varphi} \cdot \frac{\partial \varphi}{\partial t} = \nabla(D_\varphi \cdot \nabla \varphi \cdot \delta_p \cdot \nabla(\varphi \cdot P_{sat})) \quad (8)$$

where φ is the relative humidity (-); w is moisture content (kg/m^2); t is time (s); D_φ is the liquid conduction coefficient ($kg/(m \cdot s)$); δ_p is vapour permeability ($kg/(m \cdot s \cdot Pa)$).

- Energy transfer, Equation (9)

$$\frac{\partial H}{\partial T} \cdot \frac{\partial T}{\partial t} = \nabla(\lambda \cdot \nabla T) + h_v \cdot \nabla(\delta_p \cdot \nabla(\varphi \cdot P_{sat})) \quad (9)$$

where H is total enthalpy (J/m^3); T is temperature (K); λ is thermal conductivity ($W/(m \cdot K)$); h_v is latent heat of phase change (J/kg).

3.2.2 Simulation models

Given that the building elements being studied were essentially adiabatic in directions other than across the wall thickness, a 1-dimensional (1D) model was deemed sufficient for the hygrothermal analysis. Boundary conditions for simulation models of test walls from climate chamber test were assigned as measured exterior and interior climate conditions in the climate chamber test, see Figure 3.8. For simulation models of test walls from test facility measurements the data obtained from the weather station were used as the outdoor boundary conditions, see Figure 3.14 and Figure 3.15. Indoor boundary conditions were taken from the measurements in the test facility, see Figure 3.14. Thermal resistance of the internal surface was set to be $R_{si} = 0.13 (m^2 \cdot K)/W$ and the external surface to be $R_{se} = 0.04 (m^2 \cdot K)/W$. Orientation for the north-facing test walls (in the test facility) and test walls from climate chamber test was set to 0 degrees (North) and for the south-facing (in the test facility only) walls to 180 degrees (South). The latitude of the walls was set to 59.4 degrees (latitude of Tallinn, Estonia) for all test walls. The first RH and temperature measurements of each test wall were determined as initial conditions of simulation models. The initial conditions were evenly distributed between the material layers of the models.

3.2.2.1 Simulation models of test walls from climate chamber test

The simulation models of test walls (Figure 3.7) used in the climate chamber test were modified for calculations to find the limit value for initial MC in CLT panels to avoid mould growth risk on the CLT surface. The lower initial MC in CLT panels was used in the simulation model for the test walls 13MW and 13PIR. Applied initial MC of CLT was

considered as evenly distributed over all layers and was determined as 11 %. Evenly distributed MC was considered because before the experiment, the panels were kept in the same conditions as in the factory. Therefore, it was expected that the panels had achieved equilibrium MC through the entire thickness as measured after arriving from the factory. In the simulation models of test walls 20MW and 20PIR, where CLT panels were previously soaked, the initial MC was different in CLT panel layers. For the test wall 20MW, the initial MC in the top layers of the CLT panel was applied 19 % and in the middle layers 11 %. In the test wall 20PIR, the initial MC of CLT in the top layers was applied 21 %, in the middle layers 13 %.

3.2.2.2 Simulation models of test walls from test facility measurements

The simulation models of test walls (Figure 3.9) used in the test facility measurements were modified for stochastic analysis to determine hygrothermal criteria for design of CLT external walls. The initial MC of the factory-dry CLT panels was set to be 13 % ($0.053 \text{ m}^3/\text{m}^3$) over the entire cross-section. Soaked CLT panels had an initial surface MC of 26 % ($0.107 \text{ m}^3/\text{m}^3$) with the depth of 30 mm. During validation, it was changed according to the measured RH values between the CLT panel and the insulation. The central part (40 mm) in the cross-section of soaked CLT panels remained 13 %. Vapour barrier film as an interior layer in test wall type 5 was considered in the simulation model as additional resistance between the material layers of CLT and the internal insulation with vapour resistance (S_d) of $1 \times 10^{50} \text{ m}$. Air change rate (ACH) in the ventilation gap was not measured; it was assigned as a constant value of 150 1/h (0.1 m/s). Thus, it is one of the limitations of this research. However, in-depth studies of the ACH of ventilated facades have been conducted by Finch and Straube (Straube and Finch 2008) in Canadian climate (Vancouver) and by Falk and Sandin (Falk and Sandin 2013) in Swedish climate. Based on these studies, for reference, a fixed average annual ACH of 0.1 m/s was selected in our study. In addition, a sensitivity analysis was done using values of 10, 50, 100, 150 and 200 1/h for simulations. According to the sensitivity analysis, the best fit found was to use 100 and 150 1/h. For the final simulation models, the ACH value of 150 1/h was used, which has been confirmed by previous studies (Falk and Sandin 2013; Straube and Finch 2008).

3.2.3 Material properties

The properties assigned to the material layers of the simulation models of CLT test walls were selected from the Delphin 5.9 software database; Table 3.4 gives the data, together with the material ID in the database. According to the database, the properties of the materials selected for our research have been measured in IBK (Institut für Bauklimatik, Technische Universität Dresden) laboratories. The properties of the CLT were taken from the material file in the WUFI database with the ID "Stora Enso CLT", which is official information published by the CLT manufacturer Stora Enso. The material properties of "Stora Enso CLT" have been measured according to the information provided by the manufacturer at the University of Hamburg, Germany by M. Hirsch, 2013. The species of wood of CLT wood is Norway spruce (*Picea abies*). Thermal conductivity and vapour diffusion resistance factors of the CLT in Table 3.4 are given at a dry state, representing the oven-dry state of the material, i.e., 0 % moisture content. Moisture permeability (a) and sorption (b) curves of the CLT are shown in Figure 3.16. CLT properties were taken from a file made available to the public by the manufacturer (Stora Enso).

Surfaces of the PIR insulation board were considered as vapour impermeable ($S_d > 800 \text{ m}$) for imitating aluminum foil. One surface of the mineral wool interior

insulation board in test walls from climate chamber test was determined as vapour retarder layer named “Vario XtraSafe”, which has high vapour diffusion resistance variability, where S_d varies from 0 to 15 m, depending on the RH of the surrounding environment. The higher the RH in the surrounding environment, the lower the vapour resistance of the insulation board surface. At lower RH, from 0 to 20 %, the vapour resistance is highest where equivalent air layer thickness stays constant at 13 m. When RH exceeds 20 %, then vapour resistance decreases linearly together with the increase of the RH until achieving 80 %. From 80 % the vapour resistance is minimum and equivalent air layer thickness (S_d) stays near 0.5 m.

Table 3.4. Material properties of wall layers in simulation models.

ID (Delphin/Wufi)	Material	Bulk density, kg/m ³	Thermal conductivity, W/m·K	Vapour diffusion resistance factor, -	Open porosity, m ³ /m ³	Water uptake coefficient, kg/m ² ·s ^{0.5}
128	Clay plaster	1568	0.58	30	0.408	0.176
599	Gypsum board	745	0.177	11	0.719	0.179
Stora Enso CLT	CLT (5-layer)	410	0.098*	500*	0.74	0.0024
644	Mineral wool, ext. insulation	37	0.037	1	0.92	0
646	Mineral wool, int. insulation	100	0.031	1	0.92	0
580	Cellulose insulation	65	0.041	2	0.926	0.563
689	PIR insulation	38	0.022	104	0.92	0.0001
646	Wind barrier, min. wool	100	0.031	1	0.92	0

* - at oven-dry state (MC ≈ 0 %)

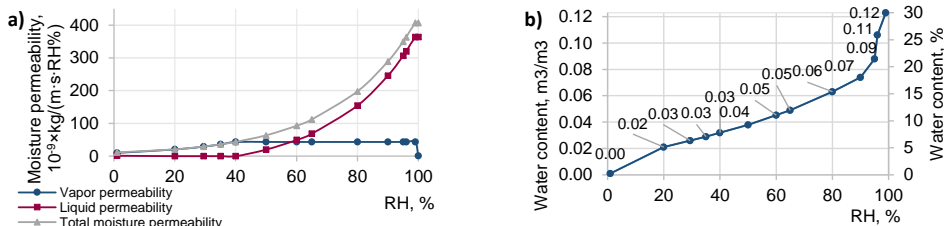


Figure 3.16. Moisture permeability (a) and sorption (b) curves of CLT.

3.2.4 Structure of stochastic analysis

Hygrothermal performance of each wall type from test facility measurements (section 3.1.4) was analysed by a stochastic approach using both discrete and continuous random variables, see Figure 3.21. A method for stochastic approach developed by Wang and Ge (2016) was used.

3.2.4.1 Discrete random variables

For the discrete random variables, the thickness of CLT and the presence of an additional air and vapour barrier between the insulation and the CLT with fixed water vapour resistance ($S_d = 2.3$ m) were used. The water vapour resistance of the air and vapour barriers available in the market varies between 0.01-2.3 m (2022a; 2022b). Small vapour resistance allows the internal membrane to be used as weather protection during construction. This work investigates the impact of an additional air and vapour barrier with fixed vapour resistance on the hygrothermal performance of the CLT wall types studied. CLT thicknesses of 100 mm, 150 mm and 200 mm were selected as the most typical use in CLT buildings. Based on discrete random variables, six different scenarios were generated for each wall type, see Figure 3.21.

3.2.4.2 Uniformly distributed continuous random variables

Ranges of material properties as uniformly distributed continuous random variables are shown in Figure 3.21. The thermal conductivity range of the insulation was selected according to the properties of different insulation products most widely used in the CLT external wall design in Northern Europe. The insulation is generally optimized between thickness and price. Therefore, the range of thermal conductivity was selected between 0.033 and 0.037 W/(m·K) for mineral wool insulation, 0.04-0.045 W/(m·K) for cellulose and 0.022-0.024 W/(m·K) for PIR insulation. The water vapour resistance (μ) ranged from 1 to 1.5 for mineral wool, 1.5-2.5 for cellulose and 60-104 for PIR insulation. The range of thermal conductivity and vapour resistance of the wind barrier refers to the selection from vapour open ($\mu=1$) and low thermal conductivity (0.033 W/(m·K)) mineral wool to vapour tight ($\mu=10$) and high thermal conductivity (0.2 W/(m·K)) wind barrier, e.g., gypsum board. Material properties of insulation and wind barrier were taken from the HAM modelling software Delphin database and product certificates (British Gypsum 2017, 2018; Kingspan 2018; Saint-Gobain 2017; Werrowool 2018).

For our stochastic analysis, 10 pairs of vapour and liquid conductivity curves were created. The pairs were formed by the total moisture permeability derived from the measured isothermal vapour resistance, discussed in section 2.2, see Figure 2.2. The ranges of water vapour resistance of CLT were selected according to the minimum and maximum measured values found in the literature (AISayegh 2012; Byttebier 2018; Meynen 2016; Zilling 2009).

The MC of CLT was considered as the EMC, which ranged from the factory-dry MC of the panel (13 %) to the EMC of the wood fibre saturation point (28 %). According to the measurements of Lipand (Lipand et al. 2021), who experimentally determined the moisture distribution of CLT in contact with water, the MC of CLT surface varies in a depth of 30 mm, see Figure 3.18. The MC of the internal ($MC_{CLT,IS}$) and external ($MC_{CLT,ES}$) surface was calculated separately as continuous random variables. All continuous random variables were uniformly distributed over 100 random numbers by Latin Hypercube Sampling.

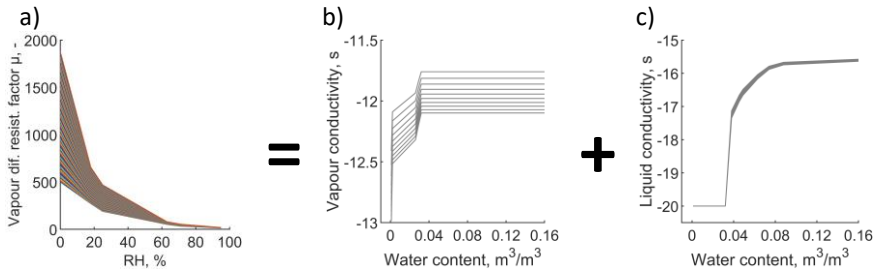


Figure 3.17. Curves of the vapour diffusion resistance factors (AlSayegh 2012; Byttebier 2018; Meynen 2016; Zilling 2009) evenly distributed (a) and derived pairs of vapour (b) and liquid (c) conductivity curves.

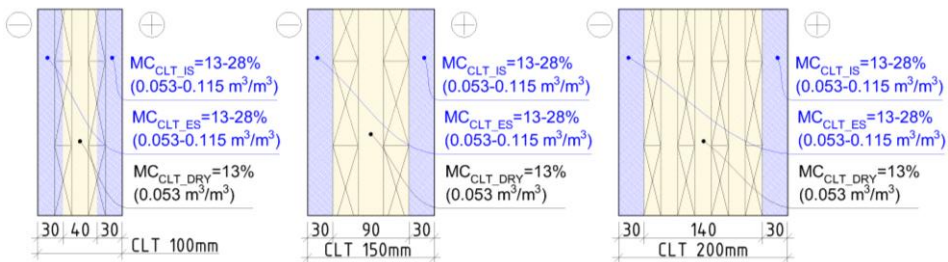


Figure 3.18. MC distribution in the cross-section of CLT panels: variation in internal ($MC_{CLT,IS}$) and external ($MC_{CLT,ES}$) surface 13-28% to a depth of 30 mm and permanently dry ($MC_{CLT,DRY}$) 13% in the middle of the panel.

3.2.4.3 Boundary conditions for data analysis

In addition to the measured environmental climatic conditions, reference boundary conditions were applied to the simulation models after validation for later data analysis.

Indoor and outdoor climate data were set as boundary conditions. Indoor temperature was calculated using the indoor temperature model for dwellings with central heating ($t_{i, central heating}$) (Ilomets et al. 2017), see Figure 3.19 a. The indoor temperature model operates on the basis of Equation (10).

$$t_{i, central heating} = \begin{cases} t_e \leq +10^\circ C \Rightarrow t_i = 22^\circ C \\ t_e > +10^\circ C \Rightarrow t_i = 0.3333 \cdot t_e + 18.667^\circ C \end{cases} \quad (10)$$

where t_e is an external temperature. The indoor RH was calculated on the basis of the indoor temperature and the moisture excess, see Figure 3.19 b. The indoor humidity model was used to calculate the indoor moisture excess that stands for ventilated occupational and living spaces with a population density more than 30 m² per person (Ilomets et al. 2017). The moisture excess by the model is 4 g/m³ at an indoor temperature below 0 °C and 1 g/m³ at an indoor temperature above +20 °C.

Estonian moisture reference year (MRY) for evaluating mould growth risk was used for the external climatic boundary conditions. MRY is a real year, which was selected by analysing Estonian climate data from 1970 to 2000 (Kalamees and Vinha 2004). MRY includes outdoor RH (Figure 3.20, a), temperature (Figure 3.20, b), diffuse (Figure 3.20, c) and direct (Figure 3.20, d) shortwave radiation on a horizontal area, rainfall intensity (Figure 3.20, e), and wind velocity (Figure 3.20, f) and direction. Orientation of the walls in the stochastic calculations was set to 0 degrees (North) and the latitude was set to

59.4 degrees (latitude of Tallinn, Estonia). Air change rate in the ventilation gap was assigned as a constant value of 150 1/h (0.1 m/s) (Falk and Sandin 2013). The hygrothermal simulations were running repeatedly over a period of five years, which is in favour of the safe side, as in practice it is rather unlikely that the critical MRY for mould growth will be repeated for such a long time. Air and rain leakages were not considered in the hygrothermal calculations.

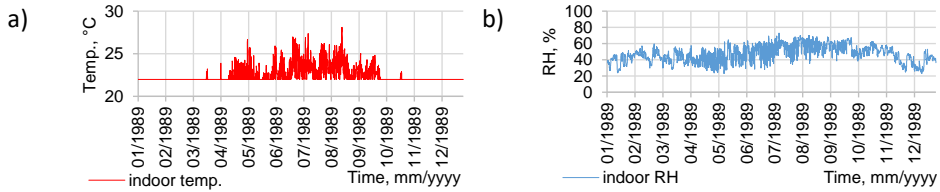


Figure 3.19. Indoor temperature (a) and RH (b).

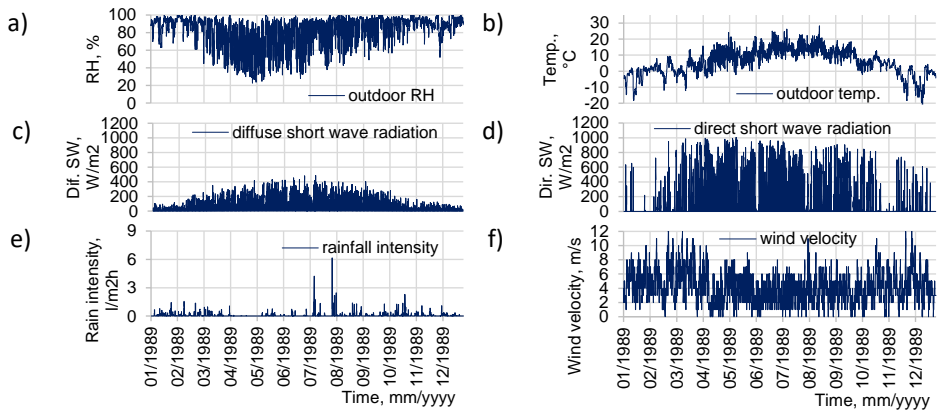
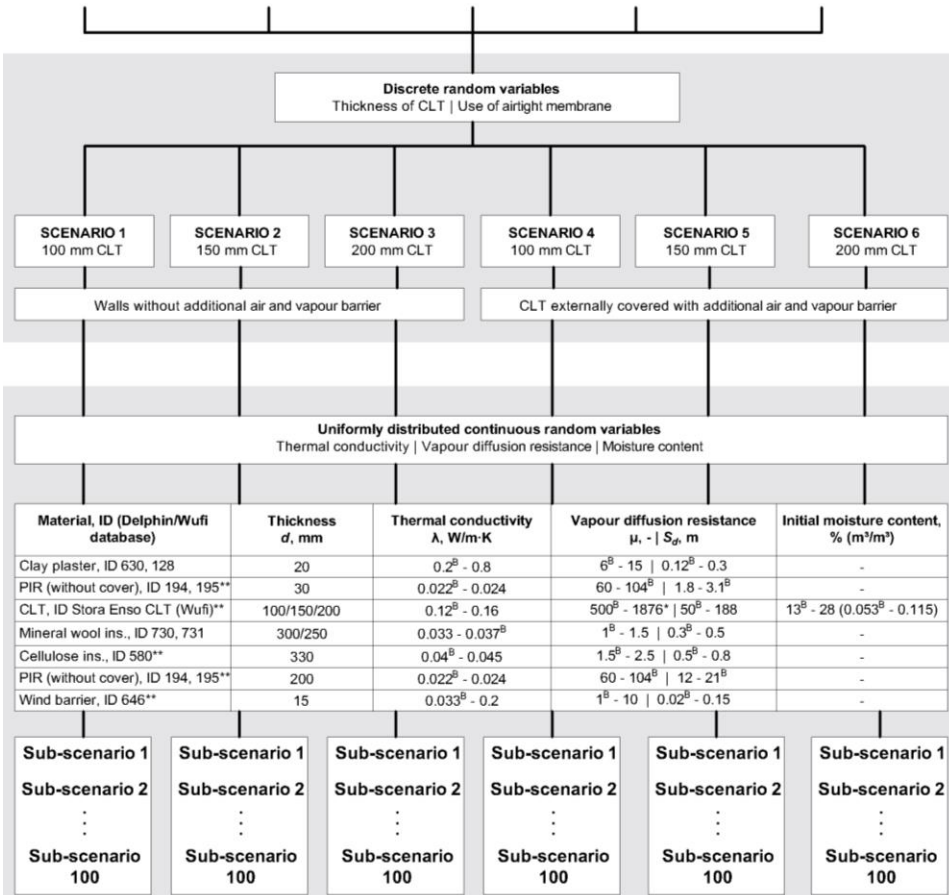
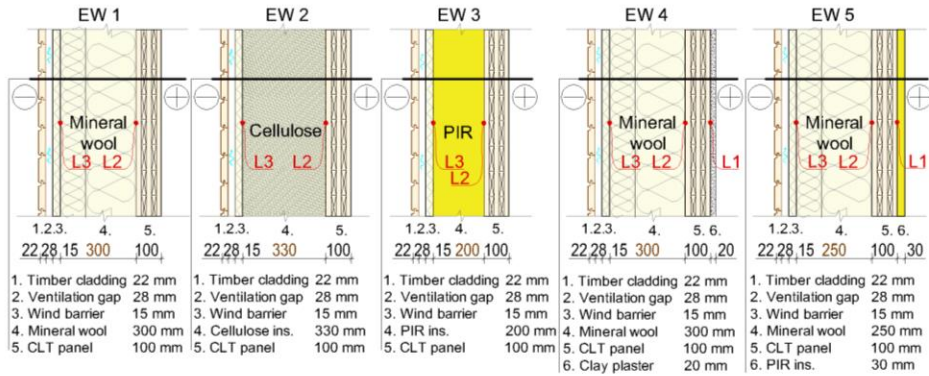


Figure 3.20. MRY outdoor RH (a), temperature (b), diffuse (c), and direct (d) shortwave radiation on a horizontal area, vertical rain density (e), and wind velocity (f).



* at oven-dry state (0 % MC); **in addition, the material properties taken from laboratory measurement reports and the product sheet (AlSayegh 2012; British Gypsum 2017, 2018; Byttebier 2018; Kingspan 2018; Saint-Gobain 2017; Werrowool 2018); ^B material properties of 'Base models'

Figure 3.21. Stochastic structure: cross-sections of CLT external test wall types as objects under study (upper), discrete random variables and the six main scenarios (middle), and continuous random variables (bottom).

3.3 Data analysis

Data for analysis were collected from both the measurements from climate chamber test (section 3.1.3) and test facility (section 3.1.4); and from simulations.

3.3.1 Validation of simulation models

The simulation models (from sections 3.2.2.1 and 3.2.2.2) were validated on the basis of comparison of three indicators: temperature, RH and partial pressure of water vapour. The simulation models were validated by comparing the measured and the calculated (simulation) results. Firstly, differences in the results were found in the absolute value (*abs. Δ*) by subtracting the measurement results from the calculation results and the difference was estimated from the error of the measuring device. Secondly, the Root-Mean-Square-Error (RMSE) was found according to Equation (11) and then normalized RMSE (NRMSE) according to Equation (12), using the mean value of the measurement results:

$$RMSE = \sqrt{\frac{\sum_{i=1}^n (s_i - m_i)^2}{n}} \quad (11)$$

$$NRMSE = \frac{RMSE}{m_{max} - m_{min}} \cdot 100, \% \quad (12)$$

where s_i – hourly calculated (simulation) result, m_i – hourly measured result, n – total number of hourly results, and m_{min} , m_{max} – the minimum and maximum measured results. RMSE indicates the standard deviation of the differences, i.e., the model error. The normalization of the RMSE shows the variability (in percent) of the differences in relation to the range of the measurements ($m_{max} - m_{min}$) and NRMSE allows comparison of the differences in the results between the observed parameters with different scales (temperature (t), partial pressure of water vapour (P_v) and RH).

3.3.2 Evaluation criteria

The hygrothermal performance of each wall assembly was evaluated by the risk of mould growth. The risk of mould was evaluated both on the basis of the measurement results (sections 3.1.3 and 3.1.4) and on the basis of the simulation results (section 3.2). The mould growth risk was evaluated using the VTT model to calculate the mould growth index (M) (Viitanen et al. 2011). The mould growth index, a numerical scale from $M = 1$ to 6 (see Table 3.5), was calculated through a function using temperature and relative humidity, exposure time to critical RH, material sensitivity to mould and relative mould index decline.

Table 3.5. Description of mould index and growth rate (Viitanen and Ojanen 2007).

Mould index M (-)	Description of the growth rate
0	No growth
1	Small amounts of mould on surface (microscope), growth initial stages
2	<10 % coverage of mould on surface (microscope)
3	10 %–30 % coverage of mould on surface (visual), new spores produced
4	30 %–70 % coverage of mould on surface (visual), moderate growth
5	>70 % coverage of mould on surface (visual), plenty of growth
6	Very heavy and tight growth, coverage around 100 %

A mould growth index below 1 ($M < 1$) represents no growth on the material surface, which was set as the evaluation criterion. The mould index was calculated on the interior (L1) and the exterior (L2) surface of CLT and on the interior surface of the wind barrier (L3), see Figure 3.21, Figure 3.9 and Figure 3.7. All locations were directly or indirectly connected to the indoor environment and therefore exceeding index 1 ($M > 1$, several mould growth colonies on the surface) was considered as the wall hygrothermally unsafe.

The mould sensitivity class varied on the CLT surface and the wind barrier when calculating the mould growth index in the stochastic analysis (section 3.2.4). On the CLT surface, we considered the sensitivity classes 'sensitive' and 'very sensitive' (Viitanen et al. 2011). The sensitivity class 'sensitive' refers to planed wood, i.e., the most common CLT panel. The 'very sensitive' sensitivity class is a solid wood panel with untreated surface (sawn surface) made of pine (*Pinus Sylvestris*) wood, e.g., nailed laminated MHM (Massiv-Holz-Mauer) panel. On the interior surface of a wind barrier, we considered the sensitivity classes 'medium resistant' and 'sensitive' (Viitanen et al. 2011). The sensitivity class 'medium resistant' refers to mineral wool materials and 'sensitive' to paper coated products, i.e., a gypsum board.

3.3.3 Probability of hygrothermal performance

The probability of hygrothermal performance was found only in a stochastic analysis (section 3.2.4). All six main scenarios based on the discrete random variables for each wall type (EW 1-5) included calculations of 100 different sub-scenarios based on the continuous random variables, making up a total of 3000 sub-scenarios, see Figure 3.21. To calculate each sub-scenario, one value from each range of continuous random variables was randomly selected.

To evaluate the hygrothermal performance of each main scenario, the number of sub-scenarios that did not exceed the evaluation criteria (mould growth index $M < 1$, described in section 3.3.2) was counted and the probability of performance was calculated accordingly. The probability of hygrothermal performance was found using a total number of 100 of sub-scenarios as 100 % of probability. For example, if 40 sub-scenarios exceeded the mould growth index 1, the probability of performance was considered to be 60 %.

3.3.4 Partial correlation coefficient

A partial correlation coefficient (PCC) (Fisher 1924; Stuart, Ord, and Arnold 2004) was used to analyse the relationship between the continuous random variables (material properties) and the calculated mould growth index. PCC was found separately between one of the variables and the mould growth index, while controlling the rest of variables. The range of PCC is between 1 and -1 and the closer to 1 or -1 the PCC, the greater the impact of the observed variable is. A positive PCC value indicates a positive or increasing influence, i.e., the higher the value of observed variable, the higher is the value of its relative variable and vice versa. PCC values between an observed variable and the mould growth index > 0.5 or < -0.5 were considered as significant, otherwise insignificant influence.

4 Results and discussion

The results of the research are divided into three main sections:

- **Air leakages** – describing the effect of cracks formation on the air leakages through CLT panel and built-in moisture on the air leakages of CLT external wall;
- **Hygrothermal performance** – describing hygrothermal behaviour of CLT external test walls, results of validation of simulation models, and hygrothermal performance of CLT wall types based on the data analysis;
- **Hygrothermal design criteria** – describing limit values that were set to ensure the safe hygrothermal performance of each studied CLT external wall type, comparing hygrothermal criteria with alternative regulations, and giving an example of how to use criteria in practice.

4.1 Air leakages

4.1.1 CLT as a material

4.1.1.1 Cracks size and locations in the CLT panel

The width and length of the cracks were measured on the surface of large scale CLT panels (S1-S4) before and after 3 months of conditioning at 25 % RH and 20 °C. Cracks on the surface of the CLT panels before conditioning were insignificant (width < 0.1 mm). The mean values of mean crack dimensions are given in Table 4.1.

Table 4.1. Mean crack length and width of CLT specimens conditioned at 25 % RH and 20 °C (MC≈7.5 %).

CLT specimen	Mean crack length, mm	Mean crack width, mm
Specimens pre-conditioned at 40 % RH and 15°C (MC≈17 %)		
S1	56	0.3
S2	143	0.4
Specimens pre-conditioned at 95 % RH and 10°C (MC≈12 %)		
S3	221	0.9
S4	468	2

CLT panels S3 and S4, which were stored in a humid environment (95 % RH), had a larger mean width and length of cracks (as expected), more than double compared to the panels conditioned at 40 % (S1 and S2). The difference in the mean values of crack widths ranged between 0.5 mm (S2 vs S3) and 1.7 mm (S1 vs S4). The length of crack widths was limited by the panel dimensions; some of the cracks ran the entire length of the panel (470 mm), see Figure 4.1 a. The difference in the widths of the cracks is explained by the surface MC of the CLT panels. This means that the panels pre-conditioned at 95 % RH had a larger decrease in surface MC (ΔMC -10 % vs ΔMC -5 %) that caused larger shrinkage in the lamination, hence larger cracks. The variation of humidity and temperature in ambient air has a significant effect on the swelling and shrinkage of the CLT laminations. Especially on the edges of the boards in the laminations. The same was concluded by Chiniforush et al. (2019) that the transverse shrinkage/swelling is largest in laminations of glulam due to moisture and temperature change. The cracks widths found in this work are insignificant compared with the allowable gap width of 6 mm according to the EN 16351 (2015). However, crack growth in the panel laminations can significantly decrease the mechanical properties (Huang et al. 2022). Autengruber et al. (2021)

predicted crack patterns in the glulam cross-section exposed to outdoor climate and referred to critical crack lengths that could affect mechanical properties.

In addition to the dimensions of the cracks, the location and shape of the cracks were evaluated. An important observation was that cracks that ran the entire length of the panel were aligned in odd and even layers, see Figure 4.1 b, c. Looking at the shapes of the cracks (Figure 4.1 b) one can see that cracks between laminations are closed by the adhesive layer. On the flat side of the specimen, cracks had formed between each lamination over the entire length of the panel (Figure 4.1 c) and this means that there is a considerable probability of some cracks aligning. Aligned cracks can lead to an opening through the panel, which is the direct source of air leakages carrying the water vapour. Location and alignment in cracks development in CLT panels were also noted in Brandner et al. studies (Brandner 2013; 2016) but were not linked to the air leakages. However, cracks do cause air leakages in CLT external wall joints (Skogstad et al. 2011).

Considering the fact that the panels had only been conditioned for 3 months and that during a real service period, the panel laminations undergo several cycles of swelling and shrinkage (summer to winter), it can be assumed that the internal tensions (caused by swelling and shrinkage) will eventually cause ruptures in the adhesive layers.

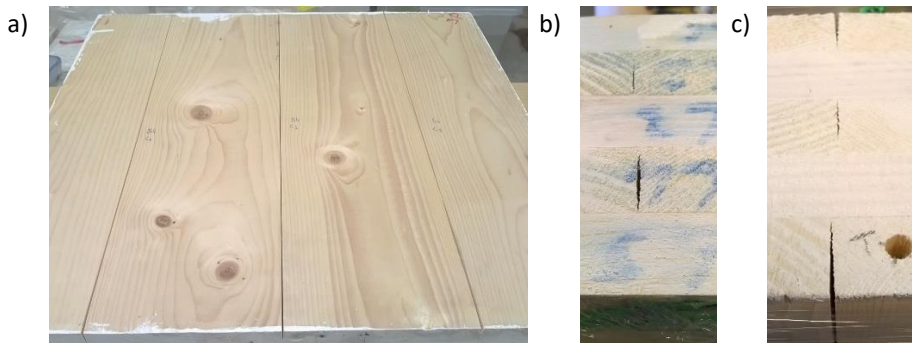


Figure 4.1. Cracks formed between laminations (a) and in odd (b) and even (c) layers.

4.1.1.2 Impact of cracks on the water vapour resistance and air permeability properties of the CLT panel

Test results of vapour permeability were recorded during 33 days of “Cup testing” for five specimens of all four types of CLT panels. The water vapour resistance factor (μ) and diffusion equivalent air layer thickness (S_d) were found for each specimen, and the results are given in Table 4.2.

The diffusion equivalent air layer thickness (S_d) of the adhesive layer ($S_{d\text{CS}2} - 2 \times S_{d\text{CS}1} = 1.25\text{ m}$) was greater than the 6-mm thick solid wood specimen; it can be said that an adhesive layer has a significant impact on the water vapour resistance of a CLT panel. The 6-mm diameter hole in the glued specimen (CS3) reduced water vapour resistance by 9 % and the 6-mm diameter hole (CS4) reduced water vapour resistance by about 30 % compared with the solid glued specimen (CS2). A decrease of 9 and 30 % in water vapour resistance is a significant change. Water vapour resistance (μ) of CLT and solid softwood (Spruce) at 50 % of RH has been found in other studies in the range of 75-150 (AISayegh 2012; Byttebier 2018; Zilling 2009), see also Figure 2.2 b. Compared to our results the vapour resistance of CLT at RH 50 % found in other studies is considerably smaller. Similar results, in the range of 200-300 of water vapour resistance can be found at 30 % of RH, see Figure 2.2 b. This indicates a high uncertainty in the environment used

in our experiment. However, given the small standard error, our conclusions about the effect of the adhesive layer and cracks (drilled holes) on water vapour resistance of CLT can be considered reliable.

Table 4.2. Vapour resistance of CLT specimens (CS1-CS4).

Specimen types	Vapour resistance μ @50 % RH, - \pm S.E.	Vapour resistance S_d @50 % RH, m \pm S.E.
CS1, 1x 6 mm lamination	185 \pm 11	1.13 \pm 0.07
CS2, 2x 12 mm bonded laminations	286 \pm 9	3.51 \pm 0.11
CS3, 2x 12 mm bonded laminations, with a $\varnothing = 2$ mm drilled hole	259 \pm 13	3.19 \pm 0.16
CS4, 2x 12 mm bonded laminations, with a $\varnothing = 6$ mm drilled hole	198 \pm 7	2.45 \pm 0.09

The results of air leakages from the first stage of pressure application (ΔP 550 Pa) did not show any airflow in the specimens of glued laminations without a drilled hole, CS2; therefore, it can be said that these specimens were impermeable to airflow, see Table 4.3. A CLT panel as an airtight material has been found in other studies as well (Gagnon and Pirvu 2011; GUT 2013).

Specimens CS3 of glued laminations with drilled holes of 2-mm diameter showed a maximum airflow of 0.13 $\text{m}^3/(\text{m}^2\cdot\text{h})$ in the first stage at ΔP 550 Pa and specimens CS4 of glued lamination with drilled holes of 6-mm diameter showed a maximum airflow of 0.34 $\text{m}^3/(\text{m}^2\cdot\text{h})$ at ΔP 550 Pa, see Table 4.2. The difference is almost threefold between specimens with 2- and 6-mm holes at ΔP 550 Pa. At ΔP 50 Pa, the difference is insignificant, 0.02 $\text{m}^3/(\text{m}^2\cdot\text{h})$.

Table 4.3. Air leakage in the CLT specimens (CS2-CS4).

Specimen types	Air leakage \dot{V} @50 Pa, $\text{m}^3/(\text{m}^2\cdot\text{h})$ \pm S.E.	Air leakage \dot{V} @550 Pa, $\text{m}^3/(\text{m}^2\cdot\text{h})$ \pm S.E.
CS2, 2x 12 mm bonded laminations	0	0
CS3, 2x 12 mm bonded laminations, with a $\varnothing = 2$ mm drilled hole	0.03 \pm 0.00	0.13 \pm 0.01
CS4, 2x 12 mm bonded laminations, with a $\varnothing = 6$ mm drilled hole	0.05 \pm 0.00	0.34 \pm 0.00

Results in the second stage of the test, where airflow in specimens CS3 and CS4 was measured in logarithmically increasing pressure difference steps, showed that airflow in the increasing pressure steps in CS4 with 6-mm diameter holes was climbing more intensely than in CS3 with 2-mm diameter holes, in other words, CS4 had a bigger growth rate in increasing pressure than CS3, see Figure 4.2.

In terms of hygrothermal performance, the impact of cracks size on the air permeability properties of a CLT panel can be significant at high pressure difference, up to ΔP 550 Pa.

Previous research by Skogstad et al. (2011) showed large airflow differences between wall element joints with initial MC of 10 % and 14 % in CLT panels without glued edges. The considerable impact of cracks on CLT panels shows that an extra layer of vapour and airtight materials for covering CLT panels in external wall assemblies may be necessary.

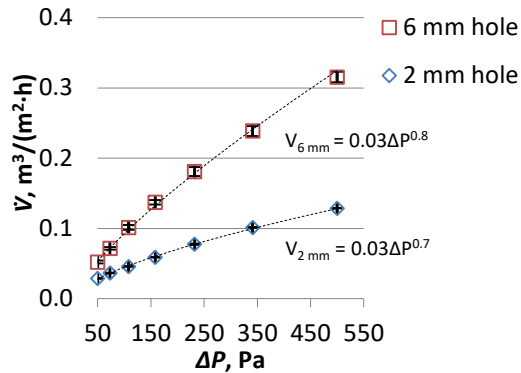


Figure 4.2. Air leakages at increasing ΔP in the CLT specimens (CS3-CS4).

4.1.1.3 Impact of indoor seasonal RH change on the crack formation and air permeability properties of the CLT panel

As concluded in the previous section, the cracks and their size can have a significant impact on the CLT air permeability properties. Therefore, next, the impact of indoor seasonal RH change, in which the critical air leakages in the CLT panel can occur, were studied.

The overall distribution of the cracks differed in each specimen, but the main difference was drawn out in different types of specimens. Thereby it was possible to recognize different patterns of cracks in the distribution, shape, and sizes in different types of specimens. The width of cracks varied from 0.1 mm to 2.5 mm. The larger crack widths occurred in the specimens with three layers (Figure 4.3) and smaller width cracks in the five-layer panels (Figure 4.4). The width of the crack depends on the thickness of the layer, the thicker the lamination (board) layer, the larger the shrinkage in the edges of the boards and, as a result, the wider are the cracks that develop. Nairn (2019) concluded in his study that the durability of mechanical properties of CLT can be increased by using thinner layers and sufficiently dry timber before panel fabrication. This results in a reduction in the growth of cracks on the CLT. On the other hand, in terms of fire resistance and delamination of CLT exposed to fire, the thicker layers (especially top layers) are beneficial (Östman et al. 2018; Schmid et al. 2018).

Larger cracks developed in the top layers of the panel (Figure 4.3 a and Figure 4.4 b), while the middle layers mostly stayed un-deformed, with only some minor cracks or gaps (Figure 4.3 b and Figure 4.4 b). Five-layer panels have three inner layers and therefore the possibility of gaps/cracks overlapping are much smaller than in three-layer panels with only one inner layer. In Figure 4.3 and Figure 4.4 it is seen the effect of “cuping” (Figure 2.3) in the top layers of laminations has caused delaminations. The delaminations in CLT panels are mostly caused by adhesive layer failure (Jahedi 2021) and low-quality bonding in the factory (Brandner 2013; Byttebier 2018). This means that the formation of cracks and thus possible air leakage through the panel also largely depends on the quality of the product.

As seen in Figure 4.5 (a), in specimens without edge bonding, the main cracks appeared as gaps between the laminations and most commonly the length of the gap occurred across the entire length of the panel from edge to edge. The area of the gaps was calculated as the area of a trapezoid formed from the measured largest and smallest width of the gap. In edge-bonded specimens, see Figure 4.5 (b), the cracks developed most commonly in the middle of the laminations with a narrowing beginning and end. The area of the cracks with narrowing beginnings and ends was calculated as the area of the rhombus formed from the measured largest width of the crack. The largest number of cracks and the largest total area of cracks appeared in specimens with higher initial MC ($\approx 13\%$).

As seen in Figure 4.6, there is a noticeable difference in the crack area between specimens with different initial MC after each conditioning step. All specimens with an initial MC of $\approx 13\%$ had an average total area of cracks greater than specimens with an initial MC of $\approx 6\%$. The biggest difference between the specimens with different initial MC was in specimens without the edge bonding and with three layers (WBE3L). Initially drier (MC $\approx 6\%$) specimens without edge bonding and with 3 layers had more than three times smaller average total area of cracks (5439 mm^2) after the final conditioning step than in the specimens with the higher initial MC ($\approx 13\%$) (17649 mm^2). Specimens with higher initial MC (13WBE3L) had also the greatest average total area of cracks after final conditioning. The smallest difference between specimens with different initial MC was in specimens without the edge bonding and with five layers (WBE5L). Specimens 13WBE5L had the average total area of cracks after final conditioning of 7308 mm^2 and 6WBE5L had 6047 mm^2 . The smallest average total area of cracks of 1152 mm^2 after final conditioning was in edge-bonded specimens with five layers and with an initial MC of $\approx 6\%$. The growth of the average crack area after each conditioning step was steady and similar in almost all specimens. Overall, the specimens with bonded edges and with initially drier laminations had a smaller average crack area after final conditioning.



Figure 4.3. Cross-sections of 3-layer and without edge-bonded panel (WBE3L) after the final conditioning step at RH of 15 %, the narrow side (a) and the long side (b) of the panel.



Figure 4.4. Cross-sections of a 5-layer and without edge-bonded panel (WBE5L) after the final conditioning step at RH of 15 %, the narrow side (a) and the long side (b) of the panel.

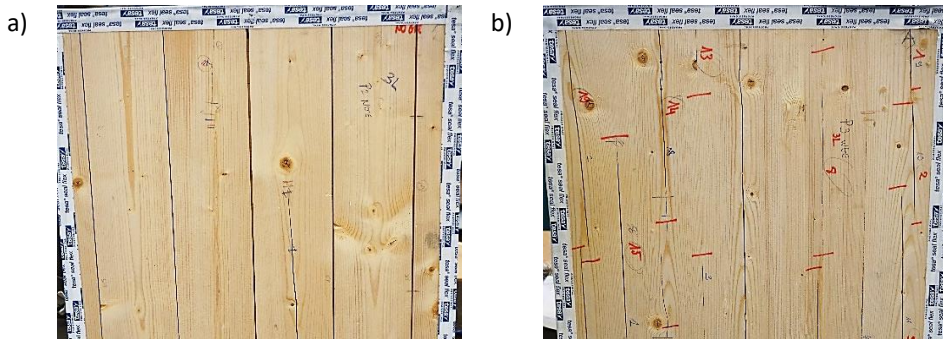


Figure 4.5. Examples of different patterns of crack distribution: cracks in the middle of the laminations (a) on the panel surface without bonded edges; gaps between the laminations (b) on the panel surface with bonded edges.

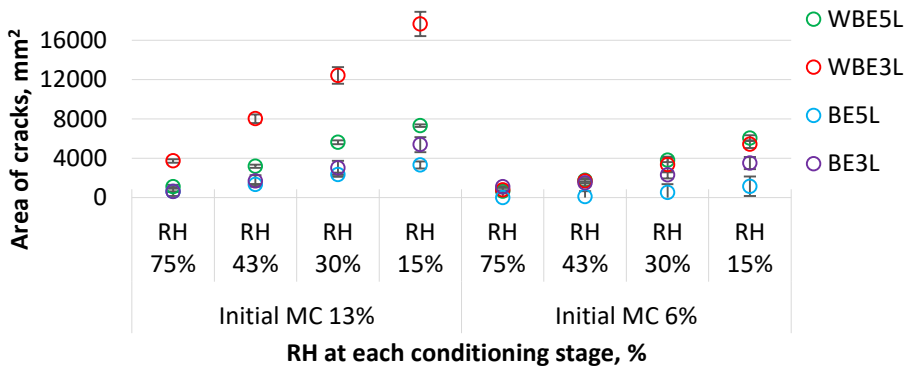


Figure 4.6. The total area of cracks on the surface of CLT specimens after each conditioning step.

The largest average air leakages at ΔP of 550 Pa after each conditioning step were in specimens with three layers, with an initial MC of $\approx 13\%$ and with bonded edges (13BE3L), see Figure 4.7. After the final conditioning step, the air leakage in the specimens 13BE3L exceeded the upper limit of the airflow meter ($1.13 \text{ m}^3/(\text{m}^2 \cdot \text{h})$).

Completely airtight after each conditioning step were all edge bonded specimens with five layers (BE5L); edge bonded three-layer specimens with an initial MC of $\approx 6\%$ (6BE3L); specimens without edge bonding, with five layers and with an initial MC of $\approx 6\%$ (6WBE5L). Almost airtight were specimens without edge bonding with five (5) layers and with an initial MC of $\approx 13\%$ (13WBE5L) where leakages appeared after conditioning in RH of 30%. After the final conditioning step, the specimens 13WBE5L had an average air

leakage of $0.02 \text{ m}^3/(\text{m}^2\cdot\text{h})$. The only specimens with an initial MC of 6 % that had air leakages after each conditioning step were three-layer specimens without bonded edges (6WBE3L). After the final conditioning step, the specimens 6WBE3L had an average air leakage of $0.26 \text{ m}^3/(\text{m}^2\cdot\text{h})$.

Results of crack area measurements showed that the production technologies for CLT panels such as edge bonding and the use of lumber with an initial MC of $\approx 6 \%$ can be recommended for avoiding large growth and development of the cracks on the panel's surface during the service life. Using initially drier lumber together with edge bonded laminations keeps the wood shrinkage lower and therefore keeps crack growth on the panel's surface at a low percentage. In the longer drying process (conditioning steps from RH 75 % to 15 %), the five-layer panels were considerably more resistant to crack growth due to a larger number of bond layers and thinner lamination layer thickness. Bond layers and dry thin laminations keep the wood steadier and the formation of internal stresses during the drying process is controlled better. Inversely, as expected, the biggest cracks appeared in specimens without bonded edges and with higher initial MC in laminations. The higher initial MC leads to greater shrinkage of the lamination in the CLT due to bigger moisture loss in the wood.

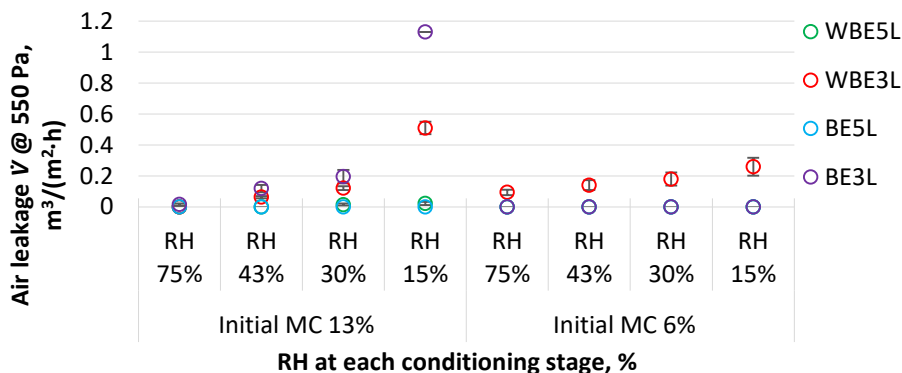


Figure 4.7. Air leakages in the CLT specimens at ΔP of 550 Pa after each conditioning step.

As seen in Figure 4.8 (a), at ΔP of 50 Pa, after the final conditioning step, the average air leakage in three-layer specimens with an initial MC of $\approx 13 \%$ and with bonded edges (13BE3L) was $0.15 \text{ m}^3/(\text{m}^2\cdot\text{h})$ and without bonded edges specimens (13WBE3L), the average air leakage of $0.1 \text{ m}^3/(\text{m}^2\cdot\text{h})$. Three-layer specimens with an initial MC of 6 % and without bonded edges (6WBE3L) had an average air leakage of $0.04 \text{ m}^3/(\text{m}^2\cdot\text{h})$ after the final conditioning step (Figure 4.8, b). In the rest of the specimens (13BE5L, 6BE5L, 13WBE5L, 6WBE5L and 6BE3L), there were no air leakages at a pressure difference of 50 Pa after the final conditioning step.

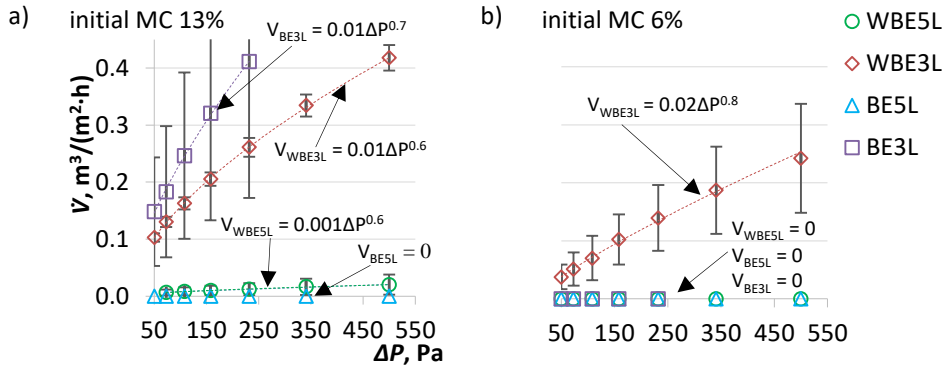


Figure 4.8. Air leakages at increasing ΔP a in the CLT specimens with initial MC of 13 % (a) and 6 % (b) after conditioning step at RH of 15 %.

The greater number of layers helps to avoid large air leakages in the CLT panels as it decreases the crack growth on the panel surface due to thinner laminations. The CLT panels with initially drier laminations showed a good resistance to crack growth and prevented large air leakages as well. Nonetheless, there was no direct correlation between the crack area and the airflow rate. Three-layer specimens with laminations of an initial MC of 13 % had overall the largest air leakages. The cause of the large air leakages was a combination of high initial MC, the larger lamination thickness and the single middle layer. It can be said that the development of cracks or gaps in the inner layers determines the airtightness of the panel. A CLT panel has an even number of inner layers (1, 3, 5 ...) in addition to the two outer layers; the results of this study showed that three inner layers are sufficient for ensuring the airtightness of CLT panels. Overall, it can be recommended that combining the technologies of using a larger number of layers, at least 5, together with initially drier laminations, initial MC of 6 %, for the production of CLT panels will result in a smaller growth of cracks on panel surfaces and smaller air leakages during the time of use. Janols et al. (2013) measured air leakages in the small CLT test house made of 3-layer panels in the period from July to December in Sweden and found that the increase of leakages was significant, but the overall the envelope remained sufficiently airtight ($n_{50} < \text{target } 0.6 \text{ h}^{-1}$). However, Cochon (2019) measured air leakages from different types of CLT panels with different edge treatments and concluded in his study that the air leakage in 3-layer panels was consistently greater than the 5-layers panels. He also concluded that the largest air leakages occurred in the panels without edge treatment (without bonded edges). The use of bonded edge technology helps to ensure the avoidance of possible air leakage threats, but in the long term, the effect might decrease as bond layers may rupture, or cracks may form in the middle of laminations.

4.1.2 Air leakages of CLT external wall

The impact of built-in moisture on the air permeability properties of CLT external walls was determined during the field measurements (section 3.1.4) of the CLT test walls. The air leakage was measured from CLT test walls with different initial MC of CLT and with different wall assemblies.

The test walls with an initially higher MC ($\approx 25 \%$) on the CLT panel surface were observed to have the largest air leakages. At 25 and 50 Pa of pressure difference,

the measured air leakages in all test walls with higher initial surface MC exceeded the set limit value of $0.9 \text{ m}^3/(\text{m}^2\text{h})$, while other test walls with the lower initial MC ($\approx 13\%$) had considerably lower air leakages, see Figure 4.9.

Test walls with a lower initial MC had air leakages below the limit value at 50 Pa of pressure difference, varying from 0.1 to $0.57 \text{ m}^3/(\text{m}^2\text{h})$, and this allowed the analysis of the effect of changes in the indoor RH on the airtightness of the test walls, see Figure 4.10. The result from the northern side test walls with lower initial MC of the CLT showed that the air leakage between the first and second measurements (Figure 3.13, a) at 50 Pa of pressure difference increased between $\Delta v = +0.03$ and $+0.4 \text{ m}^3/(\text{m}^2\text{h})$, see Figure 4.10, a. The first measurements were carried out at an RH of 56 % and the second measurements were done at an RH of 29 %, having a change in RH of $\Delta RH_{N(M2-M1)} = -27\%$, see Figure 3.13, a. The air leakage on the north side test wall EW1.2N at 50 Pa of pressure difference was $0.07 \text{ m}^3/(\text{m}^2\text{h})$ after the first measurement and $0.1 \text{ m}^3/(\text{m}^2\text{h})$ after the second. The air leakage increased by $0.03 \text{ m}^3/(\text{m}^2\text{h})$. On the test wall EW2.2N, the air leakage at 50 Pa of pressure difference was $0.18 \text{ m}^3/(\text{m}^2\text{h})$ after the first measurement and $0.57 \text{ m}^3/(\text{m}^2\text{h})$ after the second, the air leakage increased by $0.4 \text{ m}^3/(\text{m}^2\text{h})$. The third test wall on the north side EW3.2N had an air leakage of $0.11 \text{ m}^3/(\text{m}^2\text{h})$ at 50 Pa of pressure difference after the first measurement and $0.15 \text{ m}^3/(\text{m}^2\text{h})$ after the second. The air leakage increased by $0.04 \text{ m}^3/(\text{m}^2\text{h})$. The equilibrium moisture content (EMC) in the CLT panels decreased presumably about 3.8 %, based on the ambient RH and temperature, which in turn led to the increase of air leakage due to the shrinkage of laminations.

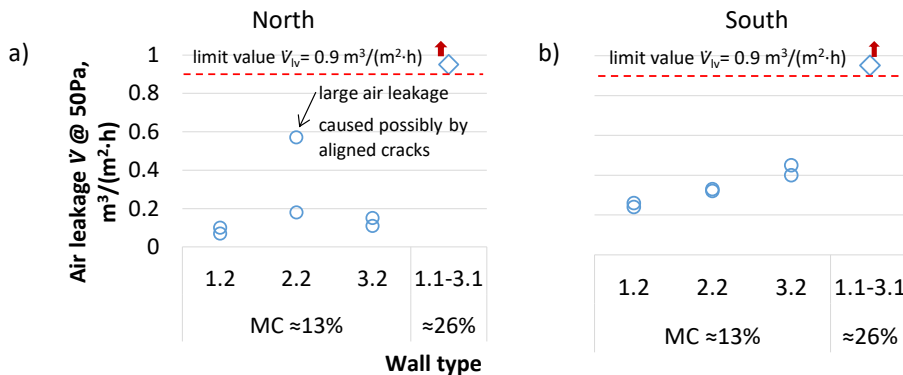


Figure 4.9. Air leakages in the northern (a) and southern (b) side CLT test walls.

The result from the southern side walls with a lower initial MC of the CLT between first and second measurements showed that the air leakage at 50 Pa of pressure difference decreased between $\Delta v = -0.01$ to $-0.05 \text{ m}^3/(\text{m}^2\text{h})$ (Figure 4.10, b) where the first measurement was done at RH of 20 % and the second measurement was at RH of 29 %, having a change in RH of $\Delta RH_{S(M2-M1)} = 16\%$, see Figure 3.13, b. The air leakage on the south side test wall EW1.2S at 50 Pa of pressure difference was $0.26 \text{ m}^3/(\text{m}^2\text{h})$ after the first measurement and $0.24 \text{ m}^3/(\text{m}^2\text{h})$ after the second, the air leakage decreased by $0.02 \text{ m}^3/(\text{m}^2\text{h})$. On the test wall EW2.2S, the air leakage at 50 Pa of pressure difference was $0.33 \text{ m}^3/(\text{m}^2\text{h})$ after the first measurement and $0.32 \text{ m}^3/(\text{m}^2\text{h})$ after the second, the air leakage decreased by $0.01 \text{ m}^3/(\text{m}^2\text{h})$. The third test wall on the south side EW3.2S had an air leakage of $0.45 \text{ m}^3/(\text{m}^2\text{h})$ at 50 Pa of pressure difference after the first measurement and $0.4 \text{ m}^3/(\text{m}^2\text{h})$ after the second, the air leakage decreased by

0.05 m³/(m²h). The EMC in the CLT panels increased presumably about 2 %, which in turn led to the decrease in air leakage due to swelling of the laminations.

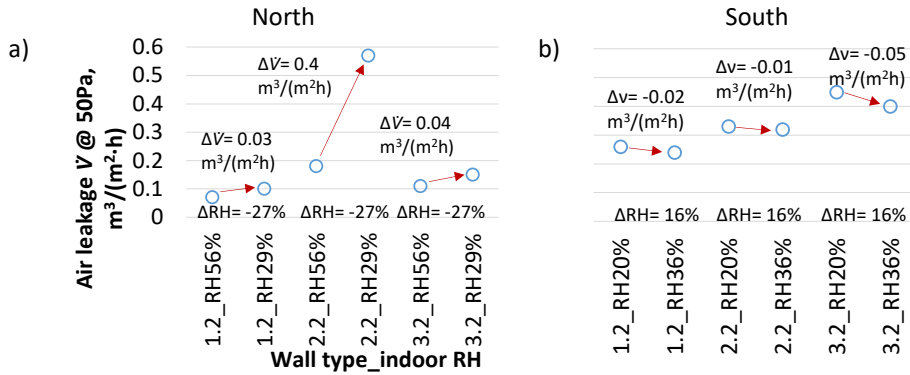


Figure 4.10. Change in air leakages between the first and the second measurement in the northern (a) and southern (b) side CLT test walls with low initial CLT MC.

The results showed a clear impact of indoor humidity on the air permeability properties of CLT walls. As indoor relative humidity decreases, air leakage in the CLT wall increases and vice versa, see Figure 4.11, a. However, the changes in air leakage (less than 0.1 m³/(m²h)) were insignificant compared with the overall air leakage values of the test walls, with an exception of one where the change was 0.4 m³/(m²h), see Figure 4.11, b. It can be assumed that the large change in air leakage may have been caused by the alignment of the cracks in the middle or at the edge of the CLT panel.

Comparison of the results regarding the effect of the indoor humidity and initial MC in CLT panels, it was revealed that the initial MC had a considerably greater impact on the air permeability properties of the CLT walls. In test walls with a high MC (≈25 %), the air leakage was higher than the limit value of 0.9 m³/(m²h) even at the minimum pressure difference of 25 Pa. Hallik and Kalamees (2019) found that the new wooden buildings constructed after 2009 in Estonia had median air leakage of 1.1 m³/h·m² at ΔP 50 Pa. This means that the CLT buildings exposed to weather conditions and being in contact with water during the construction phase cannot be considered as sufficiently airtight. Additional measures to improve the airtightness of the CLT envelope to meet the minimum requirements for energy performance are required.

In the case of dry CLT (MC ≈13 %) in the external wall, the results showed that the walls were sufficiently airtight, < 0.9 m³/(m²h), and the change in the indoor RH did not result in a change in air leakage to such an extent (the change in air leakage was between -0.05 and 0.04 m³/(m²h) with a change in RH of -27 % and 16 %) that it would have a significant impact on the airtightness of the external wall. However, there was also an exception, reflecting that in one case out of six (the ratio may be lower in reality), the formation of cracks from a change in the indoor RH may lead to a significant change in the airtightness properties of a CLT wall.

The test walls facing south had a slightly higher air leakage than the walls facing north, see Figure 4.11, a. No specific reason was given, it can be assumed that the south-facing walls dried faster due to the higher intensity of the sun, but no comparison between the panels' temperatures was done.

There was also no relation between the insulation type and the air leakage in the test walls. The test walls with, presumably, the most airtight insulation (PIR) had at times the largest air leakage $0.45 \text{ m}^3/(\text{m}^2\text{h})$ at 50 Pa and those with, presumably, the least airtight insulation (mineral wool) had the smallest air leakage $0.07 \text{ m}^3/(\text{m}^2\text{h})$ at 50 Pa.

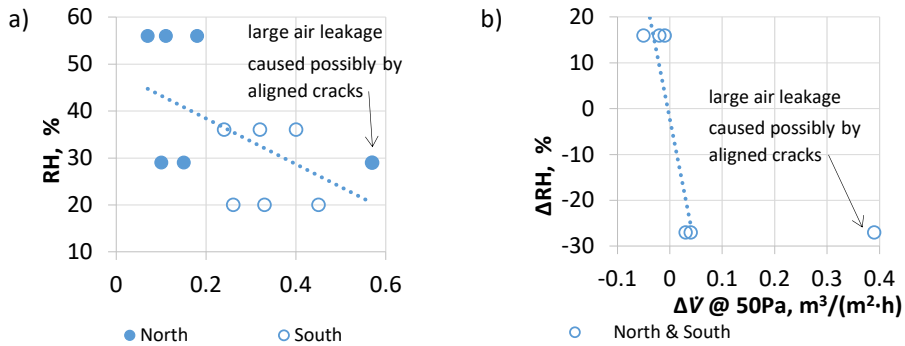


Figure 4.11. Relation between air leakage and indoor RH (a) and between air leakage and RH differences (b) in the CLT test walls with low initial CLT MC.

The results of this research showed that the CLT exposure to water and wetting of the CLT panels during construction carries more than just a risk of moisture damage. Generally, it is known that high initial MC in timber structures may lead to possible biological moisture damage such as mould growth (McClung et al. 2014; Wang and Ge 2016). Biological moisture damage risk from high MC can be managed by letting the timber structure dry out. The higher the moisture content of the CLT up to the FSP, the greater the shrinkage of the CLT lamination (Rubin, Shmulsky and Jones 2011), the greater the cracks between the laminations (Nairn 2019) and the greater the risk of air leakage. Consequently, the results of this study show that the planning and implementation of moisture safety in the construction of CLT buildings are essential if the CLT is to be considered as an airtight layer in the external wall. Using adhesive tape to ensure the airtightness of the CLT is not enough if it gets wet, as the results of this work showed. Thus, in the case of wetting, the most effective solution to ensure air tightness may be to cover the whole envelope with an airtight membrane, which, however, increases the construction cost.

Several other studies indicate that the initial high moisture content significantly affects the airtightness properties of the CLT panel. Skogstad et al. (2011) found that the dry-out from initial MC of 15 % to 10 %, when achieving equilibrium MC during service life, increased the air leakage of the CLT panels approximately up to 10 times. They concluded that airtight connections or a complete covering of the CLT external envelope with an airtight layer are necessary. Alev et al. (2014) found that the decrease of MC in wooden logs led to a significant increase in air leakage in external walls made of wooden logs due to the loosening of the seals between the logs due to weight loss.

Secondly, this study showed that a decrease in indoor humidity leads to an increase in air leakage in the test walls with low initial CLT moisture content and vice versa. The EMC of wood is related to the RH of the air and is described by sorption. As the RH decreases, the equilibrium humidity also decreases and the volume of the wood shrinks, which causes cracks and, in turn, air leakages. However, this study shows that the changes in air leakage were insignificant except for one case. Janols et al. (2013) found an increase of air leakages in the CLT envelope as well in seasonal indoor RH change,

but overall the air leakages did not surpass the target limit ($n_{50} < 0.6 \text{ h}^{-1}$). Based on the above findings, it can be concluded that the 5-layer CLT panel can be considered and used as an airtight layer in external wall construction as long as its initial factory-dry MC (about 13 %) is maintained during both construction and service life.

Thirdly, this research showed that there was no clear relation between the insulation type and the air leakage in the test walls. The airtight insulation PIR was not additionally taped, nor is it taped in practice, and thus the installation gaps caused a large enough air leakage so that the effect of the insulation on the airtightness of the external wall did not occur. This shows that the insulation layer cannot be considered as an airtight layer in CLT wall assemblies.

4.2 Hygrothermal performance of CLT external walls

4.2.1 Measurements

4.2.1.1 Climate chamber test: Impact of interior layer properties

Temperature and RH obtained from the climate chamber test experiment were collected, analysed and subsequently used to determine the performance of the test walls during the experiment. Results showed that the most critical points in all wall assemblies were between the interior insulation board and the CLT panel (L2) as well as between the exterior insulation and the wind barrier board (L5) where RH appeared at the highest values.

Between the exterior insulation and the wind barrier board (see Figure 4.12 c and d), the highest RH appeared in test wall 20PIR where it reached RH 80 % during the first “autumn” climate period (~6 weeks) when the temperature remained around 10 °C. In subsequent climate periods, the RH dropped below 80 %. In other test walls, the RH did not reach 80 % between the exterior insulation and the wind barrier (L5). Both test walls 20MW and 20PIR, at temperatures from 15 °C to 20 °C (see Figure 4.12 a and b) had RH above 80 % between the interior insulation board and the CLT panel (L2). At the same time, after 8 weeks of testing, the RH dropped below 80 % in the test wall 20MW, for the test wall 20PIR, it stayed around 90 % during the entire test. In test walls 13MW and 13PIR, the RH did not reach 80 % between the interior insulation board and the CLT panel (L2). The most critical climate period was the “autumn”, where the RH reached the highest values in all layers and where thereafter, at the beginning of the “winter” period, the RH started to decrease. As RH values were highest between the interior insulation board and the CLT (L2) at higher temperatures, this was considered as the most critical point for further modelling. Arumägi et al. (2011) field measurements showed high RH (> 75 %...80 %) between interior insulation and log wall. The accumulation of moisture on the interior surface of the log wall was caused by the absence of external insulation, which meant a significantly lower temperature compared to this study and therefore a partial pressure of water vapour approaching saturation. In this work, the accumulation of moisture was mostly caused by the dry-out of the CLT. The effect of dry-out of high initial moisture on the accumulation of moisture between the interior insulation and the log wall was noted by Alev et al. (2016; 2015).

This critical point was caused by moisture dry-out from the CLT panel towards an indoor direction and its accumulation behind the interior insulation. Test results showed that a high ($\approx 20 \%$) initial MC of CLT was problematic with both interior insulation types in the external wall assembly. A considerably higher risk was present in the wall assembly having interior insulation with high vapour diffusion resistance (PIR). Klößeiko and

Kalamees (2021) had a similar conclusion on brick walls, stating that the vapour open solutions perform better than the vapour tight PIR in terms of possible mould growth risk behind the interior insulation. Therefore, it can be said that the use of interior insulation in external wall assembly may pose a mould growth risk when CLT panels have a high initial MC ($\approx 20\%$), especially when using vapour tight interior insulation.

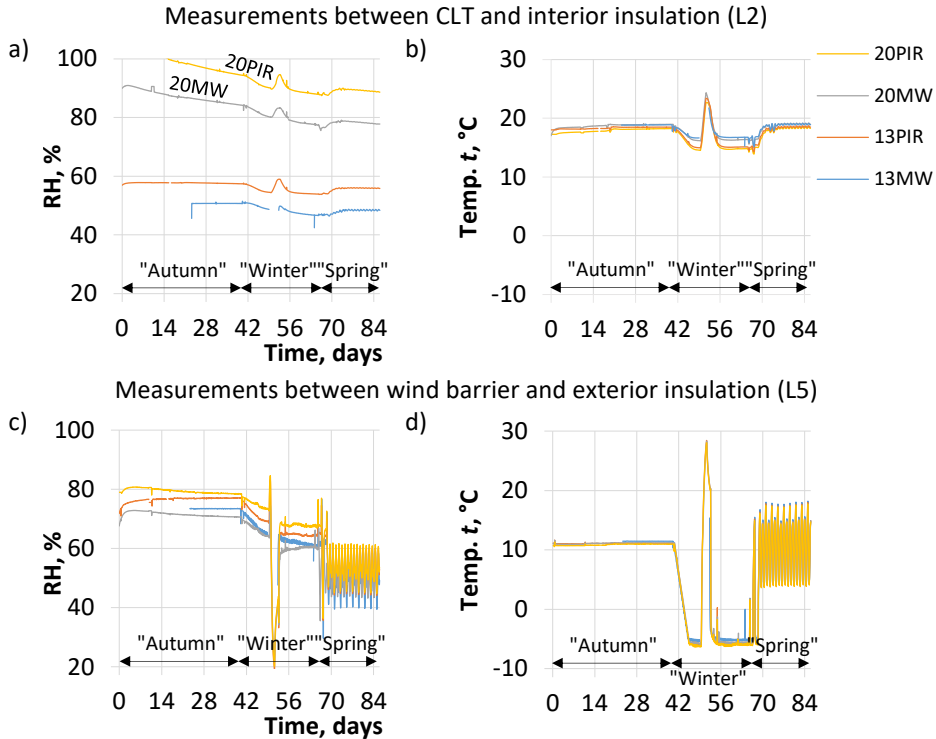


Figure 4.12. Measured relative humidity (a) and temperature (a) between interior insulation board and CLT; between exterior insulation and wind barrier, RH (c) temperature (d) respectively.

4.2.1.2 CLT external test walls exposed to real outdoor conditions

After the climate chamber test, CLT external test walls were placed to the test facility for exposure to real outdoor conditions. Temperature and RH were measured between material layers in the CLT external test walls installed in the test facility. The locations studied were between the CLT and the external insulation (location L2); between the external insulation and the wind barrier (location L3); between the CLT and the interior layer (location L1).

Measurements between the CLT and the external insulation: the RH between the CLT panel and the insulation (location L2) varied mostly between 20 and 75 % in all test walls, see PUBLICATION V (Figure A.1). In test walls with the CLT panel soaked in water before installation (EW 11-51), the RH exceeded 80 % at the beginning of the measurement period when the excess moisture in the CLT panel had dried out, see Figure 4.13. The time when the RH was over 80 % was short and the calculation results of the mould growth index did not exceed 1 in any test wall; hence, there was no risk of mould growth on the CLT surface. In the cold period, from December to March, the RH varied from

30 to 15 %, and by summer, from June to October, the RH rose above 50 % in all test walls. Smaller RH fluctuations occurred on test wall types 2 (EW 21 & EW 22) and 3 (EW 31 and EW 31), ranging from 30 to 60 %, see Figure 4.13 e-l. In the wall types insulated with mineral wool (EW1, 4 & 5), the RH ranged from 20 to 75 %, see Figure 4.13 a-d (also PUBLICATION V (Figure A.1)).

Measurements between the external insulation and the wind barrier: the RH between the insulation and the wind barrier plate (location L3) did not reach 100 % during the measurement period in any of the test walls except EW 32 North, see Figure 4.14 k and PUBLICATION V (Figure A.2). This means that no water vapour condensation risk took place except in test wall EW 32 North. In the north-oriented EW 32 test wall, the RH fluctuated continuously up to 100 % from August to November.

On the south-oriented wall (EW 31 South), RH did not reach 100 % (Figure 4.14 l). Also, the risk of mould growth (calculated according to the VTT mould index) on the surface of the wind barrier was not present in any of the walls. In the cold period, from November to February, the RH varied from 75 to 95 %, and by spring-summer, from March to September, the RH varied from 30 to 75 % in most of the test walls. Smaller RH fluctuations occurred in type 2 test walls (EW 21 & EW 22), ranging from 40 to 90 %, see Figure 4.14 e-h. The largest fluctuations occurred in type 3 walls (EW 31 & EW 32), ranging from 15 to 100 %, see Figure 4.14 7 i-l. In the wall types insulated with mineral wool (EW1, 4 & 5), the RH ranged from 20 to 95 %, see Figure 4.14 a-d, m-u and PUBLICATION V (Figure A.2).

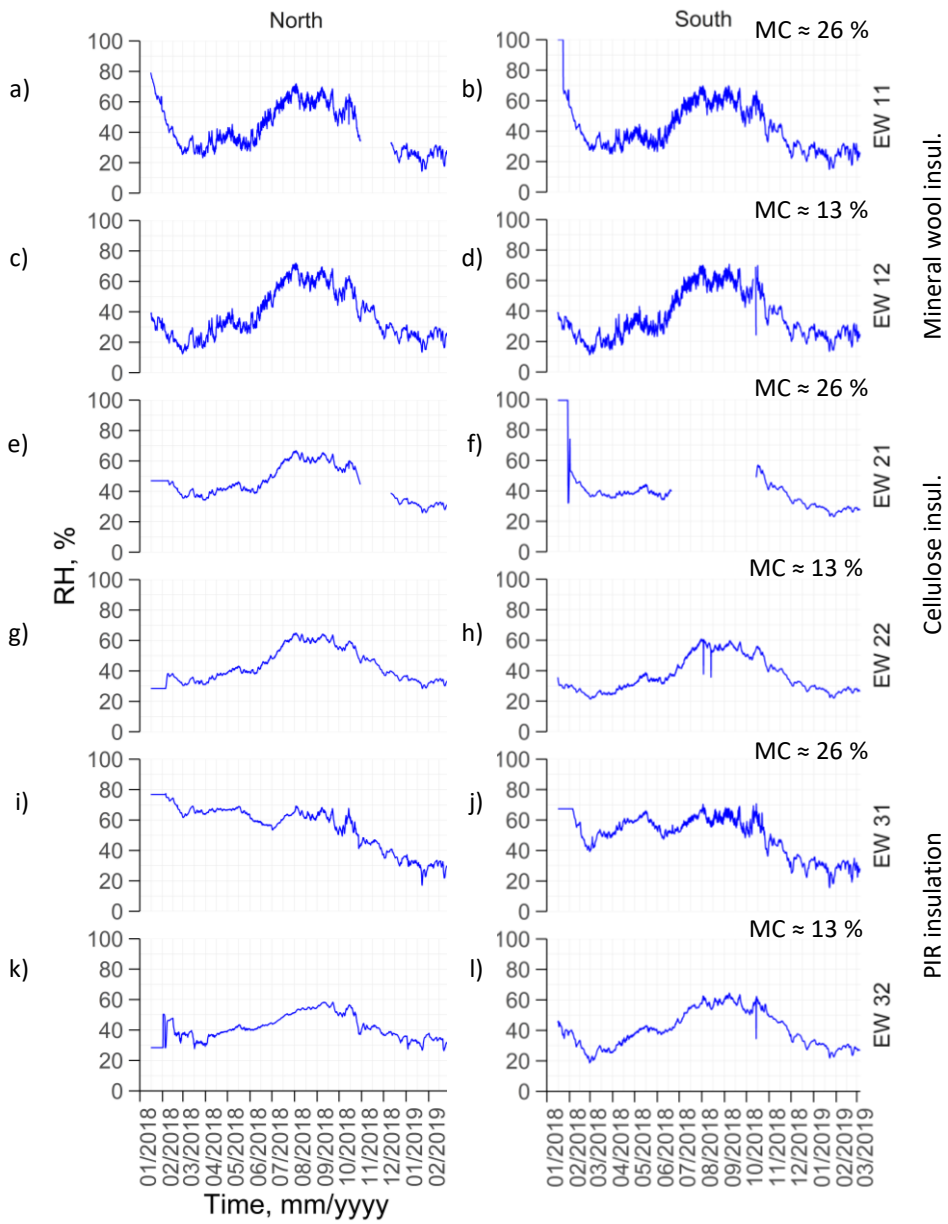


Figure 4.13. Field measurements of RH between the CLT and the insulation (L2) in types 1, 2 and 3 test walls.

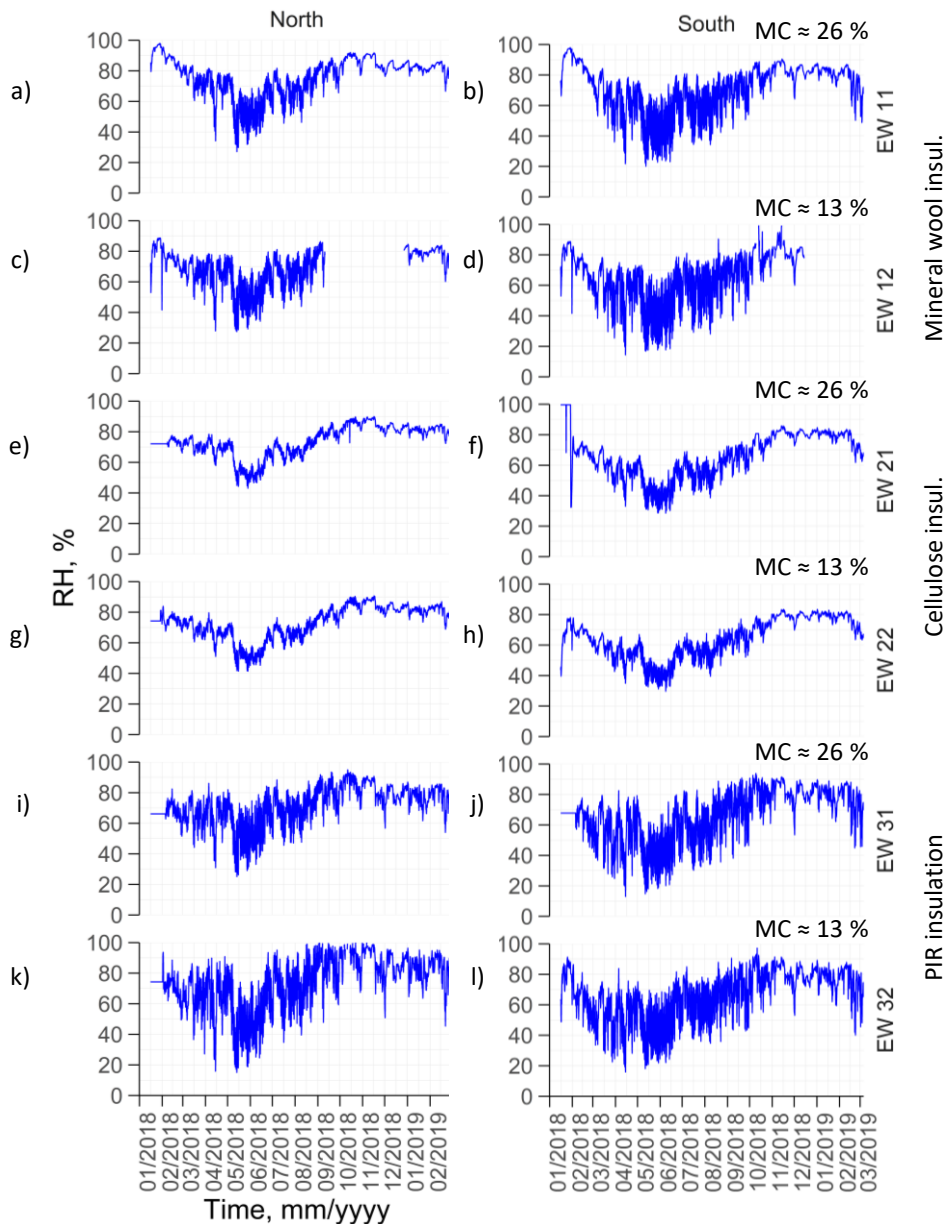


Figure 4.14. Field measurements of RH between the insulation and the wind barrier (L3) in types 1, 2 and 3 test walls.

Measurements between the CLT and the interior layer: at location L1, between the CLT and the internal layer, the RH was measured only in types 4 and 5 test walls. In type 4, the air vapour saturation limit was exceeded between the plaster and the CLT after the plaster was applied and during its drying period, see Figure 4.15 a-d. The drying time of the plaster was short enough to ensure the RH dropping below 80 % without any risk of mould growth. The calculation results of the mould index did not exceed index 1 during the dry-out. In type 5 test walls, the RH exceeded 80 % for about 90 days between the soaked CLT panel (EW 51) and the vapour barrier film, in both north- and south-oriented

external walls, see Figure 4.15 e, f. Despite long stay at high RH, no risk of mould growth on the CLT surface was detected by the calculation of the mould growth index. However, the mould index exceeded 1 if the sensitivity of the surface was reduced to 1 (rough sawn surface on wood). The RH remained stable at 60 % in walls where factory-dry panels (EW 52) were used (Figure 4.15 g, h).

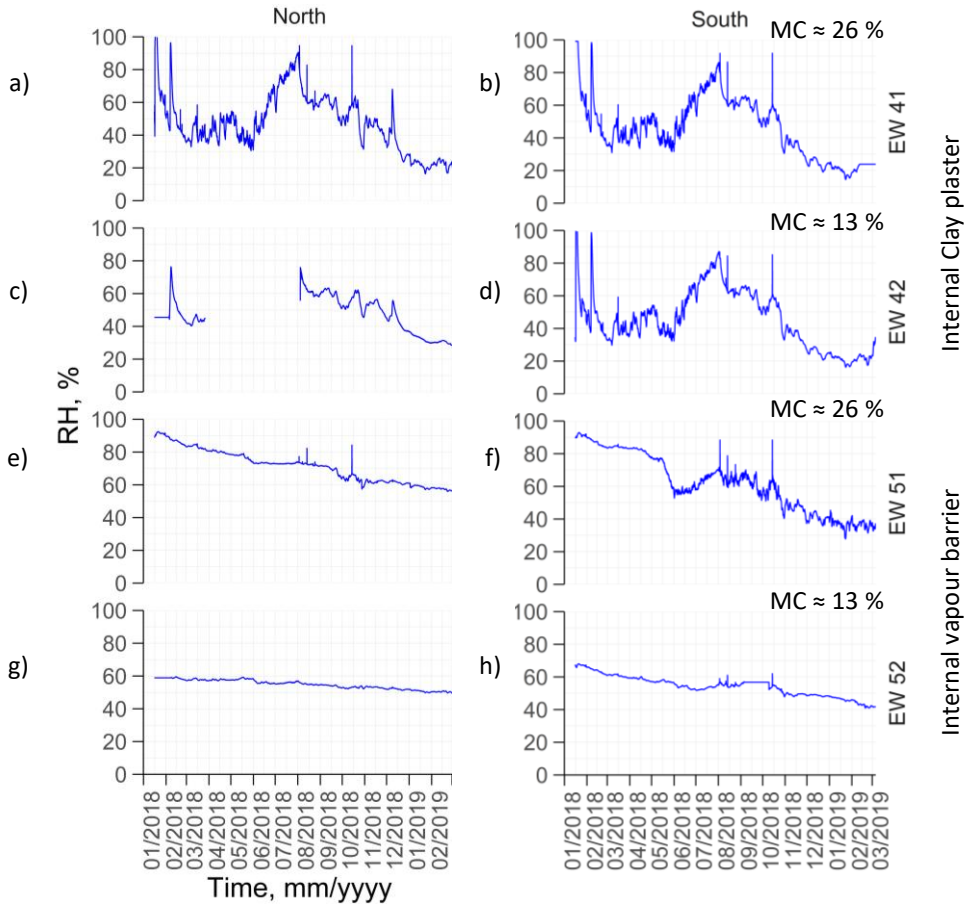


Figure 4.15. Field measurements of RH between the CLT and the interior layer (L1) in types 4 and 5 test walls.

Impact of wall orientation on field measurements: wall orientation was found to have minor impact; the results of the north- and south-facing walls did not differ much. This small effect occurred mainly due to the ventilated façade where the ventilation gap equalised the surface temperature of the wind barrier, especially on the south-facing walls, because of high solar radiation. However, the impact of the sun was observed in wall types 4 and 5, where the southern walls had a greater variation in the RH between the insulation and the wind barrier plate (location L3) than the northern walls, see Figure 4.14. Larger variations occurred mainly in the spring and summer periods, see Figure 4.14 m-u. The effect was also clearly visible in wall type 3, consisting of the CLT with PIR insulation, where a potential risk of water vapour condensation occurred on the surface of the wind barrier (location L3) on the northern wall, which was not present on the southern walls. However, it appeared only on one (EW 3.2 North) of the four walls.

Impact of CLT initial moisture content on field measurements: high initial CLT moisture content exerted strong impact, as was assumed. The dry-out of high initial moisture content at the beginning of the measurement period on the walls with soaked CLT panels significantly increased the RH between the external insulation and the CLT panel (location L2), see Figure 4.13 a, b, e, f, i, j. The same occurred between the interior layer (vapour barrier or clay plaster) and the CLT panel (location L1), see Figure 4.15 a, b. On most walls, except for wall types 2 and 3, the RH at locations L1 and L2 was greater than the critical RH of 80 % at the beginning of the drying period. However, according to the calculations of the mould growth index, dry-out of initial moisture on any wall during the measurement period posed no risk of mould growth. The measured RH in types 2 and 3 test walls with soaked CLT panels (EW 21 and EW 21) at location L2 showed a low result instead of high (expected to be over 80 %) at the beginning of the measurement period. The reason was that the start of logging of some sensors was delayed due to a technical problem of the measuring device. Therefore, the measured RH results in types 2 and 3 test walls were constant at the beginning of the measurement period, see Figure 4.13 e-k.

Impact of wall assembly on field measurements: the assembly of the walls had the greatest impact on the selection and arrangement of the layers of materials. Walls with the CLT exposure to the indoor environment or covered with water vapour permeable clay plaster demonstrated successfully that the CLT panel controls the water vapour diffusion and the RH remains low between the wind barrier and the insulation. RH also remained low in walls with high CLT initial moisture content and with low vapour permeable PIR insulation.

Comparison of external walls insulated with mineral wool and cellulose insulation showed that cellulose insulation is at an advantage due to its greater ability to bind moisture from the air. The RH remained more stable, lower and fluctuated less between material layers in cellulose insulated external test walls against walls insulated with mineral wool, see Figure 4.13 and Figure 4.14 e-h. A clear advantage was found on the walls with high CLT initial moisture content (EW 21): while almost all mineral wool insulated walls with the CLT pre-soaked (EW 11, 41 and 51) had the RH between the insulation and the CLT panel of more than 80 % at the beginning of the measurement period (dry-out period), cellulose-insulated walls had less than 75 %.

The most unexpected results were found on PIR-insulated walls. The walls had the lowest RH between the CLT and the insulation. Dry-out of the soaked CLT high initial moisture content did not result in the accumulation of moisture on the surface of the PIR insulation, as originally expected. Preliminary simulations before installing the test walls showed that moisture accumulates behind the insulation at high CLT initial MC, which in turn may cause a risk of mould growth, see Figure 4.19 a, b. A later investigation revealed that the quick dry-out was due to the low air exchange between the PIR insulation and the CLT panel. Air exchange was also considered to cause the condensation risk on the surface of the wind barrier at L3. The preliminary simulation without air leakage (PUBLICATION V, Figure 12 a-c) showed that the low vapour permeable PIR insulation controls the water vapour diffusion well, as expected and the RH varies between 30 and 90 %. Final simulation results with the air leakage showed a variation of RH between 20 and 97 %, which is similar to the field measurement results where condensation risk occurred. However, the risk of condensation may have been due to a sensor error, as was noticed in a close-up view of the measurement results (PUBLICATION V, Figure 12 d). A detailed description is presented in section 4.2.2.

The internal coating of the CLT surface with clay plaster had no significant impact and the plaster dried after installation, without posing any risk of mould growth on the CLT surface. Also, covering the CLT with a vapour barrier film and internal insulation caused no risk of mould, but the RH was over 80 % for a long time (about 3 months) at the beginning of the measurement period, see Figure 4.15 a,b. This means that further investigations are needed to address the use of internal vapour barriers and to evaluate the performance, for example, by the stochastic analysis where the boundary conditions are the reference test year.

The results from the field measurements showed that the studied CLT external walls were hygrothermally in the safe range in the observed cold and humid climate. The CLT, which is a load-bearing element, has the following additional properties: sufficient control of water vapour diffusion, relatively low thermal conductivity, and suitability to the interior as an open finishing element. Also, the CLT can be insulated both with vapour permeable and low permeable thermal insulation materials without causing any critical moisture damage risk. High insulation (thermal transmittance of the walls $U = 0.1 \text{ W}/(\text{m}^2\cdot\text{K})$) caused no water vapour condensation or mould growth risk on the surface of the wind barrier in any wall. High thermal resistance, low water vapour resistance and sufficient thickness of the mineral wool wind barrier prevented the risk of condensation and mould growth effectively. Also, covering the CLT with both vapour permeable and low permeable interior layers posed no risk of mould growth during the field measurements. Nevertheless, based on the results of this work, the key factors in terms of hygrothermal performance were sufficient dry-out capacity and high initial moisture content.

As expected, the field measurements showed that water vapour permeable insulation materials (mineral wool and cellulose insulation) provide a sufficient dry-out capacity and at high MC; CLT dried out without posing any moisture damage risk. At the same time, the use of cellulose insulation showed a clear advantage over mineral wool, demonstrating a more stable RH fluctuation. The effect of moisture buffering of cellulose insulation was proved by the lowest moisture accumulation (lowest RH at the beginning of the measurement period) between the insulation and the CLT in the walls with soaked CLT panels. Thus, the results of this work confirmed conclusions by Pihelo et al. (2016) and Ojanen et al. (2016) that the use of cellulose stabilizes high moisture fluctuations of indoor air and can prevent the risk of moisture damage better than mineral wool. Therefore, cellulose insulation is a safer choice when selecting water vapour permeable insulation for the external wall. It is preferable in particular for constructions planned without weather protection and with the CLT exposed to water contact (rain, snow) or if large fluctuations of moisture excess levels in indoor air are expected in the indoor environment during the time of use.

The most unexpected results were obtained from the test walls insulated with PIR insulation as the detected small air exchange prevented moisture accumulation and did not cause or pose any moisture damage risk during the field measurements of our study. According to previous studies, the CLT loses airtightness after exposure to water (Skogstad et al. 2011) or having three layers (Cochon 2019; Time 2020), and air leakage as an exfiltration may cause moisture damages (Kalamees and Kurnitski 2010). This shows that the insulation installed airtightly can be beneficial if the low moisture content of the CLT panel (factory dry) during construction is maintained. The effect of larger (outdoor and indoor) air leakage on the hygrothermal performance of the CLT external wall externally insulated with low vapour permeable PIR insulation needs further investigation.

The use of water low vapour permeable inner layer (vapour barrier film) posed no risk of mould growth. However, in walls with high CLT MC, moisture accumulated between the CLT and the vapour barrier film during dry-out. Although the risk of mould growth was not indicated, the probability of mould growth risk may be high at higher moisture loads (higher indoor excess moisture level or greater initial MC of CLT). In contrast, when water vapour permeable clay plaster was used as the internal layer, no large moisture accumulation occurred in the walls even at high initial CLT MC. The probability of failure (risk of mould growth on the CLT surface) when using low vapour permeable layers in the CLT external wall assembly must be determined by stochastic analysis using a variety of influencing parameters, for example, the initial moisture content and its distribution in the CLT panel, material properties, dimensions, etc. However, water vapour permeable layers are well suited for covering the CLT from the inside.

4.2.2 Modelling

4.2.2.1 Simulation models of test walls from climate chamber test

First simulation models of CLT external walls were created and validated based on the measurements in the climate chamber experiment. The adjusted material properties (see Table 3.4) were used to create the simulation models and the same climate parameters as those used in the laboratory experiment were implemented to simulate the test results. Comparing the measured and simulated results, the differences together with standard deviation (av. \pm s.d.) and minimum and maximum values (min-max) were calculated. All calculated differences can be found in PUBLICATION IV (Table 2). The differences were calculated by taking the average test result for each period in each location (L1-L5) as a base value and subtracting the result of the simulation.

The average differences in the temperature (Δt) between the test and the simulation results were from -1.1 ± 0.2 °C to 0.6 ± 0.3 °C, which is close to the error of the measuring sensors (± 0.3 °C). The temperature was similar between the test and the simulation results over all climate periods (“autumn”, “winter” and “spring”). The average differences in the relative humidity (ΔRH) were from -10.5 ± 1 % to 7.6 ± 0.3 %, compared with the error of the measuring sensors (± 2.0 %), the differences were three to five times greater. The average differences in the partial pressure of water vapour (ΔP) were from -236 ± 25 Pa to 147 ± 87 Pa. During the first period of “autumn” climate, the average differences in each layer between the simulation and the laboratory test results were smallest and differences of temperature and RH remained within the limits of the error of the sensors (ave. $\Delta t = -0.3$ °C and ave. $\Delta RH = 0.2$ %). The biggest average differences were found during the “winter” climate period. The test walls having interior insulation with variable vapour diffusion resistance (20MW and 13MW) had the biggest average differences in RH and in water vapour partial pressure between the CLT panel and the external insulation (L4) and between the interior insulation and the CLT (L2). The average difference in RH in the test wall 13MW between the CLT panel and the external insulation (L4) was 10.5 % and in partial pressure -178 Pa. In the wall 20MW, the average difference in RH between the interior insulation and the CLT (L2) was -7.5 % and in partial pressure -224 Pa. The test walls having interior insulation with high vapour resistance (20PIR and 13PIR) had the greatest average differences between the interior insulation and the CLT (L2). The average difference in RH in the test wall 13PIR between the interior insulation and the CLT (layer 2) was 6.6 % and in partial pressure was 147 Pa. In the wall 20PIR, the average difference in RH between the interior insulation and the CLT (layer 2) -3.3 % and in partial pressure -130 Pa. The overall average difference in RH and partial pressure

in the winter period was respectively -1.7 % and -43.8 Pa. The average differences between the test and simulation results in the “spring” climate period ranged between -8 % and 7.6 % in RH and between -236 Pa and 98 Pa in partial pressure. In addition to the differences in the results, Figure 4.16 shows how the simulation (SIM) results follow the trend of the measurement (LAB) results of the test wall CLT13MW.

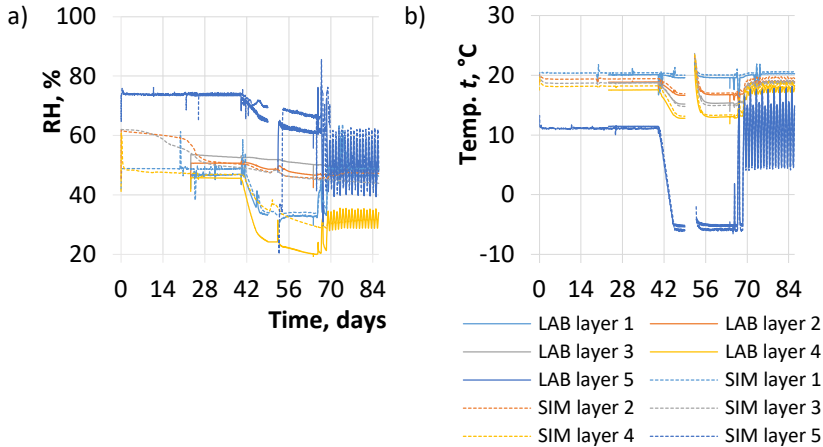


Figure 4.16. Measurements and simulations of temperature (a) and relative humidity (b) of test wall CLT 13MW.

In a previous study completed by McClung et al. (2014), which included the results of a simulation with similar wall assemblies, the overall difference between simulation and test results was $\pm 2\text{-}5\%$. It can reasonably be concluded that the simulation models were accurate and simulation results were similar to the test results. There were, however, some bigger differences that appeared in the results of RH and partial pressure of water vapour during the simulated “winter” climate period. The biggest differences mostly appeared in locations L2 and L4. It seemed that the simulations overestimated the RH in the outer layers under colder external climate conditions.

4.2.2.2 Simulation models of test walls from test facility measurements

Next, the simulation models were created and validated based on the results from field measurements. The validation was done by using NRMSE (the Normalized Root Mean Square Error). Differences as NRMSE in the measured and the calculated results of temperature (t), partial pressure of water vapour (P_v) and RH used for validation are given in Table 4.4. Comparison of the NRMSE of all parameters shows that the majority of results are up to 5 % and the vast majority up to 10 %. The smallest discrepancy in the results of all parameters based on NRMSE was at location L2 (between CLT and insulation) where most of the results were within 10 % of NRMSE (Table 3). The smallest difference in the results at L2 is also shown by the compatibility of trend lines, see Figure 4.17. An overall comparison of the trend lines of the calculation results at L2 showed that the simulation results overestimated the RH results, which is the safe side for the model when evaluating mould growth risk.

Table 4.4. NRMSE, %, of temperature (t), partial pressure of water vapour (P_v) and relative humidity (RH) at each location examined in the test walls.

Wall ID	L2, between CLT and insulation			L3, between insulation and wind barrier		
	t	P_v	RH	t	P_v	RH
NRMSE, %						
EW 11 N	10	4	4	6	6	13
EW 12 N	3	3	4	5	5	11
EW 11 S	3	6	5	6	7	11
EW 12 S	4	5	6	5	7	9
EW 21 N	7	5	6	5	4	18
EW 22 N	8	5	10	5	4	16
EW 21 S	6	5	4	4	5	8
EW 22 S	4	4	5	4	5	10
EW 31 N	6	16	25	2	8	17
EW 32 N	4	7	8	1	9	14
EW 31 S	8	10	16	2	15	19
EW 32 S	3	5	7	2	15	18
EW 41 N	10	4	6	5	5	13
EW 42 N	7	7	6	4	5	13
EW 41 S	8	6	6	6	7	11
EW 42 S	5	4	5	5	6	11
EW 51 N	16	5	8	6	5	14
EW 52 N	10	4	5	4	5	11
EW 51 S	6	5	5	6	7	10
EW 52 S	5	4	5	5	6	11
Location L1, interior layer and CLT						
EW 41 N	5	11	12			
EW 42 N	6	6	7			
EW 41 S	7	20	11			
EW 42 S	4	10	11			
EW 51 N	13	16	19			
EW 52 N	11	11	15			
EW 51 S	6	22	28			
EW 52 S	3	10	18			

NRMSE ≤ 5 %-
 NRMSE 6-10 %-
 NRMSE 11-15 %-
 NRMSE 16-20 %-
 NRMSE >20 %-

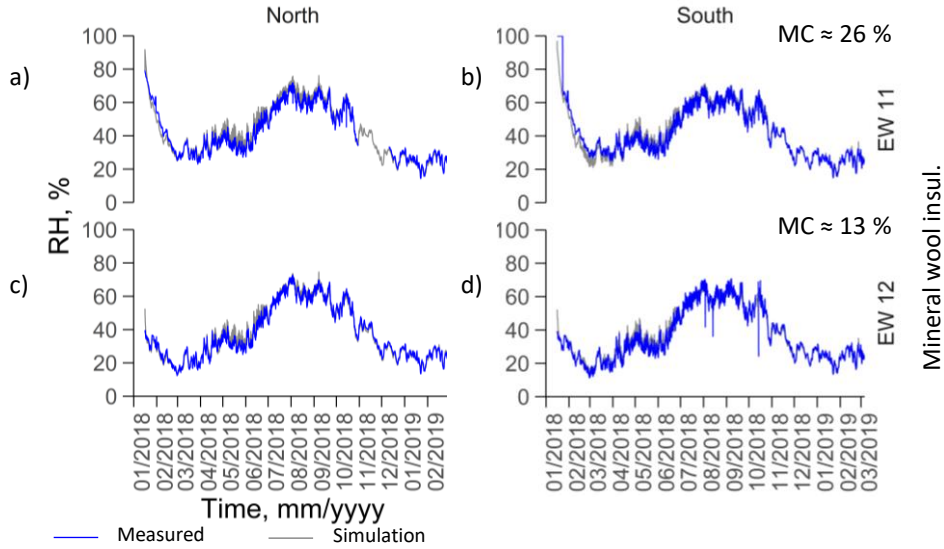


Figure 4.17. Measured and calculated RH between the CLT and the external insulation (L2) in type 1 test walls.

As an exception, there was a large difference in the NRMSE result of RH (16 and 25 %) and P_v (16 %) at location L2 for wall type 3 with high CLT initial MC (EW 31), see Figure 4.19 a, b. Also, it turned out most difficult to create a simulation model for wall type 3. Preliminary simulation results showed that RH remains stable between two materials with high water vapour resistance, PIR insulation and the CLT panel, see Figure 4.19 (preliminary calculation). However, the measured results showed a large variability of RH, influenced by the external climate. The reason was assumed to be the air gap between the PIR insulation and the plywood boards surrounding the test wall, which allowed a small air exchange as a stack effect. To confirm this, a 2D simulation model was developed and an air gap designed around the PIR insulation was connected to the outdoor (inside the ventilation gap VG, behind façade gladding FG) conditions, Figure 4.18. To achieve the best agreement of the 2D simulation results with the measurements, the width of the air gap had to be set to 3 mm. Air exchange was calculated from the difference between the outdoor temperature and the temperature between the CLT and the insulation. The hourly air exchange rate R_a was calculated according to Equation (13), (14), and (15) (Hagentoft 2001):

$$R_a = \frac{\Delta P_g}{S_g} \quad (13)$$

$$S_g = \frac{12\mu \cdot L}{b^2 \cdot A} \quad (14)$$

$$\Delta P_g = z \cdot 3.456 \cdot \left(\frac{1}{T_e} - \frac{1}{T_i} \right) \quad (15)$$

where ΔP_g (Pa) is a pressure loss inside the air gap, S_g (Pa·s/m³) – laminar airflow inside the air gap, b (m) – height of the gap, L (m) – length of the air channel, A (m²) – flow area perpendicular to the flow direction, μ (Ns/m²) – dynamic viscosity of air, z (m) – vertical distance of the air gap, T_e (°C) – hourly measured outdoor temperature (inside the VG), and T_i (°C) – hourly measured temperature between the CLT and the PIR insulation.

In the simulation, during the summer period, when the temperature difference is small, a constant of 10 1/h was set for the air exchange rate when the air exchange is dominated by the wind. The results of the 2D simulation with the air exchange rate of type 3 wall matched the measurements significantly better than in the preliminary simulation, see Figure 4.19. However, there were some major differences, especially in walls with high CLT initial MC (Figure 4.19 a, b).

The RH between the insulation and the wind barrier at L3 in type 3 walls was also greatly affected by air leakage. The preliminary simulation without air leakage showed stable RH results between 30 and 90 %. However, the final simulation with the air leakage showed a great variation of RH between 20 and 95 %, which is similar to the field measurement results. A close look (05-23 October 2018) at the field measurement results indicates a measuring sensor error (PUBLICATION V, Figure 12 d). During periods of condensation risk, RH jumps in sharp peaks to over 100 %, up to 108 %. However, the actual condensation should show a constant 100 % RH for a short time. The fact that the other three of the four type 3 test walls did not show any risk of condensation also indicates a measuring sensor error. Consequently, it can be said that real condensation on the surface of the wind barrier (L3) in the wall EW 32 North was rather unlikely.

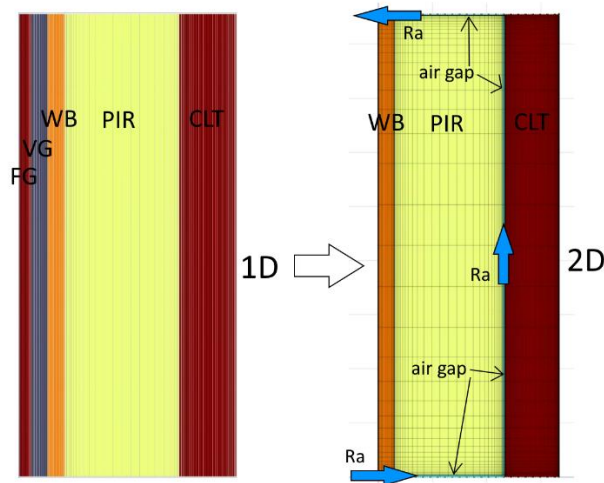


Figure 4.18. Initial 1D simulation model for test wall type 3 and final 2D model with air gaps.

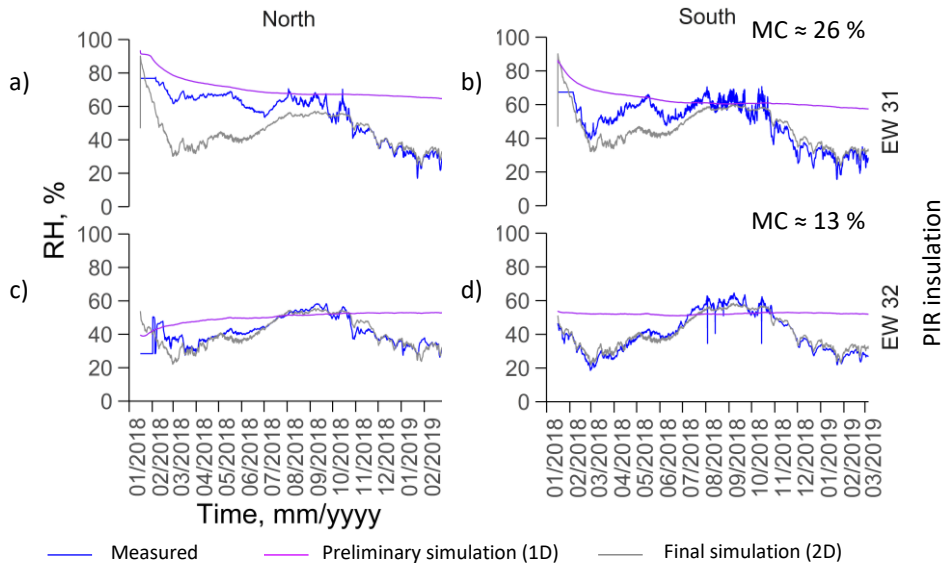


Figure 4.19. Measured and preliminary simulation (only moisture diffusion and capillary flow, without outdoor air leakage) and final simulation (with moisture diffusion and capillary flow, and outdoor air leakage) of RH between the CLT and the insulation (L2) in type 3 test walls.

Overall, the largest discrepancies occurred at location L3 where the majority of the NRMSE of the RH results were above 10 %, up to 19 %. However, the NRMSE values for temperature and pressure were low, see Table 4.4. The large discrepancy in the RH results can be attributed to the large fluctuation of the results due to solar radiation, see Figure 4.20.

At location L1, there were also some large discrepancies in the results, see Figure 4.21. The biggest difference was in the RH and P_v results in type 5 walls with high CLT initial MC (EW 51), see Figure 4.21 a, b and Table 4.4. RH results of type 5 southern wall in Figure 4.21 b show that above RH 80 %, the measurement results are compatible with the simulation and below 80 %, the simulated results keep a stable line, but the measurement results have dropped sharply. This suggests that there were small air leakages through the vapour barrier, which created uncertainty in the creation of the simulation model. The models of the other walls of type 5 also predicted a more stable result than the measurement results showed, but since the simulation results showed a higher RH, this is the safe side for the models (Figure 4.21 a, c, d). The figures show that the trend lines of the results are compatible, but the difference appears in the magnitude of the fluctuation of the results. A close look at the results (PUBLICATION V, Figure 13, 14, 15 and 16) shows that during spring the daily extremes of the measurement results are higher than in the simulation. In winter, the model underestimates the RH results by up to 5 %. The combination of two factors could have caused a large discrepancy during the cold period. First, the sensitivity analysis for finding the air exchange rate of the ventilation gap showed that the air exchange has an effect on the RH at L3. Second, there was also a larger difference between the temperature measurement and the simulation results between the CLT and the insulation (L2) during winter. This suggests that the

thermal resistance of the insulation may have been lower than expected. The heat flow was measured on the walls during field measurements, but due to the technical problems of the measuring device, the analysis of the results was incomplete.

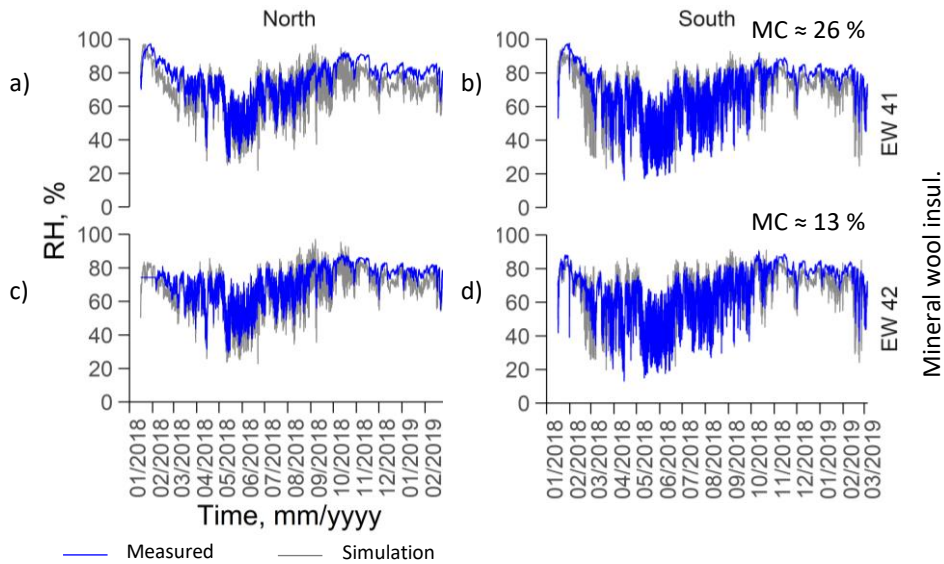


Figure 4.20. Measured and calculated RH between the insulation and the wind barrier (L3) in type 4 test walls.

At location L1, there were also some large discrepancies in the results, see Figure 4.21. The biggest difference was in the RH and P_v results in type 5 walls with high CLT initial MC (EW 51), see Figure 4.21 a, b and Table 4.4. RH results of type 5 southern wall in Figure 4.21 b show that above RH 80 %, the measurement results are compatible with the simulation and below 80 %, the simulated results keep a stable line, but the measurement results have dropped sharply. This suggests that there were small air leakages through the vapour barrier, which created uncertainty in the creation of the simulation model. The models of the other walls of type 5 also predicted a more stable result than the measurement results showed, but since the simulation results showed a higher RH, this is the safe side for the models (Figure 4.21 a, c, d).

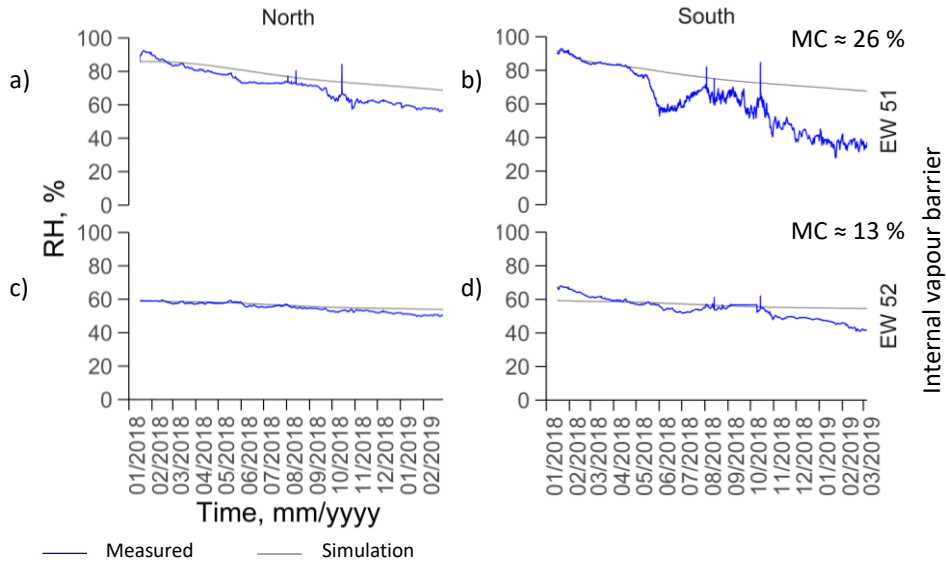


Figure 4.21. Measured and calculated RH between the CLT and the internal insulation (L1) in type 5 test walls.

In general, the vast majority of NRMSE results in the comparison of the measurement and simulation results were $\leq 10\%$ and the majority $\leq 5\%$. Several studies have used up to 10-15% NRMSE scale to evaluate the accuracy of simulation models (Cui, Zhang, and Janssen 2021; Magni et al. 2021; Tijskens, Roels, and Janssen 2018). The largest discrepancies in the measured and simulated RH results were between the insulation and the wind barrier (at location L3). Discrepancies occurred also in the RH and P_v results between the low vapour permeable layer and the CLT (type 3 walls between insulation and CLT (L2) and type 5 walls between the interior vapour barrier and the CLT (L1)). Based on the reasons for the discrepancies, limitations of this study were determined. One of the limitations is that the air exchange in the ventilation gap of the façade was not measured. The sensitivity analysis of the air exchange showed that the rate of the air exchange affects significantly the RH results between the wind barrier and the insulation. This is one of the reasons why the RH fluctuations caused by solar radiation were not estimated at high accuracy by the model. Larger discrepancies between the water low vapour permeable layers and the CLT were caused by air leakages. The limitations here are small side dimensions of the test walls; the use of low water vapour permeable materials in the CLT external walls could be studied in the future on a much larger scale. The impact of air and vapour leakages is smaller in larger-scale walls. Based on the NRMSE results in general and on the comparison of the measurement results and the simulation trend lines, it was concluded that the created simulation models were sufficiently adequate to be used in stochastic analysis (section 4.2.3.2).

The focus in this research was only on the exterior wall, and hygrothermal calculations were performed with 1D simulation models. However, several studies have indicated that the most problematic locations are the joint areas, especially the foundation and the external wall joint (Fedorik and Haapala 2017; Kalbe et al. 2020). Therefore, future research should focus on the impact of wet CLT dry-out on the hygrothermal performance of a particular 2D joint. Another important issue is the airtightness of the CLT envelope.

Several studies have shown that CLT alone may not perform as an airtight layer (Kukk et al. 2021; Kukk, Kalamees, and Kers 2019; Time 2020). Therefore, the stochastic analysis (section 4.2.3.2) also focused on the impact of additional vapour tightness (for airtightness purpose) on the hygrothermal performance of the CLT envelope.

4.2.3 Data analysis

4.2.3.1 Impact of interior layer properties on moisture dry-out of CLT external walls

The validated simulation models from the climate chamber test were used to calculate the maximum allowable MC of CLT panels in the two types of external wall assemblies: internally insulated with mineral wool having variable S_d (MW) and with vapour tight PIR. It was considered for simulations that different initial MC in the CLT panels were evenly distributed throughout the entire panel. Calculations for the mould index were made at the most critical point in the wall section for both wall assemblies, which located between the interior insulation and the CLT panel (L2). The criterion for acceptable wall performance was the following: during the five-year calculation period, no risk of mould growth, in other words, the maximum mould index during the calculation period could not exceed a value of 1 ($M < 1$, no mould growth). From Figure 4.22 b it can be seen that for wall assemblies having interior insulation with a variable vapour diffusion resistance (MW), the initial CLT MC of 17 % was the limit by which the mould growth index did not exceed 1 during the calculation period. For wall assemblies having interior insulation with a high vapour diffusion resistance (PIR), the initial CLT MC of 15 % was the limit for mould growth index not exceeding 1 during the calculation period (see Figure 4.22; b). Alev et al. found that the initial MC of logs in the external wall should be less than 14 % before adding interior insulation in the case where indoor moisture excess Δv does not exceed $< 2.5 \text{ g/m}^3$ in winter (2015); and should be less than 12 % in the case where moisture excess Δv is up to 4 g/m^3 in winter (2016).

The time at which the critical level of moisture content was considered to have dissipated was when the RH value dropped below 80 %, when the critical level for mould growth risk is avoided. With an initial MC of 15 %, the calculations showed that for wall assemblies having interior insulation with a variable vapour diffusion resistance (MW) and where the moisture could dry out to both directions (inside and outside), the RH dropped below 80 % within 6 weeks (see Figure 4.23, b). In wall assemblies having interior insulation with a high vapour diffusion resistance (PIR) and where the moisture could dry out to only one direction (towards to outdoor), the RH dropped below 80 % within 12 weeks (see Figure 4.23, a) with initial CLT MC of 15 %. The difference in moisture dissipation rate between the two wall assemblies is double. For MW wall assemblies having an initial CLT panel MC of 17 %, the RH dropped below 80 % within 17 weeks and with an initial MC of 20 %, the RH dropped within 22 weeks. In wall assemblies with PIR, the RH dropped below 80 % within 34 weeks with an initial MC of 17 % and within 64 weeks with an initial MC of 20 %. The dry-out time between the two wall assemblies is double with an initial CLT MC of 17 % and almost threefold with an initial CLT MC of 20 %.

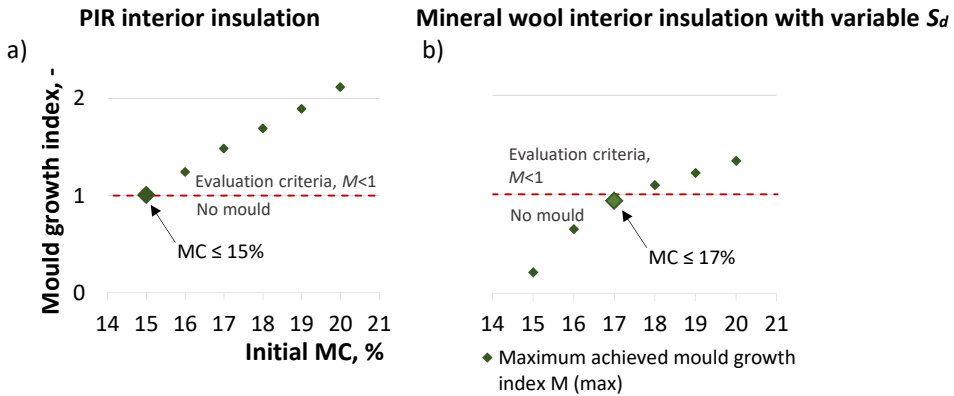


Figure 4.22. Maximum mould growth index in different initial MC of CLT panel in external wall assembly with vapour tight PIR interior insulation board (a) and with variable water vapour resistance interior mineral wool insulation board (b) during 5-year calculation period.

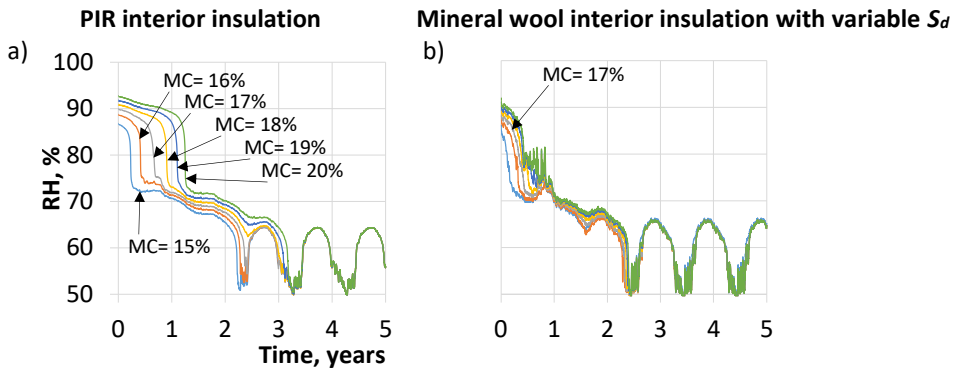


Figure 4.23. Relative humidity between interior insulation board and CLT (L2) in cases of different initial CLT MC in wall assemblies with vapour tight PIR interior insulation board (a) and with variable water vapour resistance interior mineral wool insulation board (b).

The critical moisture content of wood has previously been considered to be 20 %, above which there is a risk of mold growth (McClung et al. 2014). The results of this study showed that the risk of mould can occur even at a moisture content of less than 20 %. This means that the criteria for critical moisture content need further investigation. Although in Estonia the requirement for allowable level of MC for construction timber, strictly monitored for glue laminated timber, is between 8 to 15 %. This means that the wall assembly with PIR interior insulation meets the performance requirements without margin. The wall assembly with mineral wool interior insulation has a margin of only about 2 %. Therefore, it can be said that the use of interior insulation with a high vapour diffusion resistance in CLT walls should be undertaken with caution and only with effective supervision on the construction site. Use of effective supervision can also be recommended for use of wall assembly with mineral wool interior insulation because of the small margin of 2 % of MC. Alev and Kalamees (2016) found in their study that for vapour tight interior insulation used in log houses, the initial MC of the logs should be below 12 %. McClung et al. (2014) concluded that CLT panels with an interior membrane

with low-permeance of water vapour should be used with more caution because of the slower dry-out of CLT panels. The results of this study also showed the importance of having sufficient dry-out capacity towards both indoor and outdoor as use of vapour tight interior insulation can multiply the dry-out time of CLT by two or even more times.

4.2.3.2 Stochastic analysis

Hygrothermal performance of the CLT external wall types from the field measurements was evaluated by using a stochastic approach. The evaluation was done by simplified 1D validated simulation models (section 4.2.1.2) and the validated models were considered as base models.

Sensitivity analysis was performed prior to stochastic calculations to determine the month of the year when the CLT covering with external insulation and internal layers may pose the greatest risk of mould growth. Each month of the year (January-December) was selected as the starting point for the calculation of the mould growth index. The mould growth index in each wall type was calculated on the interior and exterior surface of the CLT panel and on the interior surface of the wind barrier. The continuous variables (highest CLT $MC_{CLT,ES/IS} = 28\%$, highest vapour resistance of the wind barrier $\mu_{WB} = 10$, etc.) that could cause the highest risk of mould growth were used in the calculations.

Most critical month to cover CLT with internal vapour tight layer (e.g., PIR insulation) was August and the smallest risk was in April (Figure 4.24, a). August was also the most critical month when CLT was externally covered with an additional air and vapour barrier and with vapour open insulation (Figure 4.24, b). The smallest risk was also in April. The most critical month to cover CLT with external vapour tight insulation (e.g., PIR insulation) was June and the smallest risk was in December (Figure 4.24, c). For the wind barrier installation, the most critical month was September and the smallest risk was in May (Figure 4.24, d). The risk of mould growth on the inner surface of the wind barrier can even be avoided by the timing of the CLT covering alone. If the wind barrier is installed in April or May, according to the sensitivity analysis, there is no risk of mould growth ($M < 1$). In all other locations, the mould growth index was above 1 in all cases.

Based on the results of sensitivity analysis, August was selected as the starting point in the stochastic calculations (see Table 4.5 and Table 4.6). Exception was made for the wall type EW3, which was externally insulated with vapour tight PIR insulation. June was selected as the starting point for wall type EW3. Also, in one scenario (with the lowest probability of performance), the risk of mould growth on the interior surface of the wind barrier was evaluated starting from September. In general, the results of the sensitivity analysis suggest that in the cold on humid climate, CLT panels should be installed and covered with the remaining wall layers in spring. Covering the CLT panel in summer carries the highest risk of mould growth, and summer is also the rainiest period in Estonia.

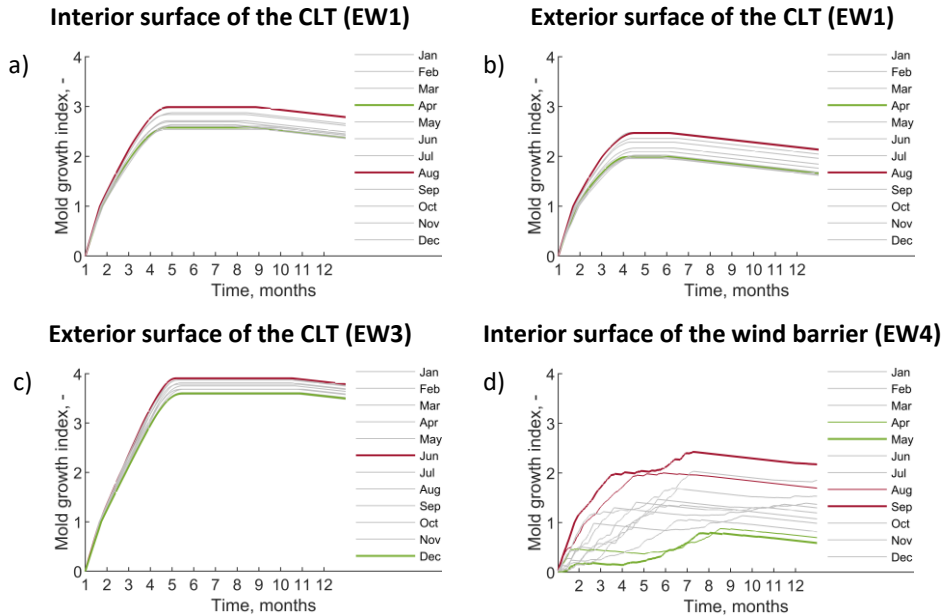


Figure 4.24. The influence of start of service life by month evaluated by the mould growth index.

Impact of additional air and vapour barrier: the results showed a clear difference between walls with uncovered and externally covered CLT panels with additional air and vapour barrier. External walls with CLT exposed to the indoor environment and externally insulated with vapour open ($S_d = 0.8$ m) insulation (e.g., mineral wool or cellulose insulation) had 100 % probability of safe hygrothermal performance, see Table 4.5 (EW1, 2 and 4, Scenarios 1-3). The addition of an air and water vapour barrier ($S_d = 2.3$ m) to the exterior surface of the CLT panel significantly decreased the probability. The probability of safe hygrothermal performance varied between 48 and 62 % in external walls of EW1, 2 and 4 having air and vapour barrier between CLT and external insulation (Scenarios 4-6), see Table 4.5.

A closer look at the results of the first year showed RH quick equilibrium in the walls without an additional air and vapour barrier (EW1, 2 and 4, Scenarios 1-3); all sub-scenarios reached the same level in almost half a year, see Figure 4.25, a. Quick equilibrium did not lead to a risk of mould growth on the CLT surface, see Figure 4.25, c. In contrast, a long equilibration occurred in the walls where an air and vapour barrier was added (Figure 4.25, b) and the maximum mould growth index in half of the sub-scenarios exceeded one, see Figure 4.25, d. A more detailed distribution of the maximum mould growth index is shown as a cumulative distribution, see Figure 4.26, a. The results of the mould growth index on the CLT external surface generally showed a short growing trend at the beginning of the calculations and after the index decreased for the rest of the calculation period, see Figure 4.25, d.

Table 4.5. The probability of safe hygrothermal performance (CLT as 'sensitive' and wind barrier 'medium resistant' to mould growth).

Scenarios	Wall type (starting point)												
	EW 1 (from August)		EW 2		EW 3 (from June)		EW 4			EW 5			
	L2	L3	L2	L3	L2	L3	L1	L2	L3	L1	L2	L3	
CLT thickness	The location where the mould risk was evaluated (L1 ^a , L2 ^b , L3 ^c) and mould growth sensitivity classes (S ^d , MR ^e)												
	S	MR	S	MR	S	MR	S	S	MR	S	S	MR	
Walls without additional air and vapour barrier													
S. 1	100 mm	100%	100%	100%	100%	32%	100%	100%	100%	100%	45%	100%	100%
S. 2	150 mm	100%	100%	100%	100%	33%	100%	100%	100%	100%	49%	100%	100%
S. 3	200 mm	100%	100%	100%	100%	34%	100%	100%	100%	100%	47%	100%	100%
CLT externally covered with additional air and vapour barrier													
S. 4	100 mm	55%	100%	54%	100%	30%	100%	100%	48%	100%	51%	58%	100%
S. 5	150 mm	59%	100%	58%	100%	30%	100%	100%	54%	100%	51%	52%	100%
S. 6	200 mm	62%	100%	53%	100%	32%	100%	100%	59%	100%	51%	62%	100%

^aL1- CLT interior surface, location between CLT and interior layer

^bL2- CLT exterior surface, location between CLT and external insulation/internal membrane

^cL3- wind barrier interior surface, location between external insulation and wind barrier

^dS- CLT as 'sensitive' to mould growth

^eMR- wind barrier as 'medium resistant' to mould growth

90-100%

80-89%

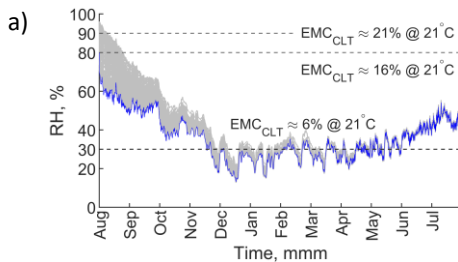
70-79%

60-69%

50-59%

<50%

EW4 without air and vapour barrier (S. 1)



EW4 with air and vapour barrier (S. 4)

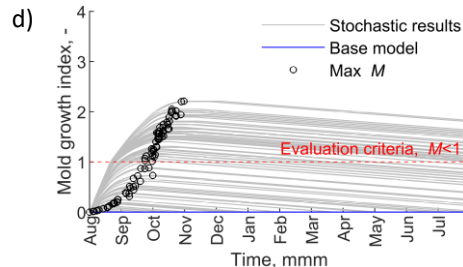
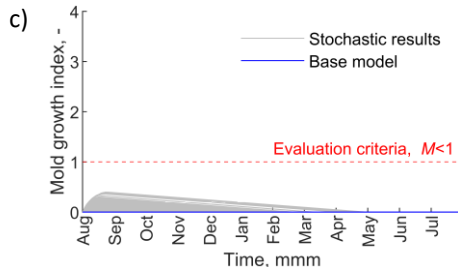
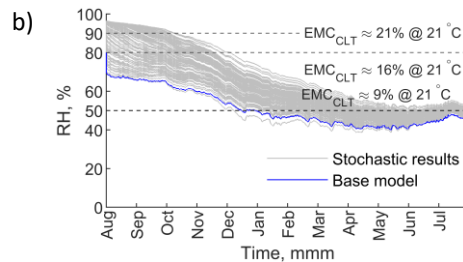


Figure 4.25. First year results of RH and mould growth index on CLT external surface (L2).

Partial correlation coefficient PCC results showed that the MC of the external surface (MC_{CLT_ES}) of the CLT alone had a significant impact (PCC > 0.5) on the mould growth index throughout the calculation period, see Figure 4.26, b. This means that the dry-out of the high MC and the moisture accumulating behind the air and vapour barrier is the main

cause of mould growth risk. The impact of the remaining studied material properties was insignificant. Therefore, the key factors in the safe hygrothermal design of the CLT external envelope are the sufficient dry-out capacity and the control of the CLT MC level during the construction phase.

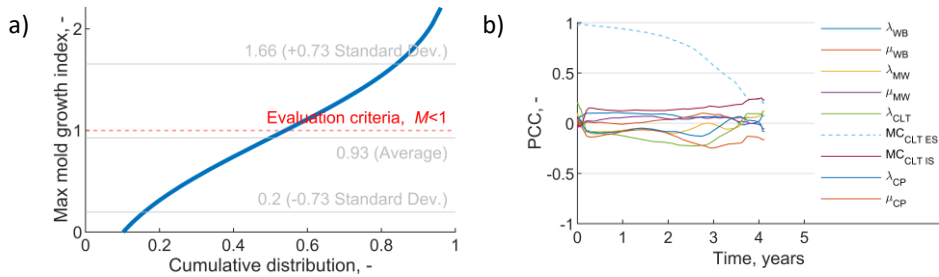


Figure 4.26. Cumulative distribution of the maximum mould growth index on the CLT external surface (a), and partial correlation coefficient between the observed material properties and the mould growth index of EW4 scenario 4.

It can be concluded that the addition of an air and vapour barrier ($S_d = 2.3$ m) makes the CLT external surface sensitive to mould growth at high CLT MC. In their study, Wang and Ge (2016) concluded that the use of a low vapour permeable water resistive barrier on the CLT external surface has a higher risk of moisture problems than a high water vapour permeable membrane. Kukk et al. (2019) found that the use of low vapour permeable ($S_d = 2.3$ m) membrane on the external surface of the mass timber panel prevents high humidity accumulation on the panel surface in the case of rainwater ingress during the service life. This confirms that low vapour permeable air and vapour barrier ($S_d = 2.3$ m) added on a wet CLT surface poses a high risk of mould growth. When installed on a dry surface (installed in the factory), it can also perform as a weather protection during the construction phase and can prevent moisture from spreading to the panel surface at rain leakage during service life.

Impact of wall assembly: externally insulated external walls with vapour tight PIR insulation (EW3) had a high risk of mould growth, regardless of the presence of an air and vapour barrier. The probability of safe hygrothermal performance varied between 30 and 34 %, see Table 4.5. This was due to the higher insulation vapour resistance rather than the air and vapour barrier ($S_{d_PIR} = 12$ m vs $S_{d_AVB} = 2.3$ m). Internally insulated external walls with vapour tight PIR insulation (EW5) had a high risk of mould as well. The probability of safe hygrothermal performance varied between 45 and 51 %, see Table 4.5.

External walls EW5, scenarios 4-6, were the only cases where CLT was covered with vapour tight layers both internally (PIR insulation) and externally (air and vapour barrier). There was a high risk of mould growth on both the interior and exterior surface, see Table 4.5. The probability of safe hygrothermal performance on the CLT interior surface was 51 % and on the exterior surface, it varied between 52 and 62 %. The PCC results of EW5, scenario 6, confirmed that the MC of the CLT surface has the greatest impact on mould growth. Importantly, the high CLT MC of the opposite surface did not affect the mould growth risk on the observed surface. The mould growth index on the CLT interior surface was significantly affected only by the MC of the interior surface, see Figure 4.27 (a), and vice versa, see Figure 4.27 (b). As the ambient conditions of the interior and exterior surface of the CLT panel in a closed external envelope are different, one surface does not affect the equilibrium of the other (Janzen and Swartman 1981). This means that if water vapour tight material layers are selected to cover the CLT panel, it is required for the

engineer to indicate in the project in which surface the material will be applied, along with a relevant notification to the constructor. This will simplify the preparation process of moisture safety planning of a CLT building during the construction phase and allows a constructor to find locations easily to monitor the CLT surface MC where its dry-out capacity is limited.

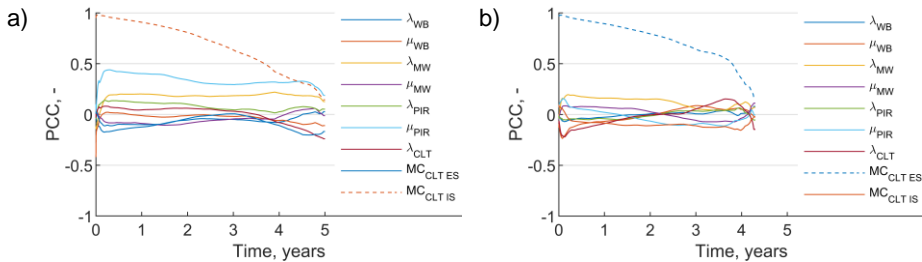


Figure 4.27. PCC between the observed material properties and the mould growth index in location L1 (a) and L2 (b) of EW5 scenario 6.

Impact of the construction phase: one of the limitations of this research was that the indoor boundary conditions for calculations started directly with the indoor environment of service life ($t_{i \min} = 22 \text{ }^\circ\text{C}$). This applies to small detached houses that are made of prefabricated elements and have a short construction phase, after which permanent heating can be applied immediately. In the case of larger buildings where the external building envelope is built on site, the indoor environment may still remain the same as the outdoor environment after installing the CLT panels on site, especially if construction starts in August. Alternatively, temporary heating can be applied for the construction phase to maintain a higher indoor temperature but still lower than service life temperature, e.g., $t_{i \min} = 15 \text{ }^\circ\text{C}$ (Kalbe et al. 2020).

A sensitivity analysis was performed to consider the effect of the indoor climate during the construction phase. We applied the indoor climate of the construction phase for the first 105 days, after which the calculation period continued with the service life of indoor climate ($t_{i \min} = 22 \text{ }^\circ\text{C}$). Four variants for the indoor climate of the construction phase were selected:

- 1) indoor and outdoor environment the same in the entire calculation period and without indoor moisture excess $t_i = t_e$, $\Delta v = 0 \text{ g/m}^3$ – indoor air exchange is ensured, windows and doors are not installed, see Figure 4.28 a, e;
- 2) indoor and outdoor environment the same, $t_i = t_e$ for the first 105 days with the indoor moisture excess in the range of $\Delta v = 0\text{-}2 \text{ g/m}^3$ – indoor without air exchange, windows and doors are installed, see Figure 4.28 b, h;
- 3) temporary heating applied to the indoor $t_{i \min} = 15 \text{ }^\circ\text{C}$ for the first 105 days with the indoor moisture excess in the range of $\Delta v = 0\text{-}2 \text{ g/m}^3$ – the presence of dehumidifiers, windows and doors are installed, see Figure 4.28 c, f, g;
- 4) temporary heating applied to the indoor $t_{i \min} = 15 \text{ }^\circ\text{C}$ for the first 105 days with the indoor moisture excess in the range of $\Delta v = 1\text{-}4 \text{ g/m}^3$ – dehumidifiers are missing, windows and doors are installed, see Figure 4.28 d.

Interior surface of CLT exposed to the indoor environment – indoor and outdoor environment the same and without indoor moisture excess, no mould growth within the first three months, see Figure 4.28 a. After the first three months, the mould growth index remained stable at 1, posing a small risk. Only factory-dry (Base model, MC = 13 %) CLT panel remained below 1. When moisture excess ($\Delta v = 0\text{-}2 \text{ g/m}^3$) was added, the risk

of mould growth occurred already after 48 days and reached a maximum mould index of 2, see Figure 4.28 b.

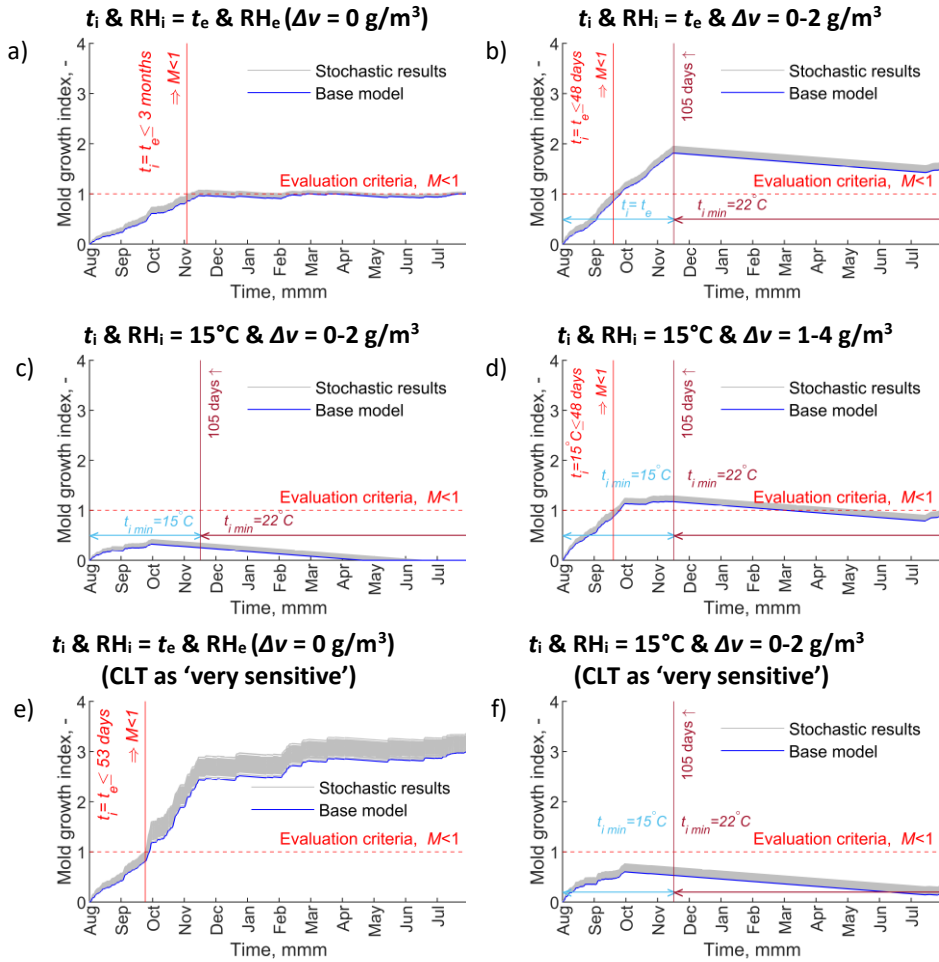
There was no risk of mould growth when temporary heating ($t_{i \min} = 15 \text{ }^\circ\text{C}$) was applied with a small moisture excess range ($\Delta v = 0\text{-}2 \text{ g/m}^3$), see Figure 4.28 c. The mould risk arose after 48 days when the moisture excess range was increased to $\Delta v = 1\text{-}4 \text{ g/m}^3$, see Figure 4.28 d. The risk of mould growth can also be avoided with temporary heating and low moisture excess range when CLT is considered as 'very sensitive' to mould, see Figure 4.28 f. However, as 'very sensitive' to mould, the CLT panel exposed to the outdoor environment ($t_i \text{ \& } RH_i = t_e \text{ \& } RH_e$) has a high risk of mould growth, which will increase in time, see Figure 4.28 e.

Exterior surface of CLT covered with vapour permeable insulation – variations in the results from the exterior surface of CLT were large and the MC had the biggest impact, see Figure 4.28 g, h. However, the risk of mould was still lower when temporary heating ($t_{i \min} = 15 \text{ }^\circ\text{C}$) was applied with a lower moisture excess range ($\Delta v = 0\text{-}2 \text{ g/m}^3$), see Figure 4.28 h.

Long-term storage of panels on the construction site and their exposure to the outdoor environment after installation can lead to the growth of mould on the panel surface. Olsson (2020a) monitored several CLT buildings in Sweden during the construction phase and from a total of 200 analysed measurement points he found that half had small growth and about a third had moderate or extensive mould growth on the CLT surface. In long-term storage, one of the possible ways to prevent mould growth on the CLT external surface is to maintain CLT as factory-dry by storing the panels water-tightly covered and by installing the CLT panels.

Secondly, in order to prevent the growth of mould on the CLT internal surface, it is highly recommended to apply temporary heating immediately after installation of the panels and to ensure a low indoor moisture excess ($\Delta v \leq 2 \text{ g/m}^3$) with air dehumidifiers.

The interior surface of CLT exposed to the indoor environment



The exterior surface of CLT (L2)

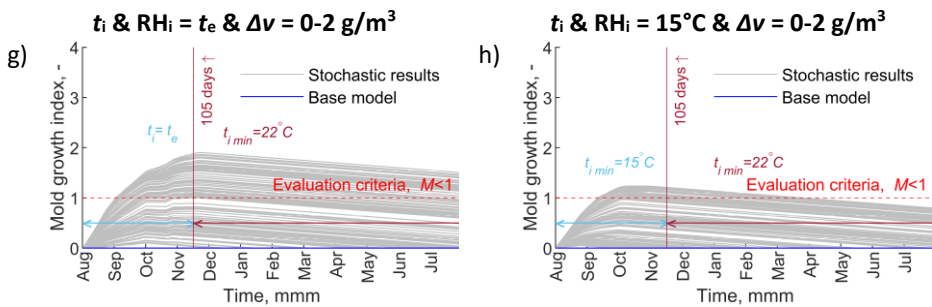


Figure 4.28. Risk of mould growth on the interior and exterior surface of the CLT (EW2) during the construction phase.

CLT as ‘very sensitive’ and the wind barrier as ‘sensitive’ to mould growth: the probability of safe hygrothermal performance decreased in all scenarios when CLT was considered as ‘very sensitive’ and the wind barrier as ‘sensitive’ to mould growth, see Table 4.6. The most significant change was observed on the interior surface of the wind barrier, especially in walls without additional air and vapour barrier. In the worst scenario (EW4, scenario 1), the probability decreased to 40 %. Figure 4.29, a, shows that the maximum mould growth index on the interior surface of the wind barrier (EW4, scenario 1) was achieved at the beginning of the calculation period. PCC results showed that vapour resistance of the wind barrier (μ_{WB}), MC of the CLT exterior surface (MC_{CLT_ES}) and thermal conductivity of the wind barrier (λ_{WB}) had significant impact ($PCC > 0.5$) on the mould growth index in the wind barrier surface, see Figure 4.29, b. In the case of high vapour resistance and thermal conductivity of the wind barrier, the high moisture excess causes the accumulation of moisture on the interior surface of the wind barrier, which in turn causes the risk mould growth, as shown by the positive results of PCC.

Table 4.6. The probability of safe hygrothermal performance (CLT as ‘very sensitive’ and wind barrier as ‘sensitive’ to mould growth).

Scenarios	Wall type (starting point)												
	EW 1 (from August)		EW 2		EW 3 (from June)		EW 4 (from August, *from September)			EW 5			
	The location where the mould risk was evaluated (L1 ^a , L2 ^b , L3 ^c) and mould growth sensitivity classes (S ^d , VS ^e)												
CLT thickness	L2	L3	L2	L3	L2	L3	L1	L2	L3*	L1	L2	L3	
	VS	S	VS	S	VS	S	VS	VS	S	VS	VS	S	
Walls without additional air and vapour barrier													
S. 1	100 mm	100%	64%	100%	64%	24%	100%	100%	100%	40%	38%	100%	55%
S. 2	150 mm	100%	52%	100%	65%	23%	100%	100%	100%	65%	36%	100%	64%
S. 3	200 mm	100%	86%	100%	60%	23%	100%	100%	100%	56%	38%	100%	60%
CLT externally covered with additional air and vapour barrier													
S. 4	100 mm	44%	95%	48%	97%	20%	100%	100%	41%	89%	43%	49%	97%
S. 5	150 mm	45%	91%	43%	94%	22%	100%	100%	47%	84%	42%	46%	95%
S. 6	200 mm	48%	99%	38%	96%	22%	100%	100%	51%	87%	38%	48%	97%

^aL1- CLT interior surface, location between CLT and interior layer

^bL2- CLT exterior surface, location between CLT and external insulation/internal membrane 90-100 %

^cL3- wind barrier interior surface, location between external insulation and wind barrier 80-89 %

^dS- wind barrier as ‘sensitive’ to mould growth 70-79 %

^eVS- CLT as ‘very sensitive’ to mould growth 60-69 %

50-59 %

<50 %

Pihelo et al. (2020) have reported that a paper coated gypsum board wind barrier with the mould sensitivity class of ‘sensitive’ is not recommended because of higher mould growth risk compared with the mineral wool-based wind barrier (‘medium resistant’). We recommend as well to select a wind barrier for the CLT external envelope with the mould sensitivity class at least ‘medium resistant’, e.g., mineral wool-based, since according to our calculations, there was no risk of mould growth.

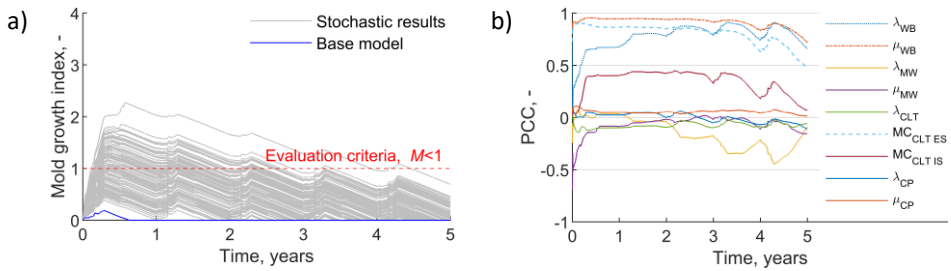


Figure 4.29. Mould growth index on the wind barrier internal surface (a) and PCC between the observed material properties and the mould growth index (b) on the internal surface of the wind barrier (L3) of EW4 scenario 1.

4.3 Hygrothermal design criteria

The hygrothermal criteria were set as limit values to ensure safe hygrothermal performance of each studied CLT external wall type from field measurements and stochastic analysis. The determination of the limit values was based on 100 % safe performance.

4.3.1 Parameter study

Stochastic analysis results showed that the hygrothermal performance of CLT external walls is most affected by the dry-out of the CLT surface MC. Therefore, the criteria were set for the CLT MC and the water vapour resistance of the material layers, which ensures the dry-out capacity of the external wall. Criteria for the CLT MC were set on both the interior (MC_{CLT_IS}) and exterior surfaces (MC_{CLT_ES}), see Table 4.7 and Table 4.8. Criteria for the water vapour resistance were set to the additional air and vapour barrier ($S_{d\ AVB}$), interior layer, e.g., clay plaster ($S_{d\ IL}$) and wind barrier ($S_{d\ WB}$). The impact of climate conditions during the construction phase was also considered.

4.3.1.1 The interior surface of CLT

The interior surface in external walls with CLT exposed to the indoor environment (EW1-3), the risk of mould growth on the CLT interior surface can be prevented when temporary heating is applied immediately after the installation of the panels. Therefore, the limit value was first set at $MC_{CLT_IS} \leq 28\%$ if the CLT interior surface is exposed to the outdoor environment for less than 3 months ($t_i = t_e$ and $\Delta v = 0\text{ g/m}^3 < 3\text{ months}$) before implementing permanent heating with $t_{i\ min} = 22\text{ }^\circ\text{C}$ (Figure 10 a) or temporary heating with $t_{i\ min} = 15\text{ }^\circ\text{C}$ (Figure 10 c) together with dehumidifiers ($\Delta v \leq 2\text{ g/m}^3$) applied immediately after the installation of the panels, see Table 4.7. In case CLT is considered as ‘very sensitive’ to mould growth, the exposing time before implementing permanent heating can only be less than 53 days, see Table 4.8.

The use of a water vapour permeable interior layer $S_{d\ IL} \leq 0.3\text{ m}$ (EW4) regardless of the mould sensitive class poses no mould risk as long as it is applied as a dry material, see Table 4.7 and Table 4.8. Layers applied as wet, e.g., clay plaster, require permanent indoor heating ($t_{i\ min} = 22\text{ }^\circ\text{C}$) for the time of application, see Table 4.7. In case CLT is regarded as ‘very sensitive’ to mould, its interior surface must be factory-dry $MC_{CLT_IS} \leq 13\%$ when the wet layer is applied, see Table 4.8.

Covering CLT internally with vapour tight PIR insulation (EW5) poses a mould growth risk even at low CLT MC, depending on whether the PIR insulation is covered or not and which coating material is used. PIR insulation without coating may pose a mould growth

risk when the CLT MC of the internal surface exceeds 18 % ($MC_{CLT\ IS} \leq 18\%$) regardless of its ambient environment, see Table 4.7. PIR covered with medium vapour resistance layers ($S_d < 1.65\ m$), e.g., paper coatings, poses mould risk when the MC exceeds 17 % ($MC_{CLT\ IS} \leq 17\%$), see Table 4.7. Vapour impermeable cover ($S_d > 800\ m$), e.g., aluminium foil, on PIR insulation poses mould risk when the CLT MC of the internal surface exceeds 16 % ($MC_{CLT\ IS} \leq 16\%$), see Table 4.7. If CLT is considered as ‘very sensitive’ to the mould growth, the limit values are $MC_{CLT\ IS} \leq 18\%$ (PIR without coating), $MC_{CLT\ IS} \leq 16\%$ (PIR coating $S_d < 1.65\ m$) and $MC_{CLT\ IS} \leq 15\%$ (PIR coating $S_d > 800\ m$) respectively, see Table 4.8.

In section 4.2.3.1 it was concluded that the critical MC in the external wall with vapour open mineral wool interior insulation is at $MC \leq 17\%$ and $MC \leq 15\%$ in the external wall with vapour tight interior PIR insulation. This means that in the case of vapour tight interior insulation, the factory-dry MC of CLT should be maintained.

4.3.1.2 The exterior surface of CLT

CLT externally insulated with vapour permeable ($S_d < 0.8\ m$) insulation, e.g., mineral wool or cellulose insulation (EW1, 2, 4 and 5), and without additional air and vapour barrier, poses no risk of mould growth on the external surface only when permanent heating ($t_{i\ min} = 22\ ^\circ C$) is applied immediately after the panels installation and closing the building envelope. Therefore, the criterion for the CLT exterior surface was set as $MC_{CLT\ ES} \leq 28\%$ ($t_{i\ min} = 22\ ^\circ C$). If the temporary heating is applied for 105 days, then the MC of the CLT external surface must be kept equal or less than $MC_{CLT\ ES} \leq 25\%$ ($t_{i\ min} = 15\ ^\circ C$). Without applying heating, the MC of the CLT external surface must be kept lower than $MC_{CLT\ ES} \leq 21\%$ ($t_i = t_e$), see Table 4.7. The limit values in case CLT is regarded as ‘very sensitive’ to the mould growth are $MC_{CLT\ ES} \leq 28\%$ ($t_{i\ min} = 22\ ^\circ C$) and $MC_{CLT\ ES} \leq 21\%$ ($t_{i\ min} = 15\ ^\circ C$) respectively, see Table 4.8.

Addition of an air and vapour barrier ($S_{d\ AVB} = 2.3\ m$) between vapour permeable insulation and CLT results in a significantly lower impact of the ambient environment of CLT, and the risk of mould is dominated by the MC. The calculations showed that the CLT MC of the external surface should not exceed $MC_{CLT\ ES} \leq 20\%$ to prevent the mould growth risk.

When CLT cannot be prevented from getting wet, the vapour resistance of an additional air and vapour barrier should be equal or less than $S_{d\ AVB} \leq 0.25\ m$, see Table 4.7. In this case, the criteria applied for the MC in the external walls (EW1, 2, 4 and 5) and without an additional barrier are the same: $MC_{CLT\ ES} \leq 28\%$ ($t_{i\ min} = 22\ ^\circ C$), $MC_{CLT\ ES} \leq 25\%$ ($t_{i\ min} = 15\ ^\circ C$) and $MC_{CLT\ ES} \leq 21\%$ ($t_i = t_e$), see Table 4.7. If CLT is considered as ‘very sensitive’ to mould growth, the limit values are $MC_{CLT\ ES} \leq 10\%$ or $S_{d\ AVB} \leq 0.05\ m$ respectively, see Table 4.8.

The use of vapour tight PIR external insulation poses a risk of mould growth on the CLT external surface at high initial MC and the criteria for the CLT MC of the external surface depend on the vapour resistance of the PIR coating; the impact of ambient environment is insignificant. PIR external insulation without coating poses a mould risk when the MC of the external surface exceeds 18 % ($MC_{CLT\ ES} \leq 18\%$), see Table 4.7. PIR covered with a medium vapour resistance layers ($S_d < 1.65\ m$) poses a mould growth risk on the external surface when its MC exceeds 17 % ($MC_{CLT\ ES} \leq 17\%$), see Table 4.7. Vapour impermeable cover ($S_d > 800\ m$), e.g., aluminium foil, on PIR insulation poses a mould risk when the CLT MC of the external surface exceeds 16 % ($MC_{CLT\ ES} \leq 16\%$), see Table 4.7. The limit values in case CLT is ‘very sensitive’ to the mould growth are $MC_{CLT\ ES} \leq 16\%$ (PIR without coating), $MC_{CLT\ ES} \leq 15\%$ (PIR coating $S_d < 1.65\ m$) and $MC_{CLT\ ES} \leq 15\%$ (PIR coating $S_d > 800\ m$) respectively, see Table 4.8.

4.3.1.3 The interior surface of the wind barrier

The criteria for the water vapour resistance of a wind barrier were determined on the basis of the wall type EW4 scenario 1. A 100 % probability of safe hygrothermal performance was achieved with a limit value of $S_{d\text{WB}} \leq 0.15$ m when the wind barrier is considered as ‘medium resistant’ to mould growth, see Table 4.7. If the wind barrier is ‘sensitive’ to mould growth, e.g., paper coated papers, the limit value for the water vapour resistance is $S_{d\text{WB}} \leq 0.03$ m, see Table 4.8 and Figure 4.30, a. The impact of the indoor environment during the construction phase is insignificant.

Table 4.7. Hygrothermal criteria for CLT external wall design (CLT as ‘sensitive’ and wind barrier ‘medium resistant’ to mould growth).

Wall type	The interior surface of the CLT	The exterior surface of the CLT		Wind barrier
		Without air and vapour barrier	Air and vapour barrier between CLT and insulation	
EW 1 CLT externally insulated with vapour permeable mineral wool	$MC_{CLT\text{IS}} \leq 28 \%$ $(t_i = t_e \text{ and } \Delta v = 0 \text{ g/m}^3 \text{ less than 3 months or } t_i = 15^\circ\text{C and } \Delta v \leq 2 \text{ g/m}^3)$ $MC_{CLT\text{IS}} \leq 13 \%$ $(t_i = t_e \text{ and } \Delta v = 0 \text{ g/m}^3 \text{ more than 3 months})$	$MC_{CLT\text{ES}} \leq 28 \%$ $(t_i = 22^\circ\text{C})$	$MC_{CLT\text{ES}} \leq 20 \%$ & $S_{d\text{AVB}} \leq 2.3 \text{ m}$ or $S_{d\text{AVB}} \leq 0.25 \text{ m}$ & $MC_{CLT\text{ES}} \leq 28 \%$ $(t_i = 22^\circ\text{C})$ or $MC_{CLT\text{ES}} \leq 25 \%$ $(t_i = 15^\circ\text{C})$ or $MC_{CLT\text{ES}} \leq 21 \%$ $(t_i = t_e)$	$S_{d\text{WB}} \leq 0.15 \text{ m}$
EW 2 CLT externally insulated with vapour permeable cellulose insulation		$MC_{CLT\text{ES}} \leq 25 \%$ $(t_i = 15^\circ\text{C})$		
EW 3 CLT externally insulated with low vapour permeable PIR insulation		$MC_{CLT\text{ES}} \leq 18 \%$ (PIR without coating) $MC_{CLT\text{ES}} \leq 17 \%$ (PIR coating $S_d < 1.65 \text{ m}$) $MC_{CLT\text{ES}} \leq 16 \%$ (PIR coating $S_d > 800 \text{ m}$)		
EW 4 CLT externally insulated with vapour permeable mineral wool and internally covered with vapour permeable clay plaster	$MC_{CLT\text{IS}} \leq 28 \%$ and $S_{d\text{IL}} \leq 0.3 \text{ m}$ $(t_i = 22^\circ\text{C only})$	$MC_{CLT\text{ES}} \leq 28 \%$ $(t_i = 22^\circ\text{C})$		
EW 5 CLT externally insulated with vapour permeable mineral wool and internally covered with low vapour permeable PIR insulation	$MC_{CLT\text{IS}} \leq 18 \%$ (PIR without coating) $MC_{CLT\text{IS}} \leq 17 \%$ (PIR coating $S_d < 1.65 \text{ m}$) $MC_{CLT\text{IS}} \leq 16 \%$ (PIR coating $S_d > 800 \text{ m}$)	$MC_{CLT\text{ES}} \leq 25 \%$ $(t_i = 15^\circ\text{C})$ $MC_{CLT\text{ES}} \leq 21 \%$ $(t_i = t_e)$		

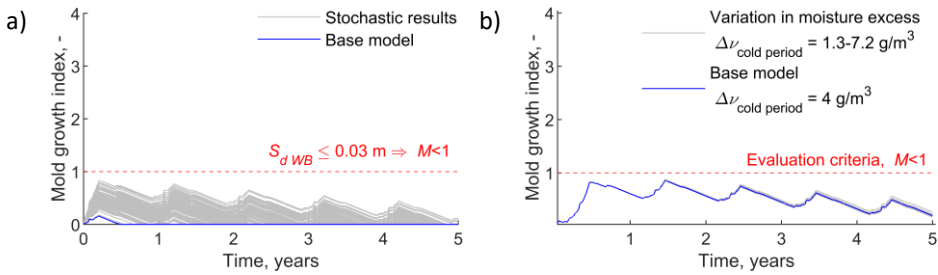


Figure 4.30. Mould growth index between the external insulation and the wind barrier (L3) in EW1 scenario 3 after the hygrothermal criteria are met (a) and sensitivity analysis with various indoor moisture excess values (b).

Table 4.8. Hygrothermal criteria for CLT external wall design (CLT as ‘very sensitive’ and wind barrier ‘sensitive’ to mould growth).

Wall type	The interior surface of the CLT	The exterior surface of the CLT		Wind barrier
		Without air and vapour barrier	Air and vapour barrier between CLT and insulation	
EW 1 CLT externally insulated with vapour open mineral wool	$MC_{CLT IS} \leq 28\%$ $(t_i = t_e$ and $\Delta v = 0 \text{ g/m}^3$ less than 53 days or $t_i = 15^\circ\text{C}$ and $\Delta v \leq 2 \text{ g/m}^3$)	$MC_{CLT ES} \leq 28\%$ $(t_i = 22^\circ\text{C})$	$MC_{CLT ES} \leq 18\%$ & $S_{d AVB} \leq 2.3 \text{ m}$ or $S_{d AVB} \leq 0.05 \text{ m}$ & $MC_{CLT ES} \leq 28\%$ $(t_i = 22^\circ\text{C})$	$S_{d WB} \leq 0.03 \text{ m}$
EW 2 CLT externally insulated with vapour open cellulose insulation			$MC_{CLT ES} \leq 21\%$ $(t_i = 15^\circ\text{C})$	
EW 3 CLT externally insulated with vapour tight PIR insulation		$MC_{CLT ES} \leq 16\%$ (PIR without coating) $MC_{CLT ES} \leq 15\%$ (PIR coating $S_d < 1.65 \text{ m}$) $MC_{CLT ES} \leq 15\%$ (PIR coating $S_d > 800 \text{ m}$)		$S_{d WB} \leq 0.15 \text{ m}$
EW 4 CLT externally insulated with vapour open mineral wool and internally covered with vapour open clay plaster	Dry internal cover: $MC_{CLT IS} \leq 28\%$ and $S_{d IL} \leq 0.3 \text{ m}$ $(t_i = 15^\circ\text{C}$ and $\Delta v \leq 2 \text{ g/m}^3$) Application of wet clay: $MC_{CLT IS} \leq 13\%$ and $S_{d IL} \leq 0.3 \text{ m}$ $(t_i = 22^\circ\text{C}$ and $\Delta v \leq 2 \text{ g/m}^3$)	$MC_{CLT ES} \leq 28\%$ $(t_i = 22^\circ\text{C})$ $MC_{CLT ES} \leq 21\%$ $(t_i = 15^\circ\text{C})$	$MC_{CLT ES} \leq 18\%$ & $S_{d AVB} \leq 2.3 \text{ m}$ or $S_{d AVB} \leq 0.05 \text{ m}$ & $MC_{CLT ES} \leq 28\%$ $(t_i = 22^\circ\text{C})$ or $MC_{CLT ES} \leq 21\%$ $(t_i = 15^\circ\text{C})$	$S_{d WB} \leq 0.03 \text{ m}$
EW 5 CLT externally insulated with vapour open mineral wool and internally covered with vapour tight PIR insulation	$MC_{CLT IS} \leq 18\%$ (PIR without coating) $MC_{CLT IS} \leq 16\%$ (PIR coating $S_d < 1.65 \text{ m}$) $MC_{CLT IS} \leq 15\%$ (PIR coating $S_d > 800 \text{ m}$)			

In addition, we performed a sensitivity analysis to determine the effect of indoor moisture excess. For this purpose, 10 moisture excess models were formed as a normal distribution. The model by Ilomets (2017) with a cold period moisture excess of 4 g/m^3 was used as the mean value for the normal distribution, the same that was used for creating the indoor RH boundary condition of this study. Moisture excess of $\pm 1.5 \text{ g/m}^3$ in the cold period was used as the standard deviation. The moisture excess values of the models in the cold period varied between 1.3 and 7.2 g/m^3 . The results showed that the indoor moisture excess has an insignificant effect on the risk of mould growth on the interior surface of the wind barrier, see Figure 4.30, b.

4.3.2 Variations in hygrothermal criteria

According to the North American standard ASHRAE 160 (2016), the mould growth index on the building material surface should not exceed 3 to avoid the mould growth problem. VTT in collaboration with IBP (Viitanen et al. 2015) have proposed the criteria as “Traffic light classification”: in interior spaces, the green light as no mould growth risk is up to mould index 1, yellow light as a small risk is between 1 and 2 and red light is above index 2. In surfaces that are not in contact with indoor air, the green light is up to mould index 2, yellow between 2 and 3 and red above 3.

The comparison with other criteria in Table 4.9 shows that the limit values differ greatly when different criteria are applied. The largest differences in the limit values occur for the CLT external surface covered with additional air and vapour barrier and externally insulated with vapour open insulation (EW1, 2, 4 and 5). For example, according to the ASHRAE standard 160-2016 criteria ($M < 3$), the high CLT moisture content of the external surface does not pose a moisture problem, but compared to our criteria ($M < 1$), the moisture content of the external surface must be kept low ($\leq 20 \%$).

When using vapour tight PIR insulation, the moisture content of the CLT internal and external surface must be kept low for all criteria, but the limit values still vary greatly ($MC_{CLT ES} \leq 16 \%$ vs $\leq 19 \%$ vs $\leq 22 \%$). The difference between the limit values for the vapour resistance of the wind barrier ($S_{d WB}$) is large as well, varying from $\leq 0.03 \text{ m}$ to $\leq 0.15 \text{ m}$.

Table 4.9. Hygrothermal criteria at different mould growth index ranges (CLT and wind barrier as ‘sensitive’ to mould growth).

Location wall type	$M < 1$	$1 < M < 2$	$2 < M < 3$
External walls with additional air and vapour barrier and with vapour open external insulation EW 1,2, 4 & 5	$MC_{CLT ES} \leq 20 \%$ or $S_{d AVB} \leq 0.25 \text{ m}$	$MC_{CLT ES} \leq 25 \%$ or $S_{d AVB} \leq 1.3 \text{ m}$	$MC_{CLT ES} \leq 28 \%$ or $S_{d AVB} \leq 2.3 \text{ m}$
External walls with vapour tight PIR external insulation EW 3	$MC_{CLT ES} \leq 18 \%$ (PIR without coating) $MC_{CLT ES} \leq 17 \%$ (PIR coating $S_d < 1.65 \text{ m}$) $MC_{CLT ES} \leq 16 \%$ (PIR coating $S_d > 800 \text{ m}$)	$MC_{CLT ES} \leq 20 \%$ (PIR without coating) $MC_{CLT ES} \leq 20 \%$ (PIR coating $S_d < 1.65 \text{ m}$) $MC_{CLT ES} \leq 19 \%$ (PIR coating $S_d > 800 \text{ m}$)	$MC_{CLT ES} \leq 23 \%$ (PIR without coating) $MC_{CLT ES} \leq 23 \%$ (PIR coating $S_d < 1.65 \text{ m}$) $MC_{CLT ES} \leq 22 \%$ (PIR coating $S_d > 800 \text{ m}$)
Wind barrier EW 1, 2, 4 & 5	$S_{d WB} \leq 0.03 \text{ m}$	$S_{d WB} \leq 0.08 \text{ m}$	$S_{d WB} \leq 0.15 \text{ m}$

4.3.3 Use of hygrothermal criteria in practice

The hygrothermal criteria are intended for engineers, constructors, manufacturers, clients – for anyone involved in the construction of CLT buildings to help ensure moisture safety during construction. Figure 4.31 shows a simplified decision flow describing how the engineer and constructor can apply criteria while designing or installing a CLT external envelope.

The first decision is made on weather protection – will the CLT building external envelope be fully weather protected during construction? When opting for full weather protection, it can be assumed that the CLT panels will remain factory-dry ($MC_{CLT ES} = 15\%$). This is followed by the question – does CLT in the external envelope have at least 5 layers? It was concluded in section 4.1.1.3 that a 5-layer CLT panel can be considered as an airtight layer, but a 3-layer panel requires an additional airtight layer. Time (2020) concluded the same in her study. Lastly, the vapour resistance of the wind barrier used in the external envelope should not exceed $S_{d WB} \leq 0.03$ m. If the requirements are met in the case of full weather protection, the CLT envelope can be considered moisture safe.

The probability of CLT getting soaked is high when the full weather protection is not applied (Olsson 2021) and an additional air and vapour barrier layer is required first. In section 4.1.2 it was concluded that the 5-layer CLT panel can be considered as an air-tight layer as long as its factory-dry moisture content is maintained during construction. The next question is – is the external insulation vapour open ($S_d \leq 0.8$ m), e.g., mineral wool and cellulose wool? This determines which criteria apply to the CLT external surface and the wind barrier, see Table 4.7. During the construction phase, it must be confirmed whether the requirements are met. If not, additional dry-out methods are required before the CLT panels are covered with the rest of the material layers. The next question is – is the CLT panel internally covered? This determines which criteria apply to the CLT internal surface, see Table 4.7.

The simplified decision flow (Figure 4.31) indicates first the complexity of ensuring moisture safety of a CLT building during the construction phase if all the requirements for full weather protection are not applied. Secondly, on the other hand, to what extent, the use of full weather protection simplifies the moisture safety supervision on construction. However, implementing full weather protection can be very costly and complicate/prolong the construction process in general. For example, building under a tent limits the selection and use of lifting equipment. Therefore, using the hygrothermal criteria for CLT external wall design, parties involved in the construction of CLT buildings (engineers, constructors, manufacturers, clients) can decide which measures to use for moisture safety, considering both cost-effectiveness, complexity and time. Kalbe et al. (2020) identified most critical joints of CLT building in the point of view of moisture safety and proposed solutions to protect CLT from wetting in the absence of full weather protection. The research concluded that with adequate preparation in design and production, weather protection can be achieved even without large-scale temporary coating, e.g., a tent covering the building, and other wall layers apart from CLT can also be used for weather protection, e.g., additional air and vapour barrier. This also confirms the importance of the hygrothermal criteria and the feasibility of using them in the preparation of weather protection for large-scale buildings where the use of a large-scale tent may be difficult.

◇ -Decision/condition $S_{d\text{ WB}}$ - vapour resistance of wind barrier $MC_{\text{CLT ES}}$ - moisture content of CLT external surface
 -Requirements $S_{d\text{ AVB}}$ - vapour resistance of air and vapour barrier $MC_{\text{CLT IS}}$ - moisture content of CLT internal surface
 $S_{d\text{ IL}}$ - vapour resistance of internal cover layer

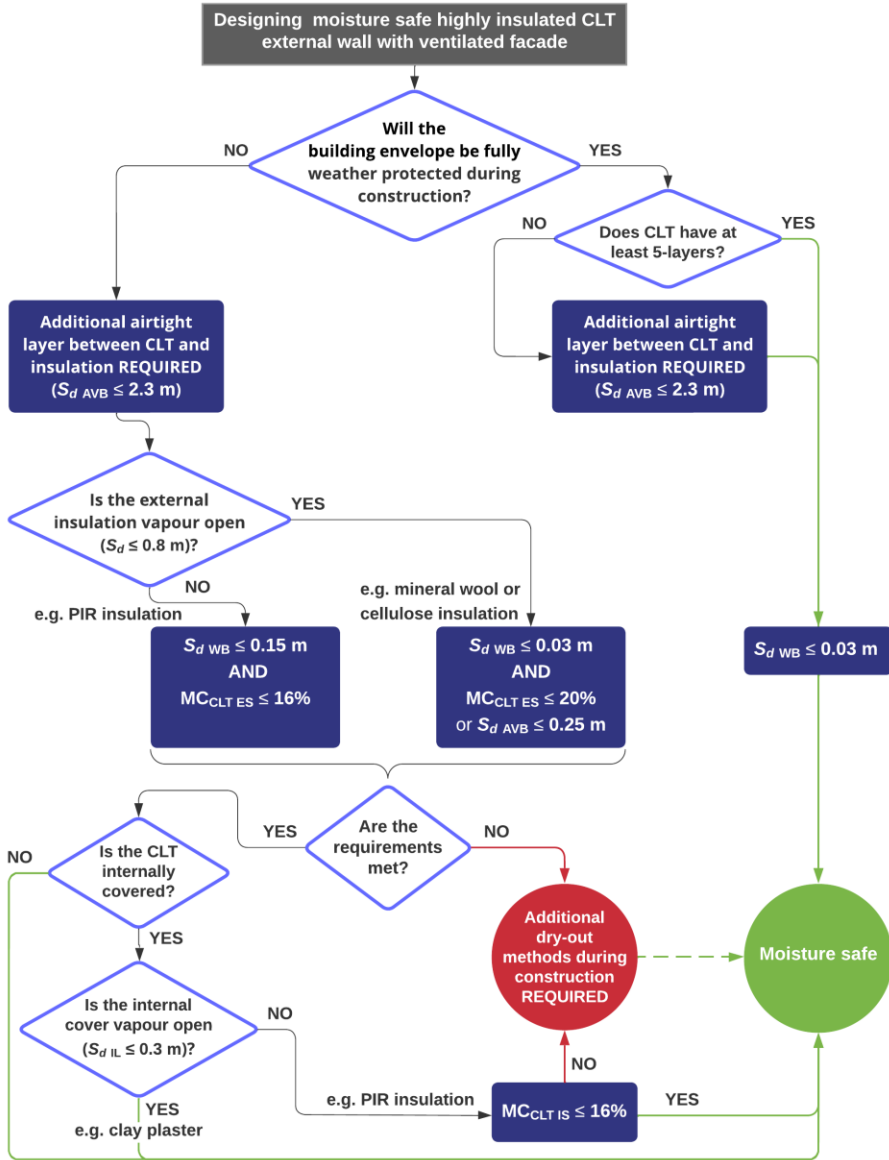


Figure 4.31. Simplified decision flowchart based on the hygrothermal criteria for CLT external wall design.

5 Conclusions

In this thesis the importance of low MC of CLT panel I during the construction phase to minimise the moisture damage risks was studied. The main objective of the thesis was to determine hygrothermal performance criteria for CLT external wall that are applicable to secure the air-tightness and moisture safety of the building envelope considering the design, production technology and built-in moisture of the CLT panel.

For that purpose several CLT wall designs were developed and their hygrothermal performance was experimentally tested. To analyse and simulate the CLT wall hygrothermal performance several simulation models were developed and the results validated by on-site data collection during the experiments. It was discovered that in addition to air leakages, built-in moisture in the CLT panel is the greatest risk that causes moisture damages in the external wall. The hygrothermal criteria were set as limit values to ensure safe hygrothermal performance of each studied CLT external wall type from field measurements. The determination of the limit values was based on 100% safe performance according to the stochastic analysis.

The data analyses showed that the key factors in the safe hygrothermal design of the CLT external wall are the sufficient dry-out capacity and the control of the CLT MC level during the construction phase. Based on the research objectives and obtained research results of the current study, the following conclusions are drawn.

The studied CLT external wall design and boundary conditions are applicable for the countries that locate in the regions of cold and humid climate.

The results of this research are applicable for the CLT external walls with ventilated cavity only.

The hygrothermal criteria for CLT external walls apply only within the ranges of variations in material properties shown in Figure 3 as uniformly distributed continuous random variables.

5.1 Air leakages in the CLT panel and external wall

- The variation of MC of CLT panels plays an important role in crack formation in the panel's laminations.
- Larger cracks occur on the CLT panel surface during the service life if the panels are pre-stored in a humid (RH > 90 %) environment compared to panels that have not been exposed to major environmental changes after production.
- Analysis of the shape and location of the cracks in the CLT panel revealed that the arrangement of formed cracks in the panel layers can be aligned, which in turn causes the crack (hole) to form through the thickness of the panel. A penetrating crack (hole) through the thickness of the panel is a source of air leakage. The size of the crack significantly affects the size of the air leakage with increasing pressure difference.
- The seasonal change in the indoor environment in cold and humid climate (RH varying from 70-20 %) affects the crack formation and airtightness of the CLT panel.

- Five-layer specimens combined with initially drier laminations had the most considerable effect on avoiding air leakages through the panel. A single middle layer is not sufficient to prevent air leakage through the cracks in the top layers and therefore 3-layer CLT panel may require an additional airtight layer. It was found that at least three middle layers (total 5 layers) are sufficient for ensuring the airtightness of CLT panels as the probability of crack formation through panel thickness is minimal.
- The effect of a change in indoor RH is small compared to the impact of built-in moisture.
- The high initial moisture content of the CLT panel significantly weakens the airtightness of the CLT external wall. CLT exposure to water during the construction is not only a risk of moisture damage and therefore the implementation of moisture safety during the construction of CLT buildings is essential if the CLT is to be considered as an airtight layer.
- The 5-layer CLT panel can be used as an air-tight layer in external wall construction as long as its initial low moisture content (about 13 %) is maintained. The type of insulation material and wall orientation has not a major effect on the airtightness of the CLT external walls.
- The insulation layer cannot be considered as an airtight layer in CLT external walls because usually the insulation is not airtight or the method of installation (PIR insulation) does not ensure sufficient airtightness.

5.2 Hygrothermal performance of CLT external walls

- The use of interior insulation in the CLT external wall poses a risk of mould growth when the CLT panel has been exposed to the built-in moisture (initial MC >20 %).
- The initial MC of CLT panel should not exceed 17 % before covering with the mineral wool interior insulation with varying vapour resistance ($S_d \approx 13 \text{ m @ RH } 20 \%$ and $S_d \approx 0.5 \text{ m @ RH } 80 \%$).
- The initial MC of CLT panel in external wall should not exceed 15 % before covering with the vapour tight PIR interior insulation ($S_d > 800 \text{ m}$ when covered with aluminum foil). Higher initial moisture content of CLT than the given limit values may pose a risk of mould growth on the CLT surface.
- CLT panel is capable of sufficient water vapour diffusion control in the external walls with ventilated facades in the cold and humid climate.
- Neither did the high levels of insulation (thermal transmittance of $U = 0.1 \text{ W/(m}^2 \cdot \text{K)}$) in the studied external walls and indoor humidity load for office and low occupancy dwellings (moisture excess of $\Delta v_{\text{tes} \leq 0^\circ \text{C}} = 3 \text{ g/m}^3$) in the cold period cause any critical moisture (condensation or mould growth) risk on the interior surface of the wind barrier.
- The high moisture content in the thin surface layer of the CLT panel may not pose mould growth risk in CLT external wall when dry-out time is short.
- The cellulose insulation compared to mineral wool has the advantage of keeping RH at a lower level between the exterior insulation and the wind barrier. Therefore, cellulose insulation can be a safer choice from the point of view of hygrothermal performance when selecting water vapour permeable insulation for the external wall.

- The use of low vapour permeable PIR external insulation can ensure stable and low RH (varying between 40 and 60 %) when low MC of CLT (MC ≈13 %) is maintained as was concluded from preliminary simulation of moisture diffusion (without outdoor air leakage). A minor air circulation with the outdoor air between the vapour tight PIR insulation and the CLT may increase significantly the RH fluctuations on the exterior surface. Only airtightly installed vapour tight insulation can be beneficial if the low moisture content of the CLT panel (factory-dry) during construction is maintained.
- The orientation (north and south) of the walls have no significant effect on the hygrothermal performance of the studied external walls with outdoor ventilated façade.

5.3 Hygrothermal design criteria

The following conclusions were made for consideration prior to design:

- In the cold and humid climate conditions, the installation and construction time of the CLT panels can have impact to the mould growth. For example, the cover of CLT panels with the remaining wall layers in spring (April-May) has a smaller risk of mould growth than covered in late summer (August-September). Installation of vapour open wind barrier in April or May can prevent the risk of mould growth alone.
- The long-term storage (>3 months) of the panels on the construction site exposed to the outdoor environment after the installation can lead to high risk of mould growth on the CLT surface.

The following conclusions were made for consideration when designing a CLT external envelope:

- In case full weather protection is used during the construction phase of a CLT building, a 5-layer CLT panel can be considered as an airtight layer, but a 3-layer panel requires additional airtight layer in the external envelope. The vapour resistance of the wind barrier should be $S_{d\text{WB}} \leq 0.03$ m with thermal resistance of $R \leq 0.075$ (m²·K)/W to prevent the risk of mould growth.
- It is recommended to select a wind barrier for the CLT external envelope with the mould sensitivity class at least 'medium resistant', e.g., mineral wool-based materials, because of no risk of mould growth according to our calculations.
- In case the CLT envelope will not be fully weather protected during the construction phase:
 - An additional air and vapour barrier layer is required as a 5-layer CLT panel can be consider as an air-tight layer only if its low MC (about 13 %) is maintained.
 - Use of an additional air and vapour barrier ($S_{d\text{AVB}} = 2.3$ m) decreases significantly the dry-out capacity of CLT and may pose high risk of mould growth at high initial MC. When installed on a dry surface, it can perform as a weather protection.
 - When selecting water vapour permeable materials for external insulation (e.g., mineral wool and cellulose wool), the following criteria were set to prevent mould growth risk: water vapour resistance of the wind barrier should not exceed $S_{d\text{WB}} \leq 0.03$ m; CLT initial MC of the

external surface should not exceed $MC_{CLT\ ES} \leq 20\%$ or vapour resistance of an additional air and vapour barrier should not exceed $S_{d\ AVB} \leq 0.25\ m$.

- In the case of vapour tight external insulation (e.g., PIR insulation), the water vapour resistance of the wind barrier should not exceed $S_{d\ WB} \leq 0.15\ m$ and the CLT initial MC of the external surface should not exceed $MC_{CLT\ ES} \leq 16\%$ to prevent mould growth risk on the CLT external surface.
- When the CLT internal surface is exposed to the indoor environment, at least temporary heating ($t_{i\ min} = 15^\circ C$) together with dehumidifiers should be applied within three months after the CLT panels have been installed to prevent the growth of mould on the internal surface during the construction phase.
- The results from stochastic analysis showed that when the CLT is internally covered with vapour tight insulation (e.g., PIR insulation), the initial MC of the internal surface should not exceed $MC_{CLT\ IS} \leq 16\%$ to prevent the mould growth risk. In the data analysis of climate chamber test results it was found that the initial MC of the CLT panel should not exceed $MC_{CLT} \leq 15\%$ when CLT is considered as 'very sensitive'. The overall recommendation is to avoid the initial MC of CLT to exceed 15% when covering with the vapour tight interior insulation.
- Covering the CLT internally with the vapour open layer, e.g., clay plaster, there are no requirements set for the MC of the internal surface. However, when applying the wet clay plaster, permanent heating ($t_{i\ min} = 22^\circ C$) must be ensured indoors.
- The mould growth risk on the observed CLT surface due to the high CLT MC is not affected by the MC on the opposite surface of the CLT. If CLT panels are covered with water vapour tight layers, the engineer should indicate in the project the surface that it will be applied to. This allows the constructor to find locations easily to monitor the CLT surface MC where its dry-out capacity is limited.

CLT thickness was found to have no significant impact on the mould growth risk since the MC of one surface does not affect the other.

6 Future studies

All measurements related to the air permeability properties of the CLT panels and external walls were performed with small-scale specimens (section 4.1.1). One of the limitations when determining the air leakages in the CLT external wall was also the measuring range of the equipment (section 4.1.2), due to which it was not possible to measure the maximum air leakages of the CLT external test walls with a high initial MC. Thus, there was no direct comparison of the air leakage values for the external walls with different initial CLT moisture content. On the contrary, the equipment used was selected to study the airtightness of the test walls in a low-leakage area (up to $0.9 \text{ m}^3/(\text{m}^2\text{h})$) and the accuracy of the results would have been significantly lower over a larger range. For more accurate studies on the air permeability properties of the CLT external building envelope, it is recommended to make measurements in a real building to study the effect of changes in the indoor RH and the built-in moisture.

The stochastic analysis of this research (section 4.2) was also limited to CLT external walls with a ventilated façade. External thermal insulation composite system (ETICS) in a timber structure external envelope has not been recommended as a solution because of high risk of moisture damage (Samuels et al. 2008). On the other hand, it has been considered as a more cost-effective alternative to a ventilated façade as well as a hygrothermally safe solution when using vapour open insulation materials (Günther, Ringhofer, Schickhofer 2016; Kukk, Kers, et al. 2019). Therefore, a future study should further explore ETICS solutions for mass timber structures using stochastic analysis.

The results from the stochastic analysis were obtained through simplified 1D calculations. This eliminates small features such as air leakages and rain intrusion. In section 4.2.1.2, a small air exchange between the PIR insulation and the CLT panel is described that significantly decreased the moisture accumulation from dry-out of CLT on the PIR insulation surface. Wang and Ge (2016) concluded that the rain leakage in the external wall has a significant impact on the increase of the CLT MC during the service life in case vapour tight layers are externally covering the CLT. Therefore, future studies should use 2D calculations to evaluate the impact of additional features such as air and rain leakage on the hygrothermal criteria.

References

- Absetz, Ilmari. 1993. "Sorption Isotherm and Moisture Diffusivity Comparison of Spruce and Pine." in *Seminarium i trämekanik, Borås October 28-29, 1993*. Borås: Statens provningsansvalt.
- Alev, Üllar and Targo Kalamees. 2016. "Avoiding Mould Growth in an Interiorly Insulated Log Wall." *Building and Environment* 105:104–15.
- Alev, Üllar, Andres Uus, and Targo Kalamees. 2015. "Comparison of Mineral Wool, Cellulose and Reed Mat for Interior Thermal Insulation of Log Walls." *Journal of Civil Engineering and Architecture Research* 2:938–46.
- Alev, Üllar, Andres Uus, Marko Teder, Martti-Jaan Miljan, and Targo Kalamees. 2014. "Air Leakage and Hygrothermal Performance of an Internally Insulated Log House." in *10th Nordic Symposium on Building Physics*. Lund, Sweden.
- AlSayegh, George. 2012. "Hygrothermal Properties of Cross Laminated Timber and Moisture Response of Wood at High Relative Humidity." Carleton University.
- Arumägi, Endrik, Simo Ilomets, Targo Kalamees, and Tanel Tuisk. 2011. "Field Study of Hygrothermal Performance of Log Wall with Internal Thermal Insulation." Pp. 1–9 in *XII DBMC 12th International Conference on Durability of Building Materials and Components, 12th - 15th April 2011, Porto, Portugal*. Porto, Portugal.
- Arumägi, Endrik, Margus Pihlak, and Targo Kalamees. 2015. "Reliability of Interior Thermal Insulation as a Retrofit Measure in Historic Wooden Apartment Buildings in Cold Climate." *Energy Procedia* 78:871–76.
- Asdrubali, F., B. Ferracuti, L. Lombardi, C. Guattari, L. Evangelisti, and G. Grazieschi. 2017. "A Review of Structural, Thermo-Physical, Acoustical, and Environmental Properties of Wooden Materials for Building Applications." *Building and Environment* 114:307–32.
- ASHRAE. 2016. *ANSI/ASHRAE 160-2016. Criteria for Moisture-Control Design Analysis in Buildings*.
- Autengruber, Maximilian, Markus Lukacevic, Christof Gröstlinger, and Josef Füssl. 2021. "Finite-Element-Based Prediction of Moisture-Induced Crack Patterns for Cross Sections of Solid Wood and Glued Laminated Timber Exposed to a Realistic Climate Condition." *Construction and Building Materials* 271:121775.
- Brandner, R., G. Flatscher, A. Ringhofer, G. Schickhofer, and A. Thiel. 2016. "Cross Laminated Timber (CLT): Overview and Development." *European Journal of Wood and Wood Products* 74(3):331–51.
- Brandner, Reinhard. 2013. "Production and Technology of Cross Laminated Timber (CLT): A State-of-the- Art Report Production and Technology of Cross Laminated Timber (CLT): A State-of-the-Art Report." in *Focus Solid Timber Solutions - European Conference on Cross Laminated Timber (CLT)*. Graz, Austria.
- Brischke, Christian, Christian Robert Welzbacher, and Andreas Otto Rapp. 2006. "Detection of Fungal Decay by High-Energy Multiple Impact (HEMI) Testing." *Holzforschung* 60(2):217–22.
- British Gypsum. 2017. *Declaration of Performance, Gyproc GTS 9, No G520*. Kirkkonummi (FIN).
- British Gypsum. 2018. *Gyproc ThermoLin PIR, Product Data Sheet - PDS-037-04*.
- Byttebier, Marcos. 2018. "Hygrothermal Performance Analysis of Cross-Laminated Timber (CLT) in Western Europe." KU Leuven.

- Caillaud, Denis, Benedicte Leynaert, Marion Keirsbulck, Rachel Nadif, S. Roussel, C. Ashan-Leygonie, V. Bex, S. Bretagne, D. Caillaud, A. C. Colleville, E. Frealle, S. Ginestet, L. Lecoq, B. Leynaert, R. Nadif, I. Oswald, G. Reboux, T. Bayeux, C. Fourneau, and M. Keirsbulck. 2018. "Indoor Mould Exposure, Asthma and Rhinitis: Findings from Systematic Reviews and Recent Longitudinal Studies." *European Respiratory Review* 27(148).
- Chang, Seong Jin, Yujin Kang, Beom Yeol Yun, Sungwoong Yang, and Sumin Kim. 2021. "Assessment of Effect of Climate Change on Hygrothermal Performance of Cross-Laminated Timber Building Envelope with Modular Construction." *Case Studies in Thermal Engineering* 28:101703.
- Chiniforush, A. A., A. Akbarnezhad, H. Valipour, and S. Malekmohammadi. 2019. "Moisture and Temperature Induced Swelling/Shrinkage of Softwood and Hardwood Glulam and LVL: An Experimental Study." *Construction and Building Materials* 207:70–83.
- Cho, Hyun Mi, Seunghwan Wi, Seong Jin Chang, and Sumin Kim. 2019. "Hygrothermal Properties Analysis of Cross-Laminated Timber Wall with Internal and External Insulation Systems." *Journal of Cleaner Production* 231:1353–63.
- Cochon, Noel Kristen. 2019. "Towards Quantifying The Air Leakage Through Cross-Laminated Timber." McMaster University, Toronto.
- Cui, Yumeng, Yufeng Zhang, and Hans Janssen. 2021. "EMPD-Based Moisture Buffering Quantification with Moisture-Dependent Properties (I): Modelling and Simulations." *Building and Environment* 205:108266.
- Curling, Simon, Carol Clausen, and Jerrold Winandy. 2002. "Relationships between Mechanical Properties, Weight Loss and Chemical Composition of Wood during Incipient Brown Rot Decay." *Forest Products Journal* 52:34–37.
- EN 12114. 2000. *Thermal Performance of Buildings - Air Permeability of Building Components and Building Elements - Laboratory Test Method*. Brussels.
- EN 13183:2002. 2002. *EN 13183-1:2002 - Moisture Content of a Piece of Sawn Timber - Part 1: Determination by Oven Dry*.
- EN 16351. 2015. "Timber Structures - Cross Laminated Timber - Requirements."
- EN 335. 2013. *Durability of Wood and Wood-Based Products - Use Classes: Definitions, Applications to Solid Wood and Wood-Based Products*. Brussels.
- EN 350. 2016. "Durability of Wood and Wood-Based Products - Testing and Classification of the Durability to Biological Agents of Wood and Wood-Based Materials."
- EN 9972. 2015. "Thermal Performance of Buildings — Determination of Air Permeability of Buildings — Fan Pressurization Method." *International Organization for Standardization*. Retrieved February 7, 2021 (<https://www.iso.org/standard/55718.html>).
- Eskola, Lari, Ûllar Alev, Endrik Arumägi, Juha Jokisalo, Anna Donarelli, Kai Sirén, and Targo Kalamees. 2016. "Airtightness, Air Exchange and Energy Performance in Historic Residential Buildings with Different Structures." [Http://Dx.Doi.Org/10.1080/14733315.2015.11684066](http://Dx.Doi.Org/10.1080/14733315.2015.11684066) 14(1):11–26.
- Falk, Jörgen and Kenneth Sandin. 2013. "Ventilated Rainscreen Cladding: Measurements of Cavity Air Velocities, Estimation of Air Change Rates and Evaluation of Driving Forces." *Building and Environment* 59:164–76.
- Fedorik, Filip and Antti Haapala. 2017. "Impact of Air-Gap Design to Hygro-Thermal Properties and Mould Growth Risk Between Concrete Foundation and CLT Frame." *Energy Procedia* 132:117–22.

- Fisher, Ronald Aylmer. 1924. "The Distribution of the Partial Correlation Coefficient." *Metron* 3:329–32.
- Flexeder, Nina, Stephan Ott, Eva Bodemer, and Stefan Winter. 2021. "Monitoring of an Office Building in Uninsulated Cross-Laminated Timber Construction Regarding Hygrothermal Component Behavior." Pp. 1–10 in *World Conference on Timber Engineering WCTE 2021*. Santiago, Chile: Centro UC de Innovación de Madera.
- Gagnon, S. and C. Pirvu. 2011. *CLT Handbook: Cross-Laminated Timber*. FPInnovations.
- Geving, Stig, Achilles Karagiozis, and Mikael Salonvaara. 2016. "Measurements and Two-Dimensional Computer Simulations of the Hygrothermal Performance of a Wood Frame Wall:" [Http://Dx.Doi.Org/10.1177/109719639702000404](http://dx.doi.org/10.1177/109719639702000404) 20(4):301–19.
- Günther, S., Ringhofer, A., Schickhofer, G. 2016. "External Thermal Insulation Composite Systems in Solid Timber Construction." in *2016 World Conference on Timber Engineering, WCTE 2016*. Vienna, Austria: Vienna University of technology.
- GUT. 2013. *Air Permeability Test on a Cross Laminated Timber. Test Report No. 812.156.024.100*. Graz.
- Hagentoft, Carl-Eric. 2001. *Introduction to Building Physics*. Studentlitteratur AB.
- Hallik, Jaanus and Targo Kalamees. 2019. "Development of Airtightness of Estonian Wooden Buildings." *Journal of Sustainable Architecture and Civil Engineering*.
- Herms, Jens Lüder. 2020. "Achieving Airtightness and Weather Protection of CLT Buildings." in *E3S Web of Conferences_NSB2020*. Vol. 172. Tallinn: EDP Sciences.
- Holm, A. and H. M. Künzel. 2003. *Two-Dimensional Transient Heat and Moisture Simulations of Rising Damp with WUFI2d*. CRC Press.
- Huang, Zirui, Dongsheng Huang, Ying Hei Chui, Yurong Shen, Hossein Daneshvar, Baolu Sheng, and Zhongfan Chen. 2022. "Modeling of Cross-Laminated Timber (CLT) Panels Loaded with Combined out-of-Plane Bending and Compression." *Engineering Structures* 250:113335.
- Humar, Miha, Christian Brischke, Linda Meyer, Dennis Jones, Nejc Thaler, Boštjan Lesar, and Mojca Žlahtic. 2014. "COST FP 1303 Cooperative Performance Test."
- Ilomets, Simo, Targo Kalamees, and Juha Vinha. 2017. "Indoor Hygrothermal Loads for the Deterministic and Stochastic Design of the Building Envelope for Dwellings in Cold Climates." *Journal of Building Physics* 41(6):547–77.
- ISO 12572. 2016. *Hygrothermal Performance of Building Materials and Products -- Determination of Water Vapour Transmission Properties -- Cup Method*.
- Jahedi, Sina. 2021. *What Causes Delamination in Cross-Laminated Timber (CLT) and How to Prevent It*. Corvallis, OR, US.
- Janols, Henrik, Mats Rönnelid, Tina Wik, Matias Brännstör, Håkan Helling, and Tommy Lövenvik. 2013. *Passive Cross Laminated Timber Buildings. Cerbof-Project No. 76*. Orsa, Sweden.
- Janzen, A. F. and R. K. Swartman. 1981. *Solar Energy Conversion II : Selected Lectures from the 1980 International Symposium on Solar Energy Utilization*. Ontario: Pergamon Books.
- Kalamees, Targo and Jarek Kurnitski. 2010. "Moisture Convection Performance of External Walls and Roofs." *Journal of Building Physics* 33(3):225–47.
- Kalamees, Targo and Juha Vinha. 2003. "Hygrothermal Calculations and Laboratory Tests on Timber-Framed Wall Structures." *Building and Environment* 38(5):689–97.
- Kalamees, Targo and Juha Vinha. 2004. "Estonian Climate Analysis for Selecting Moisture Reference Years for Hygrothermal Calculations." *Journal of Thermal Envelope and Building Science* 27(3):199–220.

- Kalbe, Kristo, Villu Kukk, and Targo Kalamees. 2020. "Identification and Improvement of Critical Joints in CLT Construction without Weather Protection" edited by J. Kurnitski and T. Kalamees. *E3S Web of Conferences* 172:10002.
- Kingspan. 2018. *Declaration of Performance, Therma TP10*. Kankaanpää (FIN).
- Klößeiko, Paul and Targo Kalamees. 2021. "Hygrothermal Performance of a Brick Wall with Interior Insulation in Cold Climate: Vapour Open versus Vapour Tight Approach." *Journal of Building Physics*.
- Kordziel, Steven, Samuel V. Glass, Charles R. Boardman, Robert A. Munson, Samuel L. Zelinka, Shiling Pei, and Paulo Cesar Tabares-Velasco. 2020. "Hygrothermal Characterization and Modeling of Cross-Laminated Timber in the Building Envelope." *Building and Environment* 177:106866.
- Van De Kuilen, J. W. G., A. Ceccotti, Zhouyan Xia, and Minjuan He. 2011. "Very Tall Wooden Buildings with Cross Laminated Timber." *Procedia Engineering* 14: 1621–28.
- Kukk, Villu, Adeniyi Bella, Jaan Kers, and Targo Kalamees. 2021. "Airtightness of Cross-Laminated Timber Envelopes: Influence of Moisture Content, Indoor Humidity, Orientation, and Assembly." *Journal of Building Engineering* 44:102610.
- Kukk, Villu, Targo Kalamees, and Jaan Kers. 2019. "The Effects of Production Technologies on the Air Permeability and Crack Development of Cross-Laminated Timber." *Journal of Building Physics* 174425911986686.
- Kukk, Villu, Jaan Kers, and Targo Kalamees. 2019. "Hygrothermal Performance of Mass Timber Wall Assembly with External Insulation Finish System." Pp. 599–607 in *Proceedings of Buildings XIV International Conference*. Clearwater, FL: ASHRAE.
- Langmans, Jelle, Ralf Klein, and Staf Roels. 2013. "Numerical and Experimental Investigation of the Hygrothermal Response of Timber Frame Walls with an Exterior Air Barrier." <https://doi.org/10.1177/1744259112473934> 36(4):375–97.
- Liisma, E., B. L. Kuus, V. Kukk, and T. Kalamees. 2019. "A Case Study on the Construction of a CLT Building without a Preliminary Roof." *Journal of Sustainable Architecture and Civil Engineering* 25(2).
- Lipand, Raina, Villu Kukk, and Targo Kalamees. 2021. "Capillary Movement of Water in a Radial Direction and Moisture Distribution in a Cross-Section of CLT Panel." Tallinn University of Technology, Tallinn.
- Lomholt, Isabelle. 2009. "Stadthaus London : Murray Grove Building." *E-Architect* (8.01.2017).
- Magni, Mara, Fabian Ochs, Samuel de Vries, Alessandro Maccarini, and Ferdinand Sigg. 2021. "Detailed Cross Comparison of Building Energy Simulation Tools Results Using a Reference Office Building as a Case Study." *Energy and Buildings* 250:111260.
- McClung, Ruth, Hua Ge, John Straube, and Jieying Wang. 2014. "Hygrothermal Performance of Cross-Laminated Timber Wall Assemblies with Built-in Moisture: Field Measurements and Simulations." *Building and Environment* 71:95–110.
- Meynen, Jasper. 2016. "Cross Laminated Timber (CLT) Bouwdelen Met Bouwvocht En Gewijzigde Luchtdichtheid." Catholic University of Leuven.
- Mjörnell, Kristina and Lars Olsson. 2019a. "Moisture Safety of Wooden Buildings – Design, Construction and Operation." *Forum Wood Building Baltic*.
- Mjörnell, Kristina and Lars Olsson. 2019b. "Moisture Safety of Wooden Buildings – Design, Construction and Operation." *Journal of Sustainable Architecture and Civil Engineering* 24(1):29–35.

- Nairn, John A. 2017. "Cross Laminated Timber Properties Including Effects of Non-Glued Edges and Additional Cracks." *European Journal of Wood and Wood Products* 75(6):973–83.
- Nairn, John A. 2019. "Predicting Layer Cracks in Cross-Laminated Timber with Evaluations of Strategies for Suppressing Them." *European Journal of Wood and Wood Products* 77(3):405–19.
- Nicolai, Andreas and John Grunewald. 2003. *Delphin 5 User Manual and Program Reference*. Dresden.
- Niklewski, J., M. Fredriksson, and T. Isaksson. 2016. "Moisture Content Prediction of Rain-Exposed Wood: Test and Evaluation of a Simple Numerical Model for Durability Applications." *Building and Environment* 97:126–36.
- Ojanen, Tuomo and Juho Laaksonen. 2016. "Hygrothermal Performance Benefits of the Cellulose Fiber Thermal Insulation Structures." in *41st IAHS International Association for Housing Science, World Congress - Sustainable Buildings*. Coimbra.
- Olsson, Lars. 2020a. "Moisture Safety in CLT Construction without Weather Protection-Case Studies, Literature Review and Interviews." *E3S Web of Conferences* (12th Nordic Building Physics Conference, NSB 2020. Tallinn).
- Olsson, Lars. 2020b. "Moisture Safety in CLT Construction without Weather Protection – Case Studies, Literature Review and Interviews." P. 10001 in *E3S Web of Conferences*. Vol. 172. EDP Sciences.
- Olsson, Lars. 2021. "CLT Construction without Weather Protection Requires Extensive Moisture Control." *Journal of Building Physics* 45(1):5–35.
- Östman, Birgi, Joachi Schmid, Michae Klippel, Ala Just, Norma Werther, and Danie Brandon. 2018. "Fire Design of CLT in Europe." *Wood and Fiber Science* 50:68–82.
- Pihelo, Peep and Targo Kalamees. 2016. "The Effect of Thermal Transmittance of Building Envelope and Material Selection of Wind Barrier on Moisture Safety of Timber Frame Exterior Wall." *Journal of Building Engineering* 6:29–38.
- Pihelo, Peep, Henri Kikkas, and Targo Kalamees. 2016. "Hygrothermal Performance of Highly Insulated Timber-Frame External Wall." *Energy Procedia* 96:685–95.
- Pihelo, Peep, Kalle Kuusk, and Targo Kalamees. 2020. "Development and Performance Assessment of Prefabricated Insulation Elements for Deep Energy Renovation of Apartment Buildings." *Energies* 2020, Vol. 13, Page 1709 13(7):1709.
- Pintos, Paula. 2019. "Mjøstårnet The Tower of Lake Mjøsa / Voll Arkitekter | ArchDaily." *ArchDaily*. Retrieved April 11, 2022 (<https://www.archdaily.com/934374/mjostarnet-the-tower-of-lake-mjosa-voll-arkitekter>).
- Pro-Clima. 2022a. *Declaration of Performance, DASAPLANO 0,01 Connect*. Schwetzingen.
- Pro-Clima. 2022b. *Declaration of Performance, Internal Air and Vapour Membrane DA*. Schwetzingen.
- Reinberg, Georg Wolfgang, Tõnu Muring, Kristo Kalbe, and Jaanus Hallik. 2013. "First Certified Passive House in Estonia." in *Proceedings of 17th International Passive House Conference*. Frankfurt, Germany: Passivhaus Institut Darmstadt.
- Saint-Gobain. 2017. *Declaration of Performance, ISOVER RKL31, No 0615-CPR-222984G-M227-2017/01/16*. Helsinki.
- Samuels, I., K. Mjörnell, and A. Jansson. 2008. "Moisture Damage in Rendered, Undrained, Well Insulated Stud Walls." Pp. 1253–60 in *Proc. 8th Symposium of Building Physics in the Nordic Countries*. Copenhagen.

- Santi, Silvia, Francesca Pierobon, Giulia Corradini, Raffaele Cavalli, and Michela Zanetti. 2016. "Massive Wood Material for Sustainable Building Design: The Massiv-Holz-Mauer Wall System." *Journal of Wood Science* 62(5):416–28.
- Schmid, Joachim, Michael Klippel, Alar Just, Andrea Frangi, and Mattia Tiso. 2018. "Simulation of the Fire Resistance of Cross-Laminated Timber (CLT)." *Fire Technology* 54(5):1113–48.
- Schmidt, Evan L., Mariapaola Riggio, Andre R. Barbosa, and Ignace Mugabo. 2019. "Environmental Response of a CLT Floor Panel: Lessons for Moisture Management and Monitoring of Mass Timber Buildings." *Building and Environment* 148:609–22.
- Schmidt, Olaf. 2010. *Wood and Tree Fungi: Biology, Damage, Protection, and Use*. Springer.
- Shmulsky, Rubin. and P. David. Jones. 2011. *Forest Products and Wood Science : An Introduction*. Sixth edit. A John Wiley & Sons, Inc.
- Shmulsky, Rubin and P. David Jones. 2011. *Forest Products and Wood Science*. Wiley-Blackwell.
- Skogstad, Hans, Lars Gullbrekken, and Kristine Nore. 2011. "Air Leakages through Cross Laminated Timber (CLT) Constructions." in *9th Nordic Symposium on Building Physics*. Tampere: Tampere: Tampere University of Technology.
- Straube, J. and G. Finch. 2008. "Ventilated Wall Claddings: Review, Field Performance, and Hygrothermal Modeling." in *Thermal Performance of Exterior Envelopes of Whole Buildings 2008*. Clearwater, Florida: ASHRAE.
- Stuart, Alan, Keith Ord, and Steven Arnold. 2004. *Kendall's Advanced Theory of Statistics, Classical Inference and the Linear Model*. Vol. 2A. 6th edition. Wiley.
- TenWolde, A., J. D. McNatt, and L. Krahn. 1988. *Thermal Properties of Wood and Wood Panel Products for Use in Buildings*. Madison.
- Tijskens, Astrid, Staf Roels, and Hans Janssen. 2018. "Neural Networks to Predict the Hygrothermal Response of Building Components in a Probabilistic Framework." in *International Building Physics Conference*. Syracuse, NY.
- Tijskens, Astrid, Staf Roels, and Hans Janssen. 2021. "Hygrothermal Assessment of Timber Frame Walls Using a Convolutional Neural Network." *Building and Environment* 193:107652.
- Time, Berit. 1998. "Hygroscopic Moisture Transport in Wood." Norwegian University of Science and Technology.
- Time, Berit. 2020. "Climate Adaptation of Wooden Buildings – Risk Reduction by Moisture Control." in *Proceedings of 12th Nordic Symposium on Building Physics (NSB 2020)*. Tallinn.
- Tuhkanen, Eero, Joosep Mölder, and Gerhard Schickhofer. 2018. "Influence of Number of Layers on Embedment Strength of Dowel-Type Connections for Glulam and Cross-Laminated Timber." *Engineering Structures* 176:361–68.
- Tveit, A. 1966. *Measurements of Moisture Sorption and Moisture Permeability of Porous Materials (Norges Byggeforskningsinstitut)*. Oslo.
- Viitanen, H., M. Krus, T. Ojanen, V. Eitner, and D. Zirkelbach. 2015. "Mold Risk Classification Based on Comparative Evaluation of Two Established Growth Models." *Energy Procedia* 78:1425–30.
- Viitanen, Hannu and Tuomo Ojanen. 2007. *Improved Model to Predict Mold Growth in Building Materials*.

- Viitanen, Hannu, Tuomo Ojanen, Ruut Peuhkuri, and Juha Vinha. 2011. "Mould Growth Modelling to Evaluate Durability of Materials." Pp. 409–16 in *XII DBMC 12th International Conference on Durability of Building Materials and Components, 12th - 15th April 2011, Porto, Portugal*, edited by M. L. Vasco Peixoto de Freitas, Helena Corvacho. Porto: FEUP Edicoes (Faculdade de Engenharia da Universidade do Porto Edicoes).
- Vinha, J., I. Valovirta, M. Korpi, A. Mikkilä, and P. Käkelä. 2005. *Rakennusmateriaalien Rakennusfysikaaliset Ominaisuudet Lämpötilan Ja Suhteellisen Kosteuden Funktiona*. Tampere: Unknown Publisher.
- Vinha, Juha. 2007. "Hygrothermal Performance of Timber-Framed External Walls in Finnish Climatic Conditions: A Method of Determining a Sufficient Water Vapour Resistance of the Internal Lining of a Wall Assembly." Tampere University of Technology.
- Wang, Lin and Hua Ge. 2016. "Hygrothermal Performance of Cross-Laminated Timber Wall Assemblies: A Stochastic Approach." *Building and Environment* 97:11–25.
- Wang, Lin and Hua Ge. 2018. "Stochastic Modelling of Hygrothermal Performance of Highly Insulated Wood Framed Walls." *Building and Environment* 146:12–28.
- Wang, Lin, Jieying Wang, and Hua Ge. 2020. "Wetting and Drying Performance of Cross-Laminated Timber Related to on-Site Moisture Protections: Field Measurements and Hygrothermal Simulations." *E3S Web of Conferences* 172:10003.
- Wang, Yingying, Wenzhuo Wang, Dengjia Wang, Yanfeng Liu, and Jiaping Liu. 2021. "Study on the Influence of Sample Size and Test Conditions on the Capillary Water Absorption Coefficient of Porous Building Materials." *Journal of Building Engineering* 43:103120.
- Werrowool. 2018. *Thermal Conductivity Test of „Tselluvill Mixture“, Test Report 11-40/EI/790-3*. Tallinn.
- WHO. 2009. *Guidelines for Indoor Air Quality: Dampness and Mould*. Copenhagen.
- Wu, Yang. 2007. "Experimental Study of Hygrothermal Properties for Building Materials." Concordia University.
- Yoo, Jiwon, Seong Jin Chang, Sungwoong Yang, Seunghwan Wi, Young Uk Kim, and Sumin Kim. 2021. "Performance of the Hygrothermal Behavior of the CLT Wall Using Different Types of Insulation; XPS, PF Board and Glass Wool." *Case Studies in Thermal Engineering* 24:100846.
- Zilling, Wolfgang. 2009. "Moisture Transport in Wood Using a Multiscale Approach." FACULTEIT INGENIEURSWETENSCHAPPEN, Leuven.

Publications

PUBLICATION I

Kukk, V.; Luciani, G.; Püssa, M.; Horta, R.; Kallakas, H.; Kers, J.; Kalamees, T., 2017. Impact of cracks to the hygrothermal properties of CLT water vapour resistance and air permeability. *Energy Procedia*, 132: The 11th Nordic Symposium on Building Physics, Trondheim, Norway, 11-14 June 2017. Ed. S. Geving, B. Time. Elsevier, 741–746.



11th Nordic Symposium on Building Physics, NSB2017, 11-14 June 2017, Trondheim, Norway

Impact of cracks to the hygrothermal properties of CLT water vapour resistance and air permeability

V. Kukk^{a*}, R. Horta^a, M. Püssa^a, G. Luciani^a, H. Kallakas^a, T. Kalamees^b, J. Kers^a

^aLaboratory of Wood Technology, Tallinn University of Technology, Teaduspargi 5, 12618 Tallinn, Estonia

^bnZEB research group, Tallinn University of Technology, Ehitajate tee 5, 19086 Tallinn, Estonia.

Abstract

Current research is focused on crack formation and propagation in cross laminated timber (CLT) panels and its impacts on the water vapour resistance and air permeability of panels. Crack formation was examined by means of climate tests with five layer CLT-panels with a thickness of 95 mm. Results of climate tests showed that decreasing the moisture content (MC) from 11 % to 7 % caused mean crack widths in panels of 0.27 mm and 0.38 mm, and an MC decreasing from 17 % to 7 % caused mean crack widths of 0.89 mm and 2.0 mm. From these test results it was concluded that in CLT panels which were produced and stored in a humid environment there was an approximate 200% increase in the mean maximum width of cracks compared to panels stored in a dry environment. The water vapour transmission increased by about 9 % with smaller cracks (that were imitated with 2 mm holes) and 30 % with larger cracks (6 mm holes). The air permeability of CLT at a maximum air pressure difference of 550 Pa was 2.25 l/(s*m²) with 2 mm holes and 5.56 l/(s*m²) with 6 mm holes. It can be concluded from the afore mentioned test results that cracks significantly influence the hygrothermal properties of CLT. Deeper investigation as to the reasons, formation and propagation procedures are needed to avoid inadvisable cracks in CLT.

© 2017 The Authors. Published by Elsevier Ltd.

Peer-review under responsibility of the organizing committee of the 11th Nordic Symposium on Building Physics.

Keywords: Cross laminated timber, cracks formation, water vapour transmission, air permeability

1. Introduction

Cross laminated timber (CLT), also known as “Engineered wood”, was initially developed in Switzerland in the early 1990s. A CLT panel as a product is a simple structure, a laminated wooden panel which can be used as both a load-bearing and an interior element.

* Corresponding author. Tel.: +372-620-2910;
E-mail address: villu.kukk@ttu.ee

Generally, a CLT panel is a cross-wisely placed multi-layer wooden panel made of lumber and adhesive (in some case nails) [1]. Adhesives used can be phenolic and aminoplastic adhesives, moisture curing one-component polyurethane adhesives (most common) or emulsion polymer isocyanate adhesives [2].

Over the last few years in Europe the use of CLT panels in buildings has increased, mostly for tall and energy efficient buildings. Murray Grove Building is a nine-storey residential building that has been assembled using a cross-laminated timber panel system pioneered by manufacturers KLH of Austria in 2009 [3]. The University of the Basque Country designed and developed an industrialised solar house prototype “The Ekihouse” in Spain [4]. The first certified passive house was also assembled using a CLT panel system [5].

Wood is known as a hygroscopic material which is able to absorb and lose moisture depending on the surrounding environment. Wood with a low MC placed in a humid environment starts to absorb water vapour from the air until the wood achieves moisture equilibrium with the surrounding environment and, vice versa, if the surrounding air gets drier in an environment where wood has achieved moisture equilibrium, it starts to lose moisture [6]. The MC of wood plays a major role in crack formation. Moisture loss and absorption in wood causes shrinkage and swelling. Shrinkage of wood is the main reason for crack formation. For example, a too quick drying process in wood may cause uneven moisture losses from the wood. When the outer surface of lumber has lost a major amount of its moisture, but the inner middle part still has its initial moisture content, then uneven shrinkage in the outer surface cause internal tensions which will break the wood cells and cracking will occur [6]. When cracks form in CLT panels they are no longer airtight, cracks also influence the water vapour permeability.

This study is focused on crack formation and its influence on changes to water vapour resistance and air permeability.

2. Methods

Four specimens (S1-S4) of 95 mm thick five-layer CLT panels (layers 19x140 mm spruce lumber boards) with length and width measurements of 470 x 500 mm were used for determining crack and split formation. Layers in the panels were glued together on their flat faces and not by the edges. Two panels (S1 and S2) were stored before testing for about two weeks at a temperature of 15 °C and a relative humidity (RH) of 40 %, simulating the environment of an indoor storage room. MC of these panels was 10.5 % and 11.2 % correspondingly. Two (S3 and S4) panels were stored for five days before testing at 10 °C and a RH 95 %, simulating an outdoor storage environment during the autumn season. MC of these panels was 16.5 % and 17.5 % correspondingly. The panels edges were given two coats of polyurethane acrylic paint, Capacryl PU-Satin, to ensure moisture in the air would move through the panels only from the flat faces. The CLT panels were placed into a climate chamber (ILKA PTK-3018) doorway for 92 days, Fig 1; left. The CLT panels in the test wall were separated with mineral wool and vapour barrier tape (Gerband 586, 50 mm wide) to prevent any major air leaks. An indoor environment corresponding to the indoor environment in Estonia during the winter months was simulated inside the climate chamber: temperature 20 °C and RH 25%. Cracks were measured on each panel on the upper surface of the external layer which was exposed to the simulated environment in the climate chamber, all other sides of the panels were not considered.

The impact of the position and dimensions of cracks on water vapour transmission was studied according to ISO 12572 standard [7], by two cross-wise glued layer specimens of a thickness of 12mm with drilled holes of 2 and 6 mm for crack simulation (6 mm hole was chosen by standard EN 16351 [2]), Fig 1; right. 35 square shapes of wooden lamellas from spruce wood (*Picea abies*) with a length of 110 mm and a thickness of 6 mm were selected and cut out from spruce board for making four type of specimens (CS1-CS4), 5 specimens for each type, total 20 specimens for carrying out the test. The surrounding conditions for carrying out the test were 23 °C ±0.5 °C, the RH inside the test cup was near 0 % (CaCl₂- particle size < 3 mm) and the external environment was RH 50 %. Final results were taken when the five last weighing's showed a constant value in mass change.

An air permeability test was carried out according to EN 12114 standard [8]. Specimens for air permeability were the same as used in the water vapour transmission test, but in this case only three specimens from each type (AS1-AS3). The test was carried out only with a positive pressure between 50 and 500 Pa at six stages with three pressure pulses before measurement. Air flow rate in every pressure difference step, for each specimen, was measured and recorded and corrected with an estimated error.

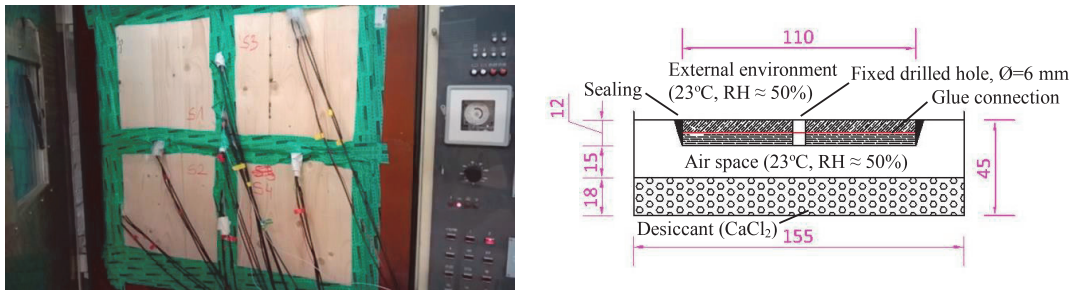


Fig 1. Test wall built up inside the climate chamber ILKA PTK-3018 doorway (left).

Final design schemes for planed and glued solid wood panels with a 6 mm diameter hole to measure the water vapour transmission (right).

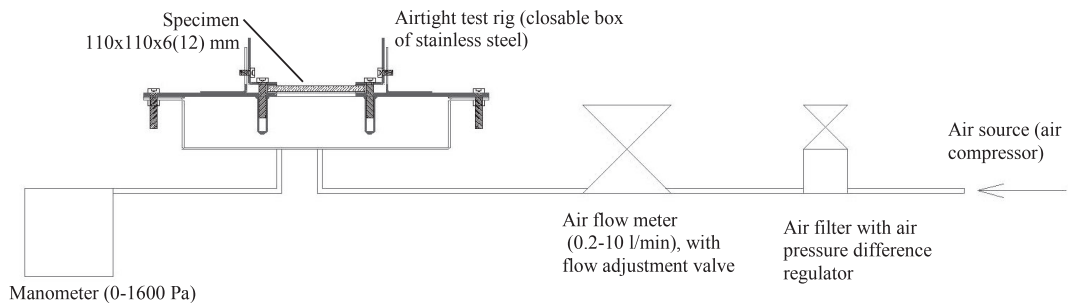


Fig 2. Equipment's complex scheme for carrying out the air permeability test.

3. Results and discussion

3.1. Crack formation in CLT panels

Before the specimens were placed into the climate chamber for testing, the existing cracks in the top surface layer in each panel were measured and, after the end of the monitoring period, the existing cracks were measured again. When measured before the monitoring period, cracks were found only in the external layer surfaces of S1 and S2.

Cracks that had occurred during the test were found in S2, S3, and S4:

- S1: no occurred cracks;
- S2: six occurred cracks of a mean length of 143 mm and a mean maximum width of 0.2 mm;
- S3: nine occurred cracks of a mean length of 221.44 mm and mean maximum width about 0.89 mm;
- S4: three occurred cracks of mean length of 468 mm and mean maximum width about 2 mm.

S3 and S4, which were stored in humid environment and had a potentially bigger threat for crack formation, did have a bigger mean maximum width of cracks, and the difference was significant, more than double. There was no correlation between the humidity of the environment and the cracks' lengths.

In addition to measuring the size of the cracks, the location and shape of the cracks were also evaluated. These values are significant as one of the threats that leads to the deterioration of the hygrothermal properties of a CLT panel is the scenario where cracks between or in the middle of laminations will align, leading to openings through the panel. If the panels are also exposed to an internal environment, openings through the panel can cause leakages of air and water vapour.

Possible sources for this threat were found in specimen four, where cracks had formed between laminations in one narrow side of the panel in odd layers (Fig 3; left a) and in the adjacent narrow side of the panel in even layers (Fig 3 left b). Looking at the shapes of the cracks (Fig 3; left a) one can see that cracks between laminations are closed by

the adhesive layer. On the flat side of the specimen, cracks had formed between each lamination over the entire length of the panel (Fig 3; right) and this means that there is a considerable probability of some cracks aligning.



Fig 3. Cracks have been formed between laminations and in odd and even layers (left) as well between laminations over the entire length of panel (left) of S4.

Taking into account the fact that the panels had only been tested for a three-month period and that during a real service period the panel laminations undergo several cycles of swelling and shrinkage, it can be assumed that the internal tensions (caused by swelling and shrinkage) will eventually cause ruptures in the adhesive layers.

MC decreased in all specimens during the first two months and then stayed stable, having reached the equilibrium MC (EMC). The change in the MC of the panels during the monitoring period showed that panels which had been stored in a humid environment before service (use in construction) and hence having a bigger MC, would have a more drastic change in MC before reaching the EMC compared to the panels stored in dry conditions. According to the statement – if the actual MC in the wood is about 2 % higher than the expected MC under the given environment conditions, the problem of occurring cracks exists, therefore it can be said that panels stored in a humid environment will have a greater threat of crack formation [9].

3.2. Water vapour transmission through the specimens

Test results were recorded during 33 days of “Cup testing” for five specimens of all four types of CLT panels. The water vapour resistance factor (μ) and diffusion equivalent air layer thickness (Sd) were found for each specimen and the results are given in Table 1.

Table 1. Test results of Cup test for four specimen’s type of CLT structural elements.

Specimen types	Water vapour resistance factor, μ		Water vapour diffusion equivalent air layer thickness, Sd (m)	
	Value	Standard error	Value	Standard error
CS1, specimens of lamellae of 6 mm thickness	185	11	1.13	0.068
CS2, specimens of glued lamellas (2x) of 12 mm thickness	286	9	3.51	0.114
CS3, specimens of glued lamellas (2x) of 12 mm thickness and with a drilled hole of 2 mm diameter	259	13	3.19	0.160
CS4, specimens of glued lamellas (2x) of 12 mm thickness and with a drilled hole of 6 mm diameter	198	7	2.45	0.087

As the resistance value for the adhesive layer is greater than the value for the 6 mm thick solid wood specimen, it can be said that an adhesive layer has a significant impact on the water vapour resistance of a CLT panel. The 2 mm diameter hole in the glued specimen reduced water vapour resistance for 9% and the 6 mm diameter hole reduced

water vapour resistance for 30 % compared with the solid glued specimen. The decrease of water vapour resistance is linear, depending directly on the size of the hole. A decrease of 9 and 30 % of water vapour resistance is quite a significant change.

Water vapour resistance factors by S_d values were calculated for simulated panels of 0.095 m thickness (area 0.0121 m²) from the results for the test specimens as follows:

- μ_1 of CLT panel with 6 mm diameter hole- $\mu_1 = S_d / 0.095 = 2.45 / 0.095 = 25.8$;
- μ_2 of CLT panel with 2 mm diameter hole- $\mu_2 = S_d / 0.095 = 3.19 / 0.095 = 33.6$;
- μ_3 of CLT panel without holes- $\mu_3 = S_d / 0.095 = 3.51 / 0.095 = 37.0$.

Comparing the results of water vapour resistance factors μ_1 to μ_3 for simulated panels with holes, where the areas are the same as in the specimens, quite considerable differences can be seen. The difference between μ_1 and μ_3 is 11.16, which is about 31% when taking μ_3 as the base value. The difference between μ_2 and μ_3 is 3.39, which is about 9% when taking μ_3 as the base value.

3.3. Air permeability properties

Results of the first stage of pressure application did not show any air flow in the specimens of glued lamellas without a drilled hole, AS1, and therefore it can be said that these specimens were impermeable to air flow. A similar result has also been reached by other studies [1,10]. As previous tests by the same team [11] had showed crack formation, the next measurements were done with drilled holes in a CLT to simulate cracks.

Specimens AS2 of glued lamellas and with drilled holes of a 2 mm diameter showed a maximum air flow of 2.25 l/(s*m²) in the first stage and specimens AS3 of glued lamellae with drilled holes of 6 mm diameter showed a maximum air flow of 5.65 l/(s*m²) in the first stage.

Results in the second stage of the test, where air flow in specimens AS2 and AS3 was measured in logarithmically increasing pressure difference steps, showed that airflow in the increasing pressure steps in AS3 with 6 mm diameter holes was climbing more intensely than in AS2 with 2 mm diameter holes, in other words AS3 had a bigger growth rate in increasing pressure than AS2 (Fig 4).

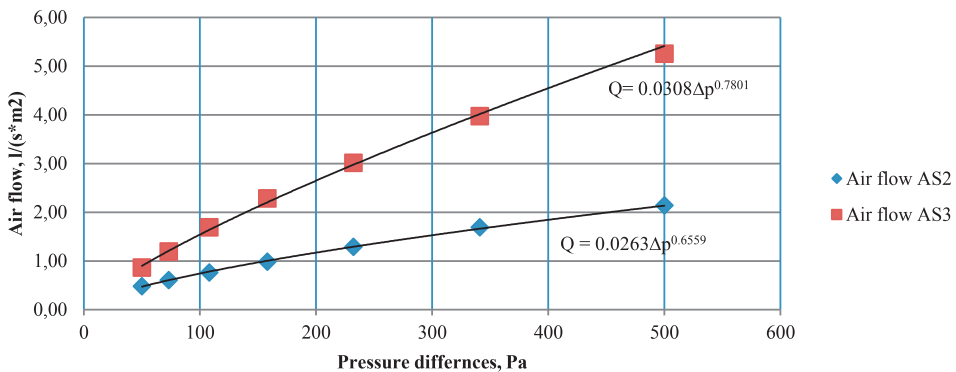


Fig 4. Growth rates of air flows of specimens S2 and S3 in second pressure test stage.

Evaluating the impact of crack growth between 2 and 6 mm simulated cracks on CLT panels, it can be said that the growth impact on water vapour resistance and on air permeability properties has been considerable for both. The impact was bigger on simulated cracks sizes for air permeability properties. A previous research by Skogstad et al. [11] showed that airflow differences through wall elements joints were 863% between MC 10% and 14% in CLT panels without glued edges. The considerable impact of cracks on CLT panels shows that extra layers of vapour and air tight materials for covering CLT panels in wall assemblies are necessary.

Conclusion

The different MC in CLT panels plays an important role in crack formation in the panel's lamellas. Specimens which had been stored in a humid environment and therefore had a potentially greater threat of crack formation, developed wider mean maximum cracks. Differences were significant, more than double compared to the specimens held in a dry environment. Based on our current results, producing CLT panels in a dry environment with an RH of about 40% helps to avoid bigger crack formations in later service life. A more in-depth study on crack formation and its influence on air leakage with different types of CLT: different number of layers, glued / not glued and different initial MC of wood, is needed.

The impact of cracks in CLT panels was considerable on the water vapour resistance properties. Based on the results of the crack formation tests it can be concluded that eventually two millimetre cracks will occur through the panel's thickness and when this happens the panel will have a 9 % lower resistance to water vapour transmission at the location of the cracks. This means that if a CLT panel is, for example, exposed to an interior environment and the wall construction does not include extra vapour tight layers between the CLT panel and insulation, then does the influence of cracks when there is a high RH between material layers require further attention in building physics analyses?

The CLT with glued lamellae and without cracks did not show any air flow and therefore it can be said that these specimens were impermeable to air. The impact of simulated cracks in CLT panels was crucial on air permeability properties. The expansion of cracks causes an increase in air leakage, and it must be noted that the expansion of cracks increases the air leakage growth rate when exposed to growing pressure, due to turbulent air flow.

Acknowledgements

This research was supported by the Estonian Centre of Excellence in Zero Energy and Resource Efficient Smart Buildings and Districts, ZEBE, grant TK146 funded by the European Regional Development Fund, and by the Estonian Research Council with Institutional research funding grant IUT1-15.

The authors wish to thank Estonian glulam producer Peetri Puit OÜ for supplying CLT specimens.

References

- [1] Gagnon S, Pirvu C. CLT handbook: cross-laminated timber. FPIInnovations; 2011.
- [2] CEN - EN 16351. Timber structures- Cross laminated timber- Requirements. 2015.
- [3] Lomholt I. Stadthaus London : Murray Grove Building. E-Architect 2009.
- [4] Irulegi O, Torres L, Serra A, Mendizabal I, Hernández R. The Ekihouse: An energy self-sufficient house based on passive design strategies. *Energy and Buildings* 2014;83:57–69. doi:10.1016/j.enbuild.2014.03.077.
- [5] Kalamees T, Paap L, Kuusk K, Muring T, Hallik J, Valge M, et al. The first year's results from the first passive house in Estonia. In: Arfvidsson J, Harderup L-E, Kumlin A, Rosencrantz B, editors. *Proceedings of 10th Nordic Symposium on Building Physics*, 15-19 June 2014 Lund, Sweden: 2014, p. 758–65.
- [6] Shmulsky R, Jones PD. *Forest Products and Wood Science*. Wiley-Blackwell; 2011.
- [7] ISO 12572. *Hygrothermal performance of building materials and products -- Determination of water vapour transmission properties -- Cup method*. 2016.
- [8] EN 12114. *Thermal performance of buildings - Air permeability of building components and building elements - Laboratory test method*. Brussels: 2000.
- [9] Fred M. Lamb. *Splits and cracks in wood*. Blacksburg, Virginia: 1992.
- [10] GUT. *Air permeability test on a cross laminated timber*. Test report no. 812.156.024.100. Graz: 2013.
- [11] Skogstad HB, Gullbrekken L, Nore K. *Air leakages through cross laminated timber (CLT) constructions*. 9th Nordic Symposium on Building Physics, Tampere, Finland, 29.05 - 02 .06: 2011.

PUBLICATION II

Kukk, V.; Kalamees, T.; Kers, J., 2019. The effects of production technologies on the air permeability and crack development of cross-laminated timber. *Journal of Building Physics*, 43 (3), 171–186.

The effects of production technologies on the air permeability and crack development of cross-laminated timber

Journal of Building Physics

1–16

© The Author(s) 2019

Article reuse guidelines:

sagepub.com/journals-permissions

DOI: 10.1177/1744259119866869

journals.sagepub.com/home/jen**Villu Kukk¹** , **Targo Kalamees¹** and **Jaan Kers²**

Abstract

In a building envelope, the cross-laminated timber is often used as an air barrier layer. The objective of this study was to evaluate the impact of production technologies such as edge bonding, different initial moisture content of lamination and number of lamination layers (three and five) on the air permeability properties of the cross-laminated timber. Air leakage and crack area in cross-laminated timber panels were measured after the panels were conditioned in environments with different relative humidities in progressive steps from humid to dry environments (relative humidity 75% → relative humidity 43% → relative humidity 30% → relative humidity 15%). The test results showed that the five-layer specimens combined with initially drier laminations had the most considerable effect on avoiding air leakages through the panel. The greater number of layers helps to avoid any overlapping of gaps between laminations that are possible sources of air leakages. Based on the results, it is recommended to combine the technologies of using a larger number of layers together with initially drier laminations to minimise the growth of cracks on panel surfaces and avoid air leakages during the time of use.

Keywords

Cross-laminated timber, production technology, crack growth, air permeability

¹Department of Civil Engineering and Architecture, Tallinn University of Technology, Tallinn, Estonia²Department of Materials and Environmental Technology, Tallinn University of Technology, Tallinn, Estonia

Corresponding author:

Villu Kukk, Department of Civil Engineering and Architecture, Tallinn University of Technology, Ehitajate tee 5, 19086 Tallinn, Estonia.

Email: villu.kukk@ttu.ee

Introduction

Airtightness of a building envelope has become its important property. The more airtight envelope and the more efficient heat recovery with reduced thickness of thermal insulation have a lower construction cost and lower energy consumption, making it financially viable (Saari et al., 2012). The building envelope is locally sensitive to exfiltration air flow, as moisture convection could cause a remarkable increase in the moisture accumulation rate on the inner surface of the sheathing (Kalamees and Kurnitski, 2010). Kayello et al. (2017) showed that frost accumulation and condensation can occur very easily due to air leakage and pose a significant risk to the integrity of the envelope. In the building envelope, a cross-laminated timber (CLT) is often used as an air barrier layer. Crack formation in CLT influences its water vapour resistance and air permeability (Kukk et al., 2017), as well as fire resistance and acoustic properties, and lowers the quality (Brandner, 2013).

Moisture movement in wood has a major role in crack formation. The important benchmark for the wood properties affected by moisture is the fibre saturation point (FSP). FSP is defined as the point where wood cell lumen does not contain free water, but the cell wall is still saturated. Properties of wood, such as volume and mass, change if the moisture content (MC) changes below FSP point. A decrease or increase in MC results, respectively, in shrinkage or swelling of wood.

The unequal decrease in MC in different wood directions (tangential, radial and longitudinal) results in unequal shrinking of wood, which causes internal stresses inside the wood. This, in turn, results in the formation of checks and cracks in the wood surface. Changes in MC in the laminations of a CLT panel result in shrinking and swelling of the wooden board's volume, which may cause cracks in board surfaces and also gaps between the edges of the boards.

This study is focused on analysing the effects of production technologies on the air permeability properties of the CLT panel. The objective is to study the effects of the number of layers in the panel, bonded edges and initial MC in lumber to crack growth in CLT panels' lamination surfaces and air permeability. It was expected that the panels with higher number of layers (five layers), with initially drier laminations (MC \approx 6%) and with edge bonding would be the most airtight panels.

Methods

Test specimens

Specimens were produced using three different technologies whose parameters are given in Table 1. The parameters of the production technologies (number of layers, edge bonding and initial MC of laminations) was determined by their direct impact on the panel air permeability. Three specimens were made for each technology combination. According to this, 24 specimens of rectangular-shaped CTL panels with dimensions of 1.4 m \times 0.4 m (0.56 m²), a thickness of 30 mm and constructed from spruce wood (*Picea abies*) were designed and produced for the air

Table 1. Parameters of specimens produced with different technologies

Edge bonding	Number of layers and initial MC of laminations			
	Three-layer panel, thickness of one layer 10 mm		Five-layer panel, thickness of one layer 6 mm	
Edge-bonded panels	I3BE3L Initial MC \approx 13%	6BE3L Initial MC \approx 6%	I3BE5L Initial MC \approx 13%	6BE5L Initial MC \approx 6%
Panels without edge bonding	I3WBE3L Initial MC \approx 13%	6WBE3L Initial MC \approx 6%	I3WBE5L Initial MC \approx 13%	6WBE5L Initial MC \approx 6%

MC: moisture content.

permeability and crack evaluation test. A small part of the flat sides of the panels was covered with adhesive tape and mastic and therefore the measurement area of each specimen for the air permeability test was considered as 0.52 m^2 ($1.375 \text{ m} \times 0.375 \text{ m}$). Layer thickness of the three-layer panels was 10 mm and of the five-layer panels was 6 mm. The initial MC of 13% represented the common moisture level of laminations in the production of the CLT panels. The initial MC of 6% represented the minimum moisture level of laminations that is required for bonding with moisture curing one-component polyurethane adhesive, which was used in the production of the CLT specimens.

Specimens were marked as follows: 6/13W/BE 3/5L, where 6/13 defines panels' initial MC of laminations (MC of 6% and MC of 13%); WBE defines panels without bonded edges and BE defines panels with bonded edges; and 3/5L defines panels with three or five layers. When panels are marked without '6/13', the specimens are separately divided by initial MC of laminations, for example, as the specimens are divided in Figure 5.

Conditioning

The laboratory test process consisted of four steps of specimen conditioning in environments with different relative humidities (RHs) supplied by a climate chamber (Figure 1, right). Before and after each conditioning step, the following three parameters were measured and recorded during a laboratory test: MC of panels, crack area on panel's top surfaces and air permeability. Conditioning steps started from an RH of 75% and continued with RH of 43%, 30% and 15%, representing the typical decrease in RH in an indoor environment during the period from summer to winter in a Nordic climate (Ilomets et al., 2017). The minimum duration of each conditioning step was 30 days, which was calculated to be the sufficient time for the specimens to attain equilibrium moisture content (EMC). The minimum duration time for conditioning was calculated with hygrothermal software WUFI 6, and the simulation results are shown in Figure 2. The temperature was at a constant 20°C during the simulation, initial state for conditioning at 75% RH was a

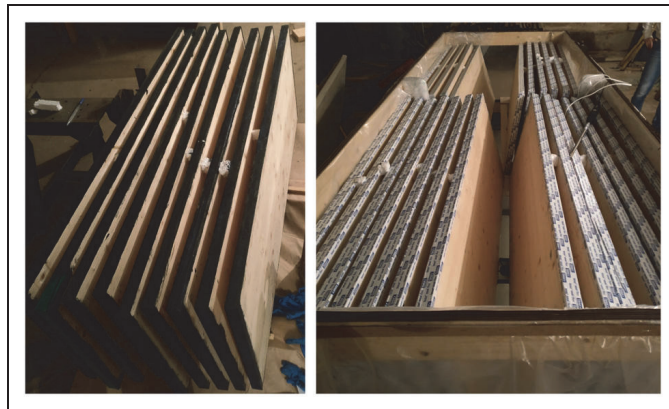


Figure 1. CLT specimens with coated edges (left) and conditioning process in the climate chamber (right).

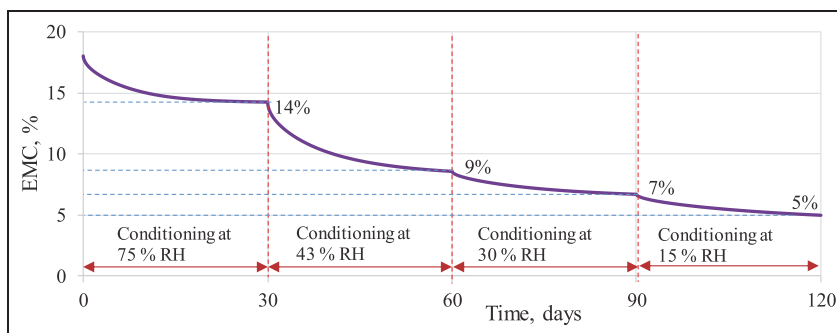


Figure 2. WUFI hygrothermal simulation of EMC (%) at 20°C of a 30-mm thick CLT panel made from Spruce at different RH conditions in 30-day interval.

selected EMC of 18% (represents the EMC at an RH of 90% at 20°C). Each conditioning at RH of 75%, 43%, 30% and 15% was done several times at various time periods until 30 days, which was found to be the sufficient minimum time to attain EMC for a 30-mm thick CLT panel made from spruce. At 20°C, the EMC of spruce at an RH of 75% is approximately 14%; at an RH of 43%, the EMC is approximately 9%; at an RH of 30%, the EMC is approximately 7%; and at an RH of 15%, the EMC is approximately 5% (Shmulsky and Jones, 2011; Simpson, 1991).

MC and crack growth

MC of panels was measured by an electronic wood moisture meter (GANN Hydromette H35). Average MC of each specimen was calculated from the three

measurements taken from different locations in one panel. Crack area results were obtained by measuring crack width and length using a crack width gauge and methodology developed by Humar et al, (2014). Cracks were measured from both flat sides of the panel, and total crack area was summed for each specimen. Cracks were defined as gaps between the laminations (Figure 3, left) and cracks in the middle of the lamination (Figure 3, right). Gaps between the laminations develop due to shrinkage of the edges of the wooden boards. Cracks appearing in the middle of the lamination (board) are expected to occur in edge-bonded panels. The rigid bond connection between the edges of the boards causes internal stresses over the cross-section of the board during the shrinkage and, as a consequence of this, cracks can form in the middle of the board top surface (Brandner, 2013). Regarding airtightness of the CLT panel, the worst resulting scenario in crack development is when gaps or cracks will overlap through all layers, thereby creating a hole through the entire thickness of the panel (Figure 3, left). It is most likely that the overlapping will occur with gaps between the layers in three-layer panels. For three-layer panels, if gaps in the outer layers occur in alignment (a gap appears in the same line in the top and bottom layers), then the appearance of a single gap in the middle layer is enough to result in an overlapping of gaps through the entire panel. A hole through the entire thickness of the panel caused by the overlapping of the gaps/cracks is a direct source of air leakage.

Air permeability

Air permeability measurements of the CLT specimens were carried out under laboratory conditions in accordance with the EN 12114 (2000) standard. The equipment used for the measurements consisted of the following (Figure 4): 0.46 m × 1.46 m hermetic test rig from powder-coated steel into which specimens were placed and sealed with ethylene propylene diene monomer (EPDM) rubber, air flow meter with integrated flow adjustment valve SMC_PFM 710 (flow rate range,

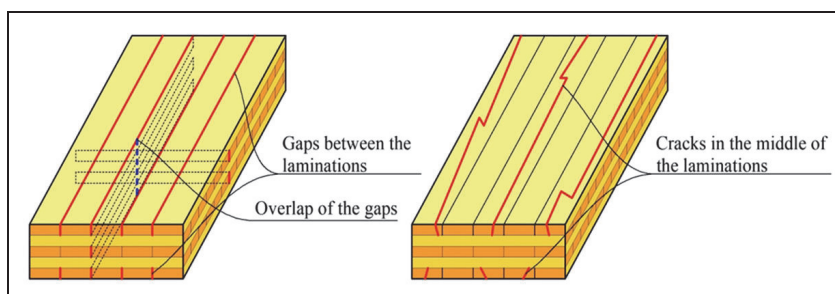


Figure 3. Gaps between the laminations, which may develop overlapping of the gaps (left), and cracks in the middle of the laminations (right) in the top layers of CLT due to swelling and shrinkage of the wood.

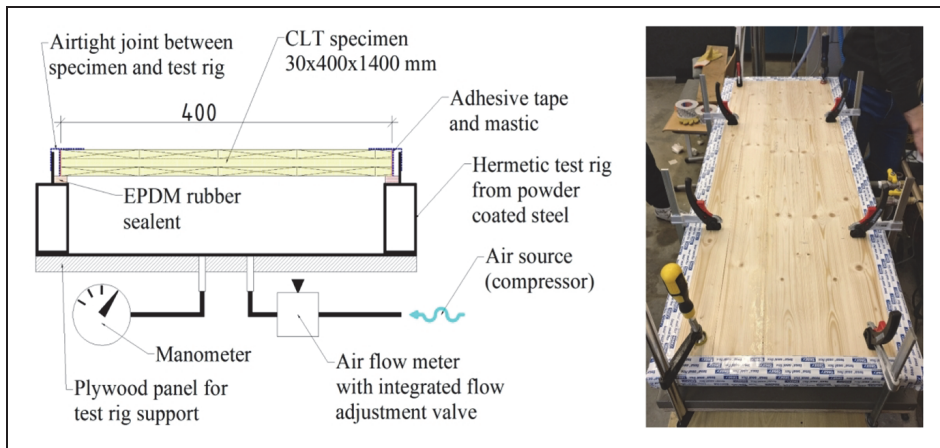


Figure 4. Equipment's complex scheme for carrying out the air permeability test (left) and CLT specimen attached and sealed to a hermetic test rig (right).

0.2–10 L/min; minimum unit setting, 0.01 L/min; and repeatability, $\pm 1\%$) and manometer for measuring air pressure difference Huba Control 699 (pressure range, 0–1600 Pa and tolerance, 0.7%). To avoid any air leakages between the connection of the test rig and specimens, all panel edges were coated with Blowerproof Liquid mastic and sealed with vapour and airtight adhesive tape (Figure 4, left and right).

Air leakage was measured only with positive pressure, and the maximum pressure difference (ΔP_{\max}) was selected to be 500 Pa and minimum (ΔP_{\min}) 50 Pa. The measurements were carried out in two stages. In the first stage, the leakage was measured by applying three overpressure impulses at a pressure difference of 550 Pa (each impulse was created with a pressure difference of 10% greater than ΔP_{\max}). In the second stage, the measurements were carried out at seven measuring points distributed in a geometric series of logarithmically growing pressure differences between and including ΔP_{\min} and ΔP_{\max} . Pressure difference in each measuring point was calculated by equation (1) in accordance with the EN 12114 (2000) standard, and starting from the first point the results were as follows: $\Delta P_1 = 50$ Pa, $\Delta P_2 = 73$ Pa, $\Delta P_3 = 108$ Pa, $\Delta P_4 = 158$ Pa, $\Delta P_5 = 232$ Pa, $\Delta P_6 = 341$ Pa and $\Delta P_7 = 500$ Pa. Each applied pressure difference, in both first and second stages, was held at least 3 s

$$\Delta P_i = 10^{\frac{-\log \Delta P_{\max} - \log \Delta P_{\min}}{N} + \log \Delta P_{\min}} \quad (1)$$

where ΔP_i (Pa) is the pressure difference in each measuring point and N is the total number of measuring points.

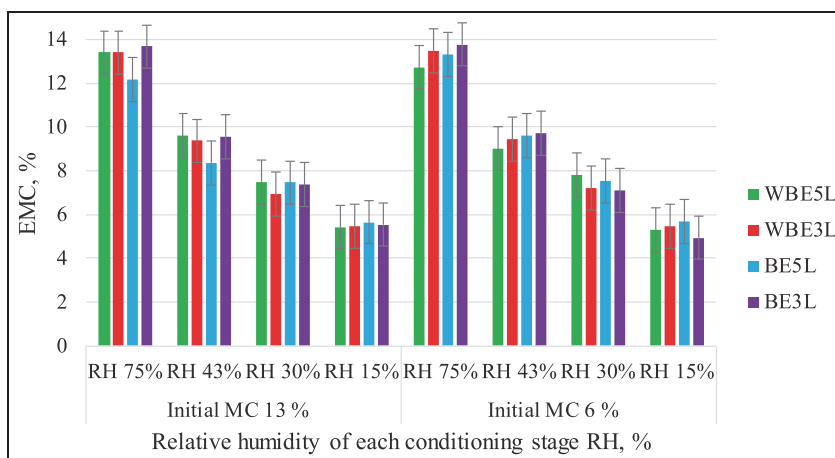


Figure 5. EMC of specimens after each conditioning step.

Measurements at different measuring points show the relation between the air flow (leakage) and pressure difference, which is characterised by the power function equation (2) taken from the EN 12114 (2000) standard

$$\dot{V} = C \times \Delta P^n \quad (2)$$

where \dot{V} (m^3/h) is the air flow rate, ΔP (Pa) is the pressure difference, C ($\text{m}^3/\text{h} \times \text{Pa}^n$) is the flow coefficient and n is the flow exponent.

Results

EMC of specimens

All specimens were conditioned equally and, as shown in Figure 5, the EMC after each conditioning step was similar in all specimens. The expected result of EMC after each conditioning step in different RHs was close in all specimens compared with the reference values (Shmulsky and Jones, 2011). The average EMC after conditioning at an RH of 75% was 13.2% over all specimens, which was close to the expected EMC of about 14%. After conditioning at an RH of 43%, the average EMC was 9.3% (expected EMC of about 8.5%), after conditioning at an RH of 30% it was 7.4% (expected EMC of about 6.5%) and after the final conditioning step (RH 15%) it was 5.4% (expected EMC of about 4.7%). Total moisture loss after the final conditioning step was about 7.8% over all specimens.

Crack area

The overall distribution of the cracks differed in each specimen, but the main difference was drawn out in different types of specimens. Thereby, different patterns of



Figure 6. Cross-sections of the three-layer and without edge-bonded panel (WBE3L) from the narrow side (top) and the long side (bottom), cut after the final conditioning step (RH 15%).



Figure 7. Cross-section of the five-layer and without edge-bonded panels (WBE5L) from the narrow side (top) and the long side (bottom), cut after the final conditioning step (RH 15%).

cracks in distribution, shape and sizes were recognised in different types of specimens. The width of cracks varied from 0.1 to 2.5 mm, larger crack widths occurred in the specimens with three layers (Figure 6) and smaller width cracks in the five-layer panels (Figure 7). The width of the crack depends on the thickness of the layer; the thicker the lamination (board) layer is, the larger the shrinkage in the edges of the boards and, as a result, the wider are the cracks that develop. Larger cracks developed in the top layers of the panel (Figure 6, top and Figure 7, top), while the middle layers mostly stayed undeformed, with only some minor cracks or gaps (Figure 6, bottom and Figure 7, bottom). Five-layer panels have three inner layers and therefore the possibility of overlapping of gaps/cracks is much lesser than in three-layer panels with only one inner layer. As shown in Figure 8(c) and (d), in specimens without edge bonding, the main cracks appeared as gaps between the laminations and most commonly the length of the gap occurred across the entire length of the panel from edge to edge. The area of the gaps was calculated as the area of a trapezoid formed from the measured largest and smallest widths of the gap. In edge-bonded specimens, Figure 8(a) and (b), the cracks developed most commonly in the middle of the laminations with a narrowing beginning and end. The area of the cracks with narrowing beginnings and ends was calculated as the area of the rhombus formed from the measured largest width of the crack. The largest number of cracks and the largest total area of cracks in one specimen appeared in specimens with an initial MC of 13%.

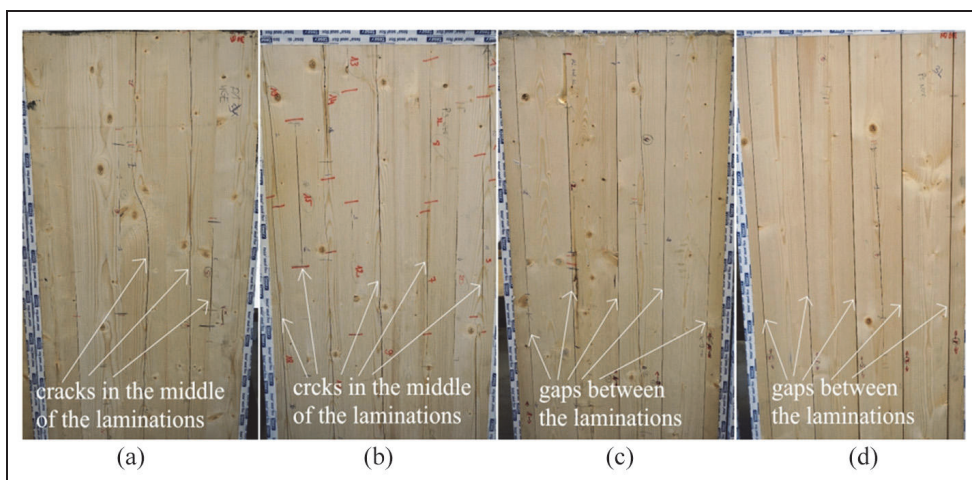


Figure 8. Examples of different patterns of crack distribution in five-layer and edge-bonded panel BE5L (a), three-layer and edge-bonded panel BE3L (b), five-layer and without edge-bonded panel WBE5L (c) and in three-layer and without edge-bonded panel WBE3L (d).

As shown in Figure 9, there is a noticeable difference in crack area between specimens with different initial MCs after each conditioning step. All specimens with an initial MC of 13.2% had an average total area of cracks greater than specimens with an initial MC of 6.2%. The biggest difference between specimens with different initial MCs was in specimens without the edge bonding and with three layers (WBE3L). Initially, drier specimens without edge bonding and with three layers (13WBE3L) had more than a three times smaller average total area of cracks after the final conditioning step than the initially moistest specimens (6WBE3L). The

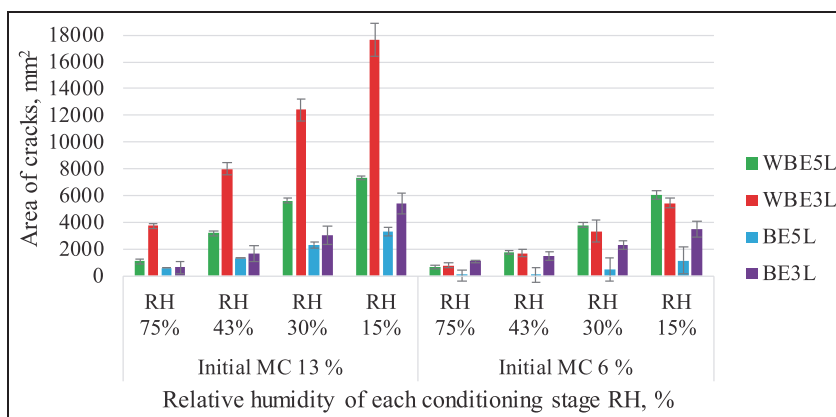


Figure 9. Average total area of cracks for each type of specimens after each conditioning step.

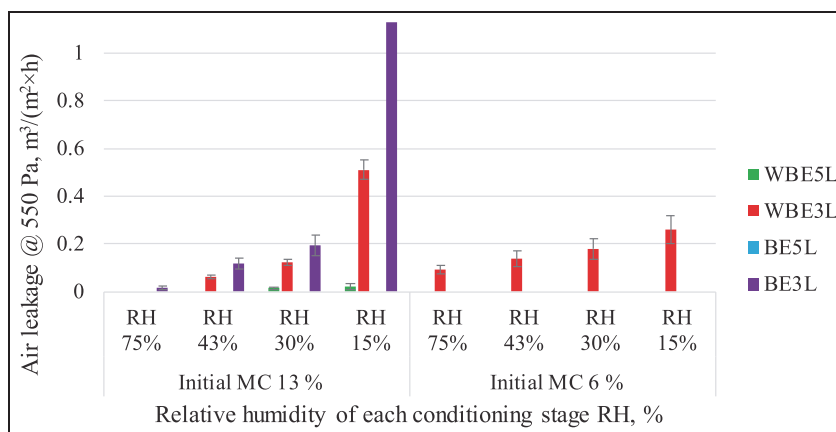


Figure 10. Average air leakages in each type of specimen at an air pressure difference of 550 Pa after each conditioning step.

average total area of cracks after final conditioning of specimen 13WBE3L was $17,649 \text{ mm}^2$ compared to 5439 mm^2 of specimen 6WBE3L. Specimen 13WBE3L also had the greatest average total area of cracks after final conditioning. The smallest difference between specimens with different initial MC was in specimens without the edge bonding and with five layers (WBE5L). Specimen 13WBE5L had the average total area of cracks after final conditioning of 7308 mm^2 and specimen 6WBE5L had 6047 mm^2 . The smallest average total area of cracks of 1152 mm^2 after final conditioning was in edge-bonded specimens with five layers and with an initial MC of 6.2%.

The growth of average crack area after each conditioning step was steady and similar in almost all specimens. Overall, the specimens with bonded edges and with initially drier laminations had a smaller average crack area after final conditioning.

Air permeability of specimens

The largest average air leakages at a pressure difference of 550 Pa after each conditioning step were in specimens with three layers, with an initial MC of 13% in laminations and with edge bonding technology (13BE3L; Figure 10). After the final conditioning step, the air leakage in the specimens 13BE3L exceeded the upper limit of the air flow meter ($1.13 \text{ m}^3/(\text{m}^2 \times \text{h})$).

After each conditioning step, edge-bonded specimens with five layers (BE5L), edge-bonded specimens with three layers and with an initial MC of 6% (6BE3L) and specimens without edge bonding with five layers and with an initial MC of 6% (6WBE5L) were completely airtight. Specimens without edge bonding with five layers and with an initial MC of 13% (13WBE5L) where leakages appeared after

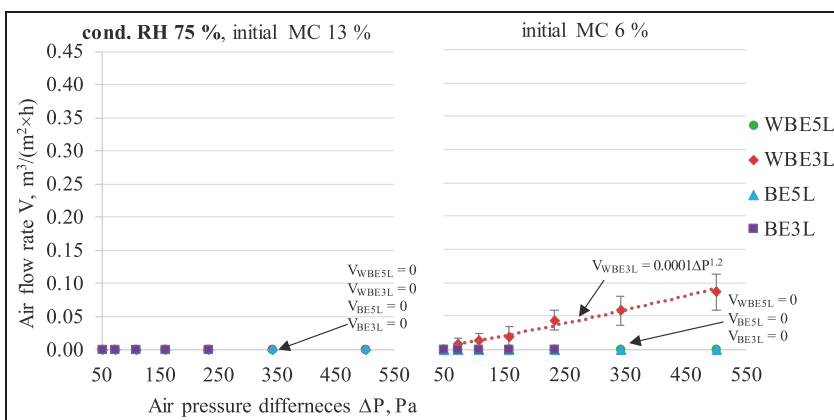


Figure 11. Air flow rate in each specimen with initial MC of 13% (left) and 6% (right) after the conditioning step in RH of 75%.

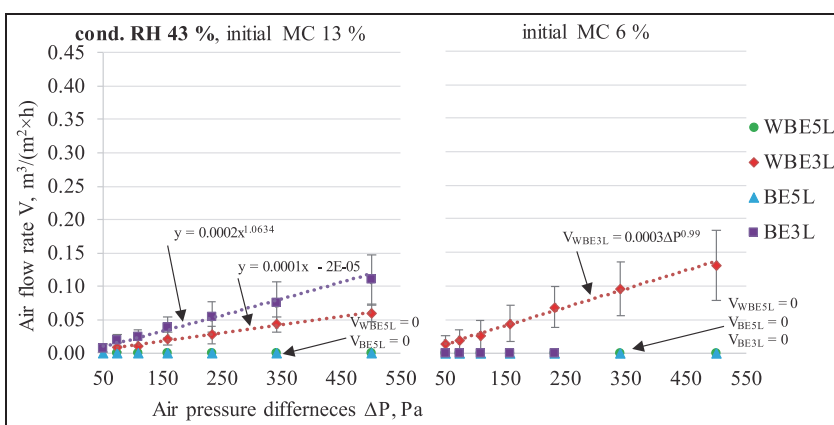


Figure 12. Air flow rate in each specimen with initial MC of 13% (left) and 6% (right) after the conditioning step in RH of 43%.

conditioning at an RH of 30% were almost airtight. After the final conditioning step, the specimen 13WBE5L had an average air leakage of $0.02 \text{ m}^3/(\text{m}^2 \times \text{h})$.

The only specimen with an initial MC of 6% that had air leakages after each conditioning step was that with three layers and without bonded edges (6WBE3L). After the final conditioning step, the specimen 6WBE3L had an average air leakage of $0.26 \text{ m}^3/(\text{m}^2 \times \text{h})$.

As shown in Figure 11 (left), Figure 12 (left) and Figure 13 (left), the biggest growth in the air flow rate appeared over all conditioning steps in specimens with an initial MC of 13% and with three layers (13WBE3L and 13BE3L), although all

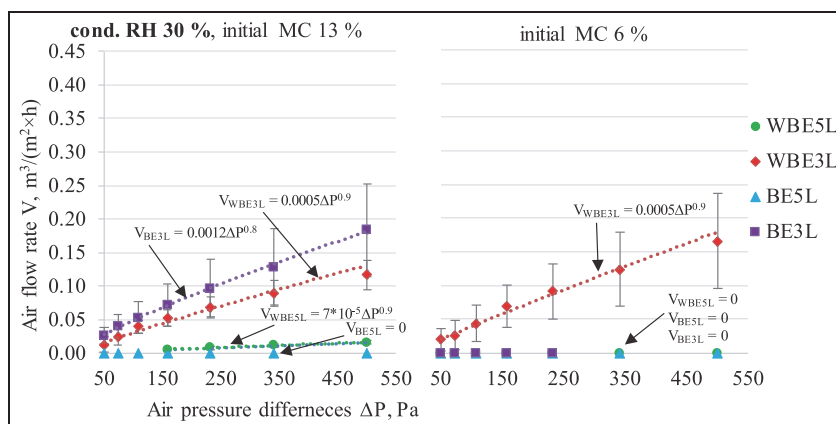


Figure 13. Air flow rate in each specimen with initial MC of 13% (left) and 6% (right) after the conditioning step in RH of 30%.

given specimens were airtight after the first conditioning step (Figure 11, left). After conditioning steps in RH of 43.5% and 30%, the growth of the air flow rate in specimens 13WBE3L and 13BE3L was steady and similar to the specimens with three layers, with an initial MC of 6% and without bonded edges (6WBE3L). The growth of air flow rate in specimens 13WBE3L and 13BE3L increased significantly after the final conditioning step at an RH of 15% (Figure 11, right).

From Figure 11 (right), it is seen that after the first conditioning step almost all specimens were airtight except the specimens with three layers with an initial MC of 6% and without bonded edges (6WBE3L). Observing the curves of the air flow rate of specimens 6WBE3L after each conditioning step, it was seen that the growth of the air flow rate was generally small. A small growth in the air flow rate was also measured in specimens without edge bonding with five layers and with an initial MC of 13% (13WBE5L).

As shown in Figure 14 (left), at a pressure difference of 50 Pa after the final conditioning step the average air leakage in specimens with three layers, with an initial MC of 13% in laminations and with edge bonding technology (13BE3L) was $0.15 \text{ m}^3/(\text{m}^2 \times \text{h})$, in specimens with three layers, with an initial MC of 13% in laminations and without edge bonding technology (13WBE3L) the average leakage was $0.1 \text{ m}^3/(\text{m}^2 \times \text{h})$. In specimens with three layers, with an initial MC of 6% in laminations and without edge bonding technology (6WBE3L), the average air leakage was $0.04 \text{ m}^3/(\text{m}^2 \times \text{h})$ at a pressure difference of 50 Pa after the final conditioning step (Figure 10, right). In the rest of the specimens (13BE5L, 6BE5L, 13WBE5L, 6WBE5L and 6BE3L), there were no air leakages at a pressure difference of 50 Pa after the final conditioning step.

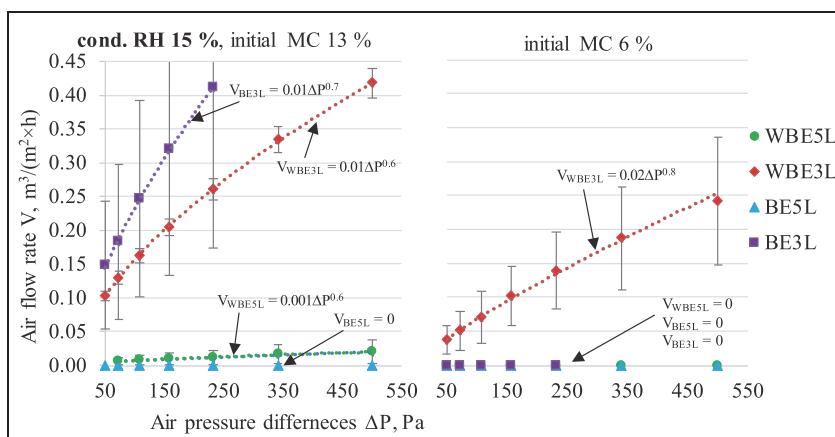


Figure 14. Air flow rate in each specimen with initial MC of 13% (left) and 6% (right) after the conditioning step in RH of 15%.

Discussion

Results of the crack area measurements showed that the production technologies of the CLT panels such as edge bonding and use of lumber with an initial MC of 6% can be recommended for avoiding large growth and development of the cracks on the panel's surface during the time of use. Using initially drier lumber together with edge-bonded laminations keeps the wood shrinkage lower and therefore keeps crack growth on the panel's surface at a low percentage. In the longer drying process (conditioning steps from RH 75% to 15%), the five-layer panels' considerable resistance to crack growth was due to a larger number of bond layers and thinner lamination layer thickness. Bond layers and dry thin laminations keep the wood steadier and controlled the formation of internal stresses during the drying process better. Inversely, as expected, the biggest cracks appeared in specimens without bonded edges and with higher initial MC in laminations. The higher initial MC leads to greater deformations from wood shrinkage in the lamination surface due to bigger moisture loss in the wood.

The greater number of layers helps to avoid any overlapping of gaps between laminations which are possible sources of air leakages (Kukk et al., 2017). The reason for better airtightness in panels with a larger number of layers is the same as it was for low crack growth, which was a larger number of bond layers and thinner laminations. In this research, the initially drier laminations showed a good resistance to crack growth and prevented bigger deformations on wood surfaces during the changes in the RH in the surrounding environment. The same effect was seen also in the air permeability test and therefore most of the specimens produced with initially drier laminations were airtight during the test. Nonetheless, there was no direct correlation between the crack area and air flow rate. Three-layer specimens

with laminations of an initial MC of 13% had overall the greatest leakages. The cause of the greater air leakages was not just a result of the initial MC, the larger lamination thickness and the single middle layer also contributed. It can be said that the development of cracks or gaps in the inner layers determines the airtightness of the panel. A CLT panel always has an even number of inner layers (1, 3, 5 ...) in addition to the two outer layers, and the results of this study showed that three inner layers are sufficient for ensuring the airtightness of CLT panels. Overall, it can be recommended that combining the technologies of using a larger number of layers, at least five, together with initially drier laminations, initial MC of 6%, for the production of CLT panels will result in the smaller growth of cracks on panel surfaces and smaller air leakages during the time of use. The use of bonded edge technology helps to ensure the avoidance of possible air leakage threats, but in the long term, the effect might decrease as bond layers may rupture, or cracks may form in the middle of laminations.

Latest measurements of airtightness of Estonian wooden buildings (Hallik and Kalamees, 2019) showed that buildings built after the enactment of the Estonian regulation of 'Minimum requirements for energy performance' had the airtightness q_{50} ranging from 0.8 to 3.1 m³/(m² × h). Based on the results of this study (air leakages at a pressure difference of 50 Pa), it can be said that similar results or better can be achieved in buildings made from all types of the investigated CLT panels. However, the connection joints of CLT panels must be airtight. This confirms that the CLT panels can be used as an airtight layer in addition to their load-bearing capacity purposes when designing a building envelope. Therefore, the CLT panels can be exposed to the indoor environment and the surface of the panel can be the final finishing element in the interior. This gives added value to the CLT panel because of its versatile use possibilities. However, in the design process, one should still consider the recommendations that are given in this study for choosing the technology of CLT to achieve long-term airtightness of the panels.

Designing a building where CLT panels are used as a main load-bearing element and will be exposed to the interior environment (without any additional internal layers in the external envelope) is important.

The large estimated error of air flow rate results was probably a result of the small number of specimens for each type, quality variation in lumber and manufacturing defects on panels (such as existing gaps between laminations and some degree of uneven distribution of adhesive). The air flow rate of specimen 13BE3L was measured to the maximum of what the equipment used could read and therefore no estimated error is shown in Figure 10.

Current research only covered one cycle of the drying process, and the results obtained in this experiment have given information about the behaviour of the panels at the beginning of their service life. For a better understanding of the air permeability properties of the panels in long-term use, it is recommended that repeated tests of several cycles are carried out in future research in the given topic.

Conclusion

In this study, three production technologies of CLT panels were analysed to determine the influence of the number of layers in the panel, bonded edges and initial MC in laminations. The main findings of this study were that the most effective technologies for avoiding large crack growth were using edge bonding together with initially drier laminations. Five-layer specimens combined with initially drier laminations had the most considerable effect on avoiding air leakages through the panel. The greater number of layers helps to avoid any overlapping of gaps between laminations that are possible sources of air leakages. Based on the results, it is recommended to combine the technologies of using a larger number of layers together with initially drier laminations to minimise the growth of cracks on panel surfaces and avoid air leakages during the time of use. The use of bonded edge technology helps to ensure the avoidance of possible air leakage threats, but in the long term, the effect might decrease as bond layers may rupture or cracks may form in the middle of laminations.

Acknowledgements

The author wishes to thank Estonian glulam producer Peetri Puit OÜ for helping to produce CLT specimens.

Declaration of Conflicting Interests

The authors declared no potential conflicts of interest with respect to the research, authorship and/or publication of this article.

Funding

The author(s) disclosed receipt of the following financial support for the research, authorship and/or publication of this article: This research was supported by the Estonian Research Council with Personal research funding PRG483 ‘Moisture safety of interior insulation, constructional moisture and thermally efficient building envelope’, Estonian Centre of Excellence in Zero Energy and Resource Efficient Smart Buildings and Districts, ZEBE, grant TK146 funded by the European Regional Development Fund.

ORCID iD

Villu Kukk  <https://orcid.org/0000-0001-7792-9035>

References

Brandner R (2013) Production and technology of cross laminated timber (CLT): a state-of-the-art report. In: *Focus solid timber solutions – European conference on cross laminated timber (CLT)*, Graz, 21–22 May.

- EN 12114 (2000) Thermal performance of buildings – Air permeability of building components and building elements – Laboratory test method.
- Hallik J and Kalamees T (2019) Development of airtightness of Estonian wooden buildings. *Journal of Sustainable Architecture and Civil Engineering* 24: 36–43.
- Humar M, Brischke C, Meyer L, et al. (2014) COST FP 1303 Cooperative Performance Test. In: *COST FP 1303 international conference*, Kranjska Gora, 10–14 May.
- Ilomets S, Kalamees T and Vinha J (2017) Indoor hygrothermal loads for the deterministic and stochastic design of the building envelope for dwellings in cold climates. *Journal of Building Physics* 41(6): 547–577.
- Kalamees T and Kurnitski J (2010) Moisture convection performance of external walls and roofs. *Journal of Building Physics* 33(3): 225–247.
- Kayello A, Ge H, Athienitis A, et al. (2017) Experimental study of thermal and airtightness performance of structural insulated panel joints in cold climates. *Building and Environment* 115: 345–357.
- Kukk V, Hortaa R, Püssaa M, et al. (2017) Impact of cracks to the hygrothermal properties of CLT water vapour resistance and air permeability. *Energy Procedia* 132: 741–746.
- Saari A, Kalamees T, Jokisalo J, et al. (2012) Financial viability of energy-efficiency measures in a new detached house design in Finland. *Applied Energy* 92: 76–83.
- Shmulsky R and Jones PD (2011) *Forest Products and Wood Science: An Introduction*, 6th ed. Chichester: John Wiley.
- Simpson WT (1991) *Dry Kiln Operator's Manual*. Madison, WI: United States Department of Agriculture.

PUBLICATION III

Kukk, V.; Bella, A.; Kers, J.; Kalamees, T., 2021. Airtightness of cross-laminated timber envelopes: Influence of moisture content, indoor humidity, orientation, and assembly. *Journal of Building Engineering*, 44.



Contents lists available at ScienceDirect

Journal of Building Engineering

journal homepage: <http://www.elsevier.com/locate/jobee>

Airtightness of cross-laminated timber envelopes: Influence of moisture content, indoor humidity, orientation, and assembly

Villu Kukk^{a, *}, Adeniyi Bella^b, Jaan Kers^b, Targo Kalamees^a

^a Tallinn University of Technology, School of Engineering, Department of Civil Engineering and Architecture, Nearly Zero Energy Buildings Research Group, Ehitajate tee 5, 19086, Tallinn, Estonia

^b Tallinn University of Technology, School of Engineering, Department of Materials and Environmental Technology, Laboratory of Wood Technology, Teaduspargi 5, 12618, Tallinn, Estonia

ARTICLE INFO

Keywords:

Cross-laminated timber
CLT
Air permeability properties
Airtightness
Initial moisture content
Moisture safety
Indoor humidity

ABSTRACT

Decrease in the relative humidity (RH) of the indoor air causes cracks in the cross-laminated timber (CLT) surface resulting in air leakages in the CLT panel. The effect of construction moisture on CLT air tightness properties is not clearly defined, which is important for moisture safe construction. The aim of this study was to investigate the effect of high MC on CLT air tightness properties compared to conventional factors such as indoor RH change, insulation type and façade orientation. An air permeability test was carried out on 12 different test walls with CLT as the airtight layer exposed to indoor environmental conditions. Test walls were constructed from CLT panels with two different initial moisture content (MC) values, $\approx 13\%$, and $\approx 26\%$, and in addition, different insulation materials were used in the wall assemblies: mineral wool, cellulose wool and polyisocyanurate (PIR) plates. Air leakage measurements were carried out at two different times, first in mid-autumn and second at the end of winter. Based on the results of this research it was concluded that high initial moisture content in the CLT panels significantly weakens the airtightness of the external wall. CLT exposure to water and wetting the CLT panels during construction carries more than a risk of moisture damage, and the planning and implementation of moisture safety in the construction of CLT buildings is therefore essential if the CLT is to be considered as an airtight layer. The effect of a change in indoor RH is small on the air permeability properties of the CLT wall. Therefore the 5-layer CLT panel can be considered and used as an air-tight layer in external wall construction as long as its initial low moisture content (about 13%) is maintained during both construction and service life.

1. Introduction

Air leakages occur in the building envelope as infiltration and exfiltration, both may cause a significant increase in total energy consumption. In addition to energy loss, air exfiltration can lead to moisture damage inside the external envelope through moisture convection. Kalamees and Kurnitski [1] investigated moisture convection inside the external wall and timber-frame attic floor connection and found that the joint is locally sensitive to exfiltration as moisture convection could cause moisture accumulation on the inner surface of the outer sheathing which creates favourable conditions for mould growth. Martin et al. [2] simulated an assembly gap in a cross-laminated timber (CLT) external wall to analyse the impact of air leakage on the energy efficiency and durability and found that infiltration significantly increased local external wall thermal transmittance and that the exfiltration may lead

to mould growth on CLT panel surfaces in the area of the assembly gap when the indoor RH exceeds 40% over the long term.

There are three main suggested technologies to improve airtightness of CLT envelopes: first is using sealing products between CLT elements; secondly giving an additional cover to the CLT joints with adhesive tape or with bitumen or airtight membrane strips; and thirdly covering the whole envelope with an airtight membrane [3]. The first two technologies are more cost-effective compared to the third and are the most commonly used. The third is the most reliable technology and mostly used if the panel itself is not airtight, for example, where an MHM (Massive-Holz-Mauer) panel is used instead of CLT. For all technologies, it is assumed that the lamination shrinkage of the CLT panel is minimal and is related only to changes in the RH of the indoor air.

For each building envelope, airtightness and hygrothermal performance must be guaranteed based on essential requirements for the envelope [4]. For CLT external envelopes, the massive wood panel is de-

* Corresponding author.

E-mail addresses: villu.kukk@taltech.ee (V. Kukk), adeniyibella@gmail.com (A. Bella), jaan.kers@taltech.ee (J. Kers), targo.kalamees@taltech.ee (T. Kalamees).

<https://doi.org/10.1016/j.jobee.2021.102610>

Received 22 September 2020; Received in revised form 20 April 2021; Accepted 23 April 2021

Available online 8 May 2021

2352-7102/© 2021 Published by Elsevier Ltd.

signed both as a load-bearing structure and as an interior finishing material. Given the standard thicknesses of the CLT panel (60–200 mm) and the water vapor resistance of the softwood ($S_d = 30\text{--}100\text{ m}$, in the dry state [5–7]), the panel also acts as an appropriate water vapor diffusion regulating layer. Therefore, a CLT external envelope in a cold and humid climate does not require any additional layers besides insulation and facade cover in terms of safe hygrothermal performance.

The wood shrinks and swells below the fibre saturation point (FSP) as the relative humidity (RH) of the environment changes [8,9]. As RH decreases, the wood loses bound moisture and shrinks, and as RH increases, moisture enters the cell walls and the wood swells. The largest volume change in wood is in the tangential direction. In cold and humid climates, the RH of indoor air is low in winter, down to 20–30% at outdoor temperatures of $-20\text{--}0\text{ }^\circ\text{C}$, but much higher in summer, over 50% [10,11]. This means that the RH changes significantly from season to season and this leads to a volume change in the wood when it is exposed to the indoor environment.

Several studies have shown that a decrease in the RH of the indoor air, during the winter season, causes cracks in the CLT surface and inside the panel, resulting in air leakages in the CLT panel. Kukkk et al. [12] investigated the impact of indoor RH decrease (from 75% to 30%, equilibrium moisture content (EMC) decrease from $\approx 15\%$ to $\approx 6\%$) to the air permeability properties of CLT panels with different production technologies and found that larger air leakages occurred in 3-layer CLT panels compared to 5-layer panels where air leakages were mostly insignificant. The same was concluded in Time [13] research indicating the need for an additional air barrier layer for the external walls with 3-layer CLT panels. Skogstad et al. [14] from SINTEF (Norwegian independent research organisation) studied the air permeability properties of the CLT panel and its connections (wall, wall to ceiling, wall to wall) and found that moisture content decrease (caused by a decrease in ambient indoor air RH) from 0.14 to 0.1 kg/kg caused air leakage in CLT connections to increase up to 10 times (mostly in wall to wall connections). They concluded that CLT constructions need to be designed with sealed connections to maintain their airtightness.

Wood shrinkage from moisture content absorbed during the construction process is higher than shrinkage that occurs as the wood dries out from its factory moisture level. During the construction process without proper weather protection, the moisture content of timber, including CLT, can be significantly higher than its factory moisture content. There are several studies and field measurements on CLT buildings [15–20] showing that the MC of water exposed CLT elements (in the outer layers), especially the joints, exceeds 25% and in some cases even more than 30% [17,20] during the construction process when the building is not weather protected.

The effect of construction moisture on CLT air tightness properties is not clearly defined in the literature and therefore the aim of this study was to investigate the effect of high MC on CLT air tightness properties compared to conventional factors such as indoor RH change, insulation type and façade orientation. Air leakage was measured from 12 CLT external test walls having two initial targeted MC values in CLT panels, $\approx 13\%$, and $\approx 26\%$. The test walls also differed in the selection of insulation material (mineral wool, cellulose wool and polyisocyanurate). 6 walls were oriented in the northern direction and the other 6 in the southern direction. The hypothesis of the work was that CLT external walls with higher initial MC have higher air leakage during the operation of the building.

2. Materials and methods

2.1. Test walls

12 (twelve) CLT external test walls with side dimensions of $850 \times 850\text{ mm}$ were examined in the current research. The walls differed in the target initial MC in the CLT panels, with MC of $\approx 13\%$, and $\approx 26\%$. The higher initial MC was gained by soaking the CLT panels in a pool filled with water. 6 walls were oriented in the northern direction and the other 6, of the same types, in the southern direction. The walls were constructed using 5-layer CLT panels with a total thickness of 100 mm, the thickness of each layer was 20 mm and the panels were made of spruce (*Picea abies*). In addition, the test walls were divided into three groups which differed in the selection of insulation material. The walls were externally insulated with 300 mm thick mineral wool (Fig. 1, right), 330 mm cellulose (Fig. 1, left), and 200 mm polyisocyanurate (PIR) insulation (Fig. 1, middle). From the outside, the walls were covered with a glass wool wind-barrier board and a ventilated timber cladding facade. Thermal transmittance was designed to be the same for all walls, $U = 0.11\text{ W}/(\text{m}^2\text{K})$, and therefore the thickness of the insulation varied. Thermal transmittance was calculated according to the standard EN ISO 6946:2017 by using equation (1).

$$U = \frac{1}{R_{si} + R_1 + R_2 + \dots + R_n + R_{se}}, \text{ W}/(\text{m}^2 \cdot \text{K}) \quad (1)$$

where U ($\text{W}/(\text{m}^2\text{K})$) is thermal transmittance of the external wall and R_T is total thermal resistance of the external wall, which was found by summing the resistance of the inner (R_{si}) and outer (R_{se}) surface and the resistance of each wall material layer (R_1, R_2, \dots, R_n). The resistances of the material layers were calculated according to the thermal conductivity given by the manufacturers.

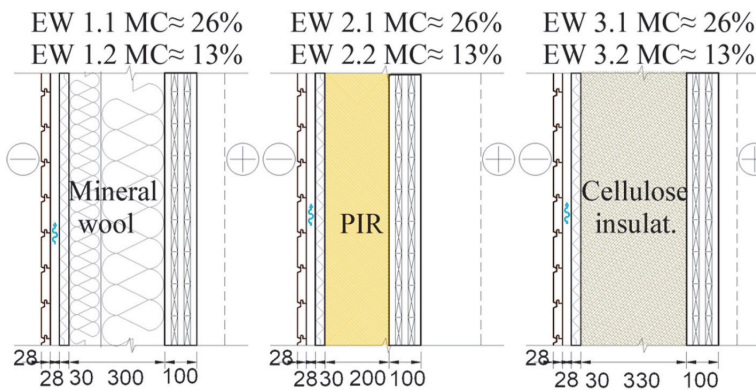


Fig. 1. Cross-sections of CLT external test wall types.

The test walls were surrounded on the sides with waterproof plywood plates to create an air and vapor tight enclosure for air permeability tests (Fig. 2, left).

2.2. Air permeability test

Air permeability measurements of the CLT walls were carried out in accordance with EN 12114 [21] and the measurements were done under real climate conditions. An airtight chamber was installed into the external wall. The airtight chamber was made of 18 mm thick film plywood and it was exposed to both the indoor and outdoor climate. The equipment used for the measurements consisted of a hermetic test rig made with flat stainless steel and plywood board which was used to cover the test wall and sealed with ethylene propylene diene monomer (EPDM) rubber, an airflow meter with integrated flow adjustment valve SMC_PFM 710 (flow rate range 0.2–10 l/min; minimum unit setting 0.01 l/min; repeatability $\pm 1\%$) and a manometer for measuring air pressure difference Huba Control 699 (Pressure range 0–1600 Pa; tolerance 0.7%), see Fig. 3.

To ensure the airtightness of the connection between the CLT panel and the plywood airtight chamber, one of the sealing methods mentioned in the introduction was used, according to which the connection was sealed with adhesive tape. Fig. 3 shows that the tape was applied to the corners of the connection, on both sides of the CLT, as well as to the corners of the plywood chamber to prevent any possible air leakage locations between the plywood and the CLT. In addition, the joint between the CLT and the plywood was filled with polyurethane foam in the thickness of the panel to ensure the rigidity of the CLT in the plywood chamber.

Air leakage was measured twice with different indoor humidity levels. The first measurements for the northern side walls were made on 30th October, with the average indoor RH of the last three months being 56% and 20 °C temperature (Fig. 4, left). The first measurements for the southern side walls were made 24th February, with the average indoor RH of the last two months being 20% and 21 °C temperature (Fig. 4, right). The second measurements for both northern and southern walls were made on 22nd March. The average indoor RH of the last three months was 29% and 21 °C temperature for the northern walls (Fig. 4, left) and the difference between the first and second measurement times was $\Delta RH_{N(M2-M1)} = -27\%$. For the southern walls, the average indoor RH of the last month before the second measurement was 36% and 19 °C temperature (Fig. 4, right), and the difference between the first and second measurement time were $\Delta RH_{S(M2-M1)} = 16\%$.

The air leakage measurements were made with only positive pressure. The maximum pressure difference (ΔP_{\max}) was selected to be 500 Pa for the first measurement and 100 Pa for the second measurement. The minimum pressure difference (ΔP_{\min}) was selected as 50 Pa and 25 Pa, respectively. The measurements included two stages and in the first stage, three overpressure impulses were applied at a pressure difference of 550 and 110 Pa (each impulse was created with a pressure difference of 10% greater than ΔP_{\max}). The measurements in the second stage were carried out at seven pressure steps. The steps were divided into a geometric series of logarithmically growing pressure differences between and including ΔP_{\min} and ΔP_{\max} . Pressure differences in pressure steps were found by equation (2) given in standard EN 12114 [21]. The first series of measurements included 7 pressure steps with pressure differences of $\Delta P_1 = 50$ Pa, $\Delta P_2 = 73$ Pa, $\Delta P_3 = 108$ Pa, $\Delta P_4 = 158$ Pa, $\Delta P_5 = 232$ Pa, $\Delta P_6 = 341$ Pa, and $\Delta P_7 = 500$ Pa; and the second series included $\Delta P_1 = 25$ Pa, $\Delta P_2 = 31$ Pa, $\Delta P_3 = 40$ Pa, $\Delta P_4 = 50$ Pa, $\Delta P_5 = 63$ Pa, $\Delta P_6 = 79$ Pa, and $\Delta P_7 = 100$ Pa. Each applied pressure difference at each pressure step was held for at least 3s.

$$\Delta P_i = 10^{\frac{\log \Delta P_{\max} - \log \Delta P_{\min}}{N} + \log \Delta P_{\min}}, Pa \quad (2)$$

where ΔP_i (Pa) is pressure difference in each pressure step, i , and N is total number of pressure steps. ΔP_{\min} and ΔP_{\max} are the selected minimum and maximum pressure difference for first and second series of measurements.

Analysis of the CLT external test walls was done based only on the results at a pressure difference of 50 Pa. The pressure difference of 50 Pa was chosen according to the air leakage rate (q_{E50}) given in EN ISO 9972: 2015 [22]. The air leakage rate is also found at a pressure difference of 50 Pa and is used to assess the air tightness of buildings in Europe. In this way, it is possible to compare the results of this research with the air tightness requirements set for buildings in Europe.

Given the small size of the test walls, the limit value of $1.0 \text{ m}^3/(\text{m}^2\text{h})$, with 10% reserve ($0.9 + 0.1 \text{ m}^3/(\text{m}^2\text{h})$), was set for the measurement results, above which the wall was considered not sufficiently airtight within the recommended norms of new nearly zero energy buildings and detached houses [23] when the results values should be applied to the whole building.

Due to the complexity of the measurement setup and large amount of time involved to perform the measurement, only one measurement was performed at each measuring point and the measurement uncertainty was calculated according to the accuracy of the equipment. Pos-



Fig. 2. CLT external test walls with the room view (left) and performing an air permeability test (right).

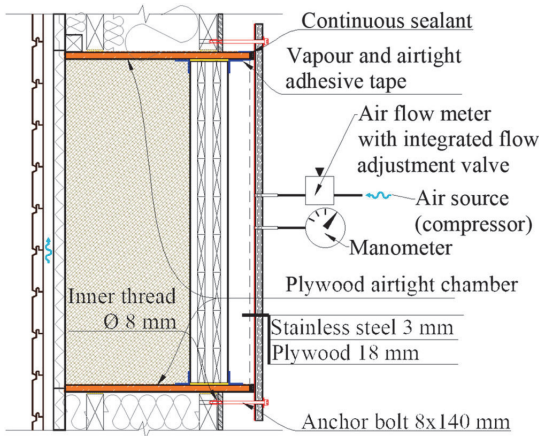


Fig. 3. Equipment kit scheme for carrying out the air permeability test (left).

sible air leakages that could have significantly increased the uncertainty were checked at the sealed connection between the hermetic test rig and the test wall with a smoke tester at a pressure difference of 1000 Pa. The uncertainty of the smallest measured result of 0.06 m³/(m²h) at the air flow measurement device repeatability of

±1% is 0.00005 m³/(m²h) and the largest measured result of 0.9 m³/(m²h) has an uncertainty of 0.0008 m³/(m²h) and therefore the uncertainties, due to their insignificant values, were not added to the results.

3. Results

The test walls with an initially higher MC (≈25%) in the CLT panels were observed to have the largest air leakages. At 25 and 50 Pa of pressure difference, the measured air leakages in all test walls with the higher initial MC exceeded the set limit value of 0.9 m³/(m²h) while other test walls with the lower initial MC (≈13%) had considerably lower air leakages (Table 1).

Test walls with a lower initial MC had air leakages below the limit value at 50 Pa of pressure difference, varying from 0.1 to 0.57 m³/(m²h), and this allowed the analysis of the effect of changes in the indoor humidity on the airtightness of the test walls, see Fig. 5. The result from the northern side test walls with lower initial MC of the CLT showed that the air leakage between the first and second measurements at 50 Pa of pressure difference increased between Δν = +0.03 and + 0.39 m³/(m²h), see Table 1 and Fig. 6, left. The first measurements were carried out at an RH of 56% and the second measurements were done at RH of 29%, having a change in RH of ΔRH_{N(M2-M1)} = -27%. The air leakage on the test wall EW1.2 N at 50 Pa of pressure difference was 0.07 m³/(m²h) after the first measurement and 0.1 m³/(m²h) after the second, the air leakage increased by 0.03 m³/(m²h). On the test wall EW2.2 N, the air leakage at 50 Pa of

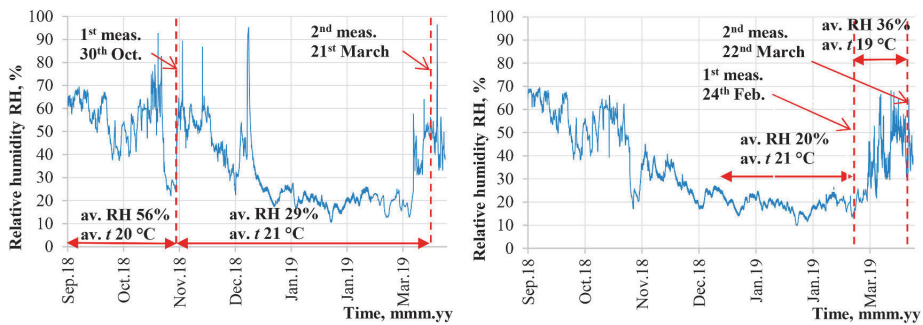


Fig. 4. Measurement times together with the environment properties of the northern (left) and southern side walls (right).

Table 1

Air flow rate values of CLT test walls after the first and second air permeability measurements.

Pressure difference, (Pa)	Measured air flow rate, ν (m ³ /(m ² h))											
	Northern side walls						Southern side walls					
	EW 1.1N	EW 1.2N	EW 2.1N	EW 2.2N	EW 3.1N	EW 3.2N	EW 1.1S	EW 1.2S	EW 2.1S	EW 2.2S	EW 3.1S	EW 3.2S
MC≈ 26%	MC≈ 13%	MC≈ 26%	MC≈ 13%	MC≈ 26%	MC≈ 13%	MC≈ 26%	MC≈ 13%	MC≈ 26%	MC≈ 13%	MC≈ 26%	MC≈ 13%	MC≈ 26%
Measurements in the first period, RH 56 %						Measurements in the first period, RH 20 %						
50	>0.9	0.07	>0.9	0.18	>0.9	0.11	>0.9	0.26	>0.9	0.33	>0.9	0.45
73	>0.9	0.09	>0.9	0.25	>0.9	0.15	>0.9	0.32	>0.9	0.39	>0.9	0.56
108	>0.9	0.12	>0.9	0.34	>0.9	0.20	>0.9	0.39	>0.9	0.48	>0.9	0.72
158	>0.9	0.14	>0.9	0.46	>0.9	0.26	>0.9	0.48	>0.9	0.59	>0.9	>0.9
232	>0.9	0.17	>0.9	>0.9	>0.9	0.32	>0.9	0.61	>0.9	0.73	>0.9	>0.9
341	>0.9	0.22	>0.9	>0.9	>0.9	0.40	>0.9	0.77	>0.9	>0.9	>0.9	>0.9
500	>0.9	0.27	>0.9	>0.9	>0.9	0.49	>0.9	>0.9	>0.9	>0.9	>0.9	>0.9
Measurements in the second period, RH 29%						Measurements in the second period, RH 36 %						
25	>0.9	0.06	>0.9	0.40	>0.9	0.11	>0.9	0.16	>0.9	0.23	>0.9	0.27
31	>0.9	0.08	>0.9	0.44	>0.9	0.12	>0.9	0.19	>0.9	0.26	>0.9	0.30
40	>0.9	0.08	>0.9	0.51	>0.9	0.13	>0.9	0.22	>0.9	0.29	>0.9	0.35
50	>0.9	0.10	>0.9	0.57	>0.9	0.15	>0.9	0.24	>0.9	0.32	>0.9	0.40
63	>0.9	0.11	>0.9	0.66	>0.9	0.17	>0.9	0.28	>0.9	0.35	>0.9	0.47
79	>0.9	0.13	>0.9	0.74	>0.9	0.20	>0.9	0.32	>0.9	0.40	>0.9	0.55
100	>0.9	0.15	>0.9	0.84	>0.9	0.23	>0.9	0.34	>0.9	0.46	>0.9	0.64

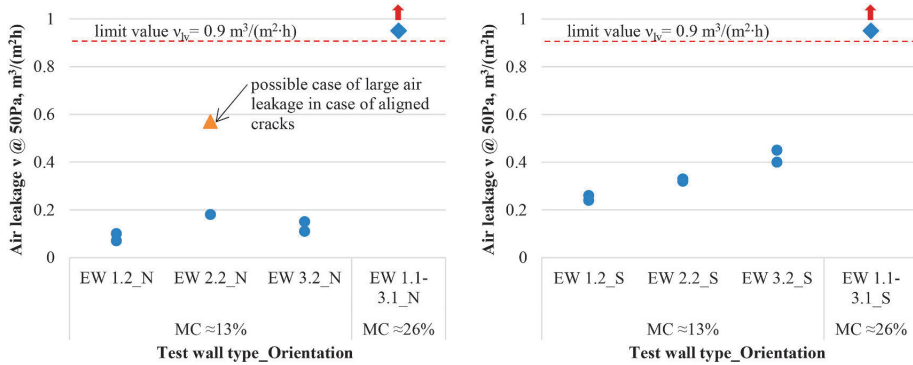


Fig. 5. Air flow rate values of northern (left) and southern (right) CLT test walls.

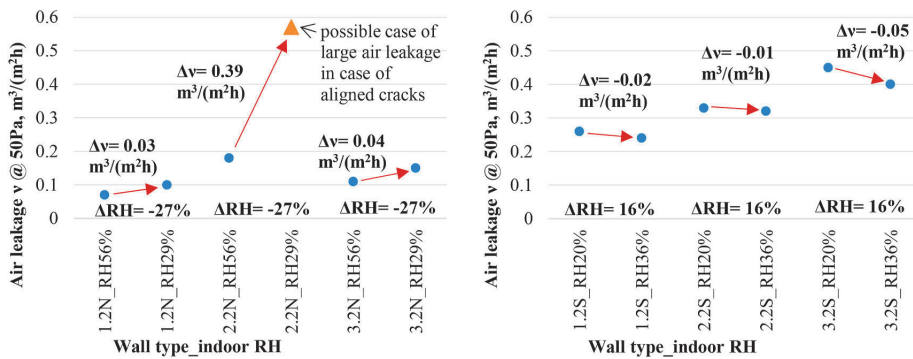


Fig. 6. Change in air leakages between first and second measurement times in northern (left) and southern walls (right).

pressure difference was $0.18 \text{ m}^3/(\text{m}^2\text{h})$ after the first measurement and $0.57 \text{ m}^3/(\text{m}^2\text{h})$ after the second, the air leakage increased by $0.39 \text{ m}^3/(\text{m}^2\text{h})$. The third test wall on the north side EW3.2 N had an air leakage of $0.11 \text{ m}^3/(\text{m}^2\text{h})$ at 50 Pa of pressure difference after the first measurement and $0.15 \text{ m}^3/(\text{m}^2\text{h})$ after the second, the air leakage increased by $0.04 \text{ m}^3/(\text{m}^2\text{h})$. The equilibrium moisture content (EMC) in the CLT panels decreased presumably about 3.8%, based on the ambient RH and temperature, which in turn led to the increase of air leakage due to the shrinkage of lamellas.

The result from the southern side walls with a lower initial MC of the CLT between first and second measurements showed that the air leakage at 50 Pa of pressure difference decreased between $\Delta v = -0.01$ to $-0.05 \text{ m}^3/(\text{m}^2\text{h})$ (Table 1 and Fig. 6, right) where the first measurement was done at RH of 20% and the second measurement was at RH of 29%, having a change in RH of $\Delta RH_{S(M2-M1)} = 16\%$. The air leakage on the test wall EW1.2S at 50 Pa of pressure difference was $0.26 \text{ m}^3/(\text{m}^2\text{h})$ after the first measurement and $0.24 \text{ m}^3/(\text{m}^2\text{h})$ after the second, the air leakage decreased by $0.02 \text{ m}^3/(\text{m}^2\text{h})$. On the test wall EW2.2S, the air leakage at 50 Pa of pressure difference was $0.33 \text{ m}^3/(\text{m}^2\text{h})$ after the first measurement and $0.32 \text{ m}^3/(\text{m}^2\text{h})$ after the second, the air leakage decreased by $0.01 \text{ m}^3/(\text{m}^2\text{h})$. The third test wall on the south side EW3.2S had an air leakage of $0.45 \text{ m}^3/(\text{m}^2\text{h})$ at 50 Pa of pressure difference after the first measurement and $0.4 \text{ m}^3/(\text{m}^2\text{h})$ after the second, the air leakage decreased by $0.05 \text{ m}^3/(\text{m}^2\text{h})$. The EMC in the CLT panels increased presumably about 2% which in turn led to the decrease of air leakage due to swelling of the lamellas.

The results showed a clear impact of the indoor humidity on the air permeability properties of CLT walls. Results showed that as indoor relative humidity decreases, air leakage in the CLT wall increases and vice versa, see Fig. 7, left. However, the changes in air leakage (less than

$0.1 \text{ m}^3/(\text{m}^2\text{h})$) were insignificant compared with the overall air leakage values of the test walls, except for one exception where the change was $0.39 \text{ m}^3/(\text{m}^2\text{h})$, see Fig. 7, right. It can be assumed that the large change in air leakage may have been caused by the alignment of the cracks in the middle or at the edge of the CLT panel.

Comparing the results when considering the effect of the indoor humidity and initial MC in CLT panels, it was seen that the last had a considerably greater impact on the air permeability properties of the CLT walls. In test walls with a high MC ($\approx 25\%$), the air leakage was higher than the limit value of $0.9 \text{ m}^3/(\text{m}^2\text{h})$ even at the minimum pressure difference of 25 Pa, therefore in such conditions, the wall cannot be considered as sufficiently airtight. In the case of dry CLT (MC $\sim 13\%$) in the external wall, the results showed that the walls were sufficiently airtight, $< 0.9 \text{ m}^3/(\text{m}^2\text{h})$, and the change in the indoor RH did not result in a change in air leakage of such an extent (the change in air leakage was between -0.05 and $0.04 \text{ m}^3/(\text{m}^2\text{h})$ with a change in RH of -27% and 16%) that it greatly impacts the airtightness of the external wall. However, there was also an exception, reflecting that in one case out of six (the ratio may be lower in reality), the formation of cracks from a change in the indoor RH may lead to a significant change in the airtightness properties of a CLT wall.

The test walls facing south had a slightly higher air leakage than the walls facing north, see Fig. 7, left. No specific reason was given, it can be assumed that the south facing walls dried faster due to the higher intensity of the sun, but a comparison between the panels temperatures was not performed.

There was also no relation between the insulation type and the air leakage in the test walls. The test walls with the, presumably, most airtight insulation (PIR) had at times the largest air leakage ($0.45 \text{ m}^3/(\text{m}^2\text{h})$ at 50 Pa) and those with, presumably, the least airtight

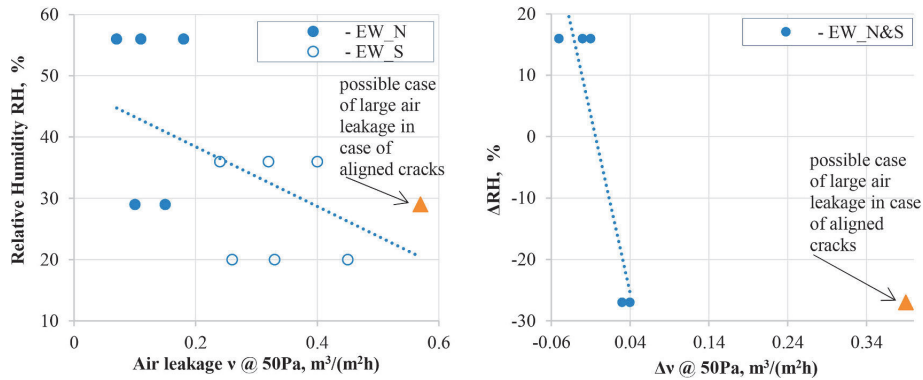


Fig. 7. Relation between air leakage and indoor RH (left) and between air leakage and RH differences (right).

insulation (mineral wool) had the smallest air leakage ($0.07 \text{ m}^3/(\text{m}^2\text{h})$) at 50 Pa).

4. Discussion

The results of this research showed that the high initial MC in the CLT panels has a great impact on the air permeability properties of the CLT test walls. The high initial moisture content ($\approx 26\%$) in the CLT panels significantly weakened the airtightness of the test walls. Air leakage exceeded the set limit value of $0.9 \text{ m}^3/(\text{m}^2\text{h})$ in all test walls with higher CLT moisture content. For comparison, the external walls with factory dry (MC 13%) CLT had significantly lower air leakages, which means that the hypothesis that external walls with higher initial CLT MC have larger air leakages was confirmed. This means that CLT exposure to water and wetting of the CLT panels during construction carries more than just a risk of moisture damage. Generally, it is known that high initial MC in timber structures may lead to possible biological moisture damage such as mould growth [12,24–27]. Biological moisture damage risk from high MC can be managed by letting the timber structure dry out. The higher the moisture content of the CLT up to the FSP, the greater the shrinkage of the CLT lamination [8,9], the greater the cracks between the laminations [26] and the greater the risk of air leakage. Consequently, the results of this study show that the planning and implementation of moisture safety in the construction of CLT buildings is essential if the CLT is to be considered as an airtight layer in the external wall. Using adhesive tape to ensure the air tightness of the CLT is not enough if it gets wet, as the results of this work showed. Thus, in the case of wetting, the only solution to ensure air tightness is covering the whole envelope with an airtight membrane, which, however, increases the construction cost.

There are several other studies which indicate that the initial high moisture content significantly affects the airtightness properties of the CLT panel. Skogstad et al. [14] found that the dry-out from initial MC of 15%–10%, when achieving equilibrium MC during service life, increased the air leakage of the CLT panels approximately up to 10 times. They concluded that airtight connections or a complete covering of the CLT external envelope with an airtight layer are necessary. Alev et al. [28] found that the decrease of MC in wooden logs led to a significant increase of air leakage in external walls made of wooden logs due to loosening of the seals between the logs due to weight loss.

Secondly, this study showed that a decrease in indoor humidity leads to an increase in air leakage in the test walls with low initial CLT moisture content, and vice versa. The EMC of wood is related to the RH of the air and is described by sorption. As the relative humidity decreases, the equilibrium humidity also decreases and the volume of the wood shrinks, which causes cracks and, in turn, air leakages. However, this study shows that the changes in air leakage were insignificant ex-

cept for one exception. Kukkk et al. [12] have found that a 5-layer panel with a low initial MC (13%) can be considered as an airtight layer, and that the air leakage in the CLT panel did not increase more than $0.01 \text{ m}^3/(\text{m}^2\text{h})$ at 50 Pa when RH in the surrounding environment decreased from 75% to 15%. Also, Time [13], found in their study that 5-layer CLT panels are airtight and sealing the structure joints is all that is necessary to achieve sufficient air tightness of the building. Based on the above findings, it can be concluded that the 5-layer CLT panel can be considered and used as an air-tight layer in external wall construction as long as its initial factory dry moisture content (about 13%) is maintained during both construction and service life. The effect of a change in indoor RH is small and therefore it is not a problem to leave the panel exposed to the indoor environmental conditions, however, it should be borne in mind that, in rare cases, this change may be significantly greater, which may have a significant effect on the airtightness of the wall.

Thirdly, this research showed that there was no clear relation between the insulation type and the air leakage in the test walls. The airtight insulation PIR was not additionally taped, nor is it taped in practice, and thus the installation gaps caused a large enough air leakage that the effect of the insulation on the airtightness of the external wall did not occur. This shows that the insulation layer cannot be considered as an airtight layer in CLT wall assemblies.

One of the limitations of the work was the measuring range of the equipment, due to which it was not possible to measure the maximum air leakages of the CLT external test walls with a high initial MC. Thus, there was no direct comparison of the air leakage values for the external walls with different initial CLT moisture content. On the contrary, the equipment used was selected to study the airtightness of the test walls in a low-leakage area (up to $0.9 \text{ m}^3/(\text{m}^2\text{h})$) and the accuracy of the results would have been significantly lower over a larger range. Another limitation was the size of the test walls. The test walls were too small to provide a direct comparison between measured air leakages from the test walls and real external walls. One of the reasons was the gross area of the connection (between the CLT and adjacent plywood) per wall area, which was larger on the test walls than it is on the actual walls. The connections of the walls (wall to wall, wall to ceiling, wall to roof connections) are usually one of the main locations of air leakages, therefore it can be assumed that the air leakage per surface area may be lower in actual CLT external walls than in the test walls in this study. In this study, the test walls were sealed with airtight tape, but the experiment revealed that the use of tape was not sufficient to ensure airtightness of CLT external walls due to the formation of large cracks in the CLT surface during the time of use.

Future studies on the air permeability properties of CLT external walls should be performed on large scale test walls or an entire building. Using a real building, it would be possible to study more accurately

the effect of the change in the indoor RH during the service time to air permeability of the CLT building.

5. Conclusions

The air permeability of three different types of CLT external test walls, with the CLT exposed to indoor environmental conditions, were examined in this study, differing in different insulation material (mineral wool, cellulose, and PIR), initial CLT moisture content ($\approx 13\%$ and $\approx 26\%$), and facade orientation (North and South). The following conclusions were drawn from the analysis of the research:

- High initial moisture content in the CLT panels significantly weakens the airtightness of the external wall. CLT exposure to water and wetting the CLT panels during construction is not only a risk of moisture damage, and the planning and implementation of moisture safety in the construction of CLT buildings is essential if the CLT is to be considered as an airtight layer.
- The effect of a change in indoor RH is small on the air permeability properties of the CLT wall. Therefore the 5-layer CLT panel can be considered and used as an air-tight layer in external wall construction as long as its initial low moisture content (about 13%) is maintained during both construction and service life.
- The type of insulation material and wall orientation did not have a major effect on the airtightness of the CLT external walls. Thus, the insulation layer cannot be considered as an airtight layer in CLT external walls.
- For more accurate studies on the air permeability properties of the CLT external building envelope, it is recommended to make measurements in a real building to study the effect of changes in the RH of the indoor humidity.

CRedit authorship contribution statement

Villu Kukkk: Conceptualization, Data curation, Writing – original draft, Methodology, Visualization, Investigation. **Adeniyi Bella:** Data curation, Writing – original draft, Visualization, Investigation. **Jaan Kers:** Supervision. **Targo Kalamees:** Supervision, Writing – review & editing.

Declaration of competing interest

The authors declare that they have no known competing financial interests or personal relationships that could have appeared to influence the work reported in this paper.

Acknowledgements

This research was supported by the Estonian Research Council with Personal research funding PRG483 “Moisture safety of interior insulation, constructional moisture, and thermally efficient building envelope”, Estonian Centre of Excellence in Zero Energy and Resource Efficient Smart Buildings and Districts, ZEBE, grant TK146 funded by the European Regional Development Fund and by the European Commission through the H2020 project Finest Twins (grant No. 856602).

The author wishes to thank Estonian CLT producer Peetri Puit OÜ for supplying CLT specimens.

References

- [1] T. Kalamees, J. Kurnitski, Moisture convection performance of external walls and roofs, *J. Build. Phys.* 33 (3) (2010) 225–247.
- [2] U. Martin, P. Blanchet, A. Potvin, Modeling the impact of assembly tolerances regarding air leaks on the energy efficiency and durability of a cross-laminated timber structure, *BioResources* 14 (1) (2019) 518–536.
- [3] J.L. Herms, Achieving airtightness and weather protection of CLT buildings, *E3S Web of Conferences NSB2020*, EDP Sciences, Tallinn, 2020.
- [4] Cpr, Regulation (EU) No 305/2011 of the European Parliament and of the Council of 9 March 2011 Laying Down Harmonised Conditions for the Marketing of Construction Products and Repealing Council Directive 89/106/EEC Text with EEA Relevance, 2011.
- [5] W. Zilling, *Moisture Transport in Wood Using a Multiscale Approach*, Catholic University of Leuven, 2009.
- [6] G. AlSageh, Hygrothermal Properties of Cross Laminated Timber and Moisture Response of Wood at High Relative Humidity, Carleton University, 2012.
- [7] J. Meynen, Cross Laminated Timber (CLT) bouwdeelen met bouwvocht en gewijzigde luchtdichtheid, Catholic University of Leuven, 2016.
- [8] R. Shmulsky, P.D. Jones, *Forest Products and Wood Science : an Introduction*, sixth ed., A John Wiley & Sons, Inc, 2011.
- [9] R. Shmulsky, P.D. Jones, *Forest Products and Wood Science*, Wiley-Blackwell, 2011.
- [10] S. Ilomets, T. Kalamees, J. Vinha, Indoor hygrothermal loads for the deterministic and stochastic design of the building envelope for dwellings in cold climates, *J. Build. Phys.* 41 (6) (2017) 547–577.
- [11] J. Vinha, et al., Internal moisture excess of residential buildings in Finland, *J. Build. Phys.* 42 (3) (2018) 239–258.
- [12] V. Kukkk, T. Kalamees, J. Kers, The effects of production technologies on the air permeability and crack development of cross-laminated timber, *J. Build. Phys.* 43 (3) (2019) 171–186, <https://doi.org/10.1177/1744259119866869>.
- [13] B. Time, Climate adaptation of wooden buildings – risk reduction by moisture control, 12th Nordic Symposium on Building Physics (NSB 2020), 2020 Tallinn.
- [14] H. Skogstad, L. Gullbrekken, K. Nore, Air leakages through cross laminated timber (CLT) constructions, 9th Nordic Symposium on Building Physics, Tampere University of Technology, 2011 Tampere: Tampere.
- [15] Olsson, L. (no date) ‘Moisture safety in CLT construction without weather protection-Case studies, literature review and interviews’..
- [16] J. Niklewski, M. Fredriksson, T. Isaksson, Moisture content prediction of rain-exposed wood: test and evaluation of a simple numerical model for durability applications, *Build. Environ.* 97 (2016) 126–136.
- [17] E. Liisma, et al., A case study on the construction of a clt building without a preliminary roof, *J. Sustain. Architect. Civ. Eng.* 25 (2) (2019).
- [18] K. Mjörnell, L. Olsson, Moisture Safety of Wooden Buildings – Design, Construction and Operation, Forum Wood Building Baltic, 2019.
- [19] E.L. Schmidt, et al., Environmental response of a CLT floor panel: Lessons for moisture management and monitoring of mass timber buildings, *Build. Environ.* 148 (2019) 609–622.
- [20] K. Kalbe, V. Kukkk, T. Kalamees, in: J. Kurnitski, T. Kalamees (Eds.), Identification and Improvement of Critical Joints in CLT Construction without Weather Protection, *E3S Web of Conferences*, vol. 172, 2020, p. 10002.
- [21] En 12114, Thermal Performance of Buildings - Air Permeability of Building Components and Building Elements - Laboratory Test Method, 2000 Brussels.
- [22] En Iso 9972:2015, Thermal Performance of Buildings — Determination of Air Permeability of Buildings — Fan Pressurization Method, International Organization for Standardization, 2015.
- [23] J. Hallik, T. Kalamees, Development of airtightness of Estonian wooden buildings, *J. Sustain. Architect. Civ. Eng.* (2019).
- [24] R. McClung, et al., Hygrothermal performance of cross-laminated timber wall assemblies with built-in moisture: field measurements and simulations, *Build. Environ.* 71 (2014) 95–110.
- [25] L. Wang, H. Ge, Hygrothermal performance of cross-laminated timber wall assemblies: a stochastic approach, *Build. Environ.* 97 (2016) 11–25.
- [26] V. Kukkk, et al., Influence of interior layer properties to moisture dry-out of CLT walls, *Can. J. Civ. Eng.* 46 (11) (2019) 1001–1009.
- [27] V. Kukkk, J. Kers, T. Kalamees, Hygrothermal performance of mass timber wall assembly with external insulation finish system, 2019 Buildings XIV International Conference, ASHRAE, Clearwater, FL, 2019, pp. 599–607.
- [28] Ü. Alev, et al., Air leakage and hygrothermal performance of an internally insulated log house, 10th Nordic Symposium on Building Physics, 2014 Lund, Sweden.

PUBLICATION IV

Kukk, V.; Külaots, A.; Kers, J.; Kalamees, T., 2019. Influence of interior layer properties to moisture dry-out of CLT walls. *Canadian Journal of Civil Engineering*, 46 (11), 1001–1009.

Influence of interior layer properties to moisture dry-out of CLT walls¹

Villu Kukk, Annegrete Külaots, Jaan Kers, and Targo Kalamees

Abstract: The objective of this study was to determine the maximum allowable initial moisture content (MC) for cross-laminated timber (CLT) walls having both exterior and interior thermal insulation. A laboratory test was conducted, for which four test walls with two different insulation solutions and two different MCs were built. Based on the test results, a simulation model was configured and simulations using the model were completed. The simulation results determined that the maximum allowable initial MC of the CLT panels was 17% for walls insulated additionally from inside with mineral wool and 15% for CLT wall assemblies insulated with polyisocyanurate (PIR). Based on these results, it was concluded that the allowable MC ranges between 8% and 16% for construction timber, and therefore, using a PIR board as interior insulation for CLT walls should be undertaken with caution given the very small margin for error in MC.

Key words: cross-laminated timber, built-in moisture, interior insulation, mould growth risk.

Résumé : L'objectif de cette étude était de déterminer la teneur maximale admissible en humidité initiale pour les murs de bois lamellé-croisé (CLT) à isolant thermique extérieur et intérieur. Un essai en laboratoire a été réalisé par la construction de quatre murs d'essai avec deux solutions d'isolant différentes et deux teneurs en humidité initiale différentes. Sur la base des résultats des essais, un modèle de simulation a été configuré et des simulations à l'aide du modèle ont été réalisées. Les résultats de la simulation ont permis de déterminer que la teneur initiale maximale en humidité admissible pour des panneaux de CLT était de 17 % pour les murs isolés également de l'intérieur avec de la laine minérale (MW) et de 15 % pour les assemblages de murs de CLT isolés avec du polyisocyanurate (PIR). Sur la base de ces résultats, il a été conclu que, pour le bois de construction, la teneur en humidité admissible varie entre 8 et 16 % et donc utiliser une planche de PIR comme isolant intérieur pour les murs en CLT doit être entrepris avec prudence étant donné la très faible marge d'erreur quant à la teneur en humidité. [Traduit par la Rédaction]

Mots-clés : bois lamellé-croisé, humidité intrinsèque, matériau isolant d'intérieur, risque de formation de moisissure.

Introduction

Because of its low embodied energy, the use of wood for the construction of buildings is a suitable for helping with the decarbonisation of building stock (EPBD 2018). Cross-laminated timber (CLT) is a novel wooden product whose use in the construction of wooden buildings is increasing because of its useful properties with respect to rigidity, strength, and environmental aspects. According to CEN – EN 16351 2015, CLT is defined as structural timber of at least three layers that are bonded crosswise; CLT products are used in a number of different types of buildings, including private residences, tall apartment houses, and public buildings.

Even though wood has a lower thermal conductivity compared with other load-bearing components, CLT components need additional thermal insulation to fulfill requirements for nearly zero energy buildings (nZEB) in the future. The thermal transmittance of the building envelope of a nZEB should be typically in the range of 0.14–0.08 W/m²K depending on the architecture and other energy performance measures (Arumägi and Kalamees 2016; Asaee et al. 2019; D'Agostino and Parker 2018; Sankelo et al. 2019). Using typical insulation materials ($\lambda \approx 0.04$ W/(m·K), insulation thickness should be around 25–45 cm. If thicker insulation is used, convection increases the heat flow and thermal transmittance of

the building envelope. Increases in insulation thickness may lead to an increased risk of mould growth and moisture damage when the insulation thickness is the only changed parameter (Gullbrekken et al. 2015; Pihelo and Kalamees 2016). To ensure that the walls of the building envelope are not too thick, modern insulation materials are needed. In general, insulation materials with lower thermal conductivity (e.g., vacuum insulation panels, polyisocyanurate (PIR), polyurethane (PUR)) are vapour tight, changing the hygrothermal performance of the building envelope. Even so, a vapour barrier may be needed in cold climates, depending on the hygrothermal loads and other properties of materials in the building envelope (Vinha 2007). If the insulation material is totally vapour tight, existing design rules may not apply any more.

The first Estonian CLT building was constructed in 2014 (Reinberg et al. 2013). Even though the building envelope was designed according to existing standards and the airtightness was well guaranteed, humidity in the externally insulated CLT panels was observed to be high, causing condensation and an elevated risk for mould development (Kalamees et al. 2014). The primary moisture source was the built-in moisture of the timber construction. Drying out of construction moisture could be an important parameter for the use of additional thermal insulation when under-

Received 14 September 2018. Accepted 4 February 2019.

V. Kukk, A. Külaots, and T. Kalamees. Department of Civil Engineering and Architecture, Tallinn University of Technology, Ehitajate tee 5, 19086 Tallinn, Estonia.

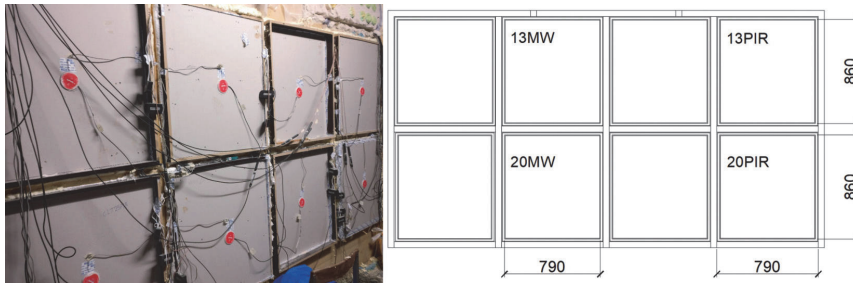
J. Kers. Department of Materials and Environmental Technology, Tallinn University of Technology, Ehitajate tee 5, 19086 Tallinn, Estonia.

Corresponding author: Villu Kukk (email: villu.kukk@ttu.ee).

¹This paper is part of a special issue entitled Durability and Climate Change.

Copyright remains with the author(s) or their institution(s). Permission for reuse (free in most cases) can be obtained from RightsLink.

Fig. 1. Interior view of the test walls in climatic chambers. [Colour online.]



taking deep energy retrofits of buildings (Pihelo et al. 2016). Considering the surface area and mass of the CLT used in building envelopes compared to the other wood frame structures, the time for drying excess moisture is potentially longer and therefore the risk of mould growth is greater. These examples show that in addition to the long-term performance, the hygrothermal performance during and after the construction of the building are also important design considerations.

In the current situation, more information is needed about the hygrothermal properties of CLT building envelopes. More specifically, information is required about the moisture levels in CLT panels to help ensure a hygrothermally safe performance of different envelopes. This is especially important for external walls that have additional insulation on the inner side of massive wood timber (Alev and Kalamees 2016) such as CLTs. Previous studies have been focused mostly on the moisture drying and airtightness of CLT envelopes. McClung et al. (2014) studied the drying behaviour of different CLT wall assemblies and showed that CLT panels with excessive moisture dried quickly (under the southern Ontario, Canada, summer or fall conditions). Fedorik and Haapala (2017) studied the impact of air gaps between the concrete foundation and the CLT frame for possible mould risk. The results did not show any significant risk for mold growth, although all results were only obtained by simulations and the test results are not currently published. Kukk et al. (2017) found that crack development on the CLT surface has significant impact on panel airtightness, and in the study undertaken by Skogstad et al. (2011), results showed the dependence of the CLT panel air permeability properties on moisture content.

Considering the current studies of the hygrothermal performance of CLT envelopes, it was determined that this study would focus on the effect of initial moisture content (MC) in CLT panels to the hygrothermal performance of CLT wall assemblies having different interior finish solutions. Thus, the objective of this study was to determine the maximum allowable initial moisture content of the CLT panel as a performance criterion for CLT walls having both exterior and interior thermal insulations.

Methods

Four test walls were built in a climatic chamber to permit the analysis of the hygrothermal performance of CLT external walls having two different insulation solutions and two different initial MCs in CLT panels under Nordic climate conditions from autumn to spring. Based on the measurement results of the 86 days of exposure in the climatic chamber, a simulation model was created for the wall under investigation and the simulation result was calibrated to those derived from the experiment. Simulations were used as a basis for calculating the maximum allowable initial MC for CLT panels.

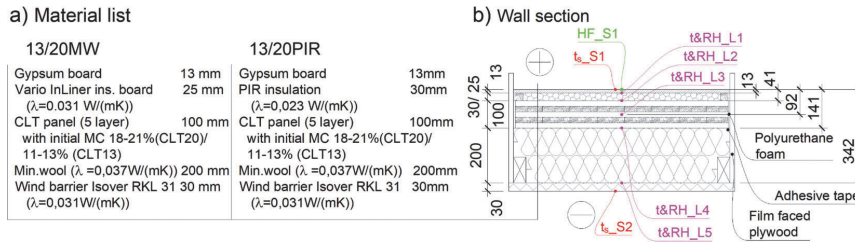
Laboratory measurements

CLT test walls

Four test walls (Fig. 1) with side dimensions of 0.79 m × 0.86 m were constructed using five layer CLT panels having a thickness of 100 mm (Fig. 2). Two levels for the target initial MC in CLT panels were chosen: 13% and 20%. The real initial MC varied depending on the humidifying results: two of the walls had an initial MC in the CLT panels of 11.9% and 12.4% and the other two had MCs of 18.7% and 20.6%. CLT panels were delivered directly from the factory, and initially, all the panels had about the same MC of 12%. The MC in the CLT panels was measured by an electronic wood moisture meter (GANN Hydromette H35). The higher initial MC was gained by soaking the CLT panels in a pool filled with water, and the MC was measured by weighing the panels at fixed intervals. Weighing was continued until the calculated weight corresponding to the desired MC was achieved. Initially, it was expected that during the 4 weeks of soaking the moisture would distribute evenly through the panel thickness; however, during the experiment, it turned out that the top layers of the wetted panels still had a much higher MC than the middle layers. Later during the modeling, the higher MC in the top layers was calculated based on the measurements of the relative humidity (RH) inside panel. The higher initial MC in the CLT panel represents the situation where the CLT has been exposed to open water (e.g., rainwater, water leakages, melting snow) during the construction period, and therefore, the moisture level in the panel has increased.

CLT test walls were designed and built with two different insulation solutions, using both interior and exterior insulations. External insulation in all test walls was 200 mm thick glass wool covered with a 30 mm thick wind barrier made of glass wool and covered by an airtight external layer. For the interior insulation, two different kinds of insulation were used. (i) On two of the test walls, 30 mm thick PIR board covered from both sides with aluminum foil was used, which was considered as a vapor tight layer, and therefore, moisture from the CLT panel could dry out to only one direction (to the outside). (ii) Two other walls incorporated glass wool board Vario InLiner and had a variable vapour diffusion resistance depending on the RH of the environment and moisture from the CLT panel could dry out to both directions (to the outside and inside). The inner layer for all test walls was gypsum board. The edges of all test walls and CLT panels were covered with 18 mm thick film-faced plywood boards ($Z_{RH90\%} = 1.14 \times 10^{10} \text{ m}^2\text{sPa/kg}$) and sealed with PUR foam and airtight adhesive tape to minimize two-dimensional moisture movement through wall. The purpose of using tape and PUR foam for sealing was to create an airtight connection between the CLT and film-faced plywood to prevent any convective moisture movement. Also, the narrow edges of the CLT panels were covered with a moisture and air barrier mastic Blowerproof Liquid ($Z = 3.92 \times 10^{11} \text{ m}^2\text{sPa/kg}$) for the same reason as the adhesive tape was used. Test walls were

Fig. 2. (a) Material layer lists of the test walls and (b) placement of measuring sensors in the wall section. [Colour online.]



marked as follows: 13/20 depending on the initial MC and either PIR or mineral wool (MW) depending on the interior surface material. The thermal transmittance of each test wall was similar: 13/20MW, 0.117 W/m²K, and 13/20PIR, 0.124 W/m²K.

The temperature (*t*), RH, and heat flux (*q*) were measured between the material layers in the test walls (Fig. 2). Both *t* and RH was measured by Omnisense A-1 temperature and humidity sensors with accuracies of ±0.3 °C from 0 °C to 60 °C (temperature sensor) and ±2.0% from 0% to 100% RH (RH sensor). Surface temperatures were measured by HOBO UX120-006M data logger together with TMC6-HD/E sensors with an accuracy of ±0.1% of reading (logger) and ±0.25 °C from 0 °C to 50 °C (sensor). Heat flux was measured by a Hukseflux HFP01 heat flux sensor with an uncertainty of calibration of ±3% (*k* = 2). Sensors were marked as follows: HF/*t*&RH/*t_s*-L/S1, where HF/*t*&RH/*t_s* defines the measured quantity (HF, heat flux; *t*&RH, temperature and RH; *t_s*, surface temperature) and L/S1 shows the location of the sensor (L1, L2, L3, ..., layer 1, 2, 3, ...; S1, inner surface; S2, outer surface).

Test environment conditions

Test walls were built in a large-scale climate chamber where it was possible to create indoor and exterior conditions on both sides of the test walls. The total duration of the test in the climate chamber was 86 days, and during the experiment, northern European climate conditions from autumn to spring were applied (Kalamees and Vinha 2003), as depicted in Fig. 3. The duration of autumn conditions (internal RH (RH_i) ≈ 50%, external RH (RH_e) ≈ 80%, internal temperature (*t_i*) ≈ +21 °C, external temperature (*t_e*) ≈ +10 °C, Δ*v* ≈ 1.6 g/m³) was about 40 days, the duration of winter conditions (RH_i ≈ 35%, RH_e ≈ 80%, *t_i* ≈ +21 °C, *t_e* ≈ -10 °C, internal moisture excess (Δ*v*) ≈ 4.5 g/m³) together with a transition period of 5 days was about 26 days, and the duration of spring conditions (RH_i ≈ 50%, RH_e ≈ 45%–70% in one cycle/day, *t_i* ≈ +21 °C, *t_e* ≈ 0 °C to +15 °C in one cycle/day, Δ*v* ≈ 7–0.18 g/m³ in one cycle/day) was about 20 days (including a transition period of 3 days). The test duration was shortened to 86 days, compared with the usual 9 months with three seasons, due to practical reasons and time limitations. It was expected that during the test, the CLT panels in wall assemblies might not reach absolute equilibrium moisture levels, but it would still be enough to investigate the dry-out capacity of CLT, and the heat, air, and moisture performance could be studied through the simulation, calibrated based on the measurements. Fluctuations in *t_e* and RH_e during a one-day cycle were applied for simulating the effect of solar radiation. It was considered equivalent to temperature change in the outdoor environment in springtime due to solar radiation during a one-day cycle in general. The outdoor temperature increase during the day and the decrease in the night was according to the exposure of the sun in general. The average change of the outdoor temperature was calculated using the climate data from March to May of the reference year that was used for finding the impact of initial moisture on durability by modeling. Exterior conditions were considered to be the environment in the ventilation gap between the wind barrier and external façade, and therefore, any additional weather

phenomena (for example, rain load) were not applied. That is the reason why an external façade was not added to the test walls. Large peaks between days 49 and 56 appeared because of technical reasons with the climate chamber. The climate chamber was switched off due to a malfunction for 6 days, and therefore, the *t* increased and the RH decreased inside the chamber.

Modeling

Simulation model

The simulation model for the test walls was made by using Delphin 5.9.3 software, which is a simulation program used for the calculation of coupled heat, moisture, and mass transport in porous building materials (Nicolai and Grunewald 2003). The model was modified for further calculations to find the maximum allowable initial MC in CLT panels for given wall assemblies. Given that the building elements being studied were essentially adiabatic in directions other than across the wall thickness, a one-dimensional model was deemed sufficient for the hygrothermal analysis. Boundary conditions for the calibration of the model were assigned as measured exterior and interior climate conditions in the climate chamber test. Calibration was made by using surface temperature and RH (assuming the same vapour pressure in air and on surface). The model was calibrated on the basis of comparison of four indicators: *t*, RH, partial pressure of water vapor (*P*), and *q*. Materials selected from the Delphin 5.9.3 software database were used to validate the calculation model (Table I).

CLT panel was defined as solid wood from spruce (*Picea*) with radial grain direction. Extra vapour resistance was added to the top surfaces of CLT lamination layers to simulate adhesive layers. Resistance was added as a vapour resistance equivalent air layer thickness (*S_d*) and according to that used in previous studies (Kukkk et al. 2017), namely *S_d* = 1.25 m. Top surfaces of the PIR insulation board were considered as vapor tight simulating aluminum foil. One surface of the Vario InLiner insulation board was determined as vapour retarder layer named “Vario XtraSafe”. It had high vapour diffusion resistance variability, where *S_d* varied from 0 to 15 m, depending on the RH of the surrounding environment. The higher the RH in the surrounding environment, the lower the vapour resistance in Vario XtraSafe surface. In the lower RH, from 0 to 15%, the vapour resistances is highest where equivalent air layer thickness stays constant at 15 m. When RH exceeds 15%, vapour resistance decreases linearly together with the increase of the RH until achieving 75%. From 75%, the vapour resistance is minimum and equivalent air layer thickness stays near 0 m.

The lower initial MC in CLT panels used in the calculation model for test walls 13MW and 13PIR was considered as evenly distributed over all layers and was 10.7%. Evenly distributed MC was considered because the panels were kept before the experiment in the same conditions as in the factory. Therefore, it was expected that the panels had achieved equilibrium MC through the entire thickness as measured after arriving from the factory. In the calculation models for test walls 20MW and 20PIR, where CLT panels were previously wetted, the initial MC was different in

Fig. 3. Indoor and exterior test environment conditions: (a) relative humidity and (b) temperature. [Colour online.]

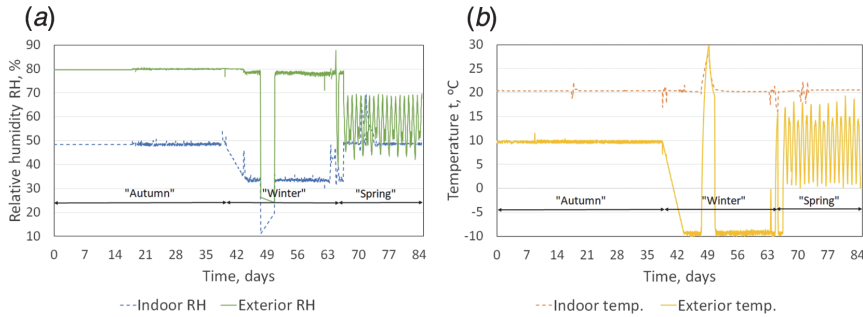


Table 1. Materials and their properties used in calculation model.

Material	Thickness (d, mm)	Bulk density (ρ , kg/m ³)	Thermal conduct. (λ , W/(m·K))	Diffusion resistance factor (μ)	Water uptake coefficient (kg/(m ² ·s ^{0.5}))
Gypsum board	13	745.1	0.21	10.9	0.179
PIR insulation board	30	35	0.023	100	1×10 ⁻⁸
Vario InLiner insulation board	25	112	0.031	1 (Vario XtrSafe RH15%/S _d = 15; RH75%/S _d = 1)	0
CLT panel (five layers)	100	437.6	0.11	474.7	0.013
Glass wool insulation	200	37	0.039	1	0
Glass wool wind barrier RKL31	30	112	0.031	1	0

CLT panel layers. In test wall 20MW, the initial MC in the top layers of the CLT panel (L5 and L1) was 19%, in the middle layers (L4 and L2) it was 16.8%, and in the inner layer (L3) it was 11.3%. In test wall 20PIR, the initial MC in the top layers (L5 and L1) was 20.6%, in the middle layers (L4 and L2) it was 16.8% and in the inner layer (L3) it was 12.5%.

Determining maximum allowable initial MC

After calibration, modelling was continued to determine the maximum allowable initial MC in CLT panels without mould growth. For external climatic conditions, the Estonian moisture reference year was used (Kalamees and Vinha 2004). Interior climatic conditions were set by standard EVS-EN ISO 13788 2012, where moisture excess class 3 was selected for the given calculations. Moisture excess class 3 is selected for detached houses and rooms where the population density is about 30 m² per person. Moisture excess in class 3 is 6 g/m³, when the temperature is below 0 °C, and 1 g/m³, when the temperature is above +20 °C (Fig. 4a). The indoor temperature was selected based on measurements in an Estonian dwelling (Ilomets et al. 2018), as shown in Fig. 4b. The performance of the CLT walls was modeled during 5-year period. The maximum allowable initial MC in CLT panels was determined during the 5-year period with the assumption that the panel has an equal degree of MC in all layers.

Evaluation criteria

Risk of mould growth on the material surface was used as the evaluation criteria for determining the maximum allowable MC in CLT panels. The evaluation by mould growth index is undertaken according to a numerical scale and the mould index is calculated through a function using temperature and RH on the material surface (Ojanen et al. 2010). When calculating the mould growth index, it is necessary to consider the sensitivity of materials to mould growth and exposure time to critical RH and temperature.

For the performance assessment, a mould index value of $M < 1$ (no growth) was used. Other values given in the figures indicate small amounts of mould on the surface $M = 1$ (microscope); several local mould growth colonies on the surface ($M = 2$; microscope);

and visual findings of mould on surface, <10% coverage, or, <50% coverage of mould ($M = 3$; microscope).

Results

Measurement results

Temperature, RH, and heat flux data obtained from the climate chamber test experiment were collected, analysed, and subsequently used to determine the performance of the test walls during the experiment. Results showed that the most critical points in all wall assemblies were between the interior insulation board and CLT panel (L2) and also between the exterior insulation and the wind barrier board, where RH appeared at the highest values. Between the exterior insulation and the wind barrier board (L5) (Figs. 5c and 5d) the highest RH appeared in test wall 20PIR where it reached RH 80% during the first “autumn” climate period (~6 weeks) when temperature remained around 10 °C. In subsequent climate periods, the RH dropped below 80%. In other test walls, the RH did not reach 80% between the exterior insulation and the wind barrier board (L5). Both test walls 20MW and 20PIR at temperatures from 15 °C to 20 °C (Figs. 5a and 5b) had a RH above 80% between the interior insulation board and CLT panel (L2). However, after 8 weeks of testing, the RH dropped below 80% in test wall 20MW; for test wall 20PIR, it stayed around 90% during the entire test. In test walls 13MW and 13PIR, the RH did not reach 80% between the interior insulation board and CLT panel (L2). The most critical climate period was “autumn”, where the RH reached the highest values in all layers; thereafter, at the beginning of the “winter” period, the RH started to decrease. As RH values were highest between the interior insulation board and CLT (L2) at higher temperatures, this was considered as the most critical point for further modelling.

Comparison of hygrothermal conditions between test results and simulations

Using the adjusted material properties given in Table 1, the test walls were modeled with the same climate parameters as used in the laboratory experiment to simulate the test results. Comparing these results, the average differences together with standard de-

Fig. 4. Moisture excess classes by (a) moisture excess values and (b) indoor temperature model dependent upon the daily average outdoor temperature. [Colour online.]

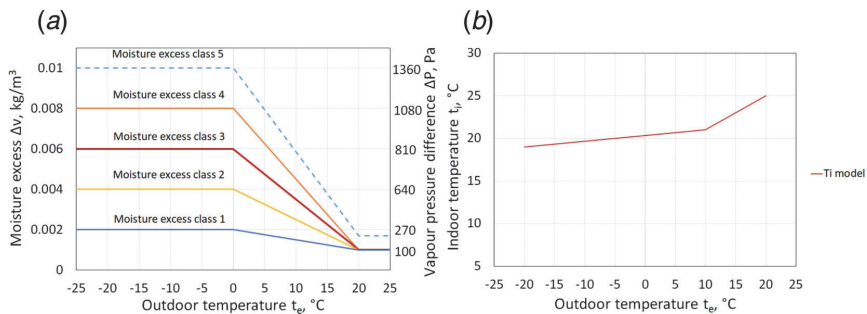
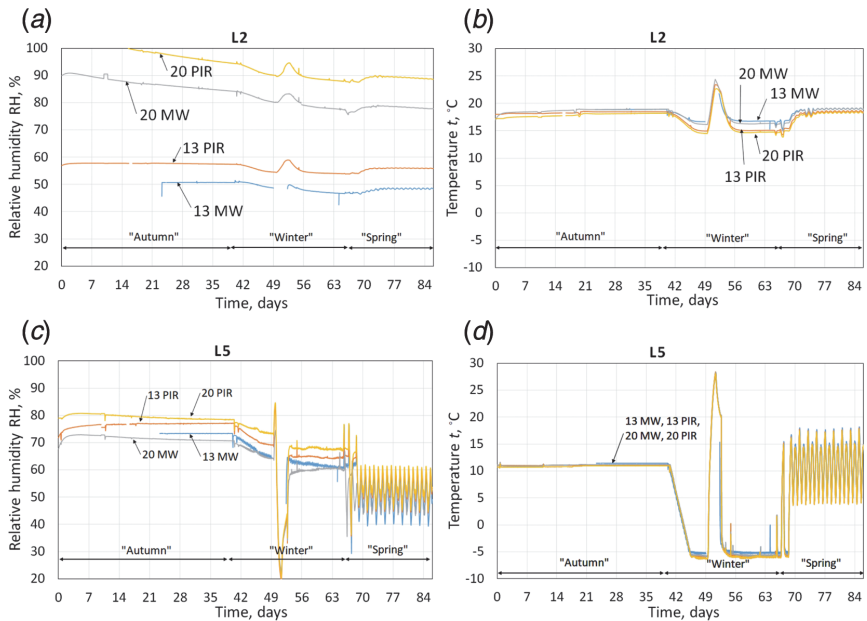


Fig. 5. Measurements from test walls of (a) relative humidity between interior insulation board and CLT, layer L2; (c) relative humidity between exterior insulation and wind barrier, layer L5; (b) temperature between interior insulation board and CLT, layer L2; (d) temperature between exterior insulation and wind barrier, layer L5. [Colour online.]



viation and minimum and maximum values were calculated (Table 2). The differences were calculated by taking the average test result for each period in each layer and subtracting the result of the simulation.

Results showed that, overall, the average differences in temperature (Δt) between test and simulation results ranged from -1.1 ± 0.2 °C to 0.6 ± 0.3 °C, which is close to the error of the measuring sensors (± 0.3 °C). The temperature was similar between the test and simulation results over all climate periods (“autumn”, “winter”, and “spring”). The average differences in RH (ΔRH) ranged from $-10.5\% \pm 1\%$ to $7.6\% \pm 0.3\%$; compared with the error of the measuring sensors ($\pm 2.0\%$), the differences were three to five times greater. The average differences in partial pressure of water vapour (ΔP) ranged from -236 ± 25 Pa to 147 ± 87 Pa and in heat flux (Δq) ranged from -0.27 ± 1.39 W/m² to 0.13 ± 1.33 W/m². During the first period of “autumn”, the average differences in each layer between simulation and laboratory test results were smallest and

the differences of temperature and RH remained within the limits of the error of the sensors (average $\Delta t = -0.3$ °C and average $\Delta RH = 0.2\%$). The biggest average differences were found during the “winter” climate period. The test walls with interior insulation with variable vapour diffusion resistance (20MW and 13MW) had the biggest average differences in RH and in water vapor partial pressure between the CLT panel and external insulation (L4) and between the interior insulation and the CLT (L2). The average difference in RH in the test wall 13MW between the CLT panel and external insulation (L4) was 10.5% and in partial pressure was -178 Pa. In wall 20MW between the interior insulation and the CLT (L2), the average difference in RH was -7.5% , and in partial pressure, the average difference was -224 Pa. The test walls with interior insulation with high vapour resistance (20PIR and 13PIR) had the greatest average differences between the interior insulation and the CLT (L2). The average difference in RH in the test wall 13PIR between the interior insulation and the CLT (L2) was 6.6%,

Table 2. Average differences ±SD (minimum, maximum) between test and simulation results.

Layer no.	Autumn climate				Winter climate				Spring climate			
	Δt, °C	ΔRH, %	ΔP, Pa	Δq, W/m ²	Δt, °C	ΔRH, %	ΔP, Pa	Δq, W/m ²	Δt, °C	ΔRH, %	ΔP, Pa	Δq, W/m ²
CLT13MW												
L1	-0.340(0.07, 0.8)	-1.74(4.1-3.5, 8.6)	-638.8(-117, 183)	0.040(1(-0.3, 1.0)	-0.580(1(-2.2, -0.4)	-1.440(7(-4.6, -0.5)	-50.14(-128, -36)	-0.24(1.5(-7.2, 10.2)	-0.350(2(-1.1, 0.6)	-2.4(11.3(-11.2, 1.6)	-788.2(7(-302, 47)	0.14(1.3(-9.4, 9.6)
L2	-0.450(0.06, 0.4)	-1.0(16.6(-3.0, 3.3)	-608.8(-178, -28)	—	-0.440(4(-19, -0.1)	1.240(6(-3.2, 2.3)	84.13(-67, 40)	—	-0.640(1(-0.9, -0.2)	1.040(2(0.4, 1.5)	-175.8(-41, 16)	—
L3	0.040(0.0, 0.2)	2.6(4.0(-0.4, 3.3)	57.2(9)	—	0.240(5(-2.1, 0.6)	4.650(5(-3.0, 5.0)	95.3(-30, 56, 127)	—	-0.140(1(-0.6, 0.1)	4.880(1(4.5, 5.1)	97.4(10, 61, 108)	—
L4	-0.640(0.07, -0.3)	-1.140(4(-1.5, 0.5)	-62.9(-71, -12)	—	-0.590(6(-3.9, -0.1)	-10.54(10(-14.2, -4.3)	-178.8(52(144, -150)	—	-0.730(2(-1.4, -0.3)	0.882(0(-2.6, 4.5)	-135.6(5(-92, 72)	—
L5	0.160(-1.06, 0.4)	-0.350(5(-1.2, 8.1)	185.9(2, 104)	—	0.660(3(-2.2, 1.2)	-5.34(10(-10.8, 5.6)	-625(-16, 24)	—	0.4(14(-4.7, 2.4)	-2.22(4.9(-13.3, 6.9)	-157.6(-290, 129)	—
CLT13PIR												
L1	-0.140(0.08, 0.3)	1.0(13.3(-2.3, 13.1)	183.2(-92, 316)	-0.140(14(-10.4, 0.4)	-0.240(1(-12.0, 0.7)	-6.24(15(-6.4, 5.6)	-19.4(49(-314, 127)	-0.3(14.4(6.3, 4.6)	-0.140(3(-1.1, 1.3)	0.8(16.6(-2.4, 3.3)	13.1(9(-14, 123)	0.0(12.2(-10.4, 9)
L2	-0.440(-0.7, -0.1)	-2.1(2.1(-5.1, 14.8)	-518.8(-73)	—	-0.440(2(-0.7, 0.8)	6.64(7(3.9, 10.6)	147.2(47(-57, 423)	—	-0.440(1(-0.8, 0.0)	7.650(3(7.1, 8.2)	882.2(0, 24)	8.820(14, 123)
L3	-0.940(0.09, -0.7)	-0.244(7(-8.02, 5)	-64.2(4(-14, -10)	—	-0.940(7(-10, 0.0)	5.240(6(1.0, 5.7)	26.4(23(-81, 63)	—	-1.140(2(-1.7, -0.8)	4.902(2(5.3, 6.1)	5.4(14(5, 6, 39)	5.4(14(5, 6, 39)
L4	-0.530(-1.1, 0.0)	2.8(10(-1.0, 5.5)	185.4(-453, 104)	—	-0.230(3(-8.9, 10.7)	-5.65(7(-4.2, 1.9)	225.9(4(-22, 174)	—	-0.660(2(-1.5, 0.0)	4.422(2(0.3, 8.6)	6.5(52(-82, 166)	6.5(52(-82, 166)
L5	0.15(1(-1.5, 1.4)	2.4(10(-1.24, 8.0)	40.6(2(-7.6, 359)	—	0.350(6(-2.4, 6.4)	-0.4(8.0(-7.9, 31.1)	225.9(4(-22, 174)	—	0.1(2.7(-3.6, 3.9)	0.1(6.9(-29.5, 10.0)	15.5(9(-352, 156)	15.5(9(-352, 156)
CLT20MW												
L1	-0.240(2(-2.0, 1.7)	1.1(2.3(-1.6, 14.6)	104.5(-267, 293)	0.1(10.2(-0.7, 1.1)	-0.340(1(-0.7, 0.2)	-1.0(2.2(-6.8, 11.0)	-4.3(46(-306, 241)	0.0(11.5(-5.1, 5.2)	-0.240(3(-4.2, 1.2)	0.143(7(-12.6, 14.1)	-12.4(2(-248, 321)	0.1(11.3(-8.1, 9.1)
L2	-0.330(4(-3.0, 0.6)	-2.6(4.7(-4.8, 0.5)	-98.2(7(-428, 25)	—	-0.740(3(-1.4, 0.1)	-7.3(11(-9.1, -5.2)	-22.4(47(-374, -116)	—	-0.530(2(-1.1, 0.0)	-8.0(10.4(-9.0, -7.2)	-236.6(25(-311, -173)	—
L3	-0.020(6(-3.8, 0.4)	-1.3(41.5(-6.8, 0.8)	-36.7(0(-354, 47)	—	-0.350(4(-1.8, 0.5)	-7.3(10.9(-8.2, -5.0)	-38.4(52(-501, -92)	—	-0.240(3(-1.4, -0.3)	-6.2(40.1(-6.3, -6.0)	-190.2(10(-296, -157)	—
L4	-0.460(8(-5.4, 0.3)	-1.9(48.8(-7.4, 11.3)	-89.2(15(-316, 205)	—	-0.950(4(-2.4, 0.4)	-5.0(25.8(-9.0, 14.7)	-19.4(59(-160, 205)	—	-0.730(3(-1.9, -0.2)	4.6(22.6(-0.7, 9.8)	61.5(9(-55, 173)	—
L5	0.2(10.1(-0.6, 1.4)	-5.3(32.0(-12.8, -0.2)	-56(3.9(-155, 282)	—	0.3(10.5(-3.4, 4.5)	-4.7(18.4(-36.5, 24.4)	318.7(-318, 362)	—	0.2(2.5(-3.2, 3.6)	-3.0(44.9(-25.8, 4.4)	-22.8(83(-369, 155)	—
CLT20PIR												
L1	-0.340(1(-0.6, 0.0)	0.9(40.3(-0.6, 1.6)	-1.4(27.4(-53.9, 15.9)	0.0(10.2(-0.7, 0.6)	-0.580(2(-1.6, 0.4)	-1.0(14.8(-7.1, 15.6)	-53.5(56(-368, 341)	-0.3(11.4(-10.0, 4.6)	-0.340(3(-1.4, 1.2)	-0.1(10.8(-2.3, 6.1)	-22.4(28(-189, 134)	0.0(11.4(-8.6, 11.3)
L2	-0.460(2(-4.8, -0.1)	5.0(22.2(10.7, 7.4)	53.6(0(-48, 159)	—	-0.730(3(-1.4, 0.1)	-3.3(17(-5.3, 1.2)	-130.4(48(-255, 4)	—	-0.660(2(-1.4, -0.5)	-4.0(10.4(-5.4, -3.3)	-157.2(23(-239, -109)	—
L3	-0.350(2(-0.7, 0.0)	5.0(6.1(-2.6, 11.3)	53.6(18(-123, 220)	—	-1.3(11.3(-3.6, 1.1)	-1.3(11.3(-3.6, 1.1)	-96.5(49(-255, 9.9)	—	-0.860(3(-1.7, -0.2)	1.9(10.2(0.8, 2.2)	-39.2(26(-133, -7)	—
L4	-0.530(3(-1.1, 0.0)	-1.8(18.6(-15.6, 9.2)	-60.5(15(-423, 129)	—	-1.1(10.5(-2.8, 0.2)	-0.1(15.4(-4.4, 16.0)	-27.7(56(-194, 285)	—	-1.0(10.3(-2.2, -0.5)	7.2(23.3(2.5, 12.0)	98.5(50(-5, 197)	—
L5	0.1(10.2(-0.6, 1.4)	1.8(18.1(-3.5, 7.2)	33.2(28(-56, 344)	—	3.0(27.8(-10.0, 32.6)	3.0(27.8(-10.0, 32.6)	18.7(6(-320, 328)	—	0.1(11.6(-2.3, 2.4)	1.2(45.1(-16.2, 10.8)	18.5(99(-119, 162)	—

and in partial pressure, the average difference was 147 Pa. In wall 20PIR between the interior insulation and the CLT (L2), the average difference in RH was -3.3%, and in partial pressure, the average difference was -130 Pa. The overall average difference in RH and partial pressure in the winter period were -1.7% and -43.8 Pa, respectively. The average differences between the test and simulation results in the “spring” climate period ranged from -8% to 7.6% in RH and from -236 Pa to 98 Pa. In Fig. 6, the measurements and simulations of temperature and RH of test wall CLT 13MW are plotted as an example.

Determination of the maximum allowable MC of CLT panels

Start time of the CLT wall assembly period

In many cases during the construction process, it is not possible to choose a suitable start date in accordance with the anticipate climate, or in other cases, the start date is postponed. Therefore, in this study, the calculations for determining the maximum allowable MC of CLT panels were made by considering the most critical month for the start of construction where, for the given wall assemblies, the risk of mould growth will be the greatest. The most critical month for the start of construction was found through using validated calculation models of test walls with an initial higher MC in CLT panels (20MW and 20PIR). Mould indices were calculated using the validated calculation models for a period of 1 year, and each month of the year was used separately as a start time. Results showed that for the wall assemblies having interior insulation with variable vapour diffusion resistance (MW), the most critical month for starting construction is December (marked as red, see Fig. 7a) where the risk to mould growth is greatest ($M \approx 1.7$). The safest month initiating construction for the same wall assembly is June, where there is no mould growth risk ($M < 1$). For wall assemblies having interior insulation with high vapour diffusion resistance (PIR), there were no differences between the most critical and safest month for starting construction. For all months, the risk for mould growth was high ($M > 3$), and for further calculations, the most critical month was chosen to be August (marked as red, see Fig. 7b).

Maximum allowable MC of CLT

The calibrated models were used to calculate the maximum allowable MC in CLT panels for the two given types of walls assemblies (MW and PIR). It was considered for calculations that different initial MCs in the CLT panels were evenly distributed throughout the entire panel. Calculations for the mould index were made at the most critical point in the wall section for both wall assemblies, which located between the interior insulation and CLT panel (L2). Criteria for acceptable wall performance were as follows: during the 5-year calculation period, no risk of mould growth, in other words, the maximum mould index during the calculation period could not exceed a value of 1 ($M < 1$, no mould growth). From Fig. 8a, it can be seen that for wall assemblies having interior insulation with a variable vapour diffusion resistance (MW), the initial MC of 17% in CLT panels was the last value that did not exceed a value of mould index 1 during the calculation period. With an initial MC of 18%, it had already exceeded the index value at that point. For wall assemblies having interior insulation with a high vapour diffusion resistance (PIR), the initial MC of 15% in CLT panels achieved almost a value of 1 for the mould index during the calculation period (Fig. 8b).

In addition to calculating the value of the mould index, the RH between interior insulation board and CLT (L2) was also calculated to permit evaluating the moisture dissipation time through the wall section. The time at which the critical level of moisture was considered to have dissipated was when the RH value dropped below 80%, which is the critical level for mould growth given suitable temperatures. With an initial MC of 15%, the calculations showed that for wall assemblies having interior insulation with a

Fig. 6. Measurements and simulations of (a) temperature and (b) relative humidity of test wall CLT 13MW. [Colour online.]

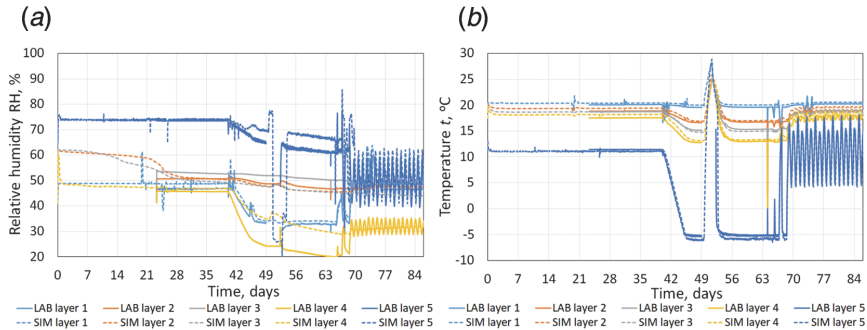


Fig. 7. Mould growth index for each month as start time of calculation in a 1-year period for test walls (a) 20MW and (b) 20PIR. [Colour online.]

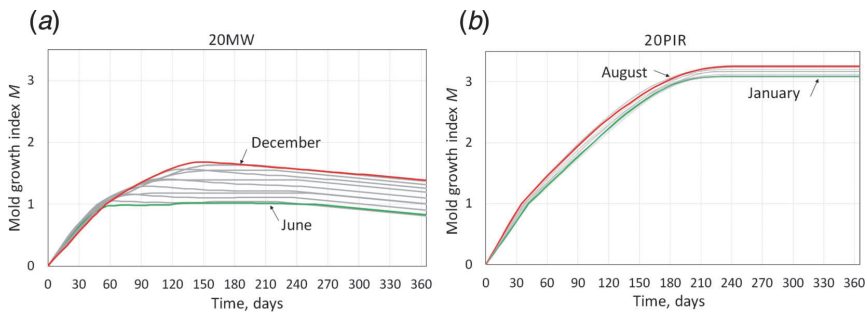
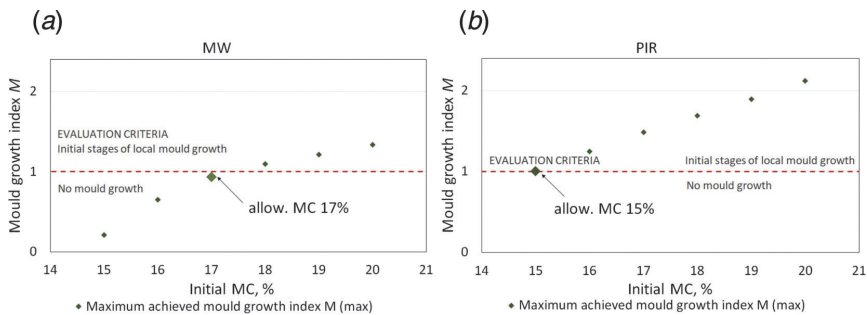


Fig. 8. Maximum achieved mould growth index for different initial MCs in CLT panels with (a) variable water vapor resistance interior mineral wool insulation board and (b) high vapor tight PIR interior insulation board during 5-year calculation period. [Colour online.]



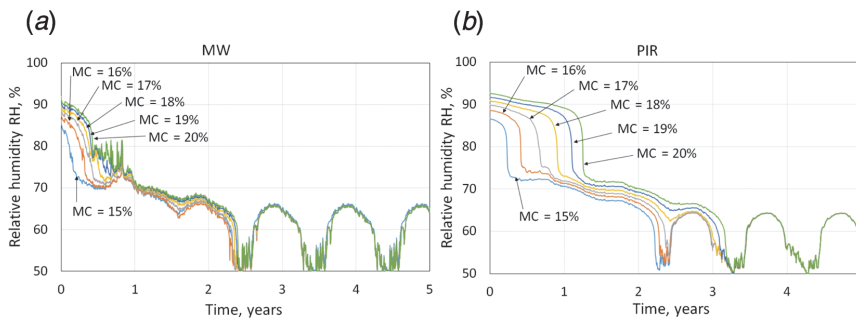
variable vapour diffusion resistance (MW) and where the moisture could dry out to both directions (inside and outside), the RH dropped below 80% within 6 weeks (Fig. 9a). In wall assemblies having interior insulation with a high vapour diffusion resistance (PIR) and where the moisture could dry out to only one direction (to the outside), as well as given the same initial MC in the CLT panels, the RH dropped below 80% within 12 weeks (Fig. 9a). The difference in moisture dissipation rate between the two wall assemblies is double. For MW wall assemblies with an initial CLT panel MC of 17%, the RH dropped below 80% within 17 weeks and with an initial MC of 20%, the RH dropped below 80% within 22 weeks. In wall assemblies of PIR, the RH dropped below 80% within 34 weeks with an initial MC of 17%, and with an initial MC of 20%, it dropped below 80% within 64 weeks. The difference

between the two wall assemblies is double with an initial MC of 17% and almost three-fold with an initial MC of 20%.

Discussion

Test results of the laboratory experiment showed that the most critical point in both types of wall assemblies (MW and PIR) was between the interior insulation and the CLT panel, especially with a higher initial MC of ~20%. This critical point was caused by moisture movement from the CLT panel towards an indoor direction and its accumulation behind the interior insulation. Test results also showed that with a higher initial MC of ~20%, both wall assemblies became critical. A considerably higher risk was present in the wall assembly having interior insulation with a high vapour diffusion resistance (PIR). This shows that there is

Fig. 9. Relative humidity between interior insulation board and CLT (L2) in cases of different initial MC in CLT panel with (a) variable water vapor resistance interior mineral wool insulation board and (b) high vapor tight PIR interior insulation board. [Colour online.]



high risk of mould growth when using interior insulation for wall assemblies with CLT panels having a higher initial MC (~20%), especially when using vapor tight insulation.

Calibration of the model with the test results showed that the overall average difference between measurements and modelling results ranged from $-1.1\text{ }^{\circ}\text{C}$ to $0.6\text{ }^{\circ}\text{C}$ in temperature, which coincided closely with the limits in error of the measurement sensors, from -10.5% to 7.6% in RH, from -236 Pa to 147 Pa in partial pressure of water vapour, and from -0.27 W/m^2 to 0.13 W/m^2 in heat flux. In a previous study completed by [McClung et al. \(2014\)](#), in which the results of a simulation with similar wall assemblies were included, the overall difference between simulation and test results was $\pm 2\%$ – 5% . It can reasonably be concluded that the calculation model was accurate and simulation results were similar to the test results. There were, however, some bigger differences that appeared in the results of RH and partial pressure of water vapor during the simulated “winter” climate period. The biggest differences mostly appeared in L2 and L4. It seemed that the simulations overestimated the RH in the outer layers under colder external climate conditions.

Modelling showed that the most critical month for starting the construction of wall assemblies with 20MW is December, when the mould growth threat is highest. For wall assemblies with 20PIR, there was no big difference in which month to start, given that the mould growth risk was high in every month. This indicates that when building with CLT panels that are insulated from the inside and with insulation having a variable vapour diffusion resistance, it is possible to mitigate the risk of mould growth by choosing the safest month for construction, i.e., when the moisture dissipation period is shortest, which is June. Insulating CLT panels from the inside using insulation having a high vapour diffusion resistance can be relied on only to keep the CLT panels in a suitable MC range for preventing the risk of mould growth. It should be noted that, as was found by [Alev and Kalamees \(2016\)](#), June was the safest month for adding MW as interior insulation for log walls.

Simulation with variations of MC in CLT panels showed that the maximum allowable MC in a wall assembly having interior insulation with variable vapour diffusion resistance was found to be 17%; at higher values of allowable MC, there may be a risk of mould growth. The maximum allowable MC in a wall assembly using interior insulation with a high vapour diffusion resistance is 15%. When comparing this value with the criteria to avoid mould growth in CLT panels to avoid mould growth used in the study by [McClung et al. \(2014\)](#), a study that was similar set of wall assemblies, it can be seen that the maximum allowable MC for both wall assemblies are below that value of 20% MC. In Estonia, however, the requirement for allowable level of MC for construction timber, strictly monitored for glue-laminated timber, is between 8% to 15%; this means that the PIR wall assembly just meets

the performance requirements and the MW wall assembly has a margin of only about 2%. Therefore, it can be said that the use of interior insulation with a high vapour diffusion resistance in CLT walls should be undertaken with caution and only with effective supervision on the construction site and proper measurement of the MC in the CLT panels before covering them with insulation given the very small margin for error. Use of effective supervision can also be recommended for use of wall assembly MW, which is insulated from the inside with insulation having a variable vapour diffusion resistance, because of the small error margin of 2% of MC. These results also show that using materials with high vapour diffusion resistance for interior insulation may have a more negative effect on external walls of solid wood compared with using materials with a variable vapour diffusion resistance. [Alev and Kalamees \(2016\)](#) found in their study that for vapour tight interior insulation used in log homes, the initial MC of the logs should be below 12%. A similar conclusion was established in the study completed by [McClung et al. \(2014\)](#) that CLT panels with an interior membrane with low permeance of water vapor should be used with more caution because of the slower drying of CLT panels. Much slower drying of CLT panels was also seen from the simulation results. In wall assembly PIR, the RH between the CLT panel and the interior insulation dropped below a critical level of 80% at least twice as slowly than for wall assembly MW. This shows the importance of having both indoor and outdoor directional ability for the drying out of excess moisture (rainwater or snow) from CLT panels at the beginning of their time of use.

In the current research, to determine the maximum allowable MC, the simulations were completed with an evenly distributed MC in the CLT panels. For the laboratory experiment described in this paper, the moisture within the wetted CLT panels was unevenly distributed and the difference between MC at the outer and inner layers was noticeably large. Much of the moisture remained in the outer layers, and the inner layers stayed dry or received only a small amount of moisture. The MC in each layer of CLT panels were not measured during the experiment and, therefore, caused uncertainties about the panel’s moisture distribution. In subsequent studies on the same topic, it will be necessary to determine how exactly moisture distributes through a CLT panel when it is exposed to excessive moisture. This knowledge could be used to refine the calculation model to obtain more accurate simulation results and from which the critical MC in CLT panels can more readily be defined.

A comparison of test and simulation results showed that during the experiment with the PIR test walls, some moisture dried out to an indoor direction but the simulation results did not reflect this. It can be stated that some moisture did dry out in a direction parallel to the exterior CLT panel surface. This indicates that in addition to a one-dimensional simulation, two-dimensional calculations are recommended for further studies on this topic.

Conclusion

Four test walls with two different interior insulation solutions and with two different initial MC in CLT panels were studied in laboratory conditions and by modelling, to permit in establish the maximum allowable initial MC as a performance criterion of CLT walls incorporating exterior and interior thermal insulation. No mould growth ($M < 1$) was used as the performance criteria for wall assemblies. Measurements and modelling results were analysed and the primary conclusions are as follows.

- Results from the laboratory test with CLT walls confirmed that it was problematic to use vapor tight interior insulation for wall assemblies, with the CLT panels having a higher initial MC (~20%).
- Overall, the agreement between test and simulation results was good and the calibrated model was considered accurate to undertake further calculations from which the maximum allowable MC in CLT panels was determined. Although some minor differences appeared during simulated “winter” climate conditions, it appeared that the simulations overestimated the RH in the outer layers during colder external climate conditions.
- The most critical month for starting the construction of wall assemblies having vapour permeable interior insulation is December. For wall assemblies with vapour tight interior insulation, there were no significant differences with respect to the month to when construction should start, given that in every month, the risk to mould growth was high.
- The maximum allowable MC in wall assemblies with vapour open interior insulation was found to be $MC \leq 17\%$, and in wall assemblies with vapour tight interior insulation, it was $MC \leq 15\%$. It was concluded that the use of vapor tight interior insulation in CLT walls should be undertaken with caution and only with effective supervision on construction site and proper measurement of MC of CLT panels before installation of the insulation, given the very small margin for error in percent MC. Effective supervision can be also recommended for wall assemblies insulated from the inside and having insulation with a variable vapour diffusion resistance, given the small margin of 2% of MC.
- For further studies on the same topic, it would be useful to determine how moisture is distributed in CLT panels when they are exposed to excessive moisture. This knowledge can be input into models to obtain more accurate simulation results from which can be determined the critical MC in CLT panels. It is recommended that for subsequent studies on this topic and in addition to one-dimensional simulations, two-dimensional simulations of construction details also be completed.

Acknowledgements

This research was supported by the Estonian Centre of Excellence in Zero Energy and Resource Efficient Smart Buildings and Districts, ZEBE, grant TK146 funded by the European Regional Development Fund, and by the Estonian Research Council with Institutional research funding grant IUT1-15. This research was also supported by the Estonian Ministry of Education and Research. EU Structural Fund (Cohesion Policy Funds) period 2014–2020, TUT Development Program for the period 2016–2022, and Doctoral School of Civil and Environmental Engineering project code 2014-2020.4.01.16-0032 have made publishing of this article possible. The Estonian glulam producer Peetri Puit OÜ is thanked for supplying CLT specimens.

References

Alev, Ü., and Kalamees, T. 2016. Avoiding mould growth in an interiorly insulated log wall. *Building Environment*, **105**: 104–115. doi:10.1016/j.buildenv.2016.05.020.

Arumägi, E., and Kalamees, T. 2016. Design of the first net-zero energy buildings

in Estonia. *Science and Technology for the Built Environment*, **22**: 1039–1049. doi:10.1080/23744731.2016.1206793.

Asaee, S.R., Ugursal, V.I., and Beausoleil-Morrison, I. 2019. Development and analysis of strategies to facilitate the conversion of Canadian houses into net zero energy buildings. *Energy Policy*, **126**: 118–130. doi:10.1016/j.enpol.2018.10.055.

CEN – EN 16351. 2015. Timber structures – Cross laminated timber – Requirements.

D’Agostino, D., and Parker, D. 2018. A framework for the cost-optimal design of nearly zero energy buildings (NZEBs) in representative climates across Europe. *Energy*, **149**: 814–829. doi:10.1016/j.energy.2018.02.020.

EPBD. 2018. Directive (EU) 2018/844 of the European Parliament and of the Council of 30 May 2018 amending Directive 2010/31/EU on the energy performance of buildings and Directive 2012/27/EU on energy efficiency. Off. J. Eur. Union.

EVS-EN ISO 13788:2012. 2012. Hygrothermal performance of building components and building elements - Internal surface temperature to avoid critical surface humidity and interstitial condensation – Calculation methods (ISO 13788:2012). Eesti Standardikeskus, Tallinn.

Fedorik, F., and Haapala, A. 2017. Impact of air-gap design to hygro-thermal properties and mould growth risk between concrete foundation and CLT frame. *Energy Procedia*, **132**: 117–122. doi:10.1016/j.egypro.2017.09.656.

Gullbrekken, L., Geving, S., Time, B., Andresen, I., and Holme, J. 2015. Moisture conditions in well-insulated wood-frame walls. Simulations, laboratory measurements and field measurements. *Wood Materials Sciences Engineering*, **10**: 232–244.

Ilo mets, S., Kalamees, T., and Vinha, J. 2018. Indoor hygrothermal loads for the deterministic and stochastic design of the building envelope for dwellings in cold climates. *Journal of Building Physics*, **41**: 547–577. doi:10.1177/1744259117718442.

Kalamees, T., and Vinha, J. 2003. Hygrothermal calculations and laboratory tests on timber-framed wall structures. *Building and Environment*, **38**: 689–697. doi:10.1016/S0360-1323(02)00207-X.

Kalamees, T., and Vinha, J. 2004. Estonian climate analysis for selecting moisture reference years for hygrothermal calculations. *Journal of Thermal Envelope and Building Science*, **27**: 199–220. doi:10.1177/1097196304038839.

Kalamees, T., Paap, L., Kuusk, K., Mauring, T., Hallik, J., Valge, M., Kalbe, K., and Tkaczyk, A.H. 2014. The first year’s results from the first passive house in Estonia. In *Proceedings of 10th Nordic Symposium on Building Physics*, 15–19 June 2014, Lund, Sweden, Edited by J. Arvidsson, L.-E. Harderup, A. Kumlin, and B. Rosencrantz, pp. 758–765.

Kukk, V., Horta, R., Püssa, M., Luciani, G., Kallaks, H., Kalamees, T., and Kers, J. 2017. Impact of cracks to the hygrothermal properties of CLT water vapour resistance and air permeability. *Energy Procedia*, **132**: 741–746. doi:10.1016/j.egypro.2017.10.019.

McClung, R., Ge, H., Straube, J., and Wang, J. 2014. Hygrothermal performance of cross-laminated timber wall assemblies with built-in moisture: field measurements and simulations. *Building and Environment*, **71**: 95–110. doi:10.1016/j.buildenv.2013.09.008.

Nicolai, A., and Grunewald, J. 2003. *Delphin 5 user manual and program reference*. Dresden.

Ojanen, T., Viitanen, H., Peuhkuri, R., Lähdesmäki, K., Vinha, J., and Salminen, K. 2010. Mold growth modeling of building structures using sensitivity classes of materials. In *Thermal Performance of the Exterior Envelopes of Buildings XI*, ASHRAE, Florida.

Pihelo, P., and Kalamees, T. 2016. The effect of thermal transmittance of building envelope and material selection of wind barrier on moisture safety of timber frame exterior wall. *Journal of Building Engineering*, **6**: 29–38. doi:10.1016/j.jobe.2016.02.002.

Pihelo, P., Lelumees, M., and Kalamees, T. 2016. Influence of moisture dry-out on hygrothermal performance of prefabricated modular renovation elements. In *Proceedings of the SBE16 Tallinn and Helsinki Conference in Energy Procedia; Build Green and Renovate Deep*, 5–7 October 2016. Edited by J. Kurmitski. Tallinn and Helsinki, Elsevier B.V., pp. 745–755.

Reinberg, G.W., Mauring, T., Kalbe, K., and Hallik, J. 2013. First certified passive house in Estonia. In *Proceedings of the 17th International Passive House Conference: 17th International Passive House Conference*. Edited by W. Feist. Passivhaus Institut Darmstadt, Frankfurt, Germany.

Sankelo, P., Jokisalo, J., Nyman, J., Vinha, J., and Sirén, K. 2019. Cost-optimal energy performance measures in a new daycare building in cold climate. *International Journal of Sustainable Energy*, **38**: 104–122. doi:10.1080/14786451.2018.1448398.

Skogstad, H., Gullbrekken, L., and Nore, K. 2011. Air leakages through cross laminated timber (CLT) constructions. In *The 9th Nordic Symposium on Building Physics*. Tampere University of Technology, Tampere.

Vinha, J. 2007. Hygrothermal performance of timber-framed external walls in Finnish climatic conditions: a method of determining a sufficient water vapour resistance of the internal lining of a wall assembly. Tampere University of Technology, Tampere.

PUBLICATION V

Kukk, V.; Kaljula, L.; Kers, J.; Kalamees, T., 2022. Designing highly insulated cross-laminated timber external walls in terms of hygrothermal performance: Field measurements and simulations. *Building and Environment*, 212.



Contents lists available at ScienceDirect

Building and Environment

journal homepage: www.elsevier.com/locate/buildenv

Designing highly insulated cross-laminated timber external walls in terms of hygrothermal performance: Field measurements and simulations

Villu Kukk^{a,*}, Laura Kaljula^b, Jaan Kers^b, Targo Kalamees^a^a Department of Civil Engineering and Architecture, Tallinn University of Technology, Ehitajate Tee 5, 19086, Tallinn, Estonia^b Department of Materials and Environmental, Technology Tallinn University of Technology, Ehitajate Tee 5, 19086, Tallinn, Estonia

ARTICLE INFO

Keywords:

Cross-laminated timber
CLT
Moisture safety
Wall assemblies
Hygrothermal performance
Initial moisture content

ABSTRACT

Keeping wood dry both under construction and service is important to prevent possible moisture damages in wooden buildings. However, practice has shown that without weather protection, wooden structures may get soaked during construction. Therefore, our aim was to evaluate the impact of vapour permeable and low permeable highly insulated external wall assemblies, façade orientation, and initial moisture content on the hygrothermal performance of cross-laminated timber (CLT) external walls. We carried out field measurements in the cold and humid Estonian climate, for which five types of test walls were designed and manufactured. Simulation models for future research were also created and validated. Field measurements showed that the CLT external walls were hygrothermally safe in the observed cold and humid climate and the CLT panel provided sufficient control of the water vapour diffusion. The use of low vapour permeable external insulation can be beneficial against vapour permeable insulation if low moisture content of the CLT panel (factory dry) during construction is maintained and insulation is installed airtightly. Cellulose insulation can be a safe choice when selecting water vapour permeable insulation for the external wall in case the construction is planned without weather protection. Mould growth risk calculations based on measured hygrothermal conditions showed that the high moisture content in the thin surface layer of the CLT panel may not be critical when dry-out time is short. The probability of failure must be determined by stochastic analysis using a variety of influencing parameters.

1. Introduction

Due to high water vapour diffusion control, low thermal conductivity and low density, as compared to steel and concrete, the cross-laminated timber (CLT) is in increasing use alongside traditional materials. CLT is characterised by structural rigidity and strength as well as small ecological footprint. A CLT panel is a multi-layer wooden composite structure made of lumber, usually softwood such as spruce and pine, produced of at least three orthogonally bonded layers [1]. In terms of hygrothermal performance, such solid wood panels as CLT are sensitive to moisture. Wood as an organic substance is known to be a nutrient for various fungi such as mould and rot, which are the primary moisture damages to wood that occur at favourable temperature and humidity. Therefore, it is essential to keep the wood dry during both construction and service. However, practice has shown that during construction, wooden structures get soaked if full weather protection is not implemented. Several studies have observed the wetting of mass timber elements both on the construction sites [2–7] and in the laboratory

conditions [5,8,9]. Their findings show that the moisture content (MC) of joints where water is absorbed at the longitudinal fibre direction from the cut-edge of the panel can increase up to 30%. On the plane surface of the panel, at the radial fibre direction, the absorption is lower. Therefore, in the design of the CLT external envelope, it is required to consider the dry-out capacity, taking into account the existence of weather protection.

In the modern construction, much emphasis is placed on energy efficiency; therefore, the target in the external envelope design is very low thermal transmittance. One of the easiest ways to achieve low thermal transmittance is to use high insulation of the envelope. The first passive house in Estonia made of CLT was built in 2013 [10]. The building was highly insulated with cellulose insulation, but the first-year measurement results showed possible condensation risk on the wind barrier surface and risk of mould growth on the insulation surface [11]. High insulation decreases the temperature between the insulation and the wind barrier and increases the risk for potential condensation. Wang and Ge [12] made a stochastic analysis of highly insulated wood frame walls

* Corresponding author. Ehitajate tee 5, 19086, Tallinn, Estonia.

E-mail address: villu.kukk@taltech.ee (V. Kukk).<https://doi.org/10.1016/j.buildenv.2022.108805>

Received 6 September 2021; Received in revised form 24 November 2021; Accepted 15 January 2022

Available online 19 January 2022

0360-1323/© 2022 Elsevier Ltd. All rights reserved.

with a ventilated cavity and found that the risk of mould in the presence of air and rain leakage is high at high internal moisture loads. Pihelo et al. [13] studied the hygrothermal performance of highly insulated timber-frame building envelopes with different insulation materials. They concluded that the use of wind barriers that have low thermal conductivity and high water vapour permeability will decrease the risk of mould growth. The use of hygroscopic cellulose insulation has advantages over mineral wool by smoothing the humidity peak levels of the indoor air and decreases the risk of mould growth [13,14]. Therefore, the assembly of the wall and the hygrothermal properties (thermal conductivity and vapour permeability) of the material layers also play an important role in the design of highly insulated external envelopes.

Many researchers have focused on the hygrothermal performance of CLT external envelopes. However, they have all used different wall configurations, evaluation criteria, and methodologies (field measurements vs. simulations). In their in-depth study of the hygrothermal performance of CLT external walls, McClung et al. [15] and Wang and Ge [16] used both field measurements and stochastic analysis. They used low and high water vapour permeable wall assemblies for the variables to study the effect of built-in moisture dry-out. Their evaluation was based on the moisture content alone (<20% and <26%), with mould and decay as the evaluation criteria. Mould, for example, grows on the surface of a material; one of the most common ways to estimate the growth is to use the mould growth index, which is calculated from the relative humidity and temperature near the surface [17]. Therefore, it is not sufficient to determine the MC alone in the risk evaluation of primary moisture damages – mould growth. Cho et al. [18] and Yoo et al. [19] evaluated the hygrothermal performance of the CLT external envelope by using the mould growth index. However, they addressed only a stationary situation, without considering any wetting scenarios of CLT; their approach was using simulation without validation based on the field measurements. Al-Sayegh [20], Byttebier [21] and Kordziel et al. [22] determined the hygrothermal properties of the CLT panel first by laboratory experiments and then used the data to create a simulation model and evaluate the hygrothermal performance in a stationary state. In their study, Kukk et al. [23–25] focused on the hygrothermal performance of the CLT external walls, considering the wetting of the panel and using a mould growth index in the evaluation of the performance. However, only few specific wall assemblies and few variables (mostly only initial MC) were used in their analyses. In summary, previous studies have evaluated the hygrothermal performance of CLT envelopes in the steady state, i.e., only at low initial CLT moisture content. In the studies addressing high CLT moisture content, either the risk of mould growth on the CLT surface is not evaluated or only a single wall assembly is used. Thus, the information on the hygrothermal performance of the CLT external envelope built without proper weather protection where the CLT achieves a high moisture content is scarce. In particular, there is little information on the variations in the performance of different wall assemblies with high initial CLT moisture content.

Therefore, our aim was to evaluate the impact of different assemblies of highly insulated external wall (vapour permeable and low permeable insulation and interior layers), orientation, and initial MC on the hygrothermal performance of CLT external walls. The results can be used for moisture safety planning in large-scale CLT construction. In the CLT building design and construction planning, it is required to decide the measures to be used for moisture safety, which in turn is closely related to the size of the construction budget. For example, the building budget is strongly affected by the expenses of a full-size temporary tent for weather protection used for a building under construction. Its planned use can save large costs on rainwater drainage and wood drying procedures that may result at the CLT exposure to the weather. A worse

case may occur when the costs of a temporary tent are not included in the budget, whereas due to extreme weather conditions, a tent is eventually required.

2. Materials and methods

Hygrothermal performance of CLT external walls was analysed through the results of our field measurements. The results were also used to create and validate simulation models for future research for stochastic analysis. Our focus was on the moisture behaviour of CLT through the parameters of temperature (t), partial pressure of water vapour (P_v) and relative humidity (RH) between each material layer in the external wall assembly. The results will reveal the impact of the initial MC of CLT on the wall structure and possible threat of mould growth on material surfaces.

2.1. Field measurements

Five external wall types (EW 1–5) with side dimensions 850×850 mm were designed to study the hygrothermal performance of the CLT in the building envelope, see Fig. 1. For each wall type, four test walls were prefabricated in the laboratory (a total of 20 test walls) and installed as part of the external wall into the nZEB technological test facility on TalTech campus, Tallinn, Estonia, see Fig. 2. Half of the test walls from each type facing north and the other half were facing south (marked EW nN/S). The test walls were also divided by the initial moisture content (MC) of the CLT. Half of the test walls were manufactured with factory dry CLT panels (MC 13%) (EW n1) and the other half with CLT surface MC up to 26% (EW n2). Higher CLT surface MC was achieved by soaking the panels in a water-filled pool for 24 days. To prevent both large water absorption along the wood grain (longitudinal direction) during soaking and rapid dry-out of the cut-edges of the CLT panel during the test, the narrow CLT edges (cut-edges) were painted with a waterproof polymer-based mastic. The high MC of the soaked CLT was measured by two methods. During soaking, the MC was determined by weighing. The aim was to achieve an MC of 25% by weight. The panels were then kept outdoors for one week for conditioning; later, before the panels were used to prefabricate the test walls, the surface moisture content was measured by the electrical resistance method using electrodes (pins). The surface MC varied between 24 and 27% in different panels and the MC also varied in the surface area. Therefore, in another study, the moisture distribution in the CLT panel was determined when the panel surface was placed in contact with water [26]. According to the panel surface, the surface high MC depth of 30 mm was later selected when creating the simulation model. Field measurements of the test walls started on January 16, 2018 and finished on March 6, 2019. The methodology was developed on the example of research by McClung R. et al. [15] and adapted according to the objectives of our work.

All external wall types were designed with a 5-layer 100 mm thick (layer thickness 20 mm) CLT panel (produced from Norway spruce, *Picea abies*), ventilated (ventilation gap 28 mm) wooden cladding (22 mm) façade, and a glass wool wind barrier (Isover RKL 30 mm). Three (EW 1–3) of the five test wall types were insulated with different insulation materials and the CLT was exposed to the indoor environment, see Fig. 1 a, b, c. In the other two wall types (EW 4–5), the CLT was covered with different interior layers and insulated with water vapour permeable mineral wool, see Fig. 1 d, e. Test wall type 1 (EW 1) was insulated with 300 mm thick glass wool insulation ($\lambda = 0.037$ W/(m·K)), type 2 (EW 2) with 330 mm thick cellulose insulation ($\lambda = 0.041$ W/(m·K)) and type 3 with 200 mm thick polyisocyanurate (PIR) ($\lambda = 0.022$ W/(m·K)). Mineral wool (glass wool in this paper) was selected for insulation because it

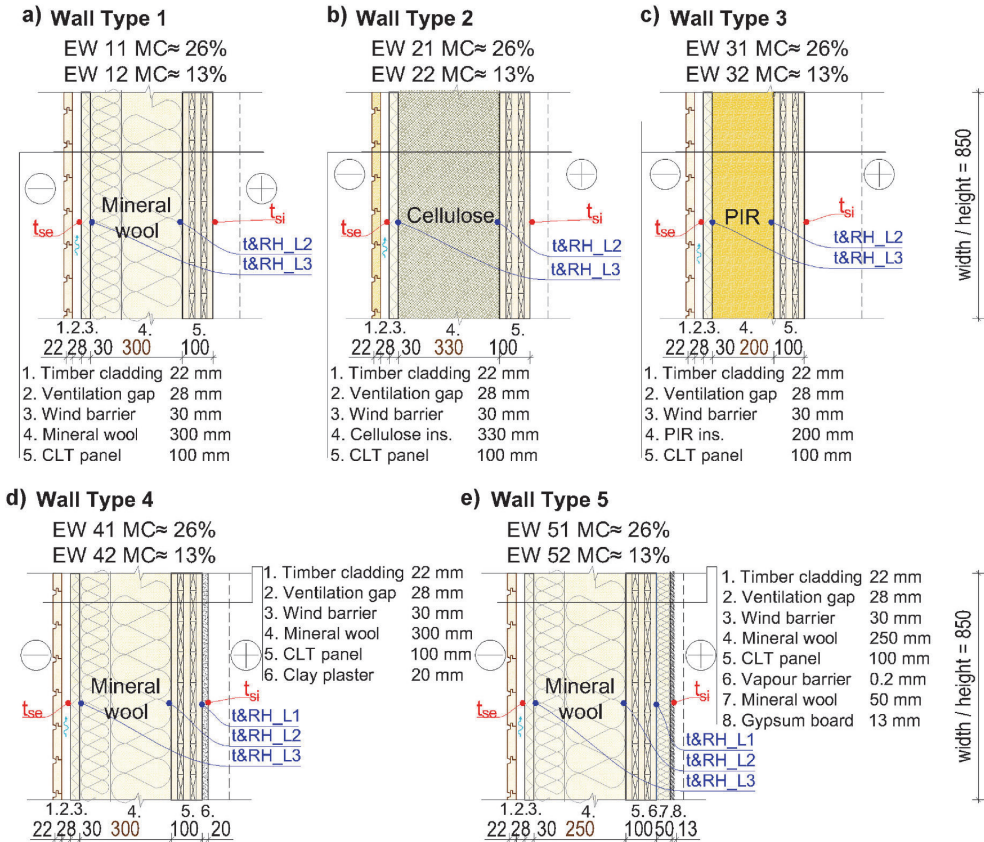


Fig. 1. Cross-sections of CLT external test wall types.

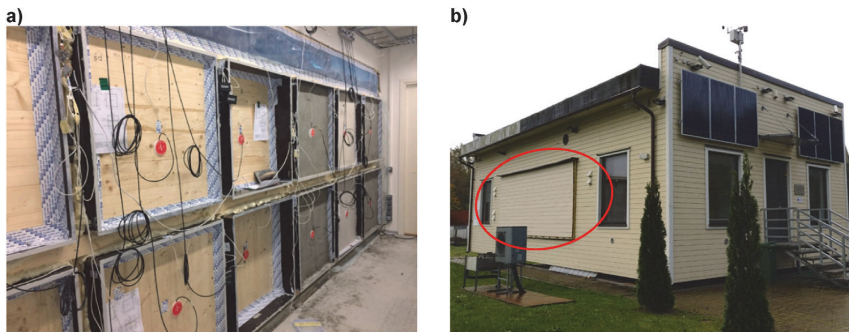


Fig. 2. Test walls installed as part of the external wall of the TalTech nZEB test facility, interior view (a) and exterior view (b, marked with a red circle). (For interpretation of the references to colour in this figure legend, the reader is referred to the Web version of this article.)

is the most common type of insulation used in the production of prefabricated wooden buildings. Cellulose insulation was selected because it provides the benefit of moisture buffering effect that can smoothen

down the humidity peak levels and dynamics of the indoor air and prevents mould growth better than non-hygroscopic insulations (such as mineral wool) [13,14]. PIR insulation has been used most frequently in

the prefabrication industry due to its very low thermal conductivity, which allows significant reduction of the wall thickness while still achieving very low thermal transmittance. Thermal transmittance was designed to be the same for all wall types ($U = 0.1 \text{ W}/(\text{m}^2 \cdot \text{K})$); therefore, thickness of the insulation varied. Thermal transmittance of each wall type was calculated at 13% CLT MC, and in the oven-dry state (0% of MC) of the remaining materials. Temperature (t) and relative humidity (RH) were measured between the material layers during our field measurements. Temperature and RH sensors (t & RH) were placed as follows: between the CLT and the insulation (L2), between the insulation and the wind barrier (L3), and between the interior layer and the CLT (L1) in wall types 4 and 5, see Fig. 1. The indoor surface temperature (t_{si}) of each wall was measured by sensors located in the interior layer surface and outdoor surface temperature sensors (t_{se}) were located on the wind barrier surface. The accuracy of the sensors was $\pm 0.3 \text{ }^\circ\text{C}$ from 0 to $60 \text{ }^\circ\text{C}$ (t sensor, Omnisense A-1), $\pm 0.5 \text{ }^\circ\text{C}$ from -10 to $85 \text{ }^\circ\text{C}$ (t_s sensor, Uniflex), and $\pm 2.0\%$ from 0% to 100% (RH sensor, Omnisense A-1). Measurement results were logged and saved at an hourly interval.

The indoor climate was controlled by automated heating and humidifiers. The target indoor temperature of both the northern and the southern walls was $21 \text{ }^\circ\text{C}$ (Fig. 3, b); the target moisture excess $\Delta v_{te} \leq 0 \text{ }^\circ\text{C} = 3 \text{ g}/\text{m}^3$ in the cold period (less than $0 \text{ }^\circ\text{C}$) and $\Delta v_{te} \geq 20 \text{ }^\circ\text{C} = 0.5 \text{ g}/\text{m}^3$ in the warm period (from $20 \text{ }^\circ\text{C}$). Moisture excess $\Delta_v, 3 \text{ g}/\text{m}^3$ in the cold period applies to residential buildings with an occupancy of $32 \text{ m}^2/$

person [27]. Indoor RH is shown in Fig. 3, a. Hourly measured values of outdoor RH (Fig. 4, a), temperature (Fig. 4, b), diffuse (Fig. 4, c) and direct (Fig. 4, d) shortwave radiation on the horizontal area, wind direction (Fig. 4 e) and velocity (Fig. 4, f), and rainfall intensity (Fig. 4, g) on the horizontal area were obtained from the nearest weather station located 3 km from the test facility.

The hygrothermal performance of the test walls was evaluated by the risk of mould growth and water vapour condensation. Initially, the risks were evaluated according to whether the RH measurements exceeded 80% between the CLT and the insulation (minimum RH for mould growth) and 100% between the insulation and the wind barrier (condensation). The dry-out period of the soaked CLT panel was also observed until the RH dropped below 80% (from a surface MC of 26% to an equilibrium MC of 15%, see Fig. 5 b). When the RH between the CLT and the insulation exceeded 80%, the mould growth risk on the CLT surface was evaluated via the mould growth index, using the VTT improved mould growth model [28]. Mould growth index M is a numerical scale from 1 to 6, which indicates the extent of mould growth. Indexes 1 and 2 indicate initial stages of mould growth (small amounts and $<10\%$ coverage of mould on the surface seen only with a microscope), 3 to 5 indicate visually visible mould coverage on the surface from 10 to over 70% and 6 indicates very heavy growth, coverage around 100% [28]. The mould index below 1 ($M < 1$) shows no growth on the material surface, which was set as the evaluation criterion. A wall

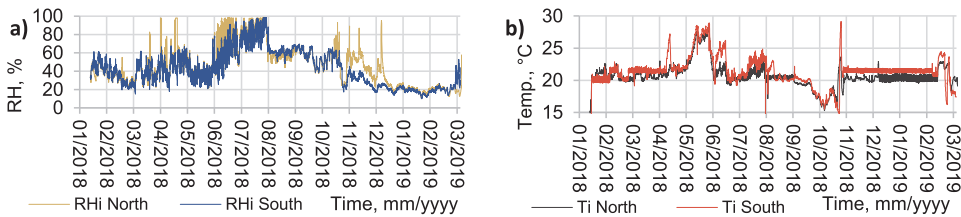


Fig. 3. Indoor RH (a) and temperature (b) in both north and south test rooms.

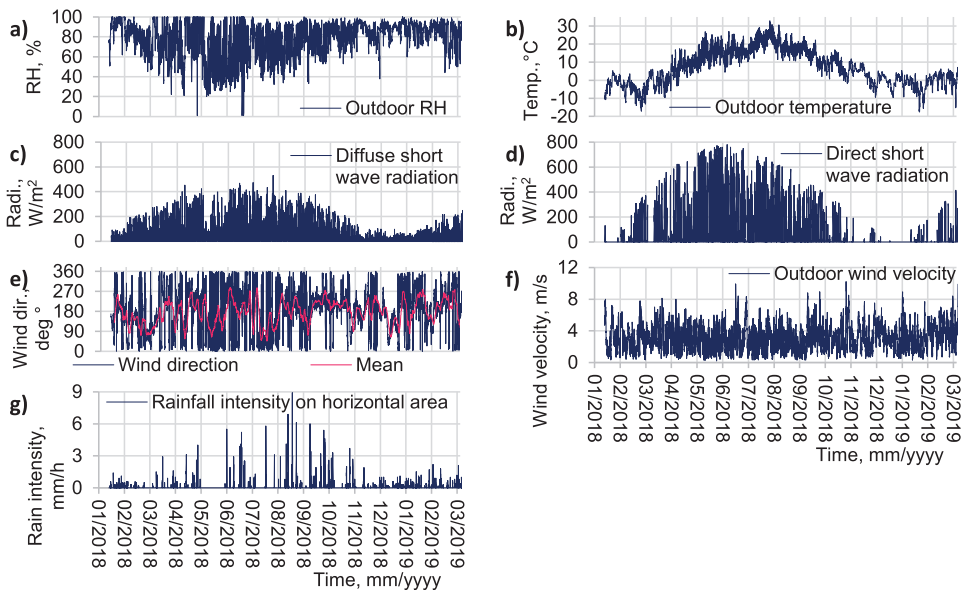


Fig. 4. Outdoor RH (a), temperature (b), diffuse (c) and direct (d) short wave radiation on the horizontal area, wind direction (e) and velocity (f) and rainfall intensity (g) on the horizontal area.

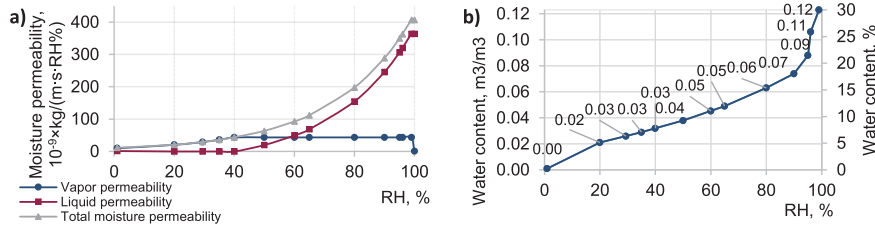


Fig. 5. Moisture permeability (a) and sorption (b) curves of CLT.

exceeding index 1 was considered as a non-hygrothermally safe wall. In other words, the building envelope design should exclude the risk of mould, regardless of the extent of mould growth. The mould growth index was calculated through a function using temperature and relative humidity, exposure time to critical RH, and considering the CLT as a very sensitive material and the surface as sensitive (planned surface) to mould growth [29]. In addition to the risk of condensation, the risk of mould growth on the surface of the wind barrier was also evaluated via a mould growth index where the material and surface sensitivity class was selected to be a medium resistant (glass wool).

2.2. Hygrothermal simulations

After completion of the field measurements, the simulation models were created using HAM (heat, air, and moisture) modelling software Delphin 5.9. The properties assigned to the material layers of the wall are given in Table 1, and the materials were selected from the Delphin software database (the material ID in the database is also included in Table 1). According to the database, the properties of the materials selected for our research have been measured in IBK (Institut für Bauklimatik, Technische Universität Dresden) laboratories. The properties of the CLT were taken from the material file in the WUFI database with the ID “Stora Enso CLT”, which is official information published by the CLT manufacturer Stora Enso. The material properties of “Stora Enso CLT” have been measured according to the information provided by the manufacturer at the University of Hamburg, Germany by M. Hirsch, 2013. The species of wood of CLT wood is Norway spruce, *Picea abies*. Thermal conductivity and vapour diffusion resistance factors of the CLT in Table 1 are given at a dry state, representing the oven-dry state of the material, i.e., 0% moisture content. Moisture permeability (a) and sorption (b) curves of the CLT are shown in Fig. 5. CLT properties were

taken from a file made available to the public by the manufacturer (Stora Enso). Orientation for the north-facing test walls was set to 0° (North) and for the south-facing walls to 180° (South). The latitude of the walls was set to 59.4° (latitude of Tallinn, Estonia). The field results measured at the site and the data obtained from the weather station were used as the indoor and outdoor boundary conditions, see Figs. 3 and 4.

Air change rate (ACH) in the ventilation gap was not measured; it was assigned as a constant value of 150 1/h (0.1 m/s). Thus, it is one of the limitations of this research. However, in-depth studies of the ACH of ventilated facades have been conducted by Finch and Straube [30] in Canadian climate (Vancouver) and by Falk and Sandin [31] in Swedish climate. Based on these studies, for reference, a fixed average annual ACH of 0.1 m/s was selected in our study. In addition, a sensitivity analysis was done using values of 10, 50, 100, 150 and 200 1/h for simulations. According to the sensitivity analysis, the best fit found was to use 100 and 150 1/h. For the final simulation models, the ACH value of 150 1/h was used, which has been confirmed by previous studies [30, 31].

The first RH and temperature measurements of each test wall were determined as initial conditions of simulation models. The initial conditions were evenly distributed between the material layers of the models. The initial MC of the factory-dry CLT panels was set to be 13% ($0.053 \text{ m}^3/\text{m}^3$) over the entire cross-section. Soaked CLT panels had an initial surface MC of 26% ($0.107 \text{ m}^3/\text{m}^3$) with the depth of 30 mm, as mentioned in section 2.1; during validation, it was changed according to the measured RH values between the CLT panel and the insulation. The central part (40 mm) in the cross-section of soaked CLT panels remained 13%. Vapour barrier film as an interior layer in test wall type 5 was considered in the simulation model as additional resistance between the material layers of CLT and the internal insulation with vapour resistance (Sd) of $1 \times 10^{50} \text{ m}$. Thermal resistance of the internal surface was set to

Table 1
Material properties.

Material ID (Delphin/Wufi database)	Material	Bulk density, kg/m^3	Thermal conductivity, $\text{W}/\text{m}\cdot\text{K}$	Vapour diffusion resistance factor, -	Open porosity, m^3/m^3	Water uptake coefficient, $\text{kg}/\text{m}^2\cdot\text{s}^{0.5}$
128	Clay plaster	1568	0.58	30	0.408	0.176
599	Gypsum board	745	0.177	11	0.719	0.179
Stora Enso CLT	CLT	410	0.098 ^a	500 ^a	0.74	0.0024
644	Glass wool insulation	37	0.037	1	0.92	0
580	Cellulose insulation	65	0.041	2	0.926	0.563
689	PIR insulation	38	0.022	104	0.92	0.0001
646	Wind barrier, glass wool	100	0.033	1	0.92	0

^a at oven-dry state.

be $R_{si} = 0.13 \text{ (m}^2 \text{ K)}/\text{W}$ and the external surface to be $R_{se} = 0.04 \text{ (m}^2 \text{ K)}/\text{W}$.

The simulation models were validated by comparing the measured and the calculated (simulation) results. Firstly, differences in the results were found in the absolute value (*abs. Δ*) by subtracting the measurement results from the calculation results and the difference was estimated from the error of the measuring device. Secondly, the Root-Mean-Square-Error (RMSE) was found according to Eq. (1) and then normalized RMSE (NRMSE) according to Eq. (2), using the mean value of the measurement results:

$$RMSE = \sqrt{\frac{\sum_{i=1}^n (s_i - m_i)^2}{n}} \quad (1)$$

$$NRMSE = \frac{RMSE}{m_{max} - m_{min}} \times 100, \% \quad (2)$$

where, s_i - hourly calculated (simulation) result, m_i - hourly measured result, n - total number of hourly results, and m_{min} , m_{max} - the minimum and maximum measured results. RMSE indicates the standard deviation of the differences, i.e., the model error. The normalization of the RMSE shows the variability (in percent) of the differences in relation to the range of the measurements ($m_{max} - m_{min}$) and NRMSE allows comparison of the differences in the results between the observed parameters with different scales (temperature (t), partial pressure of water vapour (P_v) and RH). For simplification, a colour scale was used to distribute the NRMSE results divided into five ranges:

- NRMSE ≤5% ■
- NRMSE between 6-10% ■
- NRMSE between 11-15% ■
- NRMSE between 16-20% ■
- NRMSE >20% ■

3. Results

3.1. Field measurements at each location and impact of design parameters

3.1.1. Measurements between the CLT and the insulation – location L2

The RH between the CLT panel and the insulation (location L2) varied mostly between 20 and 75% in all test walls (Fig. A1). In test walls with the CLT panel soaked in water before installation (EW 11–51), the RH exceeded 80% at the beginning of the measurement period when the excess moisture in the CLT panel had dried out, see Fig. 6. The time when the RH was over 80% was short and the calculation results of the mould growth index did not exceed 1 in any test wall; hence, there was no risk of mould growth on the CLT surface. In the cold period, from December to March, the RH varied from 30 to 15%, and by summer, from June to October, the RH rose above 50% in all test walls. Smaller RH fluctuations occurred on the test wall types 2 (EW 21 & EW 22) and 3 (EW 31 and EW 31), ranging from 30 to 60%, see Fig. 6 e-l. In the wall types insulated with mineral wool (EW1, 4 & 5), the RH ranged from 20 to 75%, see Fig. 6 a-d Fig. A1.

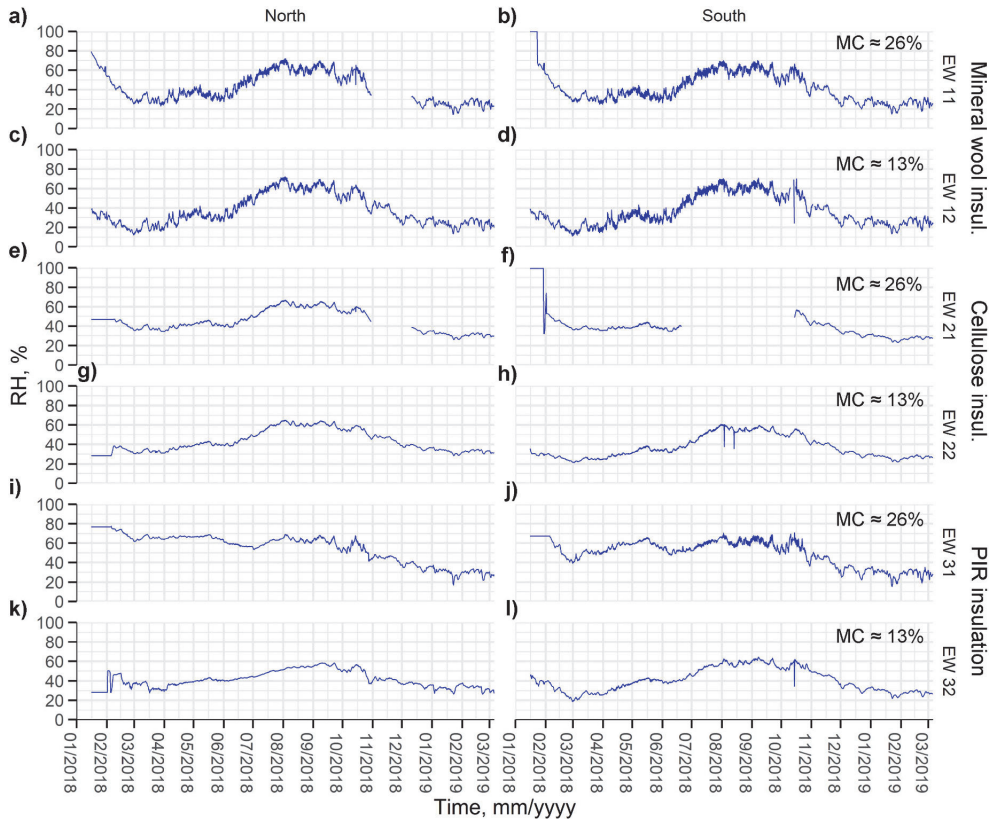


Fig. 6. Field measurements of RH between the CLT and the insulation (L2) in types 1, 2 and 3 test walls.

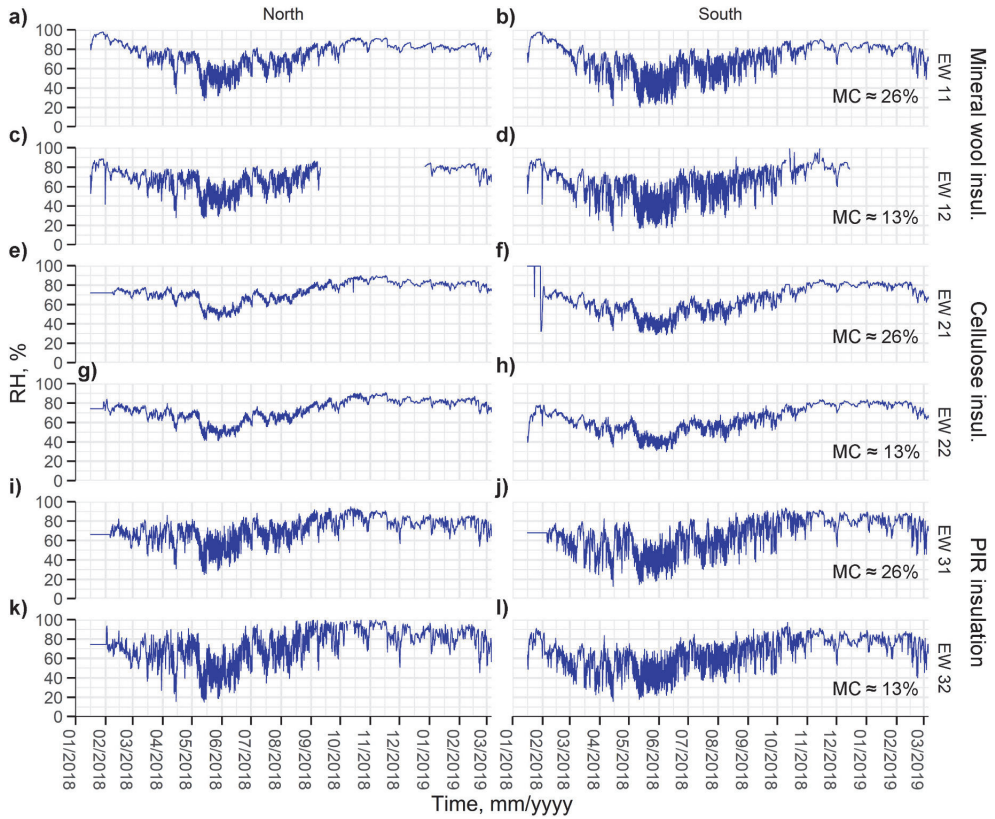


Fig. 7. Field measurements of RH between the insulation and the wind barrier (L3) in types 1, 2 and 3 test walls.

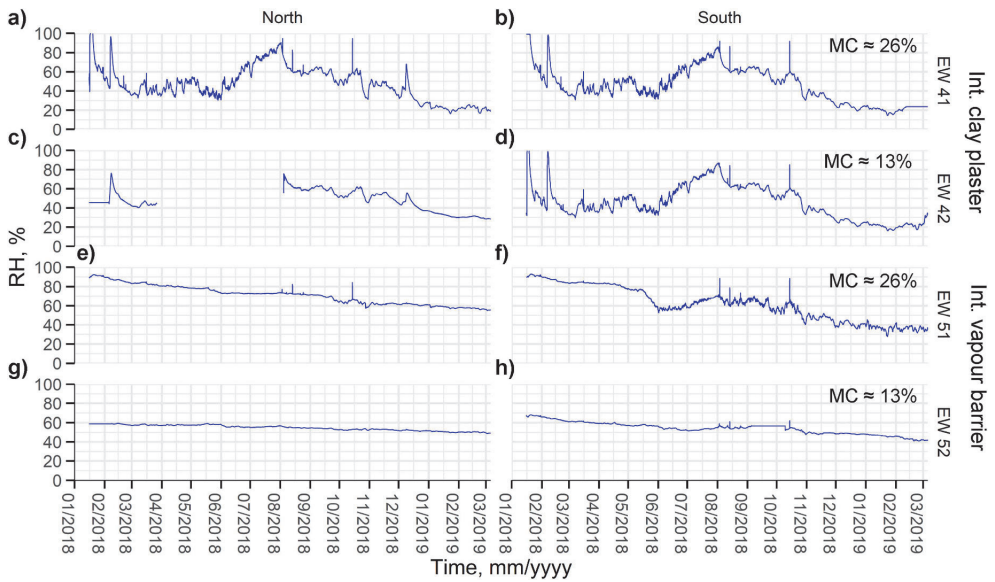


Fig. 8. Field measurements of RH between the CLT and the internal layer (L1) in types 4 and 5 test walls.

3.1.2. Measurements between the insulation and the wind barrier – location L3

The RH between the insulation and the wind barrier plate (location L3) did not reach 100% during the measurement period in any of the test walls except EW 32 North, see Fig. 7 and Fig. A2. This means that no water vapour condensation risk took place except in test wall EW 32 North. In the north-oriented EW 32 test wall, the RH fluctuated continuously up to 100% from August to November, which means that there was a risk of condensation, see Fig. 7 k. On the south-oriented wall (EW 31 South), RH did not reach 100% (Fig. 7 l). Also, the risk of mould growth (calculated according to the VTT mould index) on the surface of the wind barrier was not present in any of the walls. In the cold period, from November to February, the RH varied from 75 to 95%, and by spring-summer, from March to September, the RH varied from 30 to 75% in most of the test walls. Smaller RH fluctuations occurred in type 2 test walls (EW 21 & EW 22), ranging from 40 to 90%, see Fig. 7 e-h. The largest fluctuations occurred in type 3 walls (EW 31 & EW 32), ranging from 15 to 100%, see Fig. 7 i-l. In the wall types insulated with mineral wool (EW1, 4 & 5), the RH ranged from 20 to 95%, see Fig. 7 a-d, m-u and Fig A2.

3.1.3. Measurements between the CLT and the internal layer – location L1

At location L1, between the CLT and the internal layer, the RH was measured only in types 4 and 5 test walls. In type 4, the air vapour saturation limit was exceeded between the plaster and the CLT after the plaster was applied and during its drying period, see Fig. 8 a-d. The drying time of the plaster was short enough to ensure the RH dropping below 80% without any risk of mould growth. The calculation results of the mould index did not exceed index 1 during the dry-out. In type 5 test walls, the RH exceeded 80% for about 90 days between the soaked CLT panel (EW 51) and the vapour barrier film, in both north- and south-oriented external walls, see Fig. 8e and f. Despite long stay at high RH, no risk of mould growth on the CLT surface was detected by the calculation of the mould growth index. However, the mould index exceeded 1 if the sensitivity of the surface was reduced to 1 (rough sawn surface on wood). The RH remained stable at 60% in walls where factory dry panels (EW 52) were used (Fig. 8g and h).

3.1.4. Impact of wall orientation on field measurements

Wall orientation was found to have minor impact; the results of the north- and south-facing walls did not differ much. This small effect occurred mainly due to the ventilated façade where the ventilation gap equalised the surface temperature of the wind barrier, especially on the south-facing walls, because of high solar radiation. However, the impact of the sun was observed in wall types 4 and 5, where the southern walls had a greater variation in the RH between the insulation and the wind barrier plate (location L3) than the northern walls, see Fig. A2. Larger variations occurred mainly in the spring and summer periods, see Fig. 7 m-u. The effect was also clearly visible in wall type 3, consisting of the CLT with PIR insulation, where a potential risk of water vapour condensation occurred on the surface of the wind barrier (location L3) on the northern wall, which was not present on the southern walls. However, it appeared only on one (EW 3.2 North) of the four walls.

3.1.5. Impact of CLT initial moisture content on field measurements

High initial CLT moisture content exerted strong impact, as was assumed. The dry-out of high initial moisture content at the beginning of the measurement period on the walls with soaked CLT panels significantly increased the RH between the insulation and the CLT panel (location L2), see Fig. 6 a, b, m, n, r, s. The same occurred between the interior layer (vapour barrier or clay plaster) and the CLT panel

(location L1), see Fig. 8 a, b. On most walls, except for wall types 2 and 3, the RH at locations L1 and L2 was greater than the critical RH of 80% at the beginning of the drying period. However, according to the calculations of the mould growth index, dry-out of initial moisture on any wall during the measurement period posed no risk of mould growth. The measured RH in types 2 and 3 test walls with soaked CLT panels (EW 21 and EW 21) at location L2 showed a low result instead of high (expected to be over 80%) at the beginning of the measurement period. The reason was that the start of logging of some sensors was delayed due to a technical problem of the measuring device. Therefore, the measured RH results in types 2 and 3 test walls were constant at the beginning of the measurement period, see Fig. 6 e-k.

3.1.6. Impact of wall assembly on field measurements

The assembly of the walls had the greatest impact on the selection and arrangement of the layers of materials. Walls with the CLT exposure to the indoor environment or covered with water vapour permeable clay plaster demonstrated successfully that the CLT panel controls the water vapour diffusion and the RH remains low between the wind barrier and the insulation. RH also remained low in walls with high CLT initial moisture content and with low vapour permeable PIR insulation.

Comparison of external walls insulated with mineral wool and cellulose insulation showed that cellulose insulation is at an advantage due to its greater ability to bind moisture from the air. The RH remained more stable, lower and fluctuated less between material layers in cellulose insulated external test walls against walls insulated with mineral wool, see Figs. 6 and 7 e-h. A clear advantage was found on the walls with high CLT initial moisture content (EW 21): while almost all mineral wool insulated walls with the CLT pre-soaked (EW 11, 41 and 51) had the RH between the insulation and the CLT panel of more than 80% at the beginning of the measurement period (dry-out period), cellulose-insulated walls had less than 75%.

The most unexpected results were found on PIR-insulated walls. The walls had the lowest RH between the CLT and the insulation. Dry-out of the soaked CLT high initial moisture content did not result in the accumulation of moisture on the surface of the PIR insulation, as originally expected. Preliminary simulations, before installing the test walls showed that moisture accumulates behind the insulation at high CLT initial MC, which in turn may cause a risk of mould growth, see Fig. 11 a, b. A later investigation revealed that the quick dry-out was due to the low air exchange between the PIR insulation and the CLT panel. Air exchange was also considered to cause the condensation risk on the surface of the wind barrier at L3. In Fig. 12, the preliminary simulation without air leakage, the final simulation with air leakage and the field measurement results are compared. Clearly, in the simulation without air leakage (Fig. 12, b), the low vapour permeable PIR insulation controls the water vapour diffusion well, as expected and the RH varies between 30 and 90%. Final simulation results with the air leakage (Fig. 12, c) showed a variation of RH between 20 and 97%, which is similar to the field measurement results where condensation risk occurred (Fig. 12, a). However, the risk of condensation may have been due to a sensor error, as shown by a close-up view of the measurement results, see Fig. 12 d. A detailed description is presented in section 3.2.

The internal coating of the CLT surface with clay plaster had no significant impact and the plaster dried after installation, without posing any risk of mould growth on the CLT surface. Also, covering the CLT with a vapour barrier film and internal insulation caused no risk of mould, but the RH was over 80% for a long time (about 3 months) at the beginning of the measurement period, see Fig. 14 upper. This means that further investigations are needed to address the use of internal vapour barriers and to evaluate the performance, for example, by the stochastic

Table 2

The absolute mean difference between the measurement and the calculated results of temperature (*t*) and relative humidity (*RH*) at each location examined in the test walls.

Wall ID	Location L2, CLT and insulation		Location L3, insulation and wind barrier	
	<i>t</i> , °C	<i>RH</i> , %	<i>t</i> , °C	<i>RH</i> , %
abs. Δ				
<i>sensor accuracy:</i>				
±0.3 °C		±2.0%		±0.3 °C
				±2.0%
EW 11 N	1.3	1.8	2.0	8.2
EW 12 N	0.3	0.7	1.6	6.1
EW 11 S	0.4	2.4	1.8	7.4
EW 12 S	0.8	2.1	1.6	6.6
EW 21 N	0.7	1.7	1.8	7.2
EW 22 N	1.0	3.2	1.5	7.0
EW 21 S	0.6	2.7	1.3	4.9
EW 22 S	0.7	1.4	1.2	4.5
EW 31 N	0.6	9.8	0.5	8.7
EW 32 N	0.5	2.6	0.4	9.7
EW 31 S	1.1	7.2	0.8	11.2
EW 32 S	0.5	2.7	0.6	11.3
EW 41 N	1.2	2.4	1.9	7.7
EW 42 N	0.8	3.0	1.3	6.7
EW 41 S	1.3	2.7	1.8	7.1
EW 42 S	1.0	2.2	1.5	6.7
EW 51 N	2.4	3.9	2.2	8.2
EW 52 N	0.9	1.9	1.5	6.1
EW 51 S	1.2	2.6	1.7	6.5
EW 52 S	0.9	2.3	1.5	7.3
Location L1, interior layer and CLT				
EW 41 N	0.5	7.5		
EW 42 N	0.6	2.5		
EW 41 S	0.8	6.7		
EW 42 S	0.5	5.4		
EW 51 N	1.6	7.0		
EW 52 N	1.3	1.4		
EW 51 S	1.0	14.3	abs. Δ < sensor accuracy-	
EW 52 S	0.4	4.0		

analysis where the boundary conditions are the reference test year.

3.2. Comparison between field measurements and simulations

Differences in the measured and the calculated results of temperature (*t*) and RH used for validation are given in Table 2. NRMSE (including partial pressure of water vapour (*P_v*)) values are presented in Table 3. Table 2 shows the absolute mean differences between the measurement and the calculated results against the measuring sensor accuracy, highlighting the values that are smaller than the accuracy (marked in green). Table 3 shows the colour scale for distributing the NRMSE values, which are divided into five ranges: ≤5% (green), 6–10% (light green), 11–15% (yellow), 16–20% (light red), and >20% (red).

The vast majority of the results of the mean absolute difference exceeded the measurement sensors' accuracy (Table 2). This means that the accuracy of the model depended on the external factors (material properties, boundary conditions).

Comparison of the NRMSE of all parameters shows that the majority of results are up to 5% and the vast majority up to 10%, see Table 3. The smallest discrepancy in the results of all parameters based on NRMSE was at location L2 (between CLT and insulation) where most of the results were within 10% of NRMSE (Table 3). The smallest difference in the results at L2 is also shown by the compatibility of trend lines, see Fig. 9 and Fig. A1. An overall comparison of the trend lines of the calculation results at L2 showed that the simulation results

Table 3

NRMSE of temperature (*t*), partial pressure of water vapour (*P_v*) and relative humidity (*RH*) at each location examined in the test walls.

Wall ID	Location L2, CLT and insulation			Location L3, insulation and wind barrier		
	<i>t</i>	<i>P_v</i>	<i>RH</i>	<i>t</i>	<i>P_v</i>	<i>RH</i>
NRMSE						
EW 11 N	10%	4%	4%	6%	6%	13%
EW 12 N	3%	3%	4%	5%	5%	11%
EW 11 S	3%	6%	5%	6%	7%	11%
EW 12 S	4%	5%	6%	5%	7%	9%
EW 21 N	7%	5%	6%	5%	4%	18%
EW 22 N	8%	5%	10%	5%	4%	16%
EW 21 S	6%	5%	4%	4%	5%	8%
EW 22 S	4%	4%	5%	4%	5%	10%
EW 31 N	6%	16%	25%	2%	8%	17%
EW 32 N	4%	7%	8%	1%	9%	14%
EW 31 S	8%	10%	16%	2%	15%	19%
EW 32 S	3%	5%	7%	2%	15%	18%
EW 41 N	10%	4%	6%	5%	5%	13%
EW 42 N	7%	7%	6%	4%	5%	13%
EW 41 S	8%	6%	6%	6%	7%	11%
EW 42 S	5%	4%	5%	5%	6%	11%
EW 51 N	16%	5%	8%	6%	5%	14%
EW 52 N	10%	4%	5%	4%	5%	11%
EW 51 S	6%	5%	5%	6%	7%	10%
EW 52 S	5%	4%	5%	5%	6%	11%
Location L1, interior layer and CLT						
EW 41 N	5%	11%	12%			
EW 42 N	6%	6%	7%			
EW 41 S	7%	20%	11%			
EW 42 S	4%	10%	11%			
EW 51 N	13%	16%	19%			
EW 52 N	11%	11%	15%			
EW 51 S	6%	22%	28%			
EW 52 S	3%	10%	18%			

overestimated the RH results, which is the safe side for the model when evaluating mould growth risk.

As an exception, there was a large difference in the NRMSE result of RH (16 and 25%) and *P_v* (16%) at location L2 for wall type 3 with high CLT initial MC (EW 31), see Fig. 11 a, b. Also, it turned out most difficult to create a simulation model for wall type 3. Preliminary simulation results showed that RH remains stable between two materials with high water vapour resistance, PIR insulation and the CLT panel, see Fig. 11 (preliminary calculation). However, the measured results showed a large variability of RH, influenced by the external climate. The reason was assumed to be the air gap between the PIR insulation and the plywood boards surrounding the test wall, which allowed a small air exchange as a stack effect. To confirm this, a 2D simulation model was developed and an air gap designed around the PIR insulation was connected to the outdoor (inside the ventilation gap VG, behind façade glazing FG) conditions, see Fig. 10 a. To achieve the best agreement of the 2D simulation results with the measurements, the width of the air gap had to be set to 3 mm. Air exchange was calculated from the difference between the outdoor temperature and the temperature between the CLT and the insulation. The hourly air exchange rate *R_a* was calculated according to Eqs. (3)–(5) [32]:

$$R_a = \frac{\Delta P_g}{S_g} \tag{3}$$

$$S_g = \frac{12\mu \cdot L}{b^2 \cdot A} \tag{4}$$

$$\Delta P_g = z \cdot 3.456 \cdot \left(\frac{1}{T_e} - \frac{1}{T_i} \right) \tag{5}$$

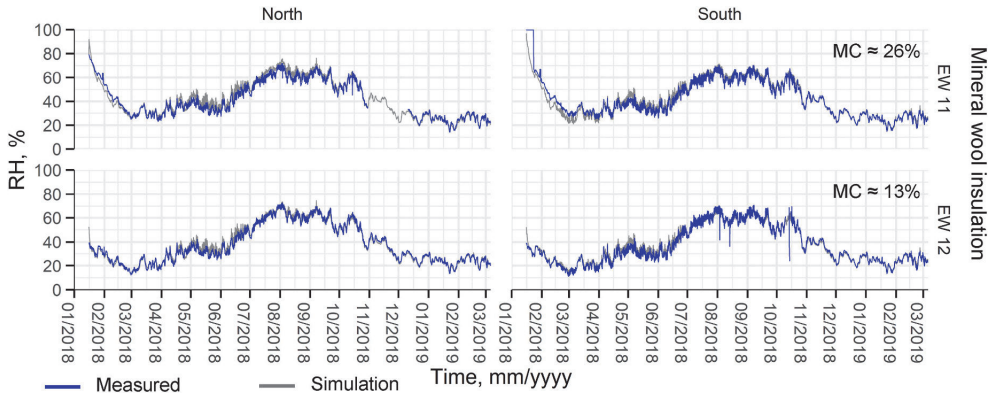


Fig. 9. Measured and calculated RH between the CLT and the insulation (L2) in type 1 test walls.

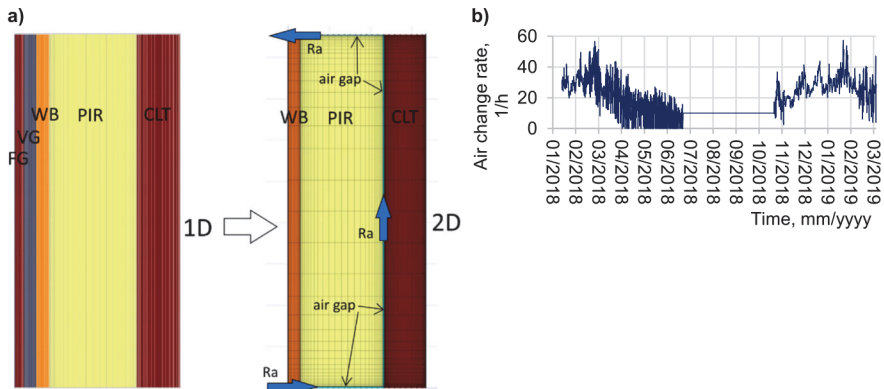


Fig. 10. Initial 1D simulation model for test wall type 3 and final 2D model with air gaps (a) and calculated air exchange rate in the air gap in type 3 test walls (b).

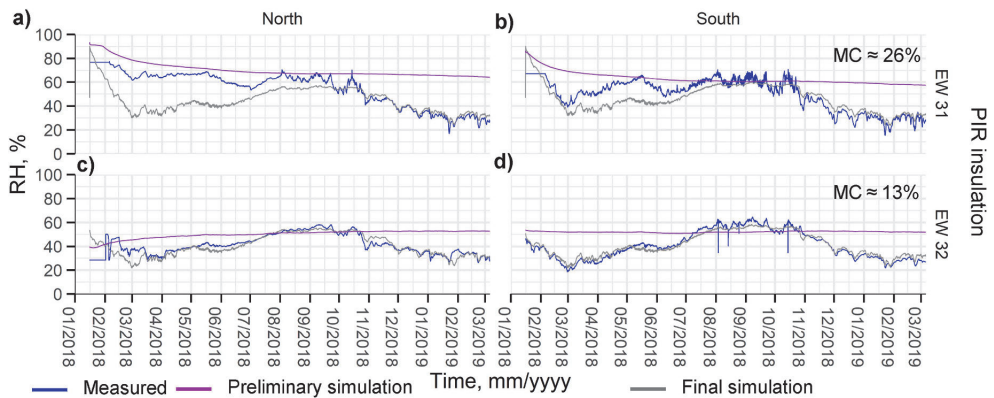


Fig. 11. Measured and preliminary simulation (only moisture diffusion and capillary flow, without outdoor air leakage) and final simulation (with moisture diffusion and capillary flow, and outdoor air leakage) of RH between the CLT and the insulation (L2) in type 3 test walls.

where, ΔP_g (Pa) is a pressure loss inside the air gap, S_g ($\text{Pa}\cdot\text{s}/\text{m}^3$) - laminar airflow inside the air gap, b (m) - height of the gap, L (m) - length of the air channel, A (m^2) - flow area perpendicular to the flow

direction, μ (Ns/m^2) - dynamic viscosity of air, z (m) - vertical distance of the air gap, T_e ($^\circ\text{C}$) - hourly measured outdoor temperature (inside the VG), and T_i ($^\circ\text{C}$) - hourly measured temperature between the CLT and the PIR insulation. In the simulation, during the summer period, when the

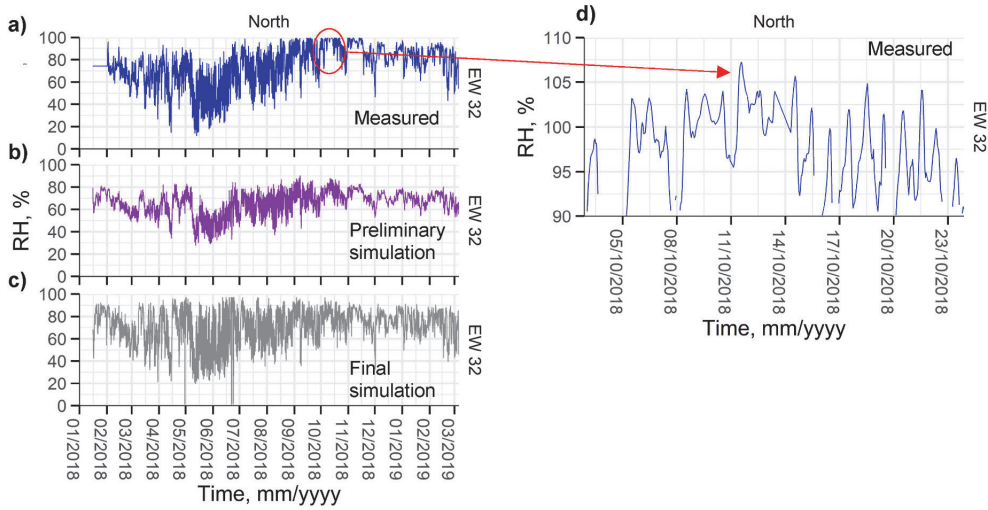


Fig. 12. Measured (a), preliminary simulation without air leakage (b), final simulation with air leakage (c) and a close look of measured (d) RH between the insulation and the wind barrier (L3) in type 3 test wall EW 32.

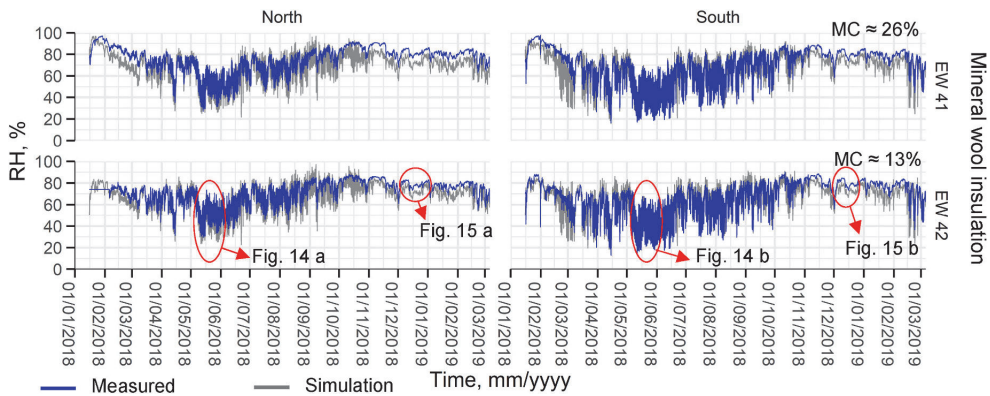


Fig. 13. Measured and calculated RH between the insulation and the wind barrier (L3) in type 4 test walls.

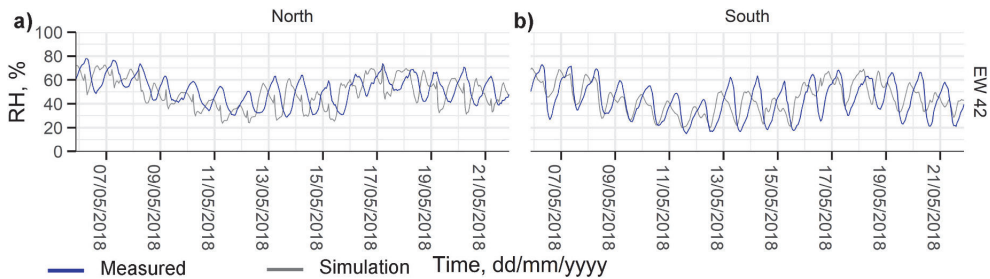


Fig. 14. Measured and calculated RH between the insulation and the wind barrier (L3) in type 4 test walls between 7 and May 21, 2018.

temperature difference is small, a constant of 10 l/h was set for the air exchange rate when the air exchange is dominated by the wind, see Fig. 10 b. The results of the 2D simulation with the air exchange rate of type 3 wall matched the measurements significantly better than in the preliminary simulation, see Fig. 11. However, there were some major

differences, especially in walls with high CLT initial MC (Fig. 11 a, b). The RH between the insulation and the wind barrier at L3 was also greatly affected by air leakage. The preliminary simulation without air leakage (Fig. 12 b) showed stable RH results between 30 and 90%. However, the final simulation with the air leakage (Fig. 12 c) showed a

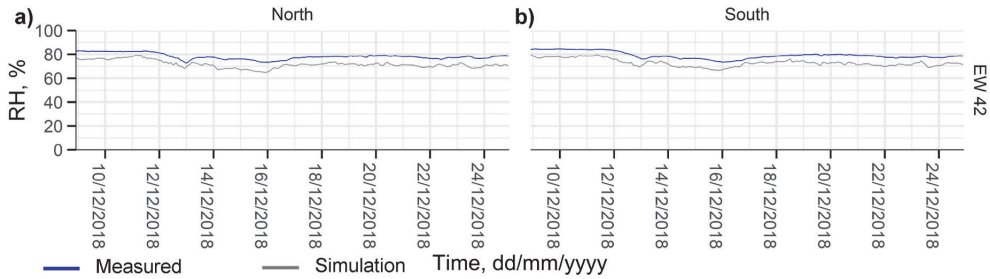


Fig. 15. Measured and calculated RH between the insulation and the wind barrier (L3) in type 4 test walls between 10 and December 24, 2018.

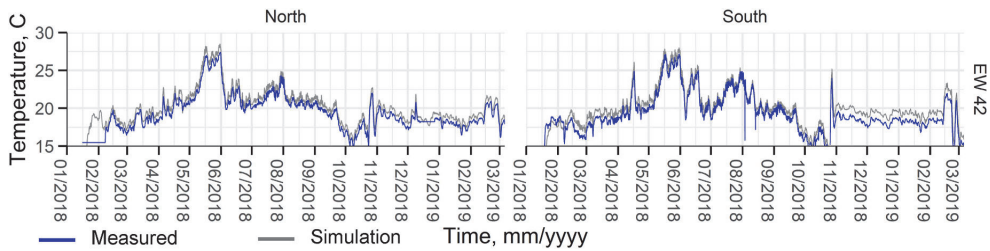


Fig. 16. Measured and calculated temperature between the CLT and the insulation (L2) in type 4 test walls.

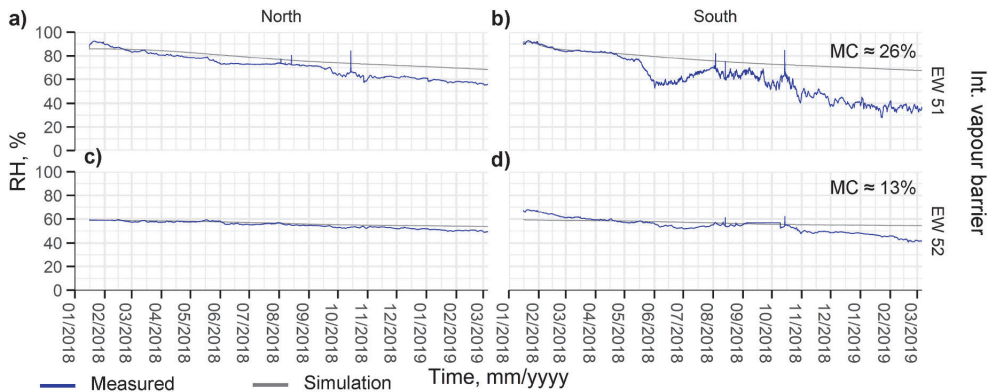


Fig. 17. Measured and calculated RH between the CLT and the internal insulation (L1) in type 5 test walls.

great variation of RH between 20 and 95%, which is similar to the field measurement results (Fig. 12 a). A close look (05–23 October 2018) at the field measurement results indicates a measuring sensor error, see Fig. 12 d. During periods of condensation risk, RH jumps in sharp peaks to over 100%, up to 108%. However, the actual condensation should show a constant 100% RH for a short time. The fact that the other three of the four type 3 test walls did not show any risk of condensation also indicates a measuring sensor error, see Fig. 7 i, j, l. Consequently, it can be said that real condensation on the surface of the wind barrier (L3) in the wall EW 32 North was rather unlikely.

Overall, the largest discrepancies occurred at location L3 where the majority of the NRMSE of the RH results were above 10%, up to 19%.

However, the NRMSE values for temperature and pressure were low, see Table 3. The large discrepancy in the RH results can be attributed to the large fluctuation of the results due to solar radiation. Fig. 13 and Fig. A2 show that the trend lines of the results are compatible, but the difference appears in the magnitude of the fluctuation of the results. A close look at the results of type 4 test walls (EW 42, externally insulated with mineral wool) shows that in late spring (between 7 and May 21, 2018), the model estimates the magnitude of the variation in the results of the north-facing wall correctly, but the results show a shift in fluctuation (Fig. 14 a). The south-facing wall model estimates the fluctuation correctly, but the measurement results show a greater effect of solar radiation. In other words, the daily extremes of the measurement results

are higher than in the simulation (Fig. 14 b). In winter (between 10 and December 24, 2018), the model underestimates the RH results by up to 5% (Fig. 15). The combination of two factors could have caused a large discrepancy during the cold period. First, the sensitivity analysis for finding the air exchange rate of the ventilation gap showed that the air exchange has an effect on the RH at L3. Second, there was also a larger difference between the temperature measurement and the simulation results between the CLT and the insulation (L2) during winter, see Fig. 16. This suggests that the thermal resistance of the insulation may have been lower than expected. The heat flow was measured on the walls during field measurements, but due to the technical problems of the measuring device, the analysis of the results was incomplete.

At location L1, there were also some large discrepancies in the results, see Fig. 17 and Fig A3. The biggest difference was in the RH and P_v results in type 5 walls with high CLT initial MC (EW 51), see Fig. 17 a, b and Table 3. RH results of type 5 southern wall in Fig. 14 b show that above RH 80%, the measurement results are compatible with the simulation and below 80%, the simulated results keep a stable line, but the measurement results have dropped sharply. This suggests that there were small air leakages through the vapour barrier, which created uncertainty in the creation of the simulation model. The models of the other walls of type 5 also predicted a more stable result than the measurement results showed, but since the simulation results showed a higher RH, this is the safe side for the models (Fig. 14 a, c, d).

4. Discussion

Our results showed that the studied CLT external walls were hygrothermally in the safe range in the observed cold and humid climate. The CLT, which is a load-bearing element, has the following additional properties: sufficient control of water vapour diffusion, relatively low thermal conductivity, suitability to the interior as an open finishing element. Also, the CLT can be insulated both with vapour permeable and low permeable thermal insulation materials without causing any critical moisture damage risk. High insulation (thermal transmittance of the walls $U = 0.1 \text{ W}/(\text{m}^2 \cdot \text{K})$) caused no water vapour condensation or mould growth risk on the surface of the wind barrier in any wall. High thermal resistance, low water vapour resistance and sufficient thickness of the mineral wool wind barrier prevented the risk of condensation and mould growth effectively. Also, covering the CLT with both vapour permeable and low permeable interior layers posed no risk of mould growth during the field measurements. Nevertheless, based on the results of this work, the key factors in terms of hygrothermal performance were sufficient dry-out capacity and high initial moisture content. The orientation (north and south) of the walls was found to have no significant effect on the hygrothermal performance of the studied external walls with outdoor ventilated façade.

As expected, the field measurements showed that water vapour permeable insulation materials (mineral wool and cellulose insulation) provide a sufficient dry-out capacity and at high MC, CLT dried out without posing any moisture damage risk. At the same time, the use of cellulose insulation showed a clear advantage over mineral wool, demonstrating a more stable and lower RH fluctuation. The effect of moisture buffering of cellulose insulation was proved by the lowest moisture accumulation (lowest RH at the beginning of the measurement period) between the insulation and the CLT in the walls with soaked CLT panels. Thus, the results of this work confirmed conclusions by Pihelo et al. [13] and Ojanen et al. [14] that the use of cellulose stabilizes high moisture fluctuations of indoor air and can prevent the risk of moisture damage better than mineral wool. Therefore, cellulose insulation is a safer choice when selecting water vapour permeable insulation for the

external wall. It is preferable in particular for constructions planned without weather protection and with the CLT exposed to water contact (rain, snow) or if large fluctuations of moisture excess levels in indoor air are expected in the indoor environment during the time of use.

The most unexpected results were obtained from the test walls insulated with PIR insulation. The preliminary simulation of factory dry CLT (MC $\approx 13\%$) with only moisture diffusion (without outdoor air leakage) showed a stable and low RH (almost constant), varying between 40 and 60%, between the insulation and the CLT. Walls with a high CLT MC were assumed to accumulate moisture on the CLT surface next to the insulation and pose a risk of moisture damage. Field measurements, on the other hand, showed similar RH results as the walls insulated with vapour permeable insulations caused by a small air exchange connected to the outdoor environment. Small air exchange did not cause or pose any moisture damage risk during the field measurements of our study. According to previous studies, the CLT loses airtightness after exposure to water [33] or having three layers [34,35], and air leakage as an exfiltration may cause moisture damages [36]. This shows that the airtightly installed insulation can be beneficial if the low moisture content of the CLT panel (factory dry) during construction is maintained. The effect of larger (outdoor and indoor) air leakage on the hygrothermal performance of the CLT external wall externally insulated with low vapour permeable PIR insulation needs further investigation.

The use of water low vapour permeable inner layer (vapour barrier film) posed no risk of mould growth. However, in walls with high CLT MC, moisture accumulated between the CLT and the vapour barrier film during dry-out. Although the risk of mould growth was not indicated by the accumulation of moisture, the dry-out time of CLT was long, almost 3 months from the start of the measurement period, because of the smaller dry-out potential. The probability of mould growth risk may be high at higher moisture loads (higher indoor excess moisture level or greater initial MC of CLT). In contrast, when water vapour permeable clay plaster was used as the internal layer, no large moisture accumulation occurred in the walls even at high initial CLT MC. Kukk et al. have previously been found that the risk of mould growth can occur even at an MC of CLT of 17% (evenly distributed through the cross-section of CLT) when using low vapour permeable interior thermal insulation [23]. They used a critical moisture reference year [37] in their calculations and selected summer as the starting period for the simulation when the dry-out period of CLT can be much longer due to the significantly higher water vapour content in the outdoor air compared to winter. This study only considered the high MC ($\approx 26\%$) in the CLT surface and used measured climate conditions (measured during the field measurements) as the boundary conditions, which were less critical in terms of the moisture damage risk compared to the reference year. Also, field measurements of this study started in the winter. In conclusion, the probability of failure (risk of mould growth on the CLT surface) when using low vapour permeable layers in the CLT external wall assembly must be determined by stochastic analysis using a variety of influencing parameters, for example, the initial moisture content and its distribution in the CLT panel, material properties, dimensions, etc. However, water vapour permeable layers are well suited for covering the CLT from the inside.

Only few external wall models showed an absolute mean difference lower than the measuring sensor accuracy. In contrast, the vast majority of NRMSE results in the comparison of the measurement and simulation results were $\leq 10\%$ and the majority $\leq 5\%$. Several studies have used up to 10–15% NRMSE scale to evaluate the accuracy of simulation models [38–40]. The largest discrepancies in the measured and simulated RH results were between the insulation and the wind barrier (at location L3). Discrepancies occurred also in the RH and P_v results between the

low vapour permeable layer and the CLT (type 3 walls between insulation and CLT (L2) and type 5 walls between the interior vapour barrier and the CLT (L1)). Based on the reasons for the discrepancies, limitations of our study were determined. One of the limitations is that the air exchange in the ventilation gap of the façade was not measured. The sensitivity analysis of the air exchange showed that the rate of the air exchange affects significantly the RH results between the wind barrier and the insulation. This is one of the reasons why the RH fluctuations caused by solar radiation were not estimated at high accuracy by the model. Larger discrepancies between the water low vapour permeable layers and the CLT were caused by air leakages. The limitations here are small side dimensions of the test walls; the use of low water vapour permeable materials in the CLT external walls could be studied in the future on a much larger scale. The impact of air and vapour leakages is smaller in larger-scale walls. Based on the NRMSE results in general and on the comparison of the measurement results and the simulation trend lines, it can be concluded that the created models are sufficiently adequate and can be used in the future research.

The focus in this research was only on the exterior wall, and hygrothermal calculations were performed with 1D simulation models. However, several studies have indicated that the most problematic locations are the joint areas, especially the foundation and the external wall joint [6,41]. Therefore, future research should focus on the impact of wet CLT dry-out on the hygrothermal performance of a particular 2D joint. Another important issue is the airtightness of the CLT envelope. Several studies have shown that CLT alone may not perform as an airtight layer [33–35]. Therefore, future studies should also focus on the impact of an additional vapour tightness (for airtightness purpose) on the hygrothermal performance of the CLT envelope.

5. Conclusions

The impact of high levels of insulation with different insulation materials (vapour permeable mineral wool and cellulose insulation and low vapour permeable PIR insulation), vapour permeable and low permeable internal layers, and dry-out of construction moisture on the hygrothermal performance of CLT external walls was evaluated by field measurements. In addition, simulation models were created and validated based on the field measurements. Our conclusions are as follows:

- Field measurement of our study showed that the designed CLT external walls performed hygrothermally in the safe range in the observed cold and humid climate. The CLT panel is capable of sufficient water vapour diffusion control. The RH between the exterior high insulation and the wind barrier varied between 15 and 95%. The high levels of insulation (thermal transmittance of $U = 0.1 \text{ W}/(\text{m}^2 \cdot \text{K})$) in the studied external walls and indoor humidity load for office and low occupancy dwellings (moisture excess of $\Delta v_{te} \leq 0^\circ\text{C} = 3 \text{ g}/\text{m}^3$) in the cold period did not cause critical moisture (condensation or mould growth) risk on the interior surface of wind barrier. This was partially prevented by the high thermal resistance and low water vapour resistance of the wind barrier.
- Mould growth risk calculations based on measured hygrothermal conditions showed that the high moisture content in the thin surface layer of the CLT panel may not be critical when dry-out time is short. The probability of failure must be determined by stochastic analysis using a variety of influencing parameters, for example, the initial moisture content and its distribution in the CLT panel, material properties, dimensions, etc.
- The comparison of walls with vapour permeable insulation showed that the use of cellulose insulation compared to mineral wool has the advantage of keeping RH at a lower level between the exterior insulation and the wind barrier (cellulose RH up 90% vs mineral

wool RH up 95%). Therefore, cellulose insulation can be a safer choice from point of view of hygrothermal performance when selecting water vapour permeable insulation for the external wall.

- The simulation of factory dry CLT ($MC \approx 13\%$) with only moisture diffusion (without outdoor air leakage) showed a stable and low RH, varying between 40 and 60%, between the CLT and the low vapour permeable external insulation (PIR). Field measurements detected a minor air circulation with the outdoor air between the PIR insulation and the CLT that increased significantly the RH fluctuations on the exterior surface of the CLT (up to 75%) and the interior surface of the wind barrier (up to 95%). This shows that the airtightly installed insulation can be beneficial if the low moisture content of the CLT panel (factory dry) during construction is maintained. The effect of larger (outdoor and indoor) air leakage on the hygrothermal performance of the CLT external wall externally insulated with low vapour permeable PIR insulation needs further investigation.
- The orientation (north and south) of the walls was found to have no significant effect on the hygrothermal performance of the studied external walls with outdoor ventilated façade.
- In the comparison of the measurement and simulation results, the vast majority of normalized root mean square error (NRMSE) result were $\leq 10\%$ and majority $\leq 5\%$. The largest discrepancies in the measured and simulated RH results were between the exterior insulation and the wind barrier (NRMSE between 8% and 19%). The limitation of using constant air exchange rate in the ventilation gap of the façade instead of measured values decreased the accuracy of the model in the estimation of the RH fluctuations caused by solar radiation. Large discrepancies were also observed behind low vapour permeable insulation and the interior layer (NRMSE between 7% and 28%). The field measurement results behind low vapour permeable layers were greatly affected by outdoor air leakage, which made it difficult to evaluate the accuracy of the simulation models. Therefore, the limitation of the work is also in small side dimensions of the test walls. The impact of air leakages is smaller in larger-scale walls. Based on the NRMSE results in general and trend line comparison of the results, the created models can be considered sufficiently adequate for use in future research.
- Future research on the hygrothermal performance of the CLT envelope should focus on
 - the impact of initial CLT moisture content in the 2D joints of building envelope
 - the impact of an additional vapour tightness (product or material for airtightness purpose) located between the exterior insulation and the CLT panel.

Declaration of competing interest

The authors declare that they have no known competing financial interests or personal relationships that could have appeared to influence the work reported in this paper.

Acknowledgments

This research was supported by the Estonian Research Council with Personal research funding PRG483 “Moisture safety of interior insulation, constructional moisture, and thermally efficient building envelope”, Estonian Centre of Excellence in Zero Energy and Resource Efficient Smart Buildings and Districts, ZEBE, grant TK146 funded by the European Regional Development Fund and by the European Commission through the H2020 project Finest Twins (grant No. 856602). The author wishes to thank Estonian glulam producer Peetri Puit OÜ for supplying CLT specimens.

Appendices.

Appendix 1

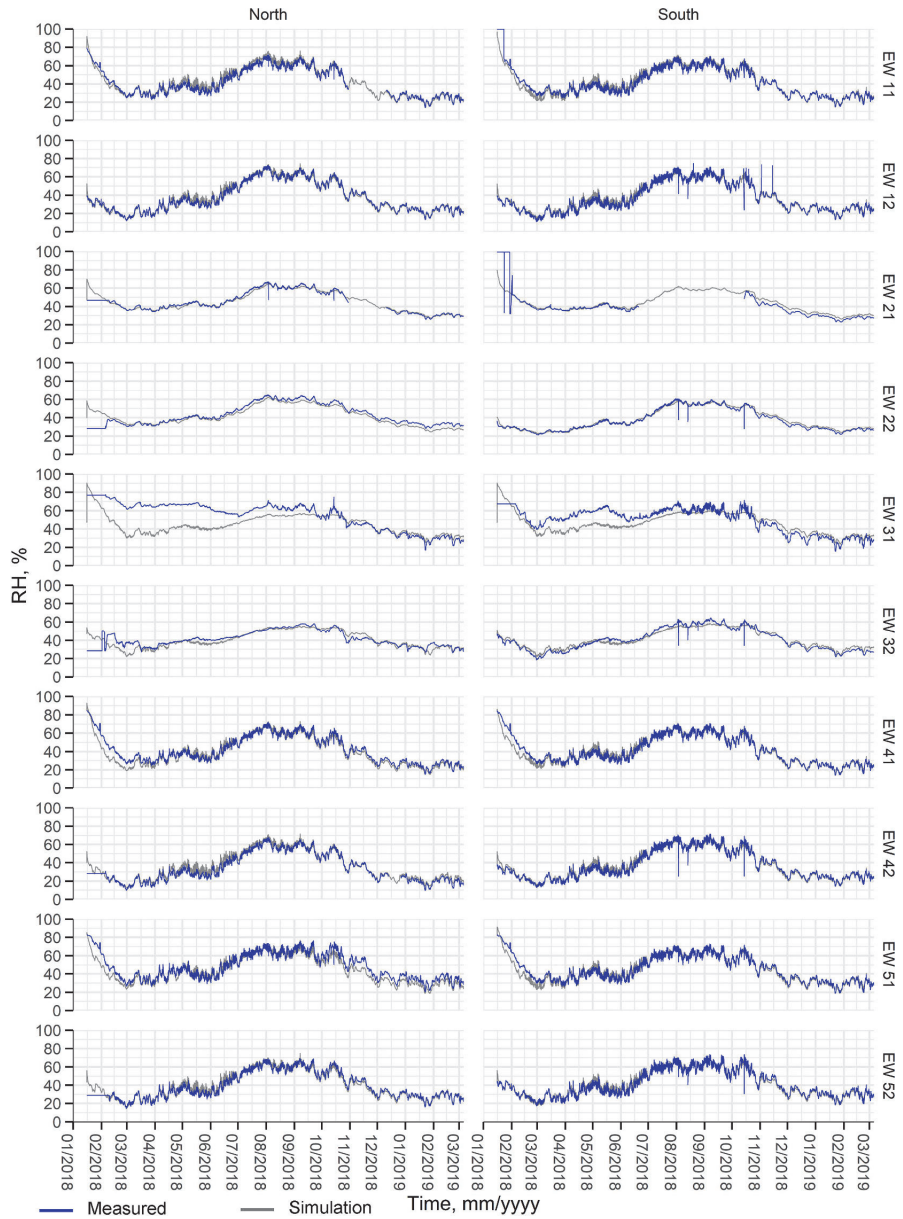


Fig. A.1. Measured and calculated RH between the CLT and the insulation (L2).

Appendix 2

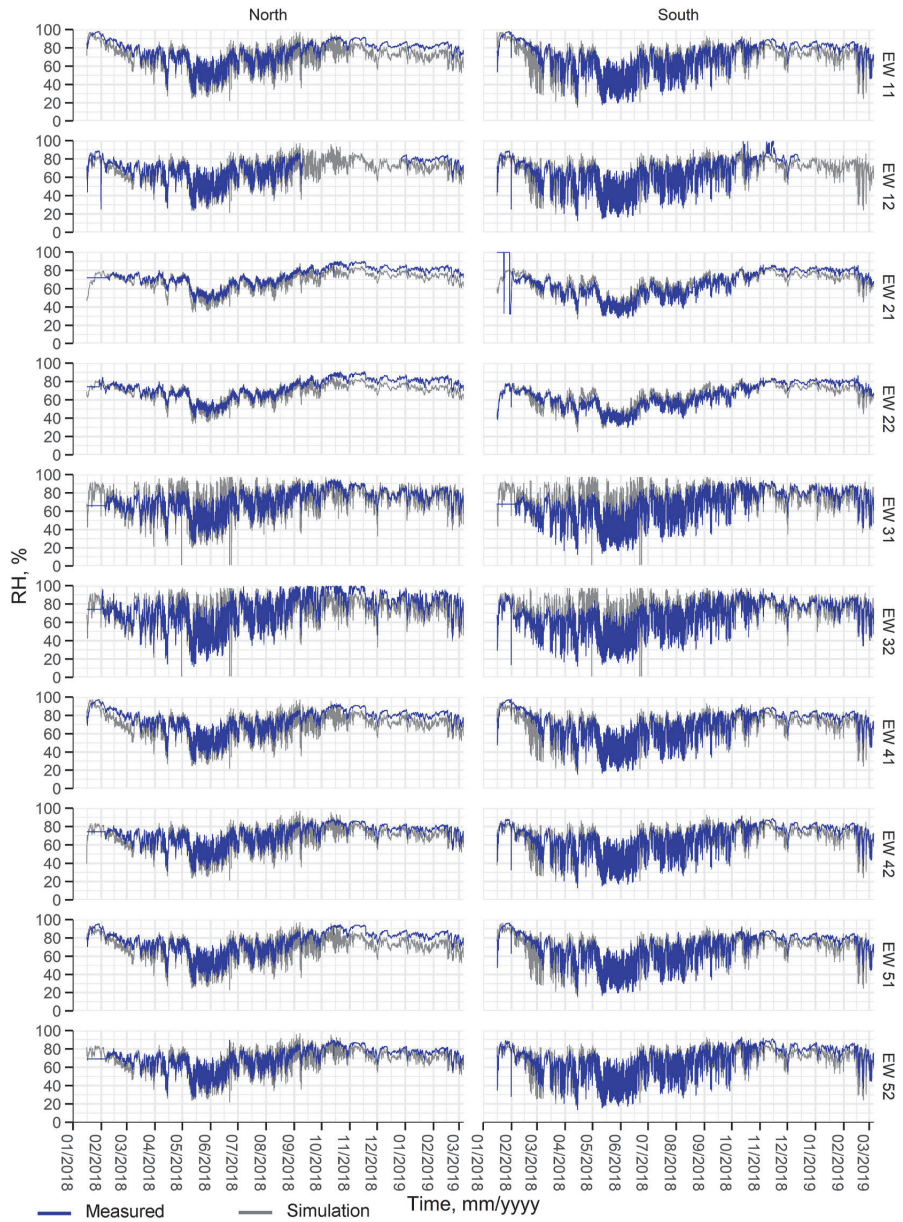


Fig. A.2. Measured and calculated RH between the insulation and the wind barrier (L3).

Appendix 3

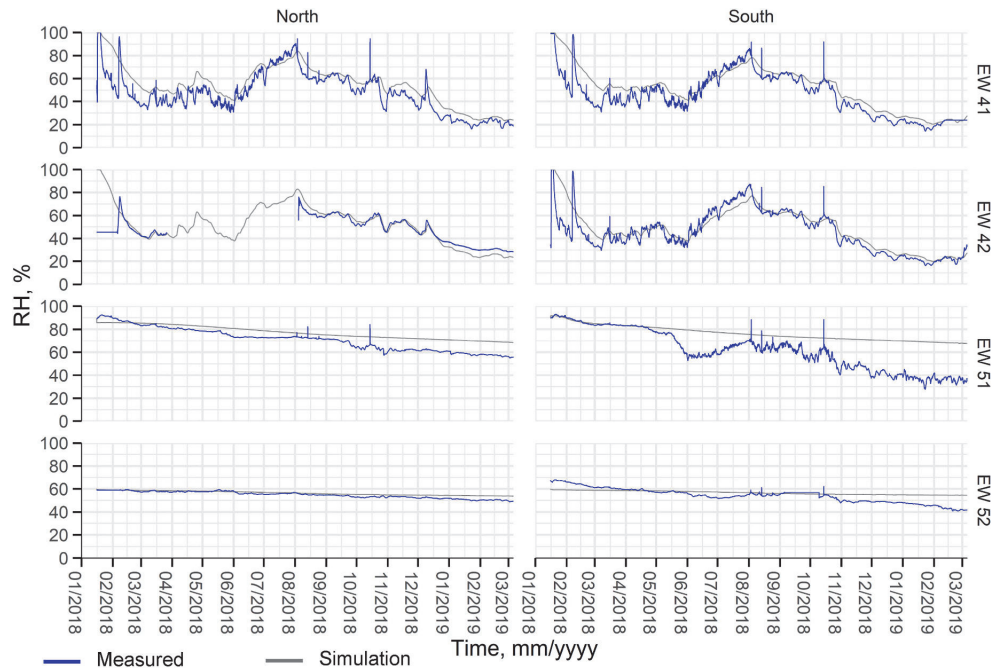


Fig. A.3. Measured and calculated RH between the CLT and the internal layer (L1).

References

- [1] EN 16351:2015 Timber Structures - Cross Laminated Timber - Requirements, 2015.
- [2] K. Mjörnell, L. Olsson, Moisture safety of wooden buildings – design, construction and operation, *J. Sustain. Architect. Civ. Eng.* 24 (2019) 29–35, <https://doi.org/10.5755/j01.sace.24.1.22341>.
- [3] L. Olsson, Moisture safety in CLT construction without weather protection – case studies, literature review and interviews, in: *E3S Web Conf.*, EDP Sciences, 2020, p. 10001, <https://doi.org/10.1051/E3SCONF/202017210001>.
- [4] J. Niklewski, M. Fredriksson, T. Isaksson, Moisture content prediction of rain-exposed wood: test and evaluation of a simple numerical model for durability applications, *Build. Environ.* 97 (2016) 126–136, <https://doi.org/10.1016/j.buildenv.2015.11.037>.
- [5] E. Liisma, B.L. Kuus, V. Kukk, T. Kalamees, A case study on the construction of a clt building without a preliminary roof, *J. Sustain. Architect. Civ. Eng.* 25 (2019), <https://doi.org/10.5755/j01.sace.25.2.22263>.
- [6] K. Kalbe, V. Kukk, T. Kalamees, Identification and improvement of critical joints in CLT construction without weather protection, *E3S Web Conf.* 172 (2020) 10002, <https://doi.org/10.1051/e3sconf/202017210002>.
- [7] L. Wang, J. Wang, H. Ge, Wetting and drying performance of cross-laminated timber related to on-site moisture protections: field measurements and hygrothermal simulations, *E3S Web Conf.* 172 (2020) 10003, <https://doi.org/10.1051/E3SCONF/202017210003>.
- [8] L. Olsson, K. Mjörnell, Laboratory investigation of sills and studs exposed to rain, in: *Proc. 5th Int. Build. Phys. Conf.*, IBPC 2012, Kyoto, 2012.
- [9] E.L. Schmidt, M. Riggio, A.R. Barbosa, I. Mugabo, Environmental response of a CLT floor panel: lessons for moisture management and monitoring of mass timber buildings, *Build. Environ.* 148 (2019) 609–622, <https://doi.org/10.1016/j.buildenv.2018.11.038>.
- [10] G.W. Reinberg, T. Mauring, K. Kalbe, J. Hallik, First certified passive house in Estonia, in: *Proc. 17th Int. Passiv. House Conf.*, Passivhaus Institut Darmstadt, Frankfurt, Germany, 2013.
- [11] T. Kalamees, L. Paap, K. Kuusk, T. Mauring, J. Hallik, M. Valge, K. Kalbe, A. H. Tkaczyk, The first year's results from the first passive house in Estonia, in: J. Arfvidsson, L.-E. Harderup, A. Kumlin, B. Rosencrantz (Eds.), *Proc. 10th Nord. Symp. Build. Phys.*, 15–19 June 2014, pp. 758–765. Lund, Sweden.
- [12] L. Wang, H. Ge, Stochastic modelling of hygrothermal performance of highly insulated wood framed walls, *Build. Environ.* 146 (2018) 12–28, <https://doi.org/10.1016/J.BUILDENV.2018.09.032>.
- [13] P. Pihelo, H. Kikkas, T. Kalamees, Hygrothermal performance of highly insulated timber-frame external wall, *Energy Proc.* 96 (2016) 685–695, <https://doi.org/10.1016/J.EGYPRO.2016.09.128>.
- [14] T. Ojanen, J. Laaksonen, Hygrothermal performance benefits of the cellulose fiber thermal insulation structures, in: 41st IAHS Int. Assoc. Hous. Sci. World Congr. - Sustain. Build., 2016. Coimbra, <http://www.iahs2016.uc.pt/projectos/iahs2016/atas/pdfs/ID110.pdf>. (Accessed 27 October 2021).
- [15] R. McClung, H. Ge, J. Straube, J. Wang, Hygrothermal performance of cross-laminated timber wall assemblies with built-in moisture: field measurements and simulations, *Build. Environ.* 71 (2014) 95–110, <https://doi.org/10.1016/J.BUILDENV.2013.09.008>.
- [16] L. Wang, H. Ge, Hygrothermal performance of cross-laminated timber wall assemblies: a stochastic approach, *Build. Environ.* 97 (2016) 11–25, <https://doi.org/10.1016/j.buildenv.2015.11.034>.
- [17] H. Viitanen, T. Ojanen, R. Peuhkuri, J. Vinha, Mould growth modelling to evaluate durability of materials, in: M.L. Vasco Peixoto de Freitas, Helena Corvacho (Eds.), XII DBMC 12th Int. Conf. Durab. Build. Mater. Components, 12th - 15th April 2011, Porto, Port., FEUP Edicoes (Faculdade de Engenharia da Universidade do Porto Edicoes), Porto, 2011, pp. 409–416.
- [18] H.M. Cho, S. Wi, S.J. Chang, S. Kim, Hygrothermal properties analysis of cross-laminated timber wall with internal and external insulation systems, *J. Clean. Prod.* 231 (2019) 1353–1363, <https://doi.org/10.1016/J.JCLEPRO.2019.05.197>.
- [19] J. Yoo, S.J. Chang, S. Yang, S. Wi, Y.U. Kim, S. Kim, Performance of the hygrothermal behavior of the CLT wall using different types of insulation; XPS, PF board and glass wool, *Case Stud. Therm. Eng.* 24 (2021) 100846, <https://doi.org/10.1016/j.csre.2021.100846>.
- [20] G. Alsayegh, Hygrothermal Properties of Cross Laminated Timber and Moisture Response of Wood at High Relative Humidity, Carleton University, 2012. https://curve.carleton.ca/system/files/etd/e7ba278b-c830-463d-ad47-5f98ea309c22/etd_pdf/ca740d27547d38a996fe4281c15c98ca/alsayegh-hygrothermalpropertiesofcrosslaminatedtimber.pdf.
- [21] M. Byttebier, Hygrothermal Performance Analysis of Cross-Laminated Timber (CLT) in Western Europe, KU Leuven, 2018. [file:///C:/Users/admin/OneDrive/project air permeability/Material/Air permeability properties of the CLT/1718_Thesis_MarcosByttebier.pdf](file:///C:/Users/admin/OneDrive/project%20air%20permeability/Material/Air%20permeability%20properties%20of%20the%20CLT/1718_Thesis_MarcosByttebier.pdf).
- [22] S. Kordziel, S.V. Glass, C.R. Boardman, R.A. Munson, S.L. Zelinka, S. Pei, P. C. Tabares-Velasco, Hygrothermal characterization and modeling of cross-laminated timber in the building envelope, *Build. Environ.* 177 (2020) 106866, <https://doi.org/10.1016/J.BUILDENV.2020.106866>.

- [23] V. Kukk, A. Külaots, J. Kers, T. Kalamees, Influence of interior layer properties to moisture dry-out of CLT walls, *Can. J. Civ. Eng.* 46 (2019) 1001–1009, <https://doi.org/10.1139/cjce-2018-0591>.
- [24] V. Kukk, R. Horta, M. Püssa, G. Luciani, H. Kallakas, T. Kalamees, J. Kers, Impact of cracks to the hygrothermal properties of CLT water vapour resistance and air permeability, *Energy Proc.* 132 (2017) 741–746, <https://doi.org/10.1016/j.egypro.2017.10.019>.
- [25] V. Kukk, J. Kers, T. Kalamees, Hygrothermal performance of mass timber wall assembly with external insulation finish system, in: *Proc. Build. XIV Int. Conf., ASHRAE, Clearwater, FL, 2019*, pp. 599–607.
- [26] R. Lipand, V. Kukk, T. Kalamees, Capillary Movement of Water in a Radial Direction and Moisture Distribution in a Cross-Section of CLT Panel, *Tallinn University of Technology*, 2021.
- [27] S. Ilomets, T. Kalamees, J. Vinha, Indoor hygrothermal loads for the deterministic and stochastic design of the building envelope for dwellings in cold climates, *J. Build. Phys.* 41 (2017) 547–577, <https://doi.org/10.1177/1744259117718442>.
- [28] H. Viitanen, T. Ojanen, Improved Model to Predict Mold Growth in Building Materials, 2007.
- [29] T. Ojanen, H. Viitanen, R. Peuhkuri, K. Lähdesmäki, J. Vinha, K. Salminen, Mold growth modeling of building structures using sensitivity classes of materials, in: *Therm. Perform. Exter. Envel. Build. XI, ASHRAE, Florida, 2010*.
- [30] J. Straube, G. Finch, Ventilated wall claddings: review, field performance, and hygrothermal modeling, in: *Therm. Perform. Exter. Envel. Whole Build. 2008, ASHRAE, Clearwater, Florida, 2008*.
- [31] J. Falk, K. Sandin, Ventilated rainscreen cladding: measurements of cavity air velocities, estimation of air change rates and evaluation of driving forces, *Build. Environ.* 59 (2013) 164–176, <https://doi.org/10.1016/j.buildenv.2012.08.017>.
- [32] C.-E. Hagentoft, *Introduction to Building Physics*, Studentlitteratur AB, 2001.
- [33] V. Kukk, A. Bella, J. Kers, T. Kalamees, Airtightness of cross-laminated timber envelopes: influence of moisture content, indoor humidity, orientation, and assembly, *J. Build. Eng.* 44 (2021) 102610, <https://doi.org/10.1016/j.jobbe.2021.102610>.
- [34] V. Kukk, T. Kalamees, J. Kers, The effects of production technologies on the air permeability and crack development of cross-laminated timber, *J. Build. Phys.* (2019), <https://doi.org/10.1177/1744259119866869>, 1744259119866869.
- [35] B. Time, Climate adaptation of wooden buildings – risk reduction by moisture control, in: *Proc. 12th Nord. Symp. Build. Phys., NSB 2020*, Tallinn, 2020.
- [36] T. Kalamees, J. Kurnitski, Moisture convection performance of external walls and roofs, *J. Build. Phys.* 33 (2010) 225–247, <https://doi.org/10.1177/1744259109343502>.
- [37] T. Kalamees, J. Vinha, Estonian climate analysis for selecting moisture reference years for hygrothermal calculations, *J. Therm. Envelope Build. Sci.* 27 (2004) 199–220, <https://doi.org/10.1177/1097196304038839>.
- [38] A. Tijskens, S. Roels, H. Janssen, Neural networks to predict the hygrothermal response of building components in a probabilistic framework, in: *Int. Build. Phys. Conf., 2018*, <https://doi.org/10.14305/ibpc.2018.ms-6.04>. Syracuse, NY. (Accessed 13 November 2021).
- [39] Y. Cui, Y. Zhang, H. Janssen, EMPD-based moisture buffering quantification with moisture-dependent properties (I): modelling and simulations, *Build. Environ.* 205 (2021) 108266, <https://doi.org/10.1016/j.buildenv.2021.108266>.
- [40] M. Magni, F. Ochs, S. de Vries, A. Maccarini, F. Sigg, Detailed cross comparison of building energy simulation tools results using a reference office building as a case study, *Energy Build.* 250 (2021) 111260, <https://doi.org/10.1016/j.enbuild.2021.111260>.
- [41] F. Fedorik, A. Haapala, Impact of air-gap design to hygro-thermal properties and mould growth risk between concrete foundation and CLT frame, *Energy Proc.* 132 (2017) 117–122, <https://doi.org/10.1016/j.egypro.2017.09.656>.

PUBLICATION VI

Kukk, V.; Kers, J.; Kalamees, T.; Wang, L.; Ge, H., 2022. Designing highly insulated cross-laminated timber external walls in terms of hygrothermal performance: A stochastic approach. *Building and Environment* (Submitted 21.03.2022, Under review).

Designing highly insulated cross-laminated timber external walls in terms of hygrothermal performance: a stochastic approach

Villu Kukk^{*1}, Jaan Kers², Targo Kalamees^{1,5}, Lin Wang³ and Hua Ge⁴

¹Tallinn University of Technology, nZEB research group

²Tallinn University of Technology, Laboratory of Wood Technology

³National Research Council Canada, Institute for Research in Construction

⁴Concordia University, Department of Building, Civil and Environmental Engineering

⁵Tallinn University of Technology, FinEst Center for Smart Cities (Finest Centre)

Abstract: In terms of hygrothermal performance, solid wood panels such as cross-laminated timber (CLT) are sensitive to moisture. However, no clear indication of critical moisture conditions for CLT envelopes exist regarding to moisture content. Therefore, our main objective in this study was to set hygrothermal criteria for the design of CLT external walls in terms of moisture conditions using a stochastic approach. The focus is on five different types of CLT external walls that differ in their dry-out. The key factors in safe hygrothermal design of the CLT external envelope are sufficient dry-out capacity and control of the CLT moisture content level during the construction phase. It was found that the vapour resistance (S_d) of the wind barrier should not exceed 0.03 m; the CLT initial moisture content of the external surface should not exceed 20% or the vapour resistance (S_d) of an additional air and vapour barrier should not exceed 0.25 m if the CLT envelope is not fully weather protected and is externally insulated with vapour open materials. In the case of vapour tight external or internal insulation, initial moisture content of the CLT surface should not exceed 16% to prevent mould growth risk.

Keywords: Cross-laminated timber, CLT, moisture safety, stochastic approach, hygrothermal performance, hygrothermal criteria

1 Introduction

A cross-laminated timber (CLT) panel is a multi-layer wooden composite structure of softwood lumber produced at least of three orthogonally bonded layers [1]. According to studies, CLT structures get soaked during construction if full weather protection is not implemented [2–7]. Most critical locations are structural joints where water is absorbed at the longitudinal fibre direction from the cut-edge of the panel and the moisture content (MC) can increase up to 30% [6,8]. Such solid wood panels as CLT are sensitive to moisture in their hygrothermal performance. Exposure to moisture can lead to growth of mould and rot on the CLT surface. Mould is harmful to human health [9,10], and rot damages the mechanical properties of wood [11]. However, it has been argued that no clear indication of the critical moisture conditions for CLT envelopes related to moisture content exist [12,13].

Several studies have addressed the hygrothermal performance of CLT external envelopes using different wall configurations, evaluation criteria, and methodologies (field measurements vs. simulations). McClung et al. [14] and Wang and Ge [15] used both field measurements and stochastic analysis to analyse low and high water vapour permeable wall assemblies with built-in moisture dry-out. Their evaluation is based on a certain level of MC alone, to find out whether the results exceeded 20% (growth of mould) or < 26% (growth of decay) without determining actual mould or decay risk. Cho et al. [16], Yoo et al. [17], Al-Sayegh [18], Bytbeier [19], and Kordziel et al. [20] evaluated the hygrothermal performance of the CLT external envelope only in a stationary situation, without considering any soaking scenarios of CLT. Kukk et al. [21–23] focused on the hygrothermal performance of CLT external walls in regard to the wetting of the panel and using a mould growth index in the evaluation of the performance. However, only few specific

* Corresponding author.

E-mail address: villu.kukk@taltech.ee

Postal address: Ehitajate tee 5, 19086 Tallinn, Estonia

wall assemblies and few variables were used in their analyses. In general, the previous studies on the hygrothermal performance of CLT external envelopes have not clearly indicated the critical moisture conditions for CLT external walls, which confirms the need to determine the hygrothermal criteria.

Therefore, our main objective was to set limit values as hygrothermal criteria for the design of CLT external walls in terms of moisture conditions using a stochastic approach to ensure safe hygrothermal performance. Hygrothermal performance was evaluated by simplified 1D validated calculation models based on the field measurements [13] of CLT test walls that were prefabricated and installed into the nZEB technological test facility on the campus of Tallinn University of Technology, Tallinn, Estonia. Continuing our field measurements, we focused on the stochastic analysis of the designed CLT external wall types. The validated models are considered as base models. Hygrothermal calculations were performed with heat, air and moisture (HAM) modelling software Delphin 5.9, and stochastic analyses were done by MatLab platform.

2 Materials and methods

2.1 External walls

The focus of this study is on five types of CLT external walls (EW 1-5) that differ in terms of dry-out capacity – use of external insulation and interior layers with high and low water vapour permeability, see Fig. 3. Wall types were designed with a 5-layer 100 mm thick (5x20 mm) CLT panel, ventilated (ventilation gap 28 mm) wooden cladding (22 mm) façade, and a glass wool wind barrier (30 mm). Thermal transmittance was designed to be the same for all wall types ($U \approx 0.1 \text{ W}/(\text{m}^2\cdot\text{K})$) and therefore insulation thickness varied.

The first test wall type (EW 1) was insulated with a 300 mm thick glass wool insulation ($\lambda = 0.037 \text{ W}/(\text{m}\cdot\text{K})$) and the second (EW 2) with a 330 mm thick cellulose insulation ($\lambda = 0.041 \text{ W}/(\text{m}\cdot\text{K})$); both insulations allowed for CLT dry-out towards the outdoor and indoor environment. The third type (EW 3) was insulated with 200 mm thick polyisocyanurate (PIR) ($\lambda = 0.022 \text{ W}/(\text{m}\cdot\text{K})$), which prevents CLT from drying out towards the outside. The fourth wall type (EW 4) was externally insulated with 300 mm thick glass wool and covered with 20 mm clay plaster on the inside. CLT in wall type 4 can dry out towards the outdoor, but there is small resistance ($\mu_{\text{plaster}} = 15$) to drying towards the indoor. The fifth type of wall is also insulated with 300 mm thick glass wool, but is covered internally with high vapour resistance ($\mu_{\text{PIR}} = 60$) 30 mm thick PIR insulation.

2.2 Structure of stochastic analysis

2.2.1 Discrete random variables

Hygrothermal performance of each wall type was analysed by a stochastic approach using both discrete and continuous random variables, see Fig. 3. A method for stochastic approach developed by Wang and Ge [15] was used. For the discrete random variables, the thickness of CLT and the presence of an additional air and vapour barrier between the insulation and CLT with fixed water vapour resistance ($S_{\bar{a}} = 2.3 \text{ m}$) were used. Several studies have shown that dry-out of soaked CLT can cause significant air leakages [24–26]. One measure to ensure the airtightness of the CLT building envelope is to apply an additional air and vapour barrier on the external surface of the CLT panel. The water vapour resistance of the air and vapour barriers available in the market varies between 0.01-2.3 m [27,28]. Small vapour resistance allows the internal membrane to be used as weather protection during construction. This work investigates the impact of an additional air and vapour barrier with fixed vapour resistance on the hygrothermal performance of the CLT wall types studied.

CLT thicknesses of 100 mm, 150 mm and 200 mm were selected as the most typical use in CLT buildings. Based on discrete random variables, six different scenarios were generated for each wall type, see Fig. 3.

2.2.2 Uniformly distributed continuous random variables

Ranges of material properties as uniformly distributed continuous random variables are shown in Fig. 3. The thermal conductivity range of the insulation was selected according to the properties of different

insulation products most widely used in the CLT external wall design in Northern Europe. The insulation is generally optimized between thickness and price. Therefore, the range of thermal conductivity was selected between 0.033 and 0.037 W/m·K for mineral wool insulation, 0.04-0.045 W/m·K for cellulose and 0.022-0.024 W/m·K for PIR insulation. The water vapour resistance ranged from 1 to 1.5 for mineral wool, 1.5-2.5 for cellulose and 60-104 for PIR insulation. The range of thermal conductivity and vapour resistance of the wind barrier refers to the selection from vapour open ($\mu=1$) and low thermal conductivity (0.033 W/m·K) mineral wool to vapour tight ($\mu=10$) and high thermal conductivity (0.2 W/m·K) wind barrier, e.g., gypsum board. Material properties of insulation and wind barrier were taken from the HAM modelling software Delphin database and product certificates [29–33].

Most of the laboratory measurements of the CLT water vapour resistance have been described as an isothermal process where the resistance is inversely proportional to the RH [18,19,34,35]. The isothermal water vapour resistance of wood includes a combination of vapour diffusion and liquid conductivity. Vapour diffusion dominates the total moisture transport in the wood up to 60% RH, from where the conductivity of the liquid begins to dominate due to capillary condensation [36,37]. For our stochastic analysis, 10 pairs of vapour and liquid conductivity curves were created. The pairs were formed by the total moisture permeability derived from the measured isothermal vapour resistance, see Fig. 1. The ranges of water vapour resistance of CLT were selected according to the minimum and maximum measured values found in the literature [18,19,34,35].

The MC of CLT was considered as the equilibrium moisture content (EMC), which ranged from the factory-dry MC of the panel (13%) to the EMC of the wood fibre saturation point (28%). According to the measurements of Lipand [38], who experimentally determined the moisture distribution of CLT in contact with water, the MC of CLT surface varies in a depth of 30 mm, see Fig. 2. The MC of the internal (MC_{CLT_IS}) and external (MC_{CLT_ES}) surface was calculated separately as continuous random variables. All continuous random variables were uniformly distributed over 100 random numbers by Latin Hypercube Sampling.

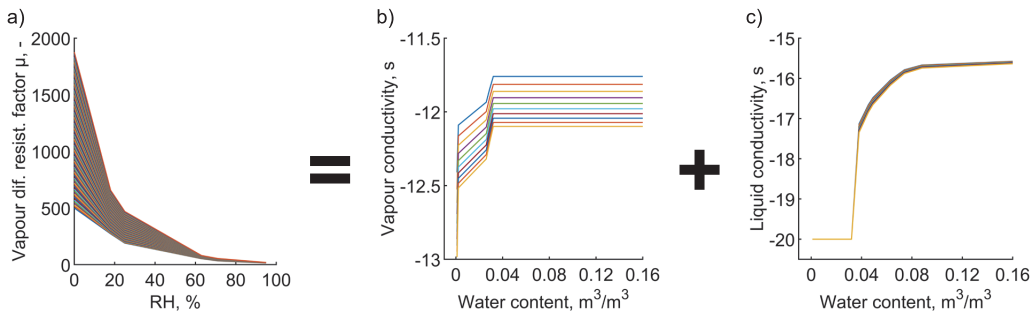


Fig. 1. Curves of the vapour diffusion resistance factors [18,19,34,35] evenly distributed (a) and derived pairs of vapour (b) and liquid (c) conductivity curves.

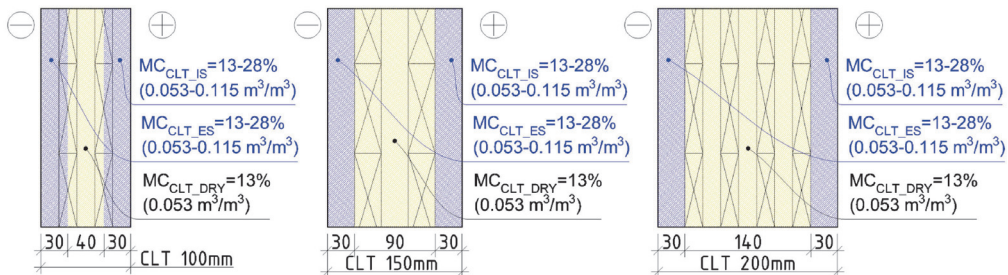
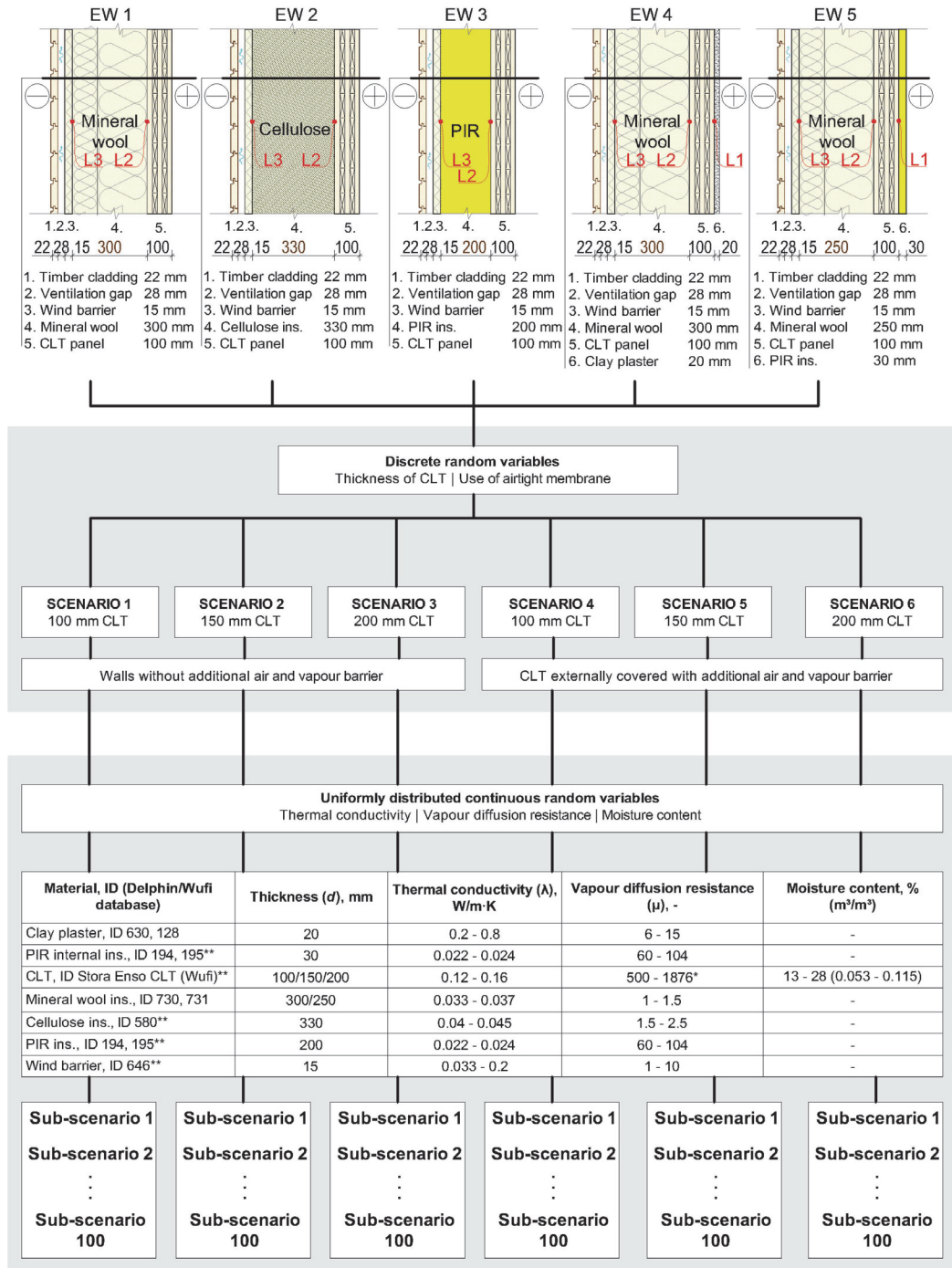


Fig. 2. MC distribution in the cross-section of CLT panels: variation in internal (MC_{CLT_IS}) and external (MC_{CLT_ES}) surface 13-28% to a depth of 30 mm and permanently dry (MC_{CLT_DRY}) 13% in the middle of the panel.



* at oven-dry state (0% MC)

**in addition, the material properties taken from laboratory measurement reports and the product sheet [18,19,29-33]

Fig. 3. Stochastic structure: cross-sections of CLT external test wall types as objects under study (upper), discrete random variables and the six main scenarios (middle), and continuous random variables (bottom).

2.2.3 Probability of hygrothermal performance

All six main scenarios based on the discrete random variables for each wall type (EW 1-5) included calculations of 100 different sub-scenarios based on the continuous random variables, making up a total of 3000 sub-scenarios, see Fig. 3. To calculate each sub-scenario, one value from each range of continuous random variables was randomly selected.

To evaluate the hygrothermal performance of each main scenario, the number of sub-scenarios that did not exceed the evaluation criteria (mould growth index $M < 1$, described in section 2.4) was counted and the probability of performance was calculated accordingly. The probability of hygrothermal performance was found using a total number of 100 of sub-scenarios as 100% of probability. For example, if 40 sub-scenarios exceeded the mould growth index 1, the probability of performance was considered to be 60%.

2.2.4 Partial correlation coefficient

A partial correlation coefficient (PCC) [39,40] was used to analyse the relationship between the continuous random variables (material properties) and the calculated mould growth index. PCC was found separately between one of the variables and the mould growth index, while controlling the rest of variables. The range of PCC is between 1 and -1 and the closer to 1 or -1 the PCC, the greater the impact of the observed variable is. A positive PCC value indicates a positive or increasing influence, i.e., the higher the value of observed variable, the higher is the value of its relative variable and vice versa. PCC values between an observed variable and the mould growth index > 0.5 or < -0.5 were considered as significant, otherwise insignificant influence.

2.3 Boundary conditions

Indoor and outdoor climate data were set as boundary conditions. Indoor temperature was calculated using the indoor temperature model for dwellings with central heating ($t_{i, central heating}$) [41], see Fig. 4 a. The indoor temperature model operates on the basis of equation 1.

$$t_{i, central heating} = \begin{cases} t_e \leq +10^\circ C \Rightarrow t_i = 22^\circ C \\ t_e > +10^\circ C \Rightarrow t_i = 0.3333 \cdot t_e + 18.667^\circ C \end{cases} \quad (1)$$

where t_e is an external temperature. The indoor RH was calculated on the basis of the indoor temperature and the moisture excess, see Fig. 4 b. The indoor humidity model was used to calculate the indoor moisture excess that stands for ventilated occupational and living spaces with a population density more than 30 m² per person [41]. The moisture excess by the model is 4 g/m³ at an indoor temperature below 0 °C and 1 g/m³ at an indoor temperature above +20 °C.

Estonian moisture reference year (MRY) for evaluating mould growth risk was used for the external climatic boundary conditions. MRY is a real year, which was selected by analysing Estonian climate data from 1970 to 2000 [42]. MRY includes outdoor RH (Fig. 5, a), temperature (Fig. 5, b), diffuse (Fig. 5, c) and direct (Fig. 5, d) shortwave radiation on a horizontal area, rainfall intensity (Fig. 5, e), and wind velocity (Fig. 5, f) and direction. Orientation of the walls in the stochastic calculations was set to 0 degrees (North) and the latitude was set to 59.4 degrees (latitude of Tallinn, Estonia). Air change rate in the ventilation gap was assigned as a constant value of 150 1/h (0.1 m/s) [13,43]. The hygrothermal simulations were running repeatedly over a period of five years, which is in favour to the safe side, as in practice it is rather unlikely that the critical MRY for mould growth will be repeated for such a long time. Air and rain leakages were not considered in the hygrothermal calculations.

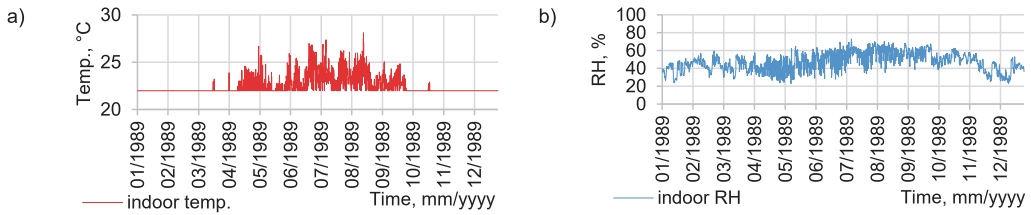


Fig. 4. Indoor temperature (a) and RH (b).

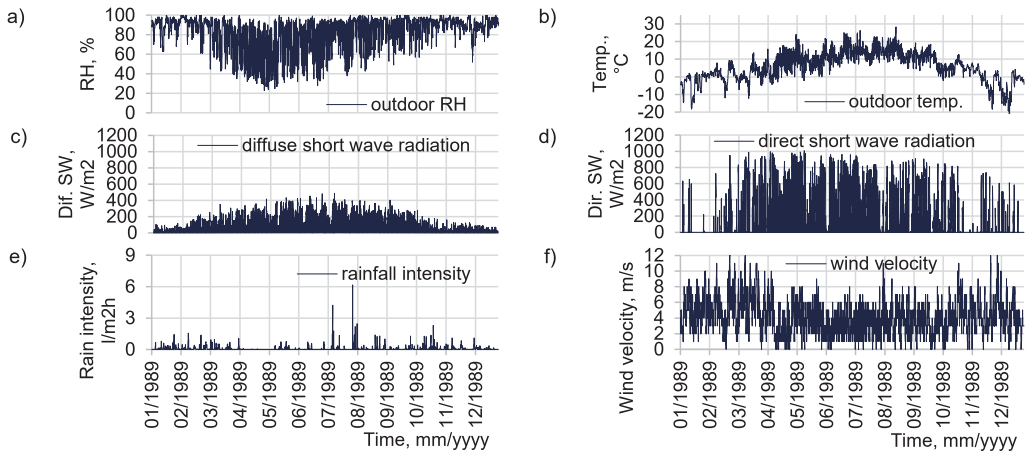


Fig. 5. MRY outdoor RH (a), temperature (b), diffuse (c), and direct (d) shortwave radiation on a horizontal area, vertical rain density (e), and wind velocity (f).

2.4 Evaluation criteria

The hygrothermal performance of each wall assembly was evaluated by the risk of mould growth on the interior (L1) and the exterior (L2) surface of CLT and on the interior surface of the wind barrier (L3), see Fig. 3. The mould growth risk was evaluated using the VTT model to calculate the mould growth index (M). The mould growth index, a numerical scale from $M=1$ to 6, was calculated through a function using temperature and relative humidity, exposure time to critical RH, material sensitivity to mould and relative mould index decline [44]. A mould growth index below 1 ($M < 1$) represents no growth on the material surface, which was set as the evaluation criterion. Exceeding index 1 ($M > 1$, several mould growth colonies on the surface) was considered as the wall hygrothermally unsafe. The hygrothermal performance of each wall type was evaluated by the probability of the risk of mould growth through 100 different sub-scenarios.

We changed the mould sensitivity class on the CLT surface and the wind barrier when calculating the mould growth index in the stochastic analysis. On the CLT surface, we considered the sensitivity classes 'sensitive' and 'very sensitive' [45]. The sensitivity class 'sensitive' refers to planed wood, i.e., the most common CLT panel. The 'very sensitive' sensitivity class is a solid wood panel with untreated surface (sawn surface) made of pine (*Pinus Sylvestris*) wood, e.g. nailed laminated MHM (Massiv-Holz-Mauer) panel. On the interior surface of a wind barrier, we considered the sensitivity classes 'medium resistant' and 'sensitive' [45]. The sensitivity class 'medium resistant' refers to mineral wool materials and 'sensitive' to paper coated products, i.e., a gypsum board.

3 Results and discussion

3.1 Determining the starting point of calculations – the impact of the start of the building's service life

Sensitivity analysis was performed prior to stochastic calculations to determine the month of the year when the CLT covering with external insulation and internal layers may pose the greatest risk of mould growth. Each month of the year (January-December) was selected as the starting point for the calculation of the mould growth index. The mould growth index in each wall type was calculated on the interior and exterior surface of the CLT panel and on the interior surface of the wind barrier. The continuous variables (highest CLT $MC_{CLT ES/IS}=28\%$, highest vapour resistance of the wind barrier $\mu_{WB}=10$, etc.) that could cause the highest risk of mould growth were used in the calculations.

Most critical month to cover CLT with internal vapour tight layer (e.g. PIR insulation) was August and the smallest risk was in April (Fig 6, a). August was also the most critical month when CLT was externally covered with an additional air and vapour barrier and with vapour open insulation (Fig 6, b). The smallest risk was also in April. The most critical month to cover CLT with external vapour tight insulation (e.g., PIR insulation) was June and the smallest risk was in December (Fig 6, c). For the wind barrier installation, the most critical month was September and the smallest risk was in May (Fig 6, d). The risk of mould growth on the inner surface of the wind barrier can even be avoided by the timing of the CLT covering alone. If the wind barrier is installed in April or May, according to the sensitivity analysis, there is no risk of mould growth ($M < 1$). In all other locations, the mould growth index was above 1 in all cases.

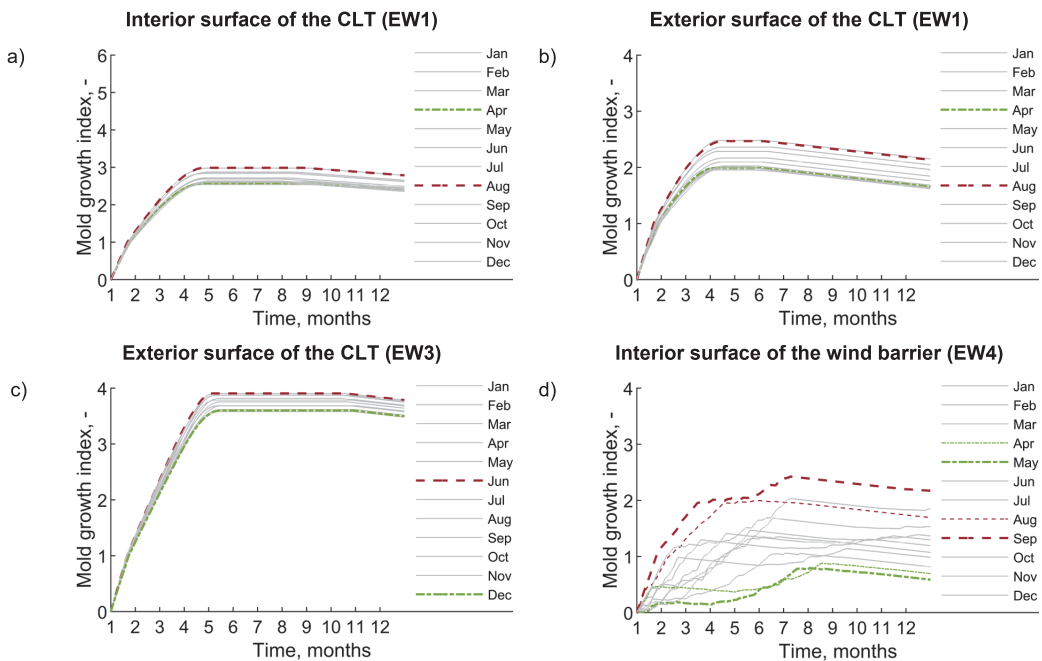


Fig. 6. The influence of start of service life by month evaluated by the mould growth index.

Based on the results of our sensitivity analysis, August was selected as the starting point in the stochastic calculations (see Tables 1 and 2). Exception was made for the wall type EW3, which was externally insulated with vapour tight PIR insulation. June was selected as the starting point for wall type EW3. Also, in one scenario (with the lowest probability of performance), the risk of mould growth on the interior surface of the wind barrier was evaluated starting from September. In general, the results of the sensitivity analysis suggest that in the cold on humid climate, CLT panels should be installed and covered with the

remaining wall layers in spring. Covering the CLT panel in summer carries the highest risk of mould growth, and summer is also the rainiest period in Estonia [46].

3.2 Stochastic analysis

3.2.1 Impact of additional air and vapour barrier

The results showed a clear difference between walls with uncovered and externally covered CLT panels with additional air and vapour barrier. External walls with CLT exposed to the indoor environment and externally insulated with vapour open ($S_d=0.8\text{m}$) insulation (e.g., mineral wool or cellulose insulation) had 100% probability of safe hygrothermal performance, see Table 1 (EW1, 2 and 4, Scenarios 1-3). The addition of an air and water vapour barrier ($S_d=2.3\text{ m}$) to the exterior surface of the CLT panel significantly decreased the probability. The probability of safe hygrothermal performance varied between 48 and 62% in external walls of EW1, 2 and 4 having air and vapour barrier between CLT and external insulation (Scenarios 4-6), see Table 1.

Table 1. The probability of safe hygrothermal performance (CLT as ‘sensitive’ and wind barrier ‘medium resistant’ to mould growth).

Scenarios	Wall type (starting point)												
	EW 1		EW 2		EW 3		EW 4			EW 5			
	(from August)				(from June)		(from August)						
	The location where the mould risk was evaluated (L1 ^a , L2 ^b , L3 ^c) and mould growth sensitivity classes (S ^d , MR ^e)												
CLT thickness	L2	L3	L2	L3	L2	L3	L1	L2	L3	L1	L2	L3	
	S	MR	S	MR	S	MR	S	S	MR	S	S	MR	
Walls without additional air and vapour barrier													
Sc. 1	100 mm	100%	100%	100%	100%	32%	100%	100%	100%	100%	45%	100%	100%
Sc. 2	150 mm	100%	100%	100%	100%	33%	100%	100%	100%	100%	49%	100%	100%
Sc. 3	200 mm	100%	100%	100%	100%	34%	100%	100%	100%	100%	47%	100%	100%
CLT externally covered with additional air and vapour barrier													
Sc. 4	100 mm	55%	100%	54%	100%	30%	100%	100%	48%	100%	51%	58%	100%
Sc. 5	150 mm	59%	100%	58%	100%	30%	100%	100%	54%	100%	51%	52%	100%
Sc. 6	200 mm	62%	100%	53%	100%	32%	100%	100%	59%	100%	51%	62%	100%

^aL1- CLT interior surface, location between CLT and interior layer

^bL2- CLT exterior surface, location between CLT and external insulation or internal membrane

^cL3- wind barrier interior surface, location between external insulation and wind barrier

^dS- CLT as ‘sensitive’ to mould growth

^eMR- wind barrier as ‘medium resistant’ to mould growth

90-100%
80-89%
70-79%
60-69%
50-59%
<50%

A closer look at the results of the first year showed RH quick equilibrium in the walls without an additional air and vapour barrier (EW1, 2 and 4, Scenarios 1-3), and all sub-scenarios reached the same level in almost half a year, see Fig. 7, a. Quick equilibrium did not lead to a risk of mould growth on the CLT surface, see Fig. 7, c. In contrast, a long equilibration occurred in the walls where an air and vapour barrier was added (Fig. 7, b) and the maximum mould growth index in half of the sub-scenarios exceeded one, see Fig. 7, d. A more detailed distribution of the maximum mould growth index is shown as a cumulative distribution, see Fig. 8, a. The results of the mould growth index on the CLT external surface generally showed a short growing trend at the beginning of the calculations and after the index decreased for the rest of the calculation period, see Fig. 7, d.

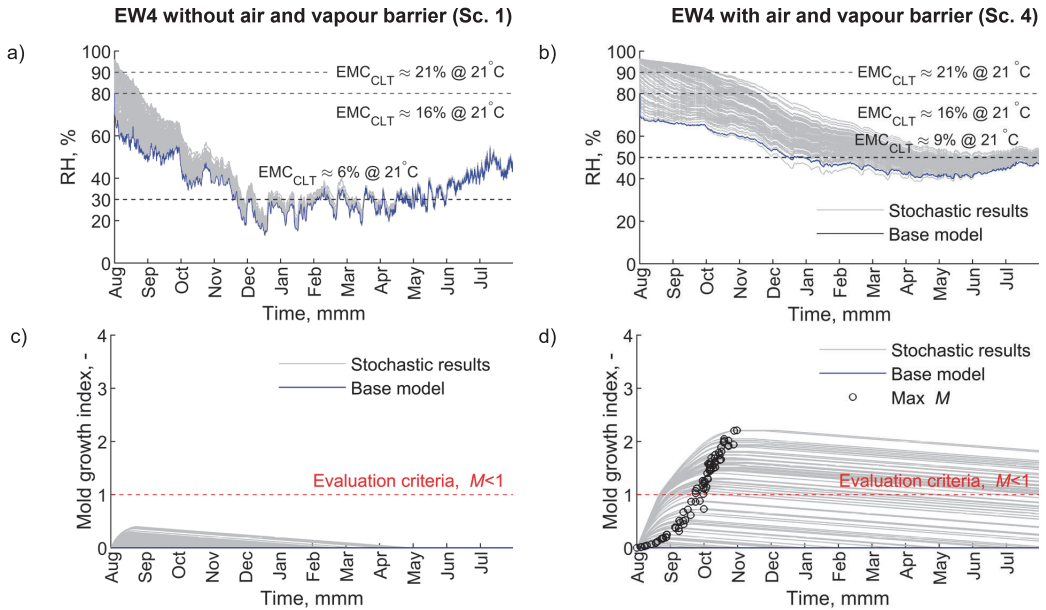


Fig. 7. First year results of RH and mould growth index on CLT external surface (L2).

PCC results showed that the MC of the external surface (MC_{CLT_ES}) of the CLT alone had a significant impact ($PCC > 0.5$) on the mould growth index throughout the calculation period, see Fig. 8, b. This means that the dry-out of the high MC and the moisture accumulating behind the air and vapour barrier is the main cause of mould growth risk. The impact of the remaining studied material properties was insignificant. Therefore, the key factors in the safe hygrothermal design of the CLT external envelope are the sufficient dry-out capacity and the control of the CLT MC level during the construction phase.

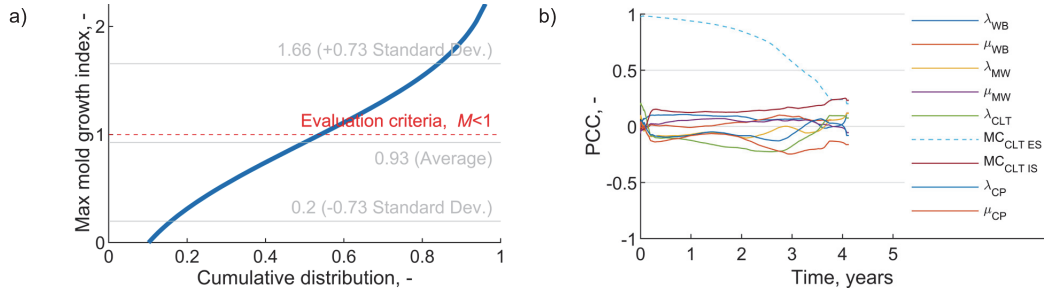


Fig. 8. Cumulative distribution of the maximum mould growth index on the CLT external surface (a), and partial correlation coefficient between the observed material properties and the mould growth index of EW4 scenario 4.

It can be concluded that the addition of an air and vapour barrier ($S_d=2.3$ m) makes the CLT external surface sensitive to mould growth at high CLT MC. In their study, Wang and Ge [15] concluded that the use of a low vapour permeable water resistive barrier on the CLT external surface has a higher risk of moisture problems than a high water vapour permeable membrane. Kukk et al. [23] found that the use of low vapour permeable ($S_d=2.3$ m) membrane on the external surface of the mass timber panel prevents high humidity accumulation on the panel surface in the case of rainwater ingress during the service life. This confirms that low vapour permeable air and vapour barrier ($S_d=2.3$ m) added on a wet CLT surface poses a high risk of mould growth. When installed on a dry surface (installed in the factory), it can also perform as a weather protection during the construction phase and can prevent moisture from spreading to the panel surface at rain leakage during service life.

3.2.2 Impact of wall assembly

Externally insulated external walls with vapour tight PIR insulation (EW3) had a high risk of mould growth, regardless of the presence of an air and vapour barrier. The probability of safe hygrothermal performance varied between 30 and 34%, see Table 1. This was due to the higher insulation vapour resistance rather than the air and vapour barrier ($S_{d,PIR}=12\text{m}$ vs $S_{d,AVB}=2.3\text{m}$). Internally insulated external walls with vapour tight PIR insulation (EW5) had a high risk of mould as well. The probability of safe hygrothermal performance varied between 45 and 51%, see Table 1.

External walls EW5, scenarios 4-6, were the only cases where CLT was covered with vapour tight layers both internally (PIR insulation) and externally (air and vapour barrier). There was a high risk of mould growth on both the interior and exterior surface, see Table 1. The probability of safe hygrothermal performance on the CLT interior surface was 51% and on the exterior surface, it varied between 52 and 62%. The PCC results of EW5, scenario 6, confirmed that the MC of the CLT surface has the greatest impact on mould growth. Importantly, the high CLT MC of the opposite surface did not affect the mould growth risk on the observed surface. The mould growth index on the CLT interior surface was significantly affected only by the MC of the interior surface, see Fig. 9 (a), and vice versa, see Fig. 9 (b). As the ambient conditions of the interior and exterior surface of the CLT panel in a closed external envelope are different, one surface does not affect the equilibrium of the other [47]. This means that if water vapour tight material layers are selected to cover the CLT panel, it is required for the engineer to indicate in the project in which surface the material will be applied, along with a relevant notification to the constructor. This will simplify the preparation process of moisture safety planning of a CLT building during the construction phase and allows a constructor to find locations easily to monitor the CLT surface MC where its dry-out capacity is limited.

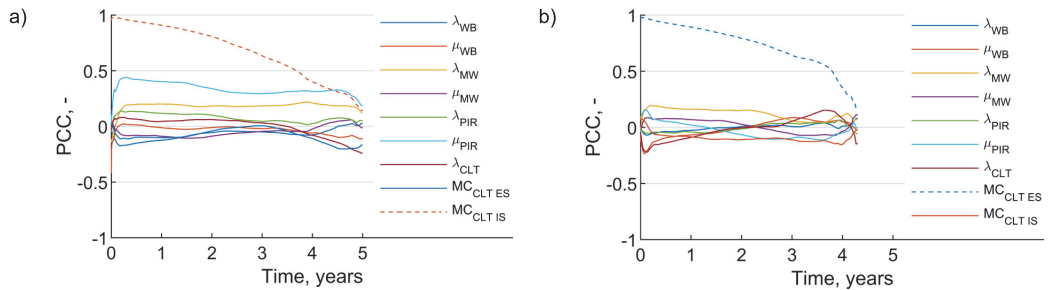


Fig. 9. PCC between the observed material properties and the mould growth index in location L1 (a) and L2 (b) of EW5 scenario 6.

CLT thickness had no significant impact on the stochastic results, since the MC of one surface does not affect the other. There was small impact only on some walls and scenarios due to thickness. For example, in walls with mineral wool external insulation with an additional air and water vapour barrier, the probability of safe hygrothermal performance was slightly higher for thicker CLT (55% vs 62%, EW1, Scenario 4 vs 6), see Table 1. Also, no significant difference was found between the external walls insulated with mineral wool and cellulose wool from the mould growth risk point of view. However, several studies have suggested that the use of cellulose insulation has some advantage over mineral wool by smoothing the humidity peak levels of the indoor air and decreasing the risk of mould growth due to its moisture buffering effect [13,48,49].

3.2.3 Impact of the construction phase

One of the limitations of this research was that the indoor boundary conditions for calculations started directly with the indoor environment of service life ($t_{i, \min} = 22\text{ }^{\circ}\text{C}$). This applies to small detached houses that are made of prefabricated elements and have a short construction phase, after which permanent heating can be applied immediately. In the case of larger buildings where the external building envelope is built on site, the indoor environment may still remain the same as the outdoor environment after installing the CLT panels on site, especially if construction starts in August. Alternatively, temporary heating can be applied

for the construction phase to maintain a higher indoor temperature but still lower than service life temperature, e.g., $t_{i \min} = 15 \text{ }^\circ\text{C}$ [6].

A sensitivity analysis was performed to consider the effect of the indoor climate during the construction phase. We applied the indoor climate of the construction phase for the first 105 days, after which the calculation period continued with the service life of indoor climate ($t_{i \min} = 22 \text{ }^\circ\text{C}$). Four variants for the indoor climate of the construction phase were selected:

- 1) indoor and outdoor environment the same in the entire calculation period and without indoor moisture excess $t_i = t_e$, $\Delta v = 0 \text{ g/m}^3$ – indoor air exchange is ensured, windows and doors are not installed, see Fig. 10 a, e;
- 2) indoor and outdoor environment the same, $t_i = t_e$ for the first 105 days with the indoor moisture excess in the range of $\Delta v = 0\text{-}2 \text{ g/m}^3$ – indoor without air exchange, windows and doors are installed, see Fig. 10 b, h;
- 3) temporary heating applied to the indoor $t_{i \min} = 15 \text{ }^\circ\text{C}$ for the first 105 days with the indoor moisture excess in the range of $\Delta v = 0\text{-}2 \text{ g/m}^3$ – the presence of dehumidifiers, windows and doors are installed, see Fig. 10 c, f, g;
- 4) temporary heating applied to the indoor $t_{i \min} = 15 \text{ }^\circ\text{C}$ for the first 105 days with the indoor moisture excess in the range of $\Delta v = 1\text{-}4 \text{ g/m}^3$ – dehumidifiers are missing, windows and doors are installed, see Fig. 10 d.

Interior surface of CLT exposed to the indoor environment– indoor and outdoor environment the same and without indoor moisture excess, no mould growth within the first three months, see Fig. 10 a. After the first three months, the mould growth index remained stable at 1, posing a small risk. Only factory-dry (Base model, MC=13%) CLT panel remained below 1. When moisture excess ($\Delta v = 0\text{-}2 \text{ g/m}^3$) was added, the risk of mould growth occurred already after 48 days and reached a maximum mould index of 2, see Fig. 10 b.

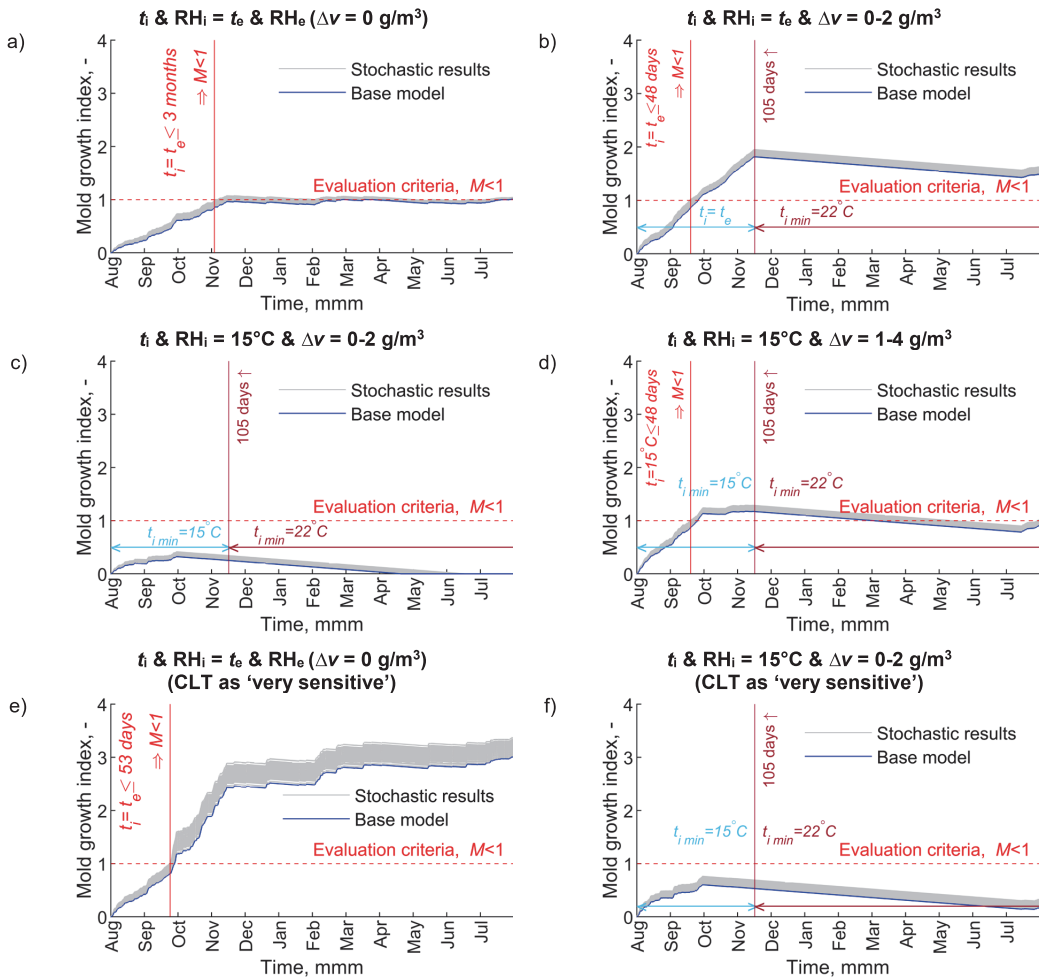
There was no risk of mould growth when temporary heating ($t_{i \min} = 15 \text{ }^\circ\text{C}$) was applied with a small moisture excess range ($\Delta v = 0\text{-}2 \text{ g/m}^3$), see Fig. 10 c. The mould risk arose after 48 days when the moisture excess range was increased to $\Delta v = 1\text{-}4 \text{ g/m}^3$, see Fig. 10 d. The risk of mould growth can also be avoided with temporary heating and low moisture excess range when CLT is considered as ‘very sensitive’ to mould, see Fig. 10 f. However, as ‘very sensitive’ to mould, the CLT panel exposed to the outdoor environment (t_i & $\text{RH}_i = t_e$ & RH_e) has a high risk of mould growth, which will increase in time, see Fig. 10 e.

Exterior surface of CLT covered with vapour permeable insulation – variations in the results from the exterior surface of CLT were large and the MC had the biggest impact, see Fig. 10 g, h. However, the risk of mould was still lower when temporary heating ($t_{i \min} = 15 \text{ }^\circ\text{C}$) was applied with a lower moisture excess range ($\Delta v = 0\text{-}2 \text{ g/m}^3$), see Fig. 10 h.

Long-term storage of panels on the construction site and their exposure to the outdoor environment after installation can lead to the growth of mould on the panel surface. Olsson [50] monitored several CLT buildings in Sweden during the construction phase and from a total of 200 analysed measurement points he found that half had small growth and about a third had moderate or extensive mould growth on the CLT surface. In long-term storage, one of the possible ways to prevent mould growth on the CLT external surface is to maintain CLT as factory dry by storing the panels water-tightly covered and by installing the CLT panels.

Secondly, in order to prevent the growth of mould on the CLT internal surface, it is highly recommended to apply temporary heating immediately after installation of the panels and to ensure a low indoor moisture excess ($\Delta v \leq 2 \text{ g/m}^3$) with air dehumidifiers.

The interior surface of CLT, exposed to the indoor environment



The exterior surface of CLT (L2)

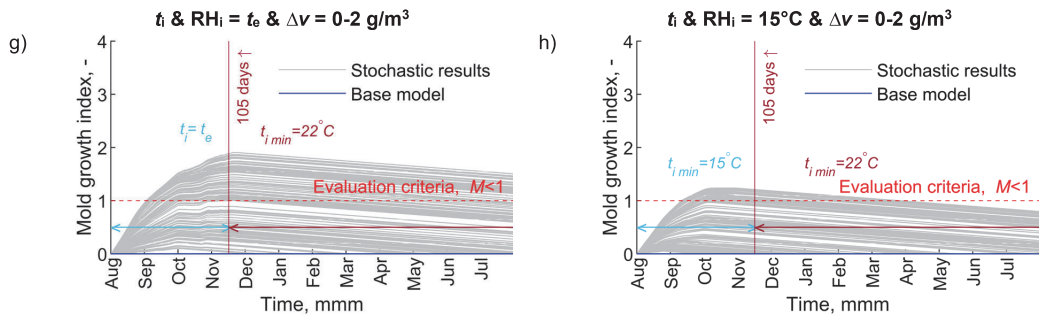


Fig. 10. Risk of mould growth on the interior and exterior surface of the CLT (EW2) during the construction phase.

3.2.4 CLT as 'very sensitive' and the wind barrier as 'sensitive' to mould growth

The probability of safe hygrothermal performance decreased in all scenarios when CLT was considered as 'very sensitive' and the wind barrier as 'sensitive' to mould growth, see Table 2. The most significant

change was observed on the interior surface of the wind barrier, especially in walls without additional air and vapour barrier. In the worst scenario (EW4, scenario 1), the probability decreased to 40%. Fig. 11, a shows that the maximum mould growth index on the interior surface of the wind barrier (EW4, scenario 1) was achieved at the beginning of the calculation period. PCC results showed that vapour resistance of the wind barrier (μ_{WB}), MC of the CLT exterior surface (MC_{CLT_ES}) and thermal conductivity of the wind barrier (λ_{WB}) had significant impact ($PCC > 0.5$) on the mould growth index in the wind barrier surface, see Fig. 11, b. In the case of high vapour resistance and thermal conductivity of the wind barrier, the high moisture excess causes the accumulation of moisture on the interior surface of the wind barrier, which in turn causes the risk mould growth, as shown by the positive results of PCC.

Table 2. The probability of safe hygrothermal performance (CLT as ‘very sensitive’ and wind barrier as ‘sensitive’ to mould growth).

Scenarios	Wall type (starting point)												
	EW 1 (from August)		EW 2		EW 3 (from June)		EW 4 (from August, *from September)			EW 5			
	L2	L3	L2	L3	L2	L3	L1	L2	L3	L1	L2	L3	
	The location where the mould risk was evaluated (L1 ^a , L2 ^b , L3 ^c) and mould growth sensitivity classes (S ^d , VS ^e)												
	VS	S	VS	S	VS	S	VS	VS	S	VS	VS	S	
Walls without additional air and vapour barrier													
Sc. 1	100 mm	100%	64%	100%	64%	24%	100%	100%	100%	40%*	38%	100%	55%
Sc. 2	150 mm	100%	52%	100%	65%	23%	100%	100%	100%	65%	36%	100%	64%
Sc. 3	200 mm	100%	86%	100%	60%	23%	100%	100%	100%	56%	38%	100%	60%
CLT externally covered with additional air and vapour barrier													
Sc. 4	100 mm	44%	95%	48%	97%	20%	100%	100%	41%	89%	43%	49%	97%
Sc. 5	150 mm	45%	91%	43%	94%	22%	100%	100%	47%	84%	42%	46%	95%
Sc. 6	200 mm	48%	99%	38%	96%	22%	100%	100%	51%	87%	38%	48%	97%

^aL1- CLT interior surface, location between CLT and interior layer

^bL2- CLT exterior surface, location between CLT and external insulation or internal membrane

^cL3- wind barrier interior surface, location between external insulation and wind barrier

^dS- wind barrier as ‘sensitive’ to mould growth

^eVS- CLT as ‘very sensitive’ to mould growth

90-100%
80-89%
70-79%
60-69%
50-59%
<50%

Pihelo et al. [51] have reported that a paper coated gypsum board wind barrier with the mould sensitivity class of ‘sensitive’ is not recommended because of higher mould growth risk compared with the mineral wool-based wind barrier (‘medium resistant’). We recommend as well to select a wind barrier for the CLT external envelope with the mould sensitivity class at least ‘medium resistant’, e.g., mineral wool-based, since according to our calculations, there was no risk of mould growth.

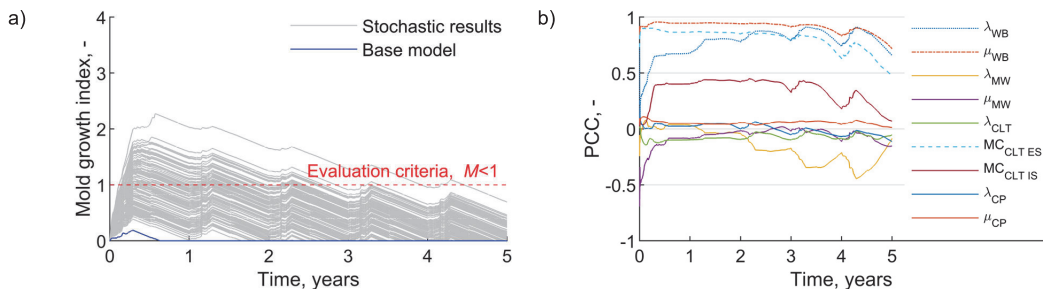


Fig. 11. Mould growth index on the wind barrier internal surface (a) and PCC between the observed material properties and the mould growth index (b) on the internal surface of the wind barrier (L3) of EW4 scenario 1.

3.3 Hygrothermal criteria

We set hygrothermal criteria as limit values to ensure safe hygrothermal performance of each studied CLT external wall type. The determination of the limit values was based on 100% safe performance. Stochastic analysis results showed that the hygrothermal performance of CLT external walls is most affected by the dry-out of the CLT surface MC. Therefore, the criteria were set for the CLT MC and the water vapour resistance of the material layers, which ensures the dry-out capacity of the external wall. Criteria for the CLT MC were set on both the interior (MC_{CLT_IS}) and exterior surfaces (MC_{CLT_ES}), see Tables 3 and 4. Criteria for the water vapour resistance were set to the additional air and vapour barrier ($S_{d\ AVB}$), interior layer, e.g., clay plaster ($S_{d\ IL}$) and wind barrier ($S_{d\ WB}$). The impact of climate conditions during the construction phase was also considered.

3.3.1 The interior surface of CLT

In external walls with CLT exposed to the indoor environment (EW1-3), the risk of mould growth on the CLT interior surface can be prevented when temporary heating is applied immediately after the installation of the panels. Therefore, the limit value was first set at $MC_{CLT_IS} \leq 28\%$ if the CLT interior surface is exposed to the outdoor environment for less than 3 months ($t_i = t_e$ and $\Delta v = 0\text{ g/m}^3 < 3\text{ months}$) before implementing permanent heating with $t_{i\ min} = 22\text{ }^\circ\text{C}$ (Fig. 10 a) or temporary heating with $t_{i\ min} = 15\text{ }^\circ\text{C}$ (Fig. 10 c) together with dehumidifiers ($\Delta v \leq 2\text{ g/m}^3$) applied immediately after the installation of the panels, see Table 3. In case CLT is considered as ‘very sensitive’ to mould growth, the exposing time before implementing permanent heating can only be less than 53 days, see Table 4.

The use of a water vapour permeable interior layer $S_{d\ IL} \leq 0.3\text{ m}$ (EW4) regardless of the mould sensitive class poses no mould risk as long as it is applied as a dry material, see Tables 3 and 4. Layers applied as wet, e.g., clay plaster, require permanent indoor heating ($t_{i\ min} = 22\text{ }^\circ\text{C}$) for the time of application, see Table 3. In case CLT is regarded as ‘very sensitive’ to mould, its interior surface must be factory dry $MC_{CLT_IS} \leq 13\%$ when the wet layer is applied, see Table 4.

Covering CLT internally with vapour tight PIR insulation (EW5) poses a mould growth risk even at low CLT MC, depending on whether the PIR insulation is covered or not and which coating material is used. PIR insulation without coating may pose a mould growth risk when the CLT MC of the internal surface exceeds 18% ($MC_{CLT_IS} \leq 18\%$) regardless of its ambient environment, see Table 3. PIR covered with medium vapour resistance layers ($S_d < 1.65\text{ m}$), e.g., paper coatings, poses mould risk when the MC exceeds 17% ($MC_{CLT_IS} \leq 17\%$), see Table 3. Vapour impermeable cover ($S_d > 800\text{ m}$), e.g., aluminium foil, on PIR insulation poses mould risk when the CLT MC of the internal surface exceeds 16% ($MC_{CLT_IS} \leq 16\%$), see Table 3. If CLT is considered as ‘very sensitive’ to the mould growth, the limit values are $MC_{CLT_IS} \leq 18\%$ (PIR without coating), $MC_{CLT_IS} \leq 16\%$ (PIR coating $S_d < 1.65\text{ m}$) and $MC_{CLT_IS} \leq 15\%$ (PIR coating $S_d > 800\text{ m}$) respectively, see Table 4.

Kukk et al. [21] found the critical MC in the external wall with vapour open mineral wool interior insulation at $MC \leq 17\%$, and $MC \leq 15\%$ in the external wall with vapour tight interior PIR insulation. This means that in the case of vapour tight interior insulation, the factory dry MC of CLT should be maintained.

3.3.2 The exterior surface of CLT

CLT externally insulated with vapour permeable ($S_d < 0.8\text{ m}$) insulation, e.g., mineral wool or cellulose insulation (EW1, 2, 4 and 5), and without additional air and vapour barrier, poses no risk of mould growth on the external surface only when permanent heating ($t_{i\ min} = 22\text{ }^\circ\text{C}$) is applied immediately after the panels installation and closing the building envelope. Therefore, the criterion for CLT exterior surface was set as $MC_{CLT_ES} \leq 28\%$ ($t_{i\ min} = 22\text{ }^\circ\text{C}$). If the temporary heating is applied for 105 days, then the MC of the CLT external surface must be kept equal or less than $MC_{CLT_ES} \leq 25\%$ ($t_{i\ min} = 15\text{ }^\circ\text{C}$). Without applying heating, the MC of the CLT external surface must be kept lower than $MC_{CLT_ES} \leq 21\%$ ($t_i = t_e$), see Table 3. The limit

values in case CLT is regarded as ‘very sensitive’ to the mould growth are $MC_{CLT\ ES} \leq 28\%$ ($t_{i\ min} = 22\ ^\circ C$) and $MC_{CLT\ ES} \leq 21\%$ ($t_{i\ min} = 15\ ^\circ C$) respectively, see Table 4.

Addition of an air and vapour barrier ($S_{d\ AVB} = 2.3\ m$) between vapour permeable insulation and CLT results in a significantly lower impact of the ambient environment of CLT, and the risk of mould is dominated by the MC. The calculations showed that the CLT MC of the external surface should not exceed $MC_{CLT\ ES} \leq 20\%$ to prevent the mould growth risk.

When CLT cannot be prevented from getting wet, the vapour resistance of an additional air and vapour barrier should be equal or less than $S_{d\ AVB} \leq 0.25\ m$, see Table 3. In this case, the criteria applied for the MC in the external walls (EW1, 2, 4 and 5) and without an additional barrier are the same: $MC_{CLT\ ES} \leq 28\%$ ($t_{i\ min} = 22\ ^\circ C$), $MC_{CLT\ ES} \leq 25\%$ ($t_{i\ min} = 15\ ^\circ C$) and $MC_{CLT\ ES} \leq 21\%$ ($t_i = t_e$), see Table 3. If CLT is considered as ‘very sensitive’ to mould growth, the limit values are $MC_{CLT\ ES} \leq 10\%$ or $S_{d\ AVB} \leq 0.05\ m$ respectively, see Table 4.

The use of vapour tight PIR external insulation poses a risk of mould growth on the CLT external surface at high initial MC and the criteria for the CLT MC of the external surface depend on the vapour resistance of the PIR coating; the impact of ambient environment is insignificant. PIR external insulation without coating poses a mould risk when the MC of the external surface exceeds 18% ($MC_{CLT\ ES} \leq 18\%$), see Table 3. PIR covered with a medium vapour resistance layers ($S_d < 1.65\ m$) poses a mould growth risk on the external surface when its MC exceeds 17% ($MC_{CLT\ ES} \leq 17\%$), see Table 3. Vapour impermeable cover ($S_d > 800\ m$), e.g., aluminium foil, on PIR insulation poses a mould risk when the CLT MC of the external surface exceeds 16% ($MC_{CLT\ ES} \leq 16\%$), see Table 3. The limit values in case CLT is ‘very sensitive’ to the mould growth are $MC_{CLT\ ES} \leq 16\%$ (PIR without coating), $MC_{CLT\ ES} \leq 15\%$ (PIR coating $S_d < 1.65\ m$) and $MC_{CLT\ ES} \leq 15\%$ (PIR coating $S_d > 800\ m$) respectively, see Table 4.

3.3.3 The interior surface of the wind barrier

The criteria for the water vapour resistance of a wind barrier were determined on the basis of the wall type EW4 scenario 1. A 100% probability of safe hygrothermal performance was achieved with a limit value of $S_{d\ WB} \leq 0.15\ m$ when the wind barrier is considered as ‘medium resistant’ to mould growth, see Table 3. If the wind barrier is ‘sensitive’ to mould growth, e.g., paper coated papers, the limit value for the water vapour resistance is $S_{d\ WB} \leq 0.03\ m$, see Table 4 and Fig. 12, a. The impact of the indoor environment during the construction phase is insignificant.

In addition, we performed a sensitivity analysis to determine the effect of indoor moisture excess. For this purpose, 10 moisture excess models were formed as a normal distribution. The model by Ilomets [41] with a cold period moisture excess of $4\ g/m^3$ was used as the mean value for the normal distribution, the same that was used for creating the indoor RH boundary condition of this study. Moisture excess of $\pm 1.5\ g/m^3$ in the cold period was used as the standard deviation. The moisture excess values of the models in the cold period varied between 1.3 and $7.2\ g/m^3$. The results showed that the indoor moisture excess has an insignificant effect on the risk of mould growth on the interior surface of the wind barrier, see Fig. 12, b.

Table 3. Hygrothermal criteria for CLT external wall design (CLT as ‘sensitive’ and wind barrier ‘medium resistant’ to mould growth).

Wall type	The interior surface of the CLT	The exterior surface of the CLT		Wind barrier
		Without air and vapour barrier	Air and vapour barrier between CLT and insulation	
EW 1 CLT externally insulated with vapour permeable mineral wool	$MC_{CLT IS} \leq 28\%$ $(t_i = t_e \text{ and } \Delta V = 0 \text{ g/m}^3 \text{ less than 3 months or } t_i = 15^\circ\text{C and } \Delta V \leq 2 \text{ g/m}^3)$ $MC_{CLT IS} \leq 13\%$	$MC_{CLT ES} \leq 28\%$ $(t_i = 22^\circ\text{C})$	$MC_{CLT ES} \leq 20\%$ and $S_{d AVB} \leq 2.3 \text{ m}$ or $S_{d AVB} \leq 0.25 \text{ m}$ and $MC_{CLT ES} \leq 28\%$ $(t_i = 22^\circ\text{C})$ or $MC_{CLT ES} \leq 25\%$ $(t_i = 15^\circ\text{C})$ or $MC_{CLT ES} \leq 21\%$ $(t_i = t_e)$	$S_{d WB} \leq 0.15 \text{ m}$
EW 2 CLT externally insulated with vapour permeable cellulose insulation		$MC_{CLT ES} \leq 25\%$ $(t_i = 15^\circ\text{C})$		
EW 3 CLT externally insulated with low vapour permeable PIR insulation	$(t_i = t_e \text{ and } \Delta V = 0 \text{ g/m}^3 \text{ more than 3 months})$	$MC_{CLT ES} \leq 18\%$ (PIR without coating) $MC_{CLT ES} \leq 17\%$ (PIR coating $S_d < 1.65 \text{ m}$) $MC_{CLT ES} \leq 16\%$ (PIR coating $S_d > 800 \text{ m}$)		
EW 4 CLT externally insulated with vapour permeable mineral wool and internally covered with vapour permeable clay plaster	$MC_{CLT IS} \leq 28\%$ and $S_{d IL} \leq 0.3 \text{ m}$ $(t_i = 22^\circ\text{C only})$	$MC_{CLT ES} \leq 28\%$ $(t_i = 22^\circ\text{C})$	$MC_{CLT ES} \leq 20\%$ and $S_{d AVB} \leq 2.3 \text{ m}$ OR $S_{d AVB} \leq 0.25 \text{ m}$ and $MC_{CLT ES} \leq 28\%$ $(t_i = 22^\circ\text{C})$ or $MC_{CLT ES} \leq 25\%$ $(t_i = 15^\circ\text{C})$ or $MC_{CLT ES} \leq 21\%$ $(t_i = t_e)$	
EW 5 CLT externally insulated with vapour permeable mineral wool and internally covered with low vapour permeable PIR insulation	$MC_{CLT IS} \leq 18\%$ (PIR without coating) $MC_{CLT IS} \leq 17\%$ (PIR coating $S_d < 1.65 \text{ m}$) $MC_{CLT IS} \leq 16\%$ (PIR coating $S_d > 800 \text{ m}$)	$MC_{CLT ES} \leq 25\%$ $(t_i = 15^\circ\text{C})$ $MC_{CLT ES} \leq 21\%$ $(t_i = t_e)$		

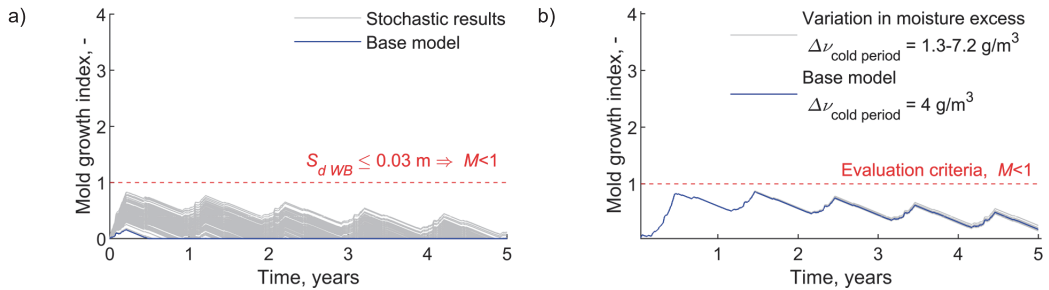


Fig. 12. Mould growth index between the external insulation and the wind barrier (L3) in EW1 scenario 3 after the hygrothermal criteria are met (a) and sensitivity analysis with various indoor moisture excess values (b).

Table 4. Hygrothermal criteria for CLT external wall design (CLT as ‘very sensitive’ and wind barrier ‘sensitive’ to mould growth).

	The interior surface of the CLT	The exterior surface of the CLT		The interior surface of the wind barrier
		Without air and vapour barrier	Air and vapour barrier between CLT and insulation	
EW 1 CLT externally insulated with vapour open mineral wool	$MC_{CLT\ ES} \leq 28\%$ ($t_i = t_e$ and $\Delta V = 0\text{ g/m}^3$ less than 53 days or $t_i = 15^\circ\text{C}$ and $\Delta V \leq 2\text{ g/m}^3$)	$MC_{CLT\ ES} \leq 28\%$ ($t_i = 22^\circ\text{C}$)	$MC_{CLT\ ES} \leq 18\%$ and $S_{d\ AVB} \leq 2.3\text{ m}$ or $S_{d\ AVB} \leq 0.05\text{ m}$ and $MC_{CLT\ ES} \leq 28\%$ ($t_i = 22^\circ\text{C}$) or $MC_{CLT\ ES} \leq 21\%$ ($t_i = 15^\circ\text{C}$)	$S_{d\ WB} \leq 0.03\text{ m}$
EW 2 CLT externally insulated with vapour open cellulose insulation		$MC_{CLT\ ES} \leq 21\%$ ($t_i = 15^\circ\text{C}$)		
EW 3 CLT externally insulated with vapour tight PIR insulation		$MC_{CLT\ ES} \leq 16\%$ (PIR without coating) $MC_{CLT\ ES} \leq 15\%$ (PIR coating $S_d < 1.65\text{ m}$) $MC_{CLT\ ES} \leq 15\%$ (PIR coating $S_d > 800\text{ m}$)		$S_{d\ WB} \leq 0.15\text{ m}$
EW 4 CLT externally insulated with vapour open mineral wool and internally covered with vapour open clay plaster	Dry internal cover: $MC_{CLT\ IS} \leq 28\%$ and $S_{d\ IL} \leq 0.3\text{ m}$ ($t_i = 15^\circ\text{C}$ and $\Delta V \leq 2\text{ g/m}^3$) Application of wet clay: $MC_{CLT\ IS} \leq 13\%$ and $S_{d\ IL} \leq 0.3\text{ m}$ ($t_i = 22^\circ\text{C}$ and $\Delta V \leq 2\text{ g/m}^3$)	$MC_{CLT\ ES} \leq 28\%$ ($t_i = 22^\circ\text{C}$) $MC_{CLT\ ES} \leq 21\%$ ($t_i = 15^\circ\text{C}$)	$MC_{CLT\ ES} \leq 18\%$ and $S_{d\ AVB} \leq 2.3\text{ m}$ or $S_{d\ AVB} \leq 0.05\text{ m}$ and $MC_{CLT\ ES} \leq 28\%$ ($t_i = 22^\circ\text{C}$) or $MC_{CLT\ ES} \leq 21\%$ ($t_i = 15^\circ\text{C}$)	$S_{d\ WB} \leq 0.03\text{ m}$
EW 5 CLT externally insulated with vapour open mineral wool and internally covered with vapour tight PIR insulation	$MC_{CLT\ IS} \leq 18\%$ (PIR without coating) $MC_{CLT\ IS} \leq 16\%$ (PIR coating $S_d < 1.65\text{ m}$) $MC_{CLT\ IS} \leq 15\%$ (PIR coating $S_d > 800\text{ m}$)			

3.3.4 Variation in hygrothermal criteria

According to the North American standard ASHRAE 160-2016 [52], the mould growth index on the building material surface should not exceed 3 to avoid the mould growth problem. VTT in collaboration with IBP [53] have proposed the criteria as ‘‘Traffic light classification’’: in interior spaces, the green light as no mould growth risk is up to mould index 1, yellow light as a small risk is between 1 and 2 and red light is above index 2. In surfaces that are not in contact with indoor air, the green light is up to mould index 2, yellow between 2 and 3 and red above 3.

The comparison with other criteria in Table 5 shows that the limit values differ greatly when different criteria are applied. The largest differences in the limit values occur for the CLT external surface covered with additional air and vapour barrier and externally insulated with vapour open insulation (EW1, 2, 4 and 5). For example, according to the ASHRAE standard 160-2016 criteria ($M < 3$), the high CLT MC of the external surface does not pose a moisture problem, but compared to our criteria ($M < 1$), the MC of the external surface must be kept low ($\leq 20\%$).

When using vapour tight PIR insulation, the MC of the CLT internal and external surface must be kept low for all criteria, but the limit values still vary greatly ($MC_{CLT\ ES} \leq 16\%$ vs $\leq 19\%$ vs $\leq 22\%$). The difference between the limit values for the vapour resistance of the wind barrier ($S_{d\ WB}$) is large as well, varying from $\leq 0.03\text{ m}$ to $\leq 0.15\text{ m}$.

Table 5. Hygrothermal criteria at different mould growth index ranges (CLT and wind barrier as ‘sensitive’ to mould growth).

Location wall type	$M < 1$	$1 < M < 2$	$2 < M < 3$
External walls with additional air and vapour barrier and with vapour open external insulation EW 1, 2, 4 & 5	$MC_{CLT\ ES} \leq 20\%$ or $S_{d\ AVB} \leq 0.25\ m$	$MC_{CLT\ ES} \leq 25\%$ or $S_{d\ AVB} \leq 1.3\ m$	$MC_{CLT\ ES} \leq 28\%$ or $S_{d\ AVB} \leq 2.3\ m$
External walls with vapour tight PIR external insulation EW 3	$MC_{CLT\ ES} \leq 18\%$ (PIR without coating) $MC_{CLT\ ES} \leq 17\%$ (PIR coating $S_d < 1.65\ m$) $MC_{CLT\ ES} \leq 16\%$ (PIR coating $S_d > 800\ m$)	$MC_{CLT\ ES} \leq 20\%$ (PIR without coating) $MC_{CLT\ ES} \leq 20\%$ (PIR coating $S_d < 1.65\ m$) $MC_{CLT\ ES} \leq 19\%$ (PIR coating $S_d > 800\ m$)	$MC_{CLT\ ES} \leq 23\%$ (PIR without coating) $MC_{CLT\ ES} \leq 23\%$ (PIR coating $S_d < 1.65\ m$) $MC_{CLT\ ES} \leq 22\%$ (PIR coating $S_d > 800\ m$)
Wind barrier EW 1, 2, 4 & 5	$S_{d\ WB} \leq 0.03\ m$	$S_{d\ WB} \leq 0.08\ m$	$S_{d\ WB} \leq 0.15\ m$

3.3.5 Use of criteria in practice

The hygrothermal criteria are intended for engineers, constructors, manufacturers, clients – for anyone involved in the construction of CLT buildings to help ensure moisture safety during construction. Fig. 13 shows a simplified decision flow describing how the engineer and constructor can apply criteria while designing or installing a CLT external envelope.

The first decision is made on weather protection – will the CLT building external envelope be fully weather protected during construction? When opting for full weather protection, it can be assumed that the CLT panels will remain factory-dry ($MC_{CLT\ ES} = 15\%$). This is followed by the question – does CLT in the external envelope have at least 5 layers? Kukk et al. [24] and Time [54] concluded that a 5-layer CLT panel can be considered as an airtight layer, but a 3-layer panel requires an additional airtight layer. Lastly, the vapour resistance of the wind barrier used in the external envelope should not exceed $S_{d\ WB} \leq 0.03\ m$. If the requirements are met in the case of full weather protection, the CLT envelope can be considered moisture safe.

The probability of CLT getting soaked is high when the full weather protection is not applied [12] and an additional air and vapour barrier layer is required first. In their study, Kukk et al. [25] concluded that the 5-layer CLT panel can be considered as an air-tight layer as long as its factory-dry MC is maintained during construction. The next question is – is the external insulation vapour open ($S_d \leq 0.8\ m$), e.g., mineral wool and cellulose wool? This determines which criteria apply to the CLT external surface and the wind barrier, see Table 3. During the construction phase, it must be confirmed whether the requirements are met. If not, additional dry-out methods are required before the CLT panels are covered with the rest of the material layers. The next question is – is the CLT panel internally covered? This determines which criteria apply to the CLT internal surface, see Table 3.

The simplified decision flow (Fig. 13) indicates first the complexity of ensuring moisture safety of a CLT building during the construction phase if all the requirements for full weather protection are not applied. Secondly, on the other hand, to what extent, the use of full weather protection simplifies the moisture safety supervision on construction.

◇ -Decision/condition
 ▭ -Requirements

$S_{d\text{ WB}}$ - vapour resistance of wind barrier
 $S_{d\text{ AVB}}$ - vapour resistance of air and vapour barrier
 $S_{d\text{ IL}}$ - vapour resistance of internal cover layer

$MC_{\text{CLT ES}}$ - moisture content of CLT external surface
 $MC_{\text{CLT IS}}$ - moisture content of CLT internal surface

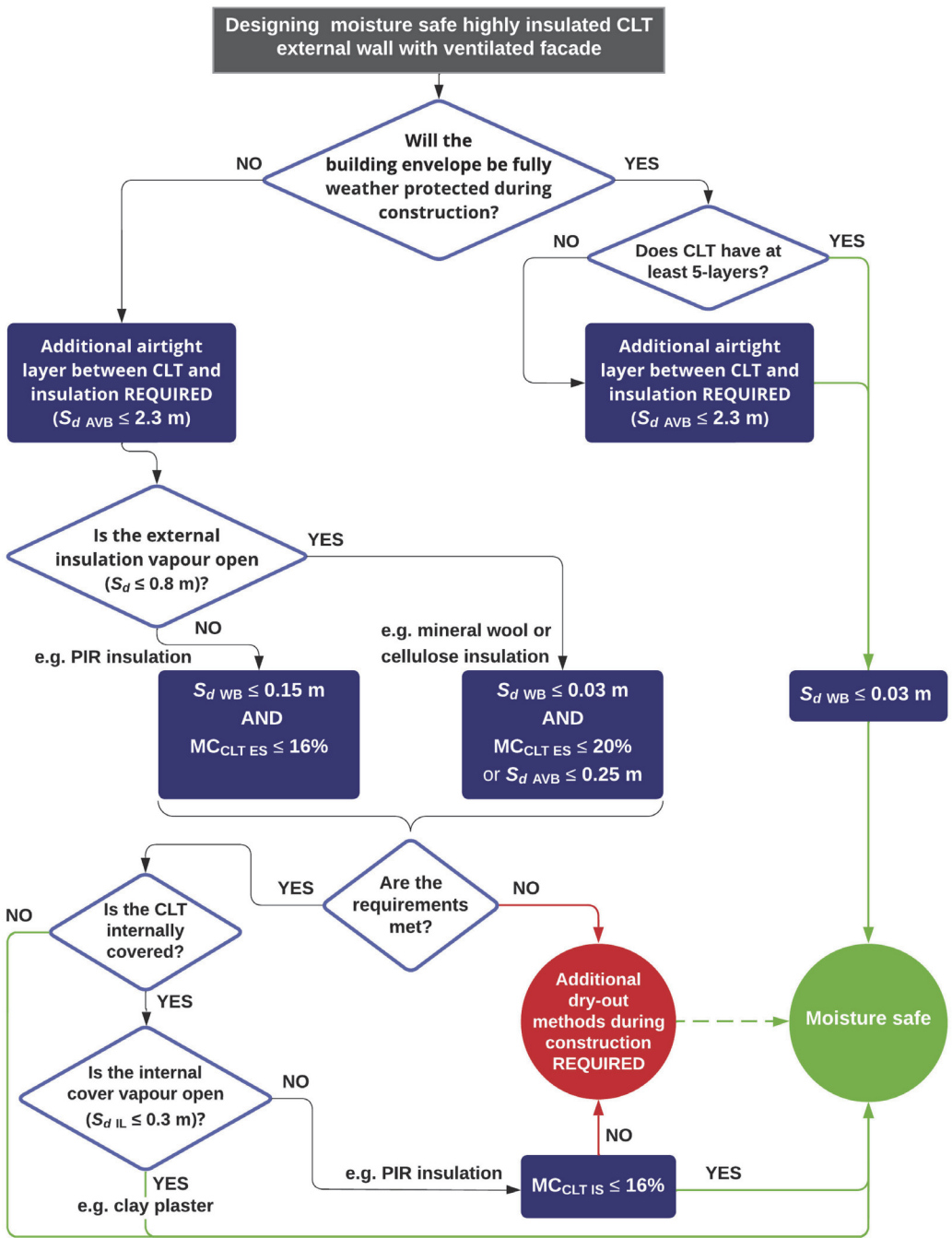


Fig. 13. Simplified decision flowchart based on the hygrothermal criteria for CLT external wall design.

3.3.6 Limitations and future study

The results of our research were obtained through simplified 1D calculations. This eliminates small features such as air leakages and rain intrusion. Kukk et al. [13] discovered a small air exchange between the PIR insulation and the CLT panel that significantly decreased the moisture accumulation from dry-out of CLT on the PIR insulation surface. Wang and Ge [15] concluded that the rain leakage in the external wall has a significant impact on the increase of the CLT MC during the service life in case vapour tight layers are externally covering the CLT. Therefore, future studies should use 2D calculations to evaluate the impact of additional features such as air and rain leakage on the hygrothermal criteria.

The stochastic analysis of our research was also limited to CLT external walls with a ventilated façade. External thermal insulation composite system (ETICS) in a timber structure external envelope has not been recommended as a solution because of high risk of moisture damage [55]. On the other hand, it has been considered as a more cost-effective alternative to a ventilated façade as well as a hygrothermally safe solution when using vapour open insulation materials [23,56]. Therefore, a future study should further explore ETICS solutions for mass timber structures using stochastic analysis.

Conclusions

The key factors in the safe hygrothermal design of the CLT external envelope are the sufficient dry-out capacity and the control of the CLT MC level during the construction phase. Our conclusions were drawn from the stochastic analysis of five types of CLT external walls in terms of hygrothermal performance.

The following conclusions were made for consideration prior to design:

- In the cold and humid climate conditions, we recommend to install the CLT panels and cover with the remaining wall layers in spring (April-May) as the risk of mould growth in spring is the lowest. The greatest risk of mould growth occurs when CLT is covered in late summer (August-September). Installation of vapour open wind barrier in April or May can prevent the risk of mould growth alone.
- The long-term storage (>3 months) of the panels on the construction site exposed to the outdoor environment after the installation can lead to high risk of mould growth on the CLT surface. To prevent the mould growth in long-term storage outdoors, low MC of CLT ($MC_{CLT IS} \leq 13\%$) must be maintained by applying full weather protection.

The following conclusions were made for consideration when designing a CLT external envelope:

- In case full weather protection is used during the construction phase of a CLT building, a 5-layer CLT panel can be considered as an airtight layer, but a 3-layer panel requires additional airtight layer in the external envelope. The vapour resistance of the wind barrier should be $S_{dWB} \leq 0.03$ m to prevent the risk of mould growth.
- We recommend to select a wind barrier for the CLT external envelope with the mould sensitivity class at least 'medium resistant', e.g., mineral wool-based materials, because of no risk of mould growth according to our calculations.
- In case the CLT envelope will not be fully weather protected during the construction phase:
 - An additional air and vapour barrier layer is required as a 5-layer CLT panel can be consider as an air-tight layer only if its low MC (about 13%) is maintained.
 - Use of an additional air and vapour barrier ($S_{dAVB}=2.3$ m) decreases significantly the dry-out capacity of CLT and may pose high risk of mould growth at high initial MC. When installed on a dry surface, it can perform as a weather protection.
 - When selecting water vapour permeable materials for external insulation (e.g., mineral wool and cellulose wool), the following criteria were set to prevent mould growth risk: water vapour resistance of the wind barrier should not exceed $S_{dWB} \leq 0.03$ m; CLT initial

MC of the external surface should not exceed $MC_{CLT ES} \leq 20\%$ or vapour resistance of an additional air and vapour barrier should not exceed $S_{d AVB} \leq 0.25$ m. The results of this study showed that from the mould growth point of view, there was no significant difference between the use of mineral wool and cellulose wool external insulation.

- In the case of vapour tight external insulation (e.g., PIR insulation), the water vapour resistance of the wind barrier should not exceed $S_{d WB} \leq 0.15$ m and the CLT initial MC of the external surface should not exceed $MC_{CLT ES} \leq 16\%$ to prevent mould growth risk on the CLT external surface.
 - When the CLT internal surface is exposed to the indoor environment, at least temporary heating ($t_{i \min} = 15^\circ\text{C}$) together with dehumidifiers should be applied within three months after the CLT panels have been installed to prevent the growth of mould on the internal surface during the construction phase.
 - When the CLT is internally covered with vapour tight insulation (e.g., PIR insulation), the initial MC of the internal surface should not exceed $MC_{CLT IS} \leq 16\%$ to prevent the mould growth risk.
 - Covering the CLT internally with the vapour open layer, e.g., clay plaster, there are no requirements for MC of the internal surface. However, when applying the wet clay plaster, permanent heating ($t_{i \min} = 22^\circ\text{C}$) must be ensured indoors.
- The mould growth risk on the observed CLT surface due to the high CLT MC is not affected by the MC on the opposite surface of the CLT. If CLT panels are covered with water vapour tight layers, the engineer should indicate in the project the surface that it will be applied to. This allows the constructor to find locations easily to monitor the CLT surface MC where its dry-out capacity is limited.
 - CLT thickness had no significant impact on the mould growth risk since the MC of one surface does not affect the other.

Acknowledgments

This research was supported by the Estonian Research Council with Personal research funding PRG483 “Moisture safety of interior insulation, constructional moisture, and thermally efficient building envelope”, Estonian Centre of Excellence in Zero Energy and Resource Efficient Smart Buildings and Districts, ZEBE, grant TK146 funded by the European Regional Development Fund and by the European Commission through the H2020 project Finest Twins (grant No. 856602). The author wishes to thank Estonian glulam producer Peetri Puit OÜ for supplying CLT specimens.

References

- [1] EN 16351:2015 Timber structures - Cross laminated timber - Requirements, (2015).
- [2] K. Mjörnell, L. Olsson, Moisture safety of wooden buildings – design, construction and operation, *J. Sustain. Archit. Civ. Eng.* 24 (2019) 29–35. <https://doi.org/10.5755/j01.sace.24.1.22341>.
- [3] L. Olsson, Moisture safety in CLT construction without weather protection – Case studies, literature review and interviews, in: E3S Web Conf., EDP Sciences, 2020: p. 10001. <https://doi.org/10.1051/E3SCONF/202017210001>.
- [4] J. Niklewski, M. Fredriksson, T. Isaksson, Moisture content prediction of rain-exposed wood: Test and evaluation of a simple numerical model for durability applications, *Build. Environ.* 97 (2016) 126–136. <https://doi.org/10.1016/j.buildenv.2015.11.037>.
- [5] E. Liisma, B.L. Kuus, V. Kukk, T. Kalamees, A case study on the construction of a clt building without a preliminary roof, *J. Sustain. Archit. Civ. Eng.* 25 (2019). <https://doi.org/10.5755/j01.sace.25.2.22263>.

- [6] K. Kalbe, V. Kukku, T. Kalamees, Identification and improvement of critical joints in CLT construction without weather protection, *E3S Web Conf.* 172 (2020) 10002. <https://doi.org/10.1051/e3sconf/202017210002>.
- [7] L. Wang, J. Wang, H. Ge, Wetting and drying performance of cross-laminated timber related to on-site moisture protections: Field measurements and hygrothermal simulations, *E3S Web Conf.* 172 (2020) 10003. <https://doi.org/10.1051/E3SCONF/202017210003>.
- [8] K. Kalbe, T. Kalamees, V. Kukku, A. Ruus, A. Annuk, Wetting circumstances, expected moisture content, and drying performance of CLT end-grain edges based on field measurements and laboratory analysis, *Build. Environ.* (2022).
- [9] WHO guidelines for indoor air quality: dampness and mould, Copenhagen, 2009. https://www.euro.who.int/__data/assets/pdf_file/0017/43325/E92645.pdf.
- [10] D. Caillaud, B. Leynaert, M. Keirsbulck, R. Nadif, S. Roussel, C. Ashan-Leygonie, V. Bex, S. Bretagne, D. Caillaud, A.C. Colleville, E. Frealle, S. Ginestet, L. Lecoq, B. Leynaert, R. Nadif, I. Oswald, G. Reboux, T. Bayeux, C. Fourneau, M. Keirsbulck, Indoor mould exposure, asthma and rhinitis: Findings from systematic reviews and recent longitudinal studies, *Eur. Respir. Rev.* 27 (2018). <https://doi.org/10.1183/16000617.0137-2017>.
- [11] S. Curling, C. Clausen, J. Winandy, Relationships between mechanical properties, weight loss and chemical composition of wood during incipient brown rot decay, *For. Prod. J.* 52 (2002) 34–37. https://pubag.nal.usda.gov/?f%5Bjournal_name%5D%5B%5D=Forest+products+journal&f%5Bpublication_year_rev%5D%5B%5D=7998-2002&f%5Bsource%5D%5B%5D=2002+v.52+no.7%2F8 (accessed March 9, 2022).
- [12] L. Olsson, CLT construction without weather protection requires extensive moisture control, *J. Build. Phys.* 45 (2021) 5–35. <https://doi.org/10.1177/1744259121996388>.
- [13] V. Kukku, L. Kaljula, J. Kers, T. Kalamees, Designing highly insulated cross-laminated timber external walls in terms of hygrothermal performance: Field measurements and simulations, *Build. Environ.* 212 (2022) 108805. <https://doi.org/10.1016/J.BUILDENV.2022.108805>.
- [14] R. McClung, H. Ge, J. Straube, J. Wang, Hygrothermal performance of cross-laminated timber wall assemblies with built-in moisture: field measurements and simulations, *Build. Environ.* 71 (2014) 95–110. <https://doi.org/10.1016/J.BUILDENV.2013.09.008>.
- [15] L. Wang, H. Ge, Hygrothermal performance of cross-laminated timber wall assemblies: A stochastic approach, *Build. Environ.* 97 (2016) 11–25. <https://doi.org/10.1016/j.buildenv.2015.11.034>.
- [16] H.M. Cho, S. Wi, S.J. Chang, S. Kim, Hygrothermal properties analysis of cross-laminated timber wall with internal and external insulation systems, *J. Clean. Prod.* 231 (2019) 1353–1363. <https://doi.org/10.1016/J.JCLEPRO.2019.05.197>.
- [17] J. Yoo, S.J. Chang, S. Yang, S. Wi, Y.U. Kim, S. Kim, Performance of the hygrothermal behavior of the CLT wall using different types of insulation; XPS, PF board and glass wool, *Case Stud. Therm. Eng.* 24 (2021) 100846. <https://doi.org/10.1016/j.csite.2021.100846>.
- [18] G. AlSayegh, Hygrothermal Properties of Cross Laminated Timber and Moisture Response of Wood at High Relative Humidity, Carleton University, 2012. https://curve.carleton.ca/system/files/etd/e7ba278b-c830-463d-ad47-5f98ca309c22/etd_pdf/ca740d27547d38a996fe4281c15c98ca/alsayegh-hygrothermalpropertiesofcrosslaminatedtimber.pdf.
- [19] M. Byttebier, Hygrothermal performance analysis of cross-laminated timber (CLT) in Western Europe, KU Leuven, 2018. [file:///C:/Users/admin/OneDrive/project air permeability/Material/Air permeability properties of the CLT/1718_Thesis_MarcosByttebier.pdf](file:///C:/Users/admin/OneDrive/project%20air%20permeability/Material/Air%20permeability%20properties%20of%20the%20CLT/1718_Thesis_MarcosByttebier.pdf).
- [20] S. Kordziel, S. V. Glass, C.R. Boardman, R.A. Munson, S.L. Zelinka, S. Pei, P.C. Tabares-Velasco,

- Hygrothermal characterization and modeling of cross-laminated timber in the building envelope, *Build. Environ.* 177 (2020) 106866. <https://doi.org/10.1016/J.BUILDENV.2020.106866>.
- [21] V. Kukk, A. Külaots, J. Kers, T. Kalamees, Influence of interior layer properties to moisture dry-out of CLT walls, *Can. J. Civ. Eng.* 46 (2019) 1001–1009. <https://doi.org/10.1139/cjce-2018-0591>.
- [22] V. Kukk, R. Horta, M. Püssa, G. Luciani, H. Kallakas, T. Kalamees, J. Kers, Impact of cracks to the hygrothermal properties of CLT water vapour resistance and air permeability, *Energy Procedia*. 132 (2017) 741–746. <https://doi.org/10.1016/J.EGYPRO.2017.10.019>.
- [23] V. Kukk, J. Kers, T. Kalamees, Hygrothermal Performance of Mass Timber Wall Assembly with External Insulation Finish System, in: *Proc. Build. XIV Int. Conf., ASHRAE, Clearwater, FL, 2019*: pp. 599–607.
- [24] V. Kukk, T. Kalamees, J. Kers, The effects of production technologies on the air permeability and crack development of cross-laminated timber, *J. Build. Phys.* (2019) 174425911986686. <https://doi.org/10.1177/1744259119866869>.
- [25] V. Kukk, A. Bella, J. Kers, T. Kalamees, Airtightness of cross-laminated timber envelopes: Influence of moisture content, indoor humidity, orientation, and assembly, *J. Build. Eng.* 44 (2021) 102610. <https://doi.org/10.1016/J.JOBE.2021.102610>.
- [26] H. Skogstad, L. Gullbrekken, K. Nore, Air leakages through cross laminated timber (CLT) constructions, in: *9th Nord. Symp. Build. Phys., Tampere: Tampere University of Technology, Tampere, 2011*. http://www.tretekknisk.no/resources/filer/publications/Air_leakages_in_cross_laminated_timber_constructions_28022011_docx_xy7tg.pdf (accessed September 5, 2018).
- [27] Declaration of Performance, DASAPLANO 0,01 connect Pro-Clima, Schwetzingen, 2022. <https://ee.proclima.com/tooted/sisemised-kangad/dasaplano-001-connect>.
- [28] Declaration of Performance, internal air and vapour membrane DA Pro-Clima, Schwetzingen, 2022. <https://ee.proclima.com/tooted/sisemised-kangad/da/kuidas-see-tootab>.
- [29] Gyproc ThermaLin PIR, Product Data Sheet - PDS-037-04, Br. Gypsum, Saint-Gobain. (2018). <https://www.british-gypsum.com/products/board-products/gyproc-thermaline-pir-63mm#articles>.
- [30] Declaration of Performance, Therma TP10, Kankaanpää (FIN), n.d. <https://www.kingspan.com/fi/fi-fi/tuotteet/eristeet/suoritustasoilmoitukset/therma-tp10>.
- [31] Thermal Conductivity Test of „Tselluvill mixture“, Test report 11-40/EI/790-3, Tallinn, 2018. https://media.voog.com/0000/0003/1367/files/18-355_Thermal__Werrowool.pdf.
- [32] Declaration of Performance, Gyproc GTS 9, no G520, Kirkkonummi (FIN), 2017. <https://www.gyproc.ee/tooted/kipsplaadid-ja-muud-plaadid/plaadid-vaelisseintesse/gyproc-gts-9>.
- [33] Declaration of Performance, ISOVER RKL31, No 0615-CPR-222984G-M227-2017/01/16, Helsinki, 2017. <https://www.isover.ee/tooted/isover-rkl-31>.
- [34] J. Meynen, Cross Laminated Timber (CLT) bouwdelen met bouwvocht en gewijzigde luchtdichtheid, Catholic University of Leuven, 2016.
- [35] W. Zilling, Moisture transport in wood using a multiscale approach, *FACULTEIT INGENIEURSWETENSCHAPPEN*, 2009. <https://bwk.kuleuven.be/bwf/PhDs/> (accessed June 17, 2020).
- [36] J. Vinha, I. Valovirta, M. Korpi, A. Mikkilä, P. Käckelä, Rakennusmateriaalien rakennusfysikaaliset ominaisuudet lämpötilan ja suhteellisen kosteuden funktiona, Unknown Publisher, Tampere, 2005. <https://trepo.tuni.fi/handle/10024/128233> (accessed September 28, 2021).
- [37] C.-E. Hagentoft, *Introduction to Building Physics*, Studentlitteratur AB, 2001.

- [38] R. Lipand, V. Kukk, T. Kalamees, Capillary Movement of Water in a Radial Direction and Moisture Distribution in a Cross-section of CLT panel, Tallinn University of Technology, 2021.
- [39] A. Stuart, K. Ord, S. Arnold, Kendall's Advanced Theory of Statistics, Classical Inference and the Linear Model, 6th edition, Wiley, 2004. <https://www.wiley.com/en-us/Kendall's+Advanced+Theory+of+Statistics,+Volume+2A,+Classical+Inference+and+the+Linear+Model,+6th+Edition-p-9780470689240> (accessed March 9, 2022).
- [40] R.A. Fisher, The Distribution of the Partial Correlation Coefficient, *Metron*. 3 (1924) 329–332. <https://hdl.handle.net/2440/15182> (accessed March 9, 2022).
- [41] S. Ilomets, T. Kalamees, J. Vinha, Indoor hygrothermal loads for the deterministic and stochastic design of the building envelope for dwellings in cold climates, *J. Build. Phys.* 41 (2017) 547–577. <https://doi.org/10.1177/1744259117718442>.
- [42] T. Kalamees, J. Vinha, Estonian Climate Analysis for Selecting Moisture Reference Years for Hygrothermal Calculations, *J. Therm. Envel. Build. Sci.* 27 (2004) 199–220. <https://doi.org/10.1177/1097196304038839>.
- [43] J. Falk, K. Sandin, Ventilated rainscreen cladding: Measurements of cavity air velocities, estimation of air change rates and evaluation of driving forces, *Build. Environ.* 59 (2013) 164–176. <https://doi.org/10.1016/j.buildenv.2012.08.017>.
- [44] T. Ojanen, H. Viitanen, R. Peuhkuri, K. Lähdesmäki, J. Vinha, K. Salminen, Mold Growth Modeling of Building Structures Using Sensitivity Classes of Materials, in: *Therm. Perform. Exter. Envel. Build. XI, ASHRAE, Florida, 2010*.
- [45] H. Viitanen, T. Ojanen, R. Peuhkuri, J. Vinha, Mould Growth Modelling to Evaluate Durability of Materials, in: M.L. Vasco Peixoto de Freitas, Helena Corvacho (Ed.), XII DBMC 12th Int. Conf. Durab. Build. Mater. Components, 12th - 15th April 2011, Porto, Port., FEUP Edicoes (Faculdade de Engenharia da Universidade do Porto Edicoes), Porto, 2011: pp. 409–416.
- [46] Observation data, Est. Weather Serv. Repub. Est. Environ. Agency. (n.d.). <https://www.ilmateenistus.ee/ilm/ilmavaatlused/vaatlusandmed/?lang=en>.
- [47] A.F. Janzen, R.K. Swartman, Solar energy conversion II: selected lectures from the 1980 International Symposium on Solar Energy Utilization, Pergamon Books, Ontario, 1981. <https://doi.org/10.1016/C2013-0-03320-8> (accessed January 28, 2022).
- [48] T. Ojanen, J. Laaksonen, Hygrothermal performance benefits of the cellulose fiber thermal insulation structures, in: 41st IAHS Int. Assoc. Hous. Sci. World Congr. - Sustain. Build., Coimbra, 2016. <http://www.iahs2016.uc.pt/projectos/iahs2016/atas/pdfs/ID110.pdf> (accessed October 27, 2021).
- [49] P. Pihelo, H. Kikkas, T. Kalamees, Hygrothermal Performance of Highly Insulated Timber-frame External Wall, *Energy Procedia*. 96 (2016) 685–695. <https://doi.org/10.1016/J.EGYPRO.2016.09.128>.
- [50] L. Olsson, Moisture safety in CLT construction without weather protection-Case studies, literature review and interviews, E3S Web Conf. (2020). <https://doi.org/10.1051/e3sconf/2020172>.
- [51] P. Pihelo, K. Kuusk, T. Kalamees, Development and Performance Assessment of Prefabricated Insulation Elements for Deep Energy Renovation of Apartment Buildings, *Energies* 2020, Vol. 13, Page 1709. 13 (2020) 1709. <https://doi.org/10.3390/EN13071709>.
- [52] ASHRAE, ANSI/ASHRAE 160-2016. Criteria for Moisture-control Design Analysis in Buildings, 2016.
- [53] H. Viitanen, M. Krus, T. Ojanen, V. Eitner, D. Zirkelbach, Mold Risk Classification Based on Comparative Evaluation of Two Established Growth Models, *Energy Procedia*. 78 (2015) 1425–

1430. <https://doi.org/10.1016/J.EGYPRO.2015.11.165>.

- [54] B. Time, Climate adaptation of wooden buildings – risk reduction by moisture control, in: Proc. 12th Nord. Symp. Build. Phys. (NSB 2020), Tallinn, 2020.
- [55] I. Samuels, K. Mjörnell, A. Jansson, Moisture damage in rendered, undrained, well insulated stud walls, in: Proc. 8th Symp. Build. Phys. Nord. Ctries., Copenhagen, 2008: pp. 1253–1260.
- [56] G. Günther, S., Ringhofer, A., Schickhofer, External thermal insulation composite systems in solid timber construction, in: 2016 World Conf. Timber Eng. WCTE 2016, Vienna University of technology, Vienna, Austria, 2016.

Curriculum vitae

Personal data

Name: Villu Kukk
Date of birth: 29.03.1989
Place of birth: Ulvi, Mustvee Parish, Jõgeva County, Estonia
Citizenship: Estonian

Contact data

E-mail: villu.kukk@taltech.ee

Education

2017–2022 PhD, Civil and Environmental Engineering, Tallinn University of Technology
2014–2016 MSc, Wood Technology, Tallinn University of Technology
2008–2014 MSc, Rural Engineering, Estonian University of Life Science
1997–2008 Avinurme High school

Language competence

Estonian Native language
English Fluent

Professional employment

2022–... Expert, Tallinn University of Technology
2017–2022 Early Stage Researcher, Tallinn University of Technology
2014–2017 Production House OÜ, Budget manager and quantity surveyour

Research and development work

2022–... ForestValue 2022-2025 project “WoodLCC - Enhanced Life-Cycle-Costing in wood construction by novel methods for service life planning”
2017–2020 EU Horizon 2020 project “Cost reduction of new Nearly Zero-Energy Wooden buildings in the Northern Climatic Conditions” (NERO)

Elulookirjeldus

Isikuandmed

Nimi: Villu Kukk
Sünniaeg: 29.03.1989
Sünnikoht: Ulvi, Mustvee vald, Jõgevamaa
Kodakondsus: Eesti

Kontaktandmed

E-post: villu.kukk@taltech.ee

Hariduskäik

2017–2022 PhD, Ehitus ja arhitektuur, Tallinna Tehnikaülikool
2014–2016 MSc, Puidutehnoloogia, Tallinna Tehnikaülikool
2008–2014 MSc, Maaehitus, Maaülikool
1997–2008 Keskkharidus, Avinurme Gümnaasium

Keelteoskus

Eesti keel Emakeel
Inglise keel Kõrgtase

Teenistuskäik

2022–... Ekspert, Tallinna Tehnikaülikool
2017–2022 doktorant-nooremteadur, Tallinna Tehnikaülikool
2014–2017 Ehitusprojektide eelarvestaja, Production House OÜ

Teadus- ja arendustegevus

2022–... ForestValue 2022-2025 projekt "WoodLCC - puitehituse täiustatud elutsükli kuluarvestuse meetodite uuringud"
2017–2020 Euroopa Liidu Horizon2020 projekt "Uute puidust liginullenergiahoonete maksumuse vähendamine põhjamaises kliimas" (NERO)

Publications / Teaduspublikatsioonid

Articles in peer-reviewed scientific journals

Teadusartiklid, mis avaldatud eelretsenseeritavates teadusajakirjades

- Kukk, V.;** Kers, J.; Kalamees, T.; Wang, L.; Ge, H. (2022). Impact of built-in moisture on the design of hygrothermally safe cross-laminated timber external walls: A stochastic approach. *Building and Environment* (Under review)
- Kalbe, K.; Kalamees, T.; **Kukk, V.;** Ruus, A.; Annuk, A. (2022). Wetting circumstances, expected moisture content, and drying performance of CLT end-grain edges based on field measurements and laboratory analysis. *Building and Environment*. DOI: 10.1016/j.buildenv.2022.109245
- Kukk, V.;** Kaljula, L.; Kers, J.; Kalamees, T. (2022). Designing highly insulated cross-laminated timber external walls in terms of hygrothermal performance: Field measurements and simulations. *Building and Environment*, 212, #108805. DOI: 10.1016/j.buildenv.2022.108805.
- Kukk, V.;** Bella, A.; Kers, J.; Kalamees, T. (2021). Airtightness of cross-laminated timber envelopes: Influence of moisture content, indoor humidity, orientation, and assembly. *Journal of Building Engineering*, 44, #102610. DOI: 10.1016/j.jobe.2021.102610.
- Kukk, V.;** Kers, J.; Kalamees, T. (2020). Field measurements and simulation of an massive wood panel envelope with ETICS. *Wood Material Science and Engineering*, 1–8. DOI: 10.1080/17480272.2020.1712738.
- Liisma, E.; Kuus, B. L.; **Kukk, V.;** Kalamees, T. (2019). A case study on the construction of a CLT building without a preliminary roof. *Journal of Sustainable Architecture and Civil Engineering*, 25 (2), 53–62. DOI: 10.5755/j01.sace.25.2.22263.
- Kukk, V.;** Külaots, A.; Kers, J.; Kalamees, T. (2019). Influence of interior layer properties to moisture dry-out of CLT walls. *Canadian Journal of Civil Engineering*, 46 (11), 1001–1009. DOI: 10.1139/cjce-2018-0591.
- Kukk, V.;** Kalamees, T.; Kers, J. (2019). The effects of production technologies on the air permeability and crack development of cross-laminated timber. *Journal of Building Physics*, 43 (3), 171–186. DOI: 10.1177/1744259119866869.

Articles in peer-reviewed conference proceedings

Artiklid, mis avaldatud eelretsenseeritavates konverentsiväljaannetes

- Kukk, V.;** Kers, J.; Kalamees, T. (2021). The use of an internal airtight membrane in CLT external wall in terms of hygrothermal performance. *Journal of Physics: Conference Series*, 2069: 8th International Building Physics Conference (IBPC 2021) 25-27 August 2021, Copenhagen, Denmark. IOP Publishing Ltd, #012208. DOI: 10.1088/1742-6596/2069/1/012208.
- Kalbe, K.; **Kukk, V.;** Kalamees, T. (2021). Weather exposed CLT construction – observations and improvement concept. *Proceedings of The II Forum Wood Building Baltic: II Forum Wood Building Baltic*, Riga, 2021. Riia, Läti Vabariik: Riga Technical University, 84–85.

- Kalbe, K.; **Kukk, V.**; Kalamees, T. (2020). Identification and improvement of critical joints in CLT construction without weather protection. *E3S Web of Conferences: 12th Nordic Symposium on Building Physics (NSB 2020)*, 172: 12th Nordic Symposium on Building Physics (NSB 2020).. Ed. J. Kurnitski and T. Kalamees. Tallinn, Estonia, September 6-9, 2020: EDP Sciences. DOI: 10.1051/e3sconf/202017210002.
- Kukk, V.**; Kers, J.; Kalamees, T. (2019). Hygrothermal Performance of Mass Timber Wall Assembly with External Insulation Finish System. In: *Thermal Performance of the Exterior Envelopes of Whole Buildings. 14th International Conference on Thermal Performance of the Exterior Envelopes of Whole Buildings 2019*; Clearwater; United States; 9 December 2019 through 12 December 2019.
- Kukk, V.**; Kalamees, T. (2018). Hygrothermal performance of cross-laminated timber walls with interior insulation. *Proceedings of the CIB / NRC Symposium Durability and Climate, Change. Changing Climatic loads as may affect the Durability of Building Materials, Components and Assemblies*, CIB Publication 414: National Research Council Canada, Construction Research Center, Ottawa, Canada 21 September, 2018. Ed. Michael A. Lacasse. CIB - International Council for Research and Innovation in Building and Construction, 23–24.
- Kukk, V.**; Kers, J.; Kalamees, T. (2018). The effects of production technologies on the air permeability properties of cross laminated timber. *IBPC2018 Proceedings: 7th International Building Physics Conference (IBPC2018)*, Syracuse, NY, USA. September 23-26.2018. Syracuse CoE, 349–354.
- Kukk, V.**; Luciani, G.; Püssa, M.; Horta, R.; Kallakas, H.; Kers, J.; Kalamees, T. (2017). Impact of cracks to the hygrothermal properties of CLT water vapour resistance and air permeability. *Energy Procedia*, 132: *The 11th Nordic Symposium on Building Physics, Trondheim, Norway, 11-14 June 2017*. Ed. S. Geving, B. Time. Elsevier, 741–746. DOI: 10.1016/j.egypro.2017.10.019.

ISSN 2585-6901 (PDF)
ISBN 978-9949-83-838-7 (PDF)